TE KUNENGA KI PŪREHUROA | MASSEY UNIVERSITY

UNIVERSITY OF NEW ZEALAND

Global warming responses within the New Zealand alpine radiation of acridid grasshoppers

A thesis submitted in partial fulfilment of the requirements for the degree of

Doctor of Philosophy

in

Ecology

at Massey University, Manawatū, New Zealand

Fabio Leonardo Meza-Joya

2024

To Eli,

who always has backed me in all my endeavours

Thesis abstract

We are living in the Anthropocene, where humans are directly and indirectly altering climatic regimes, leading to warmer conditions with multifarious effects on the biosphere. Well-documented ecological responses to planetary heating include distributional, phenological, and/or phenotypical shifts. Anthropogenic global warming is predicted to significantly impact alpine ecosystems, yet our current understanding of alpine species responses to both ongoing and future global warming is limited. My thesis bridges this gap by investigating the influence of past and future climates on New Zealand's endemic alpine short-horn grasshoppers (Orthoptera: Acrididae), as representatives of New Zealand's alpine fauna. As one of the most ubiquitous herbivores in alpine areas worldwide, grasshoppers provide a marvellous lens to examine responses of native systems to increasing temperatures and explore the mechanisms behind such responses. For this, I used an integrative approach combining phylogeographic tools, demographic statistics, phenotypic data (size and shape), niche models and niche metrics, and genotype–phenotype–environment associations. My findings indicate that (1) distinct climatic, biological, and geophysical factors controlled population structuring of grasshopper species during the Pleistocene with a legacy of spatially separate intraspecific lineages; (2) departures from current climatic conditions are projected to vary with geography, and so species exposure and vulnerability to climate change will vary; (3) habitat loss predicted over the next 50 years of warming will lead to smaller and more-fragmented populations with reduced adaptive potential; (4) differences in niche features between diverging intraspecific lineages may lead to lineage-specific responses; (5) distinct climatic factors influence body size clines, and this might strongly influence potential phenotypic responses. An unexpected and important result is that closely related species are predicted to respond in different ways to climate change, suggesting such responses are more evolutionarily labile than conserved. Collectively, this body of research offers valuable insights into the eco-evolutionary responses of alpine organisms to global warming with broad implications for alpine biota everywhere in the world. The thermal environment is a powerful abiotic driver of evolution, and as we face unparalleled rates of warming, understanding how temperature hinder or foster evolution is critical for assisting management decisions that embrace evolutionary resilience.

Declaration by author

The research carried out for my doctoral thesis has been used in whole or in part for this qualification only. The research is my original work, except as indicated by appropriate attribution in the text and/or acknowledgments; quotation marks have been used where required; and I take responsibility for the content and quality of this thesis. I have clearly stated the contribution of others in jointly authored works, which can be found at the end of each chapter. The "Statement of Contribution to Doctoral Thesis Containing Publications (DRC16)", has been completed for each research chapter within the thesis, and is included in the electronic copy at the start of each chapter.

Acknowledgments

I deeply thank and owe my achievement to Steve and Mary, my superb supervisors, for believing in me from the beginning, for their natural care towards their students, for being assertive and constructive in every single feedback, and for their invaluable support in challenging times. My sincere gratitude goes to Dr Emily Koot (Plant and Food Research) for her insightful feedback on the chapter that we co-authored and Dr Claire Newell (Broken River Ski Area) for her assistance in plant identification. To Eli, Mari, Andrea, Evans, and Cheten, thank you for joining me on my field expeditions. I would also like to thank all members of the Phoenix Lab group for the stimulating talks we have shared: Eliana, Mari, David, Michelle, Shogo, Nim, Cheten, Nyasha, Julien, Mathie, Gillian, and Simon (and everyone else who has come and gone). I would like to acknowledge our lab technicians (Shaun, Cleland, and Tracy) and all of the ski fields that granted us access for grasshopper and plant collections: Broken River, Rainbow Ski Area, Mt Olympus Ski Field, Mt Hutt Ski Area, Fox Peak Ski Field, and Cardrona Alpine Resort. This research was supported by funding from the Miss E. L. Hellaby Indigenous Grasslands, the Orthopterists' Society's Theodore J. Cohn Research Fund, and the Massey University Doctoral Scholarship. Eli, you have always backed me in all my endeavours, been courageous from the beginning, nothing but love for you. To Alberto and Cristabel, thank you for your friendship and for warmly welcoming me (and Eli) into your circle. Last but not least, I want to thank my loved ones in Colombia, who have supported me in every possible way during this journey. Mum and Monis, you are always in my thoughts, I am just terrible at staying connected every week. To my friends in Colombia and elsewhere, thanks for bearing with me in my doctoral quest.

Publications during candidature

Peer-reviewed journal article, included in this thesis:

Meza-Joya, F. L., Morgan-Richards, M., & Trewick, S. A. (2022). Relationships among body size components of three flightless New Zealand grasshopper species (Orthoptera, Acrididae) and their ecological applications. *Journal of Orthoptera Research, 31*(1), 91–103. https://doi.org/10.3897/jor.31.79819

Meza-Joya. F. L., Morgan-Richards, M., Koot, E. M., & Trewick, S. A. (2023). Global warming leads to habitat loss and genetic erosion of alpine biodiversity. *Journal of Biogeography, 50*, 961–975. https://doi.org/10.1111/jbi.14590

Article submitted for publication in a peer-reviewed journal, included in this thesis:

Meza-Joya, F. L., Morgan-Richards, M., & Trewick, S. A. Phenotypic and genetic divergence in a cold-adapted grasshopper may lead to lineage-specific responses to rapid climate change. *Diversity and Distributions*, under review.

Table of Contents

“*Each fresh peak ascended teaches something.*” – Sir Martin Convay

Sharp forest–alpine vegetation transition along an elevational gradient at Hamilton Peak (Broken River Ski Area), Craigieburn Forest Park, South Island. The road/track climbs steeply from Mistletoe Flat Campsite (799 m) to Nervous Knob (1,820 m, where the picture was taken), and then to Hamilton Peak (1,922 m).

Chapter One

Thesis introduction: Earth's climate as a key driver of biodiversity patterns

"As exemplifying the effects of climatal changes on distribution, I have attempted to show how important has been the influence of the modern Glacial period, which I am fully convinced simultaneously affected the whole world, or at least great meridional belts."

(Darwin, 1859, p. 407)

Earth's climate and biogeography

Earth's atmospheric conditions have always exerted selective pressure on life on our planet, driving broad-scale migrations and extinctions (Eyles, 2008; Huntley & Webb, 1989; Stanley, 1998). The Cenozoic era—the last 65 million years of Earth's history—saw abrupt changes in global climate, from widespread warming with ice-free poles to extreme cooling with massive polar ice-sheets, and the onset of orbitally-driven glacial–interglacial cycles at ~2.58 million years ago (Mya), that signalled the start of the ongoing Pliocene–Quaternary glaciation (Zachos et al., 2001). This is a time of repeated gradual glaciation and rapid deglaciation, with a sharp transition about 800 kiloyears ago (kya) from short (41-kyr) to extended (100-kyr) glacial phases (Herbert, 2023; Ruddiman & Raymo, 1988; Tziperman & Gildor, 2003). During the most recent glacial period, culminating in the Last Glacial Maximum (GLM; ~26–19 kya), global ice volume was ~52^6 km^3 greater and global sea levels were ~130 m lower than today (Clark et al., 2009; Lambeck et al., 2014). While the onset of full-glacial conditions was attained first in the Southern Hemisphere, polar ice sheets were more extensive in the North (Clark et al., 2009; Denton et al., 2020). The Earth is now undergoing an inter-glacial cycle, a time of relative rapid warmth that marked the onset of the last ice recession about 18 kya (Denton et al., 2020).

The Pliocene–Quaternary glacial onset and demise denote one of the largest and fastest natural climate shifts in Earth's recent history, shaping much of the landscape and

biogeography we see today. Periods of cooling and glacial advance are inferred to have imposed changes in habitat availability for warm-adapted species, promoting range contractions and extinctions (Davis & Shaw, 2001; Hewitt, 2004). Cold-adapted organisms in turn, could have experienced population and range expansion, and greater connectivity via valley corridors (Carmelet-Rescan et al., 2021; Endo et al., 2015; Galbreath et al., 2009; Hewitt, 2004; Trewick et al., 2000). Rapid global warming at the start of the present interglacial signalled one of the largest megafaunal extinctions in Earth's history, the Quaternary extinction event (Iwase et al., 2012; Koch & Barnosky, 2006; Post, 2013). Populations of warm-adapted species underwent rapid expansion as ice sheets receded and climate amelioration allowed the recolonisation of higher latitudes and the occupation of newly expanded habitats (Taberlet et al., 1998; Lessa et al., 2003; Hewitt 2004), along with possible bursts of speciation (e.g. Milá et al., 2007). Cold-adapted species worldwide are inferred to have experienced range contraction as temperatures increased after the LGM and alpine environments shifted to higher elevations and latitudes (e.g. Ikeda, 2022; Muellner-Riehl, 2019; Trewick et al., 2011), a trend that continues today at an increased rate (Bellard et al., 2012; Freeman et al., 2018; Walther et al., 2002).

We are living in the Anthropocene, where humans are directly and indirectly altering climatic trajectories, leading to warmer conditions with manifold effects on the biosphere (Steffen et al., 2018; McGaughran et al., 2021). Anthropogenic global warming is a major threat to global biodiversity (Loarie et al., 2009; Thomas et al., 2004; Warren et al., 2018), with predictions for species loss as high is 55% by the end of this century under the most extreme scenarios (Román-Palacios & Wiens, 2020). Whether anthropogenic or not, climate varies across the landscape according to latitude and elevation, and such climate isoclines serve as analogues for studying potential species responses to accelerated climate warming (De Frenne et al., 2013; Hodkinson, 2005). While most environments will be at some risk, global warming is predicted to have the greatest impact on the species composition and biodiversity of high elevation and latitude ecosystems (Boggs & Murphy, 1997; Galbreath et al., 2009; Thuiller et al., 2005; Walther et al., 2002). Growing evidence suggest that the rate of warming is amplified with elevation, such that high-mountain environments are more sensitive to rapid increases in temperature than low elevation areas (MRI, 2015). Some of the effects of rising temperatures are now observed across thermal gradients, such as those created by

elevational clines in high mountainous areas (Greenwood & Jump, 2014). Therefore, mountain environments are a sensitive barometer of global climate change, which can yield rapid shifts in the distribution and connectivity of alpine ecosystems (Greenwood & Jump, 2014; Koot et al., 2022; MacDonald et al., 2000).

Montane alpine environments: isolated, biodiverse, and rapidly changing

The alpine zone of mountains represents the only terrestrial biogeographic unit with global distribution (Körner, 2003; Qian et al., 2021). Plant communities above alpine treelines (elevational) resembles that of polar treelines (latitudinal), but the vegetation transition varies strikingly between gradients (Körner, 2021; Qian et al., 2021). Mountainous topography results in abrupt environmental changes over short vertical distances, with sharp transitions in vegetation and hydrology (Frazier & Brewington, 2019; Grabherr et al., 2010). The alpine belt in a mountain system refers to the area located between the natural climatic limit of trees and the permanent snowline (Grabherr et al., 2010). The tree limit on continental mountains varies worldwide, reaching its maximum between tropical and subtropical areas (> 4,000 m) and decreasing towards the poles (Körner, 1998; Jobbágy & Jackson, 2000; Rita et al., 2023). At the global scale, latitude-driven temperature variation is a prime predictor of treeline formation and maintenance, although regional and local-scale topoclimatic conditions and human disturbance regimens also play a role (Greenwood & Jump, 2014; Harsch et al., 2009; Körner & Paulsen, 2004; Rita et al., 2023). Mountains on islands tend to have lower treelines than their continental counterparts (Irl et al., 2016, Leuschner, 1996), likely reflecting the influence of regional climatic factors and impoverished woody species pools (Irl et al., 2016).

Alpine ecosystems on distinct mountains are often separated by deep forested or rangeland areas, hence from a biogeographic view they are analogous to oceanic islands for plant and animal diversity, with populations evolving independently from those on other isolated summits (Mayr & Diamond, 1976; Pauli & Halloy, 2019; Qian et al., 2021). Montane alpine ecosystems are shaped by the significant environmental challenges imposed on life, including diurnal and seasonal extremes in temperature and water availability, strong winds and elevated ultraviolet radiation during a short growth

season (Chinn & Chinn, 2020; Koot et al., 2022). Because the extent of alpine habitat tends to be attenuated with elevation due to the shape of mountains, the majority of terrestrial species inhabiting them tend to have a fragmented distribution within habitat patches that decrease in size with elevation (Pauli & Halloy, 2019). Although the total area of montane alpine ecosystems represents only 2.6% of the Earth's terrestrial surface (Körner, 2021; Körner et al., 2011), they are often recognised as biodiversity hotspots containing a rich variety of plant and animal species and high levels of endemism (Beniston, 2003; Frazier & Brewington, 2019). These cold and isolated alpine ecosystems are among those where global warming impacts are forecasted to be more severe and detectable early on (Grabherr et al., 2010).

Mountains are heating faster than lowlands (Frazier & Brewington, 2019; Greenwood & Jump, 2014; Pauli & Halloy, 2019), with enhanced rates of warming at higher elevations (MRI, 2015). A number of predictive modelling studies forecast major redistributions of native and exotic forest habitat under future warming (e.g. Dyderski et al., 2018; Mathias et al., 2023; Pecchi et al., 2020), and this is reflected by rising treelines and snowlines, and reduction in snowpack depth and endurance (e.g. Cazzola Gatti et al., 2019; Klein et al., 2016). This poses a serious threat for the ecological integrity of alpine ecosystems and their cold-adapted specialised biota (Beniston, 2003; Frazier & Brewington, 2019; Greenwood & Jump, 2014). Treeline advance into higher elevations reduce alpine habitat space given the finite shape of the mountains, and this limits opportunities for alpine biota to persist (Greenwood & Jump, 2014; Koot et al., 2022; Pauli & Halloy, 2019). Cliffs and rocky areas limiting tree growth might become critical as treelines advance, allowing small and scattered patches of alpine habitat to persist (Greenwood & Jump, 2014). Accelerating warming and human disturbance on alpine areas may encourage the establishment of invasive species, thus altering ecosystem processes by filling new functional roles (Beniston, 2003; Frazier & Brewington, 2019; Greenwood & Jump, 2014).

Alpine fauna responses to anthropogenic global warming

Changes in the distribution and connectivity of alpine ecosystems and reduction in snowpack depth and persistence (e.g. Cazzola Gatti et al., 2019; Klein et al., 2016) may

result in new abiotic gradients. To survive, alpine organisms may respond with acclimation, adaptation, relocation, or extinction (Corlett & Westcott, 2013; Frazier & Brewington, 2019; Parmesan, 2006). The literature on species responses to climate change is vast to say the least, and I do not review that literature here. Instead, I highlight the responses that are of interest for the present research, that is, range and phenotypic shifts. For alpine fauna, upward range shifts are most commonly documented, and such shifts are often accompanied by range contractions seen as local extinctions (Reviewed in Parmesan, 2006). Compelling examples of upward shifts of alpine animals around the world include mammals (e.g. Büntgen et al., 2017; McCain et al., 2021; Schai-Braun et al., 2021), birds (e.g. Pernollet et al., 2015; Tingley et al., 2012; Schai-Braun et al., 2021), and insects (e.g. Gilgado et al., 2022; Kerner et al., 2023; Wilson et al., 2005). While these upward shifts are occurring at either or both elevational fronts (i.e. trailing and leading), shifts in the leading edge may become restricted with time owing the finite shape of the mountains, leading alpine biota to a "summit trap" (Koot et al., 2022; Moritz et al., 2008; Wilson et al., 2005).

Although these range shifts may alleviate the immediate effects of global warming, species are still likely to encounter novel environmental conditions (abiotic and biotic) in their expanded range (Jacobsen, 2020; Kerner et al., 2023; Parmesan, 2006). For example, decreasing oxygen availability at higher elevations might prevent some ectothermic animals with limited ability to adjust their metabolic rate to shift upwards (Jacobsen, 2020). Notably, alpine species are not shifting ranges as intact communities but are instead experiencing species-specific range shifts (e.g. McCain et al., 2021; Moritz et al., 2008; Tingley et al., 2012). This may lead to novel biotic interactions and disruptions of ecosystem services, which increases the difficulty in predicting the ecological outcomes of climatic change. For example, variation in the rate of migration between alpine butterflies and their host plants may disrupt biotic interactions or decelerate further butterfly shifts if they are not able to adapt to new hosts (Kerner et al., 2023). For poor-dispersing alpine animals inhabiting remote islands the threat of climate change is even greater: geographic isolation (i.e. unsuitable habitat matrix surrounding both islands and mountaintops) act as very efficient dispersal filters and short elevational spans (i.e. lower topography compared to major continental landmasses) limit the available habitat area to colonise (see Frazier & Brewington, 2019; Harter et al., 2015; Koot et al., 2022).

Growing evidence indicate some animal species are shrinking in body size in response to warming (Gardner et al., 2011; Martins et al., 2023). Such directional shift is predicted by Bergmann's rule (Bergmann, 1847), a trend where larger species (or individuals) occur at higher, colder latitudes and elevations, owing to the relative thermal efficiency for a lower surface-to-volume ratio of endotherms. While this mechanism does not apply to ectotherms, parallel size distribution is common in Orthoptera and other insects (Shelomi, 2012; Mousseau, 1997; Whitman, 2008). Compelling examples of intraspecific body size declines in alpine species are scarce, but a few datasets have shown links between rising temperatures and body size declines in alpine mammals (Mason et al., 2014; Pettorelli et al., 2007; Tafani et al., 2013; Reiner et al., 2021) and birds (Delgado et al., 2019). Empirical evidence of warming-driven size declines in ectotherms is limited to montane moth assemblages from Borneo, but in this case size restructuring involves uphill shifts of relatively small species (Wu et al., 2019). As warming appears to affect species or groups of taxa whose optimal size is sensitive to temperature (i.e. displaying intraspecific or interspecific Bergmann's clines), body size shrinking through time may result from both within-species size shifts and community-level changes due to species redistribution (Martins et al., 2023; Tian & Benton, 2020; Wu et al., 2019).

These, though, are not the only impacts of climate change on alpine organisms. Shifts in phenology have been reported for a few alpine species (e.g. Sedlacek et al., 2022). Moreover, climate change can also impact behaviour and physiology (reviewed in Parmesan, 2006), and this might also be relevant for alpine taxa. Indeed, temperature is a powerful abiotic driver of evolution, and any aspect of an organism's biology that is linked to its capacity to adapt to its thermal environment is likely to be influenced by global warming (Ryding et al., 2021).

Genetic consequences of upward range shift

Phylogeographic inferences indicate alpine species' ranges have been contracting since the demise of the last glacial peak (Hewitt, 2004; Galbreath et al., 2009; Trewick et al., 2000), with genetic and evolutionary consequences (Excoffier et al., 2009; Hewitt, 2004; Parmesan, 2006). As the Earth warmed, montane alpine populations colonised newly-

formed alpine habitat at higher elevations and were extirpated from areas that became unsuitable at lower elevations (Trewick et al., 2000). Yet this pattern could have varied depending on species dispersal abilities, topography, landscape configuration, among other factors (e.g. Carmelet-Rescan et al., 2021; Galbreath et al., 2009; Trewick et al., 2000), which adds difficulty to draw general predictions for the genetic effects of past elevational shifts (Galbreath et al., 2009). However, three general patterns emerge: first, alpine specialists might retain high genetic diversity from larger populations in the recent glacial past (Carmelet-Rescan et al., 2021; Trewick et al., 2000). Second, signatures of gene flow may remain from when their populations were not isolated on mountain peaks (Carmelet-Rescan et al., 2021; Galbreath et al., 2009). Third, long-term lack of genetic connectivity might result in deep divergence from nearby populations (Hewitt, 1996; Taberlet et al., 1998; Trewick et al., 2000). Despite this, current genetic structure and diversity in alpine species may depend, to a large degree, on their glacial–postglacial range shifting history (Alsos et al., 2009).

Recent simulation studies have expanded our ability to understand how range contractions impact the genetic makeup of populations. The common output is that regardless the pattern and speed of range contraction, this process always decreases neutral genetic diversity (Arenas et al., 2012; Rogan et al., 2023). Yet lineages and alleles in the trailing edge of a contracting population are more likely to go extinct (Cobben et al., 2011; Arenas et al., 2012). Moreover, range contractions can result in highly-structured phylogenetic trees, indicative of past demographic contraction (Excoffier et al., 2009). These predictions are much in line with inferences from phylogeographic, niche modelling and fossil data, suggesting that habitat fragmentation in response to future warming will reduce genetic diversity and increased population isolation of some alpine species (e.g. Alsos et al., 2009, Carmelet-Rescan et al., 2021; Koot et al., 2022), and empirical evidence on contemporary upward range shifts of alpine taxa indicate similar outputs (e.g. Jordan et al., 2016; Rubidge et al., 2012). While vulnerability to genetic erosion partly depends on the spatial distribution of genetic diversity within a species (e.g. Alsos et al., 2009), studies investigating the effects of climate change on biodiversity often overlook intraspecific genetic variation. This is relevant as the ability of species and populations to keep pace with future climate change depends on their evolutionary adaptive potential, and thus on sufficient genetic variation upon which natural selection can act (Frankham, 2003; Martin, 2023; Pauls et al., 2013).

Mechanisms for warming-driven range and phenotypic shifts

While species' range shifts are perhaps the best-documented response to global warming, their underlying mechanisms are less understood (Diamond, 2023). Organisms shift their ranges to stay in quasi-equilibrium with the climate envelope they are adapted to (Bellard et al., 2012), but for shifting they still rely on plasticity (i.e. phenotypic variation produced by a single genotype in distinct environments) and genetic adaptation (i.e. change in allele frequencies in population traits due to selection) to modulate range dynamics (Atkins & Travis, 2010; Diamond, 2023; Martin et al., 2023). Key range-limiting traits (e.g. heat tolerance and dispersal ability) are of special interest at this respect. For instance, limited plasticity in thermal tolerance may increase organismal sensitivity to warming temperatures (Seebacher et al., 2015), promoting upward shifts (Jacobsen, 2022). Moreover, greater dispersal abilities can evolve via plastic and/or genetic changes (e.g. Thomas et al., 2001), even if such dispersal propensity is phenotypically cryptic, that is, mediated by increased production of molecular energy (Hanski et al., 2004). Likewise, phenotypic plasticity and/or genetic adaptation are the main ways in which organism phenotypes can change in response in situ to global warming (Ryding et al., 2021).

Although warming-driven reduction in body size is often interpreted as an adaptive response in the context of Bergmann's rule (Gardner et al., 2011), obtaining clear evidence for genetic adaptive evolution in the wild represents a major ongoing challenge (Teplitsky et al., 2008; Merilä & Hendry, 2014). While the current view is that phenotypic plasticity is a prime mechanism to rapidly buffer the effects of warming (Merilä & Hendry, 2014), adaptation via heritable changes in physiology, morphology, and phenology are likely (e.g. Bradshaw & Holzapfel, 2001; Sedlacek et al., 2022; Thomas et al., 2001). However, disentangling genetic and plastic responses is challenging as they are not mutually exclusive, can interact, and both may or may not be adaptive (Martin et al., 2023). Whether genetic or plastic, adaptative responses result in phenotypes suited to new conditions. Moreover, plasticity and genetic adaptation can contribute separately or collectively to keep pace with climate change, yet within their own limits (Martin et al., 2023). In some cases, plasticity might foster evolution by buying time for selection to act, in others it might shield evolution by delaying selective responses increasing extinction risk (Chevin & Hoffmann, 2017; Martin et al., 2023;

Vinton et al., 2022), and in other situations plasticity is itself subject to natural selection (Nussey et al., 2005).

New Zealand alpine biodiversity: grasshoppers as a case study

New Zealand Aotearoa is one of the most isolated and topographically diverse continental islands worldwide (Halloy & Mark, 2003; Trewick & Bland, 2012). Today, New Zealand consists of two main islands (South Island Te Waipounamu and North Island Te Ika-a-Māui), but its shape and size have changed markedly over millions of years, significantly affecting the evolutionary trajectories of alpine organisms (Halloy & Mark, 2003; McGlone et al., 2001; Trewick & Bland, 2012). The alpine environment is relatively young compared to the age of the land surface (Heenan & McGlone 2013), although there has been significant variation in topography between islands (Trewick & Bland, 2012). The New Zealand Southern Alps Kā Tiritiri o Te Moana has dominated the South Island landscape, climate and to a large extent biogeography over approximately the past five million years, but North Island has a different and geologically younger landscape with the oldest axial ranges rising ~1 Mya (Trewick & Bland, 2012). Rapid uplift of mountains generated the first alpine environments in this region since the Jurassic–Cretaceous (Heenan & McGlone, 2013).

New Zealand alpine environments host a diverse assemblage of biotic lineages, including 768 vascular plant taxa, and many bryophytes and lichens (Mark, 2012). While the alpine vertebrate fauna is limited in species (21 birds and 24 lizards), invertebrates are major contributors to alpine biodiversity (Buckley et al., 2022; Halloy & Mark, 2003; Mark, 2012). A remarkable aspect of New Zealand's alpine environment is the high diversity and endemism of brachypterous and flightless insect communities, including alpine adapted, short-horned Catantopinae grasshoppers (Buckley et al., 2022; Nakano et al., 2023). Alpine insects that have endured Pleistocene climate cycling have been critical for advancing our understanding of the role of climatic change on high mountain life evolution and are germane for predicting responses to glacial and interglacial conditions (e.g. Carmelet-Rescan et al., 2021; King et al., 2020; Trewick et al., 2000). This is the situation of the flightless alpine grasshoppers (Orthoptera: Acrididae), which are the product of an endemic radiation largely associated with the Southern Alps of New

Zealand, whose species display freeze-tolerance adaptations (Hawes, 2015; Koot et al. 2020). This monophyletic group radiated ~13–15 Mya, long before Pleistocene climate cycling began (Koot et al., 2020), so their current distributions and intraspecific diversity could reveal responses to glacial and interglacial conditions (e.g. Carmelet-Rescan et al., 2021).

New Zealand alpine grasshoppers have experienced a number of changes to their taxonomic designation due to their conserved morphology, examination of poorly-informative characters (e.g. internal male genitalia), and limited sample size (see Bigelow, 1967). This resulted in some species being transferred between genera and new genera being proposed to accommodate species (Bigelow, 1967; Hutton, 1897). Currently, there are four recognised genera containing 13 species of endemic alpine grasshoppers in New Zealand (Bigelow, 1967): *Alpinacris* (Bigelow, 1967), *Brachaspis* (Hutton, 1897), *Paprides* (Hutton, 1897), and *Sigaus* (Hutton 1897). Most species are found in mountains of the Southern Alps and only one species of *Sigaus* is found occupying alpine habitats in North Island (Bigelow, 1967; Trewick & Morris, 2008). Systematic research using genetic mitochondrial markers have unveiled deep levels of intraspecific divergence (Carmelet-Rescan et al., 2021; Trewick, 2001; Trewick, 2008; Trewick & Morris, 2008), while complete mitogenome phylogenetic analysis indicates a single colonisation event into the alpine environment and misleading current taxonomy (Koot et al., 2020). While a new taxonomic proposal consisting of a single genus (*Sigaus* Hutton) for the New Zealand alpine grasshopper radiation was published by the time this chapter was written (Trewick et al., 2023), here I follow Bigelow's (1967) taxonomy as all research chapters were completed before the updated proposal was published.

Scope of the dissertation

The biotic consequences of climate change have attracted considerable attention since the pace of the anthropogenic climate crisis became recognised (Singer, 2017; Warren et al., 2018). The alpine state of New Zealand and its endemic fauna provide a marvellous lens to examine responses of native systems to environmental shifts because they remain relatively intact but are very sensitive to increasing temperatures (Chinn & Chinn, 2020; Koot et al., 2022). Will New Zealand alpine specialists undergo adaptive evolution in

response to ongoing and future global warming, or is the Earth heating too quickly for evolution to keep pace? Emerging evidence suggests that New Zealand alpine biota not only have a greater capacity to rapidly evolve in novel environments (e.g. McCulloch et al., 2019), but also that adaptive evolution may be occurring in response to climate change (e.g. Becker et al., 2013). Recent predictive modelling on alpine grasshoppers has forecasted species-specific range shifts in response to warming (Koot et al., 2022). This is in line with phylogeographic studies unveiling high levels of intraspecific variation (genetic and phenotypic) within some alpine insects (e.g. Carmelet-Rescan et al., 2021; King et al., 2020; Trewick et al., 2000), suggesting adaptation might enable some lineages to persist under warmer conditions. However, our current understanding of species responses to both ongoing and future global warming is limited, and this thesis aims at integrating several subdisciplines, ranging from morphology to phylogeography, to fill this knowledge gap.

In this thesis I examine the influence of past and future climate change on New Zealand's endemic alpine grasshoppers, as representatives of New Zealand's alpine fauna. This thesis is based on publications and is divided into six chapters. This introduction (Chapter One) briefly elaborates the theoretical framework from where my research derives and presents the scope and outline of the doctoral thesis. Four research chapters (Chapter Two to Chapter Five) compose the main body of the thesis and are written as independent publishable research articles. These chapters are hereby presented in publishable format. Chapter Two has been published in *Journal of Biogeography*, Chapter three in *Journal of Orthoptera Research*, Chapter Four has been submitted for peer-review in *Diversity and Distributions*, and Chapter Five is intended to be submitted to *Proceedings of the Royal Society B: Biological Sciences*. As papers are co-authored, I use "we" and "our" in these chapters to be inclusive of co-authors (see "Declaration by Author" on page iv). My proportional contribution is indicated in the Statement of Contribution form (DRC16) at the beginning of each chapter. The final chapter (Chapter Six) summarizes the major findings of this research and discuss how integrative approaches, historical data, and novel technologies provide exciting opportunities to improve confidence in our predictions on biotic responses to global warming.

Thesis Outline

Our planet is rapidly warming, meaning biotic entities do not have the luxury of time (Chevin & Hoffmann, 2017). Do New Zealand's alpine grasshoppers have the capacity to rapidly track their favourable climate space to cope with anthropogenic warming over the next 50 years? My second chapter integrates phylogeography, ecological niche modelling and climatic niche comparisons to investigate how changing conditions in the Southern Alps influences three flightless alpine grasshopper species with partly overlapping ranges. This chapter aims to (1) identify availability and vulnerability of potential habitat based on climate proxies, (2) analyse how historical processes and barriers to movement shape the current distribution of genetic variation, and (3) predict the impact of future climate change on its distribution and potential loss of genetic diversity. If LGM conditions promoted species-specific patterns of spatial distribution of intraspecific diversity, then anthropogenic warming over the next 50 years could result in uneven genetic erosion even among sympatric and closely related species.

Choosing an ecologically meaningful body size metrics is critical to draw robust inferences on the relationship between size and global warming (Bailey et al., 2020). Which body size metric better reflects overall changes in body size in New Zealand's alpine grasshoppers? My third chapter used empirical data on distinct size proxies (linear dimensions and mass) of three alpine grasshopper species, and frequentist hierarchical and non-hierarchical statistical modelling to examined intraspecific relationships among size metrics across species, while accounting for size dimorphism. This aims to (1) quantify the effects of ethanol preservation on body mass estimates, (2) examine length–mass relationships to identify robust predictors of overall body size, and (3) develop species-specific statistical modes to estimate distinct body size metrics from easy-to-obtain size measurement (e.g. femur length). Knowledge about the relationships between body size components has important ecological applications in the context of global warming and provide a tool for making size metrics from different sources (e.g. museum specimens, published datasets, and fresh sampling) comparable.

Species responses to global warming might depend on intraspecific diversity (Seaborn et al., 2021). Will intraspecific variation in alpine species provide the evolutionary potential to persist or lead to lineage-specific responses to rapid global warming? My fourth chapter combines demographic statistics, phylogeographic tools, phenotypic data (size

and shape), niche models and niche analyses, and genotype–phenotype–environment associations to investigate the evolutionary processes underlying genetic and phenotypic diversity in the sole flightless and cold-adapted grasshopper endemic to North Island, and project its suitable space in time. This chapter (1) examines the influence of palaeo-geophysical changes on population connectivity and demography, and correlation with morphological variation, (2) estimates the relative role of genetic drift and selection on patterns of phenotypic differentiation across this species range, and (3) predicts the impact of future climate change on its distribution and potential loss of intraspecific genetic and phenotypic diversity. Such integrative approach provides a robust framework to investigate possible drivers of local adaptation and to identify populations that require conservation resources to avoid loss of evolutionary potential.

Environmental clines serve as analogues for predicting species responses to the current climate warming (Hodkinson, 2005). Do New Zealand's alpine grasshoppers exhibit clinal variation in body size across environmental gradients? My fifth chapter used empirical data on distinct body size components of three flightless alpine grasshopper species (structural size, body mass, and body condition) and Bayesian hierarchical statistical modelling to test for biogeographic clines in body size and sexual size dimorphism, and to explore climate–size associations. This aims to (1) assess whether Bergmann clines occur across latitude and elevation at intraspecific level, (2) identify potential drivers of clinal variation by considering the role of selection and gene flow (within species), and multiple environmental gradients (different species on the same mountain), and (3) identify sex-specific changes in body size across biogeographic and climate gradients creating clinal change in size dimorphism. Biogeographic clines in morphology can illuminate the evolutionary forces driving organismal trait disparity and inform phenotypic adjustments to changing environmental conditions.

As argued across these chapters, the major findings of this thesis are not limited to the grasshopper study system (or arthropods, for that matter) but might have broad implications for alpine biota anywhere in the world.

References

Alsos, I. G., Alm, T., Normand, S., & Brochmann, C. (2009). Past and future range shifts and loss of diversity in dwarf willow (*Salix herbacea* L.) inferred from genetics, fossils and modelling. *Global Ecology and Biogeography*, *18*(2), 223–239. https://doi.org/10.1111/j.1466-8238.2008.00439.x

Arenas, M., Ray, N., Currat, M., & Excoffier, L. (2012). Consequences of range contractions and range shifts on molecular diversity. *Molecular Biology and Evolution*, *29*(1), 207–218. https://doi.org/10.1093/molbev/msr187

Atkins, K. E., & Travis, J. M. J. (2010). Local adaptation and the evolution of species' ranges under climate change. *Journal of Theoretical Biology*, *266*, 449–457. https://doi.org/10.1016/j.jtbi.2010.07.014

Bailey, L. D., Kruuk, L. E., Allen, R., Clayton, M., Stein, J., & Gardner, J. L. (2020). Using different body size measures can lead to different conclusions about the effects of climate change. *Journal of Biogeography*, *47*, 1687–1697. https://doi.org/10.1111/jbi.13850

Becker, M., Gruenheit, N., Steel, M., Voelckel, C., Deusch, O., Heenan, P. B., ... & Lockhart, P. J. (2013). Hybridization may facilitate in situ survival of endemic species through periods of climate change. *Nature Climate Change*, *3*(12), 1039–1043. https://doi.org/10.1038/nclimate2027

Bellard, C., Bertelsmeier, C., Leadley, P., Thuiller, W., & Courchamp, F. (2012). Impacts of climate change on the future of biodiversity. *Ecology Letters*, *15*(4), 365–377. https://doi.org/10.1111/j.1461-0248.2011.01736.x

Beniston, M. (2003). Climatic change in mountain regions: A review of possible impacts. *Climatic change*, *59*, 5–31. https://doi.org/10.1023/A:1024458411589

Bigelow, R. S. (1967). *The grasshoppers (Acrididae) of New Zealand*. University of Canterbury Publications.

Boggs, C. L., & Murphy, D. D. (1997). Community composition in mountain ecosystems: Climatic determinants of montane butterfly distributions. *Global Ecology and Biogeography Letters*, *6*(1), 39–48. https://doi.org/10.2307/2997525

Bradshaw, W. E., & Holzapfel, C. M. (2001). Genetic shift in photoperiodic response correlated with global warming. *Proceedings of the National Academy of Sciences*, *98*(25), 14509–14511. https://doi.org/10.1073/pnas.241391498

Buckley, T. R., Hoare, R. J., & Leschen, R. A. (2022). Key questions on the evolution and biogeography of New Zealand alpine insects. *Journal of the Royal Society of New Zealand*, *54*(1), 30–54. https://doi.org/10.1080/03036758.2022.2130367

Büntgen, U., Greuter, L., Bollmann, K., Jenny, H., Liebhold, A., Galván, J. D., ... & Mysterud, A. (2017). Elevational range shifts in four mountain ungulate species from the Swiss Alps. *Ecosphere*, *8*(4), e01761. https://doi.org/10.1002/ecs2.1761

Carmelet-Rescan, D., Morgan-Richards, M., Koot, E. M., & Trewick, S. A. (2021). Climate and ice in the last glacial maximum explain patterns of isolation by distance inferred for alpine grasshoppers. *Insect Conservation and Diversity*, *14*(5), 568–581. https://doi.org/10.1111/icad.12488

Cazzola Gatti, C. R., Callaghan, T., Velichevskaya, A., Dudko, A., Fabbio, L., Battipaglia, G., & Liang, J. (2019). Accelerating upward treeline shift in the Altai Mountains under last-century climate change. *Scientific Reports*, *9*(1), 7678. https://doi.org/10.1038/s41598-019-44188-1

Chevin, L. M., & Hoffmann, A. A. (2017). Evolution of phenotypic plasticity in extreme environments. *Philosophical Transactions of the Royal Society B: Biological Sciences*, *372*(1723), 20160138. https://doi.org/10.1098/rstb.2016.0138

Chinn, W. G. H., & Chinn, T. J. H. (2020). Tracking the snow line: Responses to climate change by New Zealand alpine invertebrates. *Arctic, Antarctic, and Alpine Research*, *52*(1), 361–389. https://doi.org/10.1080/15230 430.2020.1773033

Clark, P. U., Dyke, A. S., Shakun, J. D., Carlson, A. E., Clark, J., Wohlfarth, B., Mitrovica, J. X., Hostetler, S.W., & McCabe, A. M. (2009). The Last Glacial Maximum. *Science*, *35*, 710–714. https://doi.org/10.1126/science.117287

Cobben, M. M. P., Verboom, J., Opdam, P. F. M., Hoekstra, R. F., Jochem, R., Arens, P., & Smulders, M. J. M. (2011). Projected climate change causes loss and redistribution of genetic diversity in a model metapopulation of a medium-good disperser. *Ecography*, *34*(6), 920–932. https://doi.org/10.1111/j.1600-0587.2011.06713.x

Corlett, R. T., & Westcott, D. A. (2013). Will plant movements keep up with climate change? *Trends in Ecology & Evolution*, *28*(8), 482–488. https://doi.org/10.1016/j.tree.2013.04.003

Davis, M. B., & Shaw, R. G. (2001). Range shifts and adaptive responses to quaternary climate change. *Science*, *292*(5517), 673–679. https://doi.org/10.1126/science.292.5517.673

De Frenne, P., Graae, B. J., Rodríguez-Sánchez, F., Kolb, A., Chabrerie, O., Decocq, G., ... & Verheyen, K. (2013). Latitudinal gradients as natural laboratories to infer species' responses to temperature. *Journal of Ecology*, *101*(3), 784–795. https://doi.org/10.1111/1365-2745.12074

Delgado, M. D. M., Bettega, C., Martens, J., & Päckert, M. (2019). Ecotypic changes of alpine birds to climate change. *Scientific Reports*, *9*(1), 16082. https://doi.org/10.1038/s41598-019-52483-0

Denton, G. H., Anderson, R. F., Toggweiler, J. R., Edwards, R. L., Schaefer, J. M., & Putnam, A. E. (2010). The last glacial termination. *Science*, *328*(5986), 1652–1656. https://doi.org/10.1126/science.1184119

Diamond, S. E. (2018). Contemporary climate-driven range shifts: Putting evolution back on the table. *Functional Ecology*, *32*(7), 1652–1665. https://doi.org/10.1111/1365-2435.13095

Dyderski, M. K., Paź, S., Frelich, L. E., & Jagodziński, A. M. (2018). How much does climate change threaten European forest tree species distributions? *Global Change Biology*, *24*(3), 1150–1163. https://doi.org/10.1111/gcb.13925

Endo, Y., Nash, M., Hoffmann, A. A., Slatyer, R., & Miller, A. D. (2015). Comparative phylogeography of alpine invertebrates indicates deep lineage diversification and historical refugia in the Australian Alps. *Journal of Biogeography*, *42*(1), 89–102. https://doi.org/10.1111/jbi.12387

Excoffier, L., Foll, M., & Petit, R. J. (2009). Genetic consequences of range expansions. *Annual Review of Ecology, Evolution, and Systematics*, *40*, 481–501. https://doi.org/10.1146/annurev.ecolsys.39.110707.173414

Eyles, N. (2008). Glacio-epochs and the supercontinent cycle after~ 3.0 Ga: Tectonic boundary conditions for glaciation. *Palaeogeography, Palaeoclimatology, Palaeoecology*, 258, 89–129. https://doi.org/10.1016/j.palaeo.2007.09.021

Frankham, R. (2003). Genetics and conservation biology. *Comptes Rendus Biologies*, *326*, 22–29. https://doi.org/10.1016/S1631-0691(03)00023-4

Frazier, A. G., Brewington, L., Goldstein, M. I., & DellaSala, D. A. (2020). *Current changes in alpine ecosystems of Pacific Islands*. In M. I. Goldstein & D. A. DellaSala (Eds.), *Encyclopedia World's Biomes* (pp. 607–619). Elsevier. https://doi.org/10.1016/B978-0-12-409548-9.11881-0

Freeman, B. G., Lee-Yaw, J. A., Sunday, J. M., & Hargreaves, A. L. (2018). Expanding, shifting and shrinking: The impact of global warming on species' elevational distributions. *Global Ecology and Biogeography*, *27*(11), 1268–1276. https://doi.org/10.1111/geb.12774

Galbreath, K. E., Hafner, D. J., & Zamudio, K. R. (2009). When cold is better: Climate-driven elevation shifts yield complex patterns of diversification and demography in an alpine specialist (American pika, *Ochotona princeps*). *Evolution*, *63*(11), 2848–2863. https://doi.org/10.1111/j.1558-5646.2009.00803.x

Gardner, J. L., Peters, A., Kearney, M. R., Joseph, L., & Heinsohn, R. (2011). Declining body size: A third universal response to warming? *Trends in Ecology & Evolution*, *26*(6), 285–291. https://doi.org/10.1016/j.tree.2011.03.005

Gilgado, J. D., Rusterholz, H. P., & Baur, B. (2022). Millipedes step up: Species extend their upper elevational limit in the Alps in response to climate warming. *Insect Conservation and Diversity*, *15*(1), 61–72. https://doi.org/10.1111/icad.12535

Grabherr, G., Gottfried, M., & Pauli, H. (2010). Climate change impacts in alpine environments. *Geography Compass*, *4*(8), 1133–1153. https://doi.org/10.1111/j.1749-8198.2010.00356.x

Greenwood, S., & Jump, A. S. (2014). Consequences of treeline shifts for the diversity and function of high altitude ecosystems. *Arctic, Antarctic, and Alpine Research*, *46*(4), 829–840. https://doi.org/10.1657/1938-4246-46.4.829

Halloy, S. R., & Mark, A. F. (2003). Climate-change effects on alpine plant biodiversity: A New Zealand perspective on quantifying the threat. *Arctic, Antarctic, and Alpine*

Research, *35*, 248–254. https://doi.org/10.1657/1523-0430(2003)035[0248:CEOAPB]2.0.CO;2

Hanski, I., Erälahti, C., Kankare, M., Ovaskainen, O., & Sirén, H. (2004). Variation in migration propensity among individuals maintained by landscape structure. *Ecology Letters*, *7*(10), 958–966. https://doi.org/10.1111/j.1461-0248.2004.00654.x

Harsch, M. A., Hulme, P. E., McGlone, M. S., & Duncan, R. P. (2009). Are treelines advancing? A global meta-analysis of treeline response to climate warming. *Ecology Letters*, *12*(10), 1040–1049. https://doi.org/10.1111/j.1461-0248.2009.01355.x

Harter, D. E., Irl, S. D., Seo, B., Steinbauer, M. J., Gillespie, R., Triantis, K. A., ... & Beierkuhnlein, C. (2015). Impacts of global climate change on the floras of oceanic islands–Projections, implications and current knowledge. *Perspectives in Plant Ecology, Evolution and Systematics*, *17*(2), 160–183. https://doi.org/10.1016/j.ppees.2015.01.003

Hawes, T. C. (2015). Canalization of freeze tolerance in an alpine grasshopper. *Cryobiology*, *71*(2), 356–359. https://doi.org/10.1016/j.cryobiol.2015.07.008

Heenan, P. B., & McGlone, M. S. (2013). Evolution of New Zealand alpine and open-habitat plant species during the late Cenozoic. *New Zealand Journal of Ecology*, *37*(1), 105–113. http://www.jstor.org/stable/24060763

Herbert, T. D. (2023). The Mid-Pleistocene Climate Transition. *Annual Review of Earth and Planetary Sciences*, 51, 389–418. https://doi.org/10.1146/annurev-earth-032320-104209

Hewitt, G. M. (1996). Some genetic consequences of ice ages, and their role in divergence and speciation. *Biological Journal of the Linnean Society*, *58*(3), 247–276. https://doi.org/10.1111/j.1095-8312.1996.tb01434.x

Hewitt, G. M. (2004). Genetic consequences of climatic oscillations in the quaternary. *Philosophical Transactions of the Royal Society, B: Biological Sciences*, *359*(1442), 183–195. https://doi.org/10.1098/rstb.2003.1388

Hodkinson, I. D. (2005). Terrestrial insects along elevation gradients: Species and community responses to altitude. *Biological Reviews of the Cambridge Philosophical Society*, *80*, 489–513. https://doi.org/10.1017/S1464793105006767

Huntley, B., & Webb, T. (1989). Migration: Species' response to climatic variations caused by changes in the Earth's orbit. *Journal of Biogeography*, *16*(1), 5–19. https://doi.org/10.2307/2845307

Ikeda, H. (2022). Decades-long phylogeographic issues: Complex historical processes and ecological factors on genetic structure of alpine plants in the Japanese archipelago. *Journal of Plant Research*, *135*, 191–201. https://doi.org/10.1007/s1026 5-022-01377-w

Irl, S. D., Anthelme, F., Harter, D. E., Jentsch, A., Lotter, E., Steinbauer, M. J., & Beierkuhnlein, C. (2016). Patterns of island treeline elevation–a global perspective. *Ecography*, *39*(5), 427–436. https://doi.org/10.1111/ecog.01266

Iwase, A., Hashizume, J., Izuho, M., Takahashi, K., & Sato, H. (2012). Timing of megafaunal extinction in the late Late Pleistocene on the Japanese Archipelago. *Quaternary International*, *255*, 114–124. https://doi.org/10.1016/j.quaint.2011.03.029

Jacobsen, D. (2020). The dilemma of altitudinal shifts: Caught between high temperature and low oxygen. *Frontiers in Ecology and the Environment*, *18*(4), 211-218. https://doi.org/10.1002/fee.2161

Jobbagy, E. G., & Jackson, R. B. (2000). Global controls of forest line elevation in the northern and southern hemispheres. *Global Ecology and Biogeography*, *9*(3), 253–268. https://doi.org/10.1046/j.1365-2699.2000.00162.x

Jordan, S., Giersch, J. J., Muhlfeld, C. C., Hotaling, S., Fanning, L., Tappenbeck, T. H., & Luikart, G. (2016). Loss of genetic diversity and increased subdivision in an endemic alpine stonefly threatened by climate change. *PloS One*, *11*(7), e0157386. https://doi.org/10.1371/journal.pone.0157386

Kerner, J. M., Krauss, J., Maihoff, F., Bofinger, L., & Classen, A. (2023). Alpine butterflies want to fly high: Species and communities shift upwards faster than their host plants. *Ecology*, *104*(1), e3848. https://doi.org/10.1002/ecy.3848

King, K. J., Lewis, D. M., Waters, J. M., & Wallis, G. P. (2020). Persisting in a glaciated landscape: Pleistocene microrefugia evidenced by the tree wētā Hemideina maori in central South Island, New Zealand. *Journal of Biogeography*, *47*(11), 2518–2531. https://doi.org/10.1111/jbi.13953

Klein, G., Vitasse, Y., Rixen, C., Marty, C., & Rebetez, M. (2016). Shorter snow cover duration since 1970 in the Swiss Alps due to earlier snowmelt more than to later snow onset. *Climatic Change*, *139*, 637–649. https://doi.org/10.1007/s10584-016-1806-y

Koch, P. L., & Barnosky, A. D. (2006). Late Quaternary extinctions: State of the debate. *Annual Review of Ecology, Evolution, and Systematics*, *37*, 215–250. https://doi.org/10.1146/annurev.ecolsys.34.011802.132415

Koot, E. M., Morgan-Richards, M., & Trewick, S. A. (2020). An alpine grasshopper radiation older than the mountains, on Kā Tiritiri o te Moana (southern Alps) of Aotearoa (New Zealand). *Molecular Phylogenetics and Evolution*, *147*, 106783. https://doi.org/10.1016/j.ympev.2020.106783

Koot, E. M., Morgan-Richards, M., & Trewick, S. A. (2022). Climate change and alpine adapted insects: Modelling environmental envelopes of a grasshopper radiation. Royal *Society Open Science*, *9*, 211596. https://doi.org/10.1098/rsos.211596

Körner, C. (1998). A re-assessment of high elevation treeline positions and their explanation. *Oecologia*, *115*(4), 445–459. https://doi.org/10.1007/s004420050540

Körner, C. (2021). *Alpine plant life: Functional plant ecology of high mountain ecosystems*. Springer International Publishing. https://doi.org/10.1007/978-3-030-59538-8

Körner, C., & Paulsen, J. (2004). A world-wide study of high altitude treeline temperatures. *Journal of Biogeography*, *31*(5), 713–732. https://doi.org/10.1111/j.1365-2699.2003.01043.x

Körner, C., Paulsen, J., & Spehn, E. M. (2011). A definition of mountains and their bioclimatic belts for global comparisons of biodiversity data. *Alpine Botany*, 121, 73–78. https://doi.org/10.1007/s00035-011-0094-4

Lambeck, K., Rouby, H., Purcell, A., Sun, Y., & Sambridge, M. (2014). Sea level and global ice volumes from the Last Glacial Maximum to the Holocene. Proceedings of the National Academy of Sciences, 111(43), 15296–15303. https://doi.org/10.1073/pnas.1411762111

Lessa, E. P., Cook, J. A., & Patton, J. L. (2003). Genetic footprints of demographic expansion in North America, but not Amazonia, during the Late Quaternary.

Proceedings of the National Academy of Sciences, *100*(18), 10331–10334. https://doi.org/10.1073/pnas.1730921100

Leuschner, C. (1996). Timberline and alpine vegetation on the tropical and warm-temperate oceanic islands of the world: Elevation, structure and floristics. *Vegetatio, 123*, 193–206 (1996). https://doi.org/10.1007/BF00118271

Loarie, S. R., Duffy, P. B., Hamilton, H., Asner, G. P., Field, C. B., & Ackerly, D. D. (2009). The velocity of climate change. *Nature*, *462*, 1052–1055. https://doi.org/10.1038/nature08649

MacDonald, G. M., Velichko, A. A., Kremenetski, C. V., Borisova, O. K., Goleva, A. A., Andreev, A. A., ... & Gattaulin, V. N. (2000). Holocene treeline history and climate change across northern Eurasia. *Quaternary Research*, *53*(3), 302–311. https://doi.org/10.1006/qres.1999.2123

Mark, A. F. (2012). *Above the treeline; A nature guide to alpine New Zealand*. Craig Potton Publishing.

Martin, R. A., da Silva, C. R., Moore, M. P., & Diamond, S. E. (2023). When will a changing climate outpace adaptive evolution? *Wiley Interdisciplinary Reviews Climate Change*, *14*(6), e852. https://doi.org/10.1002/wcc.852

Martins, I. S., Schrodt, F., Blowes, S. A., Bates, A. E., Bjorkman, A. D., Brambilla, V., ... & Dornelas, M. (2023). Widespread shifts in body size within populations and assemblages. *Science, 381*, 1067–1071. https://doi.org/10.1126/science.adg6006

Mason, T., Apollonio, M., Chirichella, R., Willis, S., & Stephens, P. (2014). Environmental change and long-term body mass declines in an alpine mammal. *Frontiers in Zoology*, *11*(69), 69. https://doi.org/10.1186/s12983-014-0069-6

Mathias, S., van Galen, L. G., Jarvie, S., & Larcombe, M. J. (2023). Range reshuffling: Climate change, invasive species, and the case of *Nothofagus* forests in Aotearoa New Zealand. *Diversity and Distributions, 29*, 1402–1419. https://doi.org/10.1111/ddi.13767

Mayr, E., & Diamond, J. M. (1976). Birds on islands in the sky: Origin of the montane avifauna of northern Melanesia. *Proceedings of the National Academy of Sciences*, *73*(5), 1765–1769. https://doi.org/10.1073/pnas.73.5.1765

McCain, C. M., King, S. R., & Szewczyk, T. M. (2021). Unusually large upward shifts in cold-adapted, montane mammals as temperature warms. *Ecology*, *102*(4), e03300. https://doi.org/10.1002/ecy.3300

McCulloch, G. A., Foster, B. J., Ingram, T., & Waters, J. M. (2019). Insect wing loss is tightly linked to the treeline: Evidence from a diverse stonefly assemblage. *Ecography*, *42*(4), 811–813. https://doi.org/10.1111/ecog.04140

McGaughran, A., Laver, R., & Fraser, C. (2021). Evolutionary responses to warming. *Trends in Ecology & Evolution*, *36*(7), 591–600. https://doi.org/10.1016/j.tree.2021.02.014

McGlone, M. S., Duncan, R. P., & Heenan, P. B. (2001). Endemism, species selection and the origin and distribution of the vascular plant flora of New Zealand. *Journal of Biogeography*, *28*(2), 199–216. https://doi.org/10.1046/j.1365-2699.2001.00525.x

Merilä, J., & Hendry, A. P. (2014). Climate change, adaptation, and phenotypic plasticity: The problem and the evidence. *Evolutionary Applications*, *7*(1), 1–14. https://doi.org/10.1111/eva.12137

Milá, B., McCormack, J. E., Castaneda, G., Wayne, R. K., & Smith, T. B. (2007). Recent postglacial range expansion drives the rapid diversification of a songbird lineage in the genus Junco. *Proceedings of the Royal Society B: Biological Sciences*, *274*(1626), 2653–2660. https://doi.org/10.1098/rspb.2007.0852

Moritz, C., Patton, J. L., Conroy, C. J., Parra, J. L., White, G. C., & Beissinger, S. R. (2008). Impact of a century of climate change on small-mammal communities in Yosemite National Park, USA. *Science*, *322*(5899), 261–264. https://doi.org/10.1126/science.1163428

Mountain Research Initiative EDW Working Group. (2015). Elevation-dependent warming in mountain regions of the world. *Nature Climate Change*, *5*, 424–430. https://doi.org/10.1038/nclim ate2563

Muellner-Riehl, A. N. (2019). Mountains as evolutionary arenas: Patterns, emerging approaches, paradigm shifts, and their implications for plant phylogeographic research in the Tibeto-Himalayan region. *Frontiers in Plant Science*, *10*, 195. https://doi.org/10.3389/fpls.2019.00195

Nakano, M., Morgan-Richards, M., Clavijo-McCormick, A., & Trewick, S. A. (2023). Abundance and distribution of antennal sensilla on males and females of three sympatric species of alpine grasshopper (Orthoptera: Acrididae: Catantopinae) in Aotearoa New Zealand. *Zoomorphology*, *142*, 51–62. https://doi.org/10.1007/s00435-022-00579-z

Nussey, D. H., Postma, E., Gienapp, P., & Visser, M. E. (2005). Selection on heritable phenotypic plasticity in a wild bird population. *Science*, *310*, 304–306. https://doi.org/10.1126/science.1117004

Parmesan, C. (2006). Ecological and evolutionary responses to recent climate change. *Annual Review of Ecology, Evolution, and Systematics*, *37*, 637–669. https://doi.org/10.1146/annurev.ecolsys.37.091305.110100

Pauli, H., & Halloy, S. (2019). *High mountain ecosystems under climate change*. Oxford University Press. https://doi.org/10.1093/acrefore/97801 90228 620.013.764

Pauls, S. U., Nowak, C., Bálint, M., & Pfenninger, M. (2013). The impact of global climate change on genetic diversity within populations and species. *Molecular Ecology*, *22*(4), 925–946. https://doi.org/10.1111/mec.12152

Pecchi, M., Marchi, M., Moriondo, M., Forzieri, G., Ammoniaci, M., Bernetti, I., ... & Chirici, G. (2020). Potential impact of climate change on the forest coverage and the spatial distribution of 19 key forest tree species in Italy under RCP4. 5 IPCC trajectory for 2050s. *Forests*, *11*(9), 934. https://doi.org/10.3390/f11090934

Pernollet, C. A., Korner-Nievergelt, F., & Jenni, L. (2015). Regional changes in the elevational distribution of the Alpine Rock Ptarmigan *Lagopus muta helvetica* in Switzerland. *Ibis*, *157*(4), 823–836. https://doi.org/10.1111/ibi.12298

Pettorelli, N., Pelletier, F., von Hardenberg, A., Festa-Bianchet, M., & Côté, S. (2007). Early onset of vegetation growth vs. rapid green-up: Impacts on juvenile mountain ungulates. *Ecology*, 88, 381–390. https://doi.org/10.1890/06-0875

Post, E. (2013). *Ecology of climate change: The importance of biotic interactions*. Princeton University Press. https://doi.org/10.1515/9781400846139

Qian, H., Ricklefs, R. E., & Thuiller, W. (2021). Evolutionary assembly of flowering plants into sky islands. *Nature Ecology & Evolution*, *5*(5), 640–646. https://doi.org/10.1038/s41559-021-01423-1

Reiner, R., Zedrosser, A., Zeiler, H., Hackländer, K., & Corlatti, L. (2021). Forests buffer the climate-induced decline of body mass in a mountain herbivore. *Global Change Biology*, *27*(16), 3741–3752. https://doi.org/10.1111/gcb.15711

Rita, A., Saracino, A., Cieraad, E., Saulino, L., Zotti, M., Idbella, M., ... & Bonanomi, G. (2023). Topoclimate effect on treeline elevation depends on the regional framework: A contrast between Southern Alps (New Zealand) and Apennines (Italy) forests. *Ecology and Evolution*, *13*(1), e9733. https://doi.org/10.1002/ece3.9733

Rogan, J. E., Parker, M. R., Hancock, Z. B., Earl, A. D., Buchholtz, E. K., Chyn, K., ... & Fitzgerald, L. A. (2023). Genetic and demographic consequences of range contraction patterns during biological annihilation. *Scientific Reports*, *13*(1), 1691. https://doi.org/10.1038/s41598-023-28927-z

Román-Palacios, C., & Wiens, J. J. (2020). Recent responses to climate change reveal the drivers of species extinction and survival. *Proceedings of the National Academy of Sciences*, *117*(8), 4211–4217. https://doi.org/10.1073/pnas.1913007117

Ruddiman, W. F., & Raymo, M. E. (1988). Northern Hemisphere climate regimes during the past 3 Ma: Possible tectonic connections. *Philosophical Transactions of the Royal Society of London B: Biological Sciences*, *318*(1191), 411–430. https://doi.org/10.1098/rstb.1988.0017

Rubidge, E. M., Patton, J. L., Lim, M., Burton, A. C., Brashares, J. S., & Moritz, C. (2012). Climate-induced range contraction drives genetic erosion in an alpine mammal. *Nature Climate Change*, *2*, 285–288. https://doi.org/10.1038/nclimate1415

Ryding, S., Klaassen, M., Tattersall, G. J., Gardner, J. L., & Symonds, M. R. (2021). Shape-shifting: Changing animal morphologies as a response to climatic warming. *Trends in Ecology & Evolution*, *36*(11), 1036–1048. https://doi.org/10.1016/j.tree.2021.07.006

Schai-Braun, S. C., Jenny, H., Ruf, T., & Hackländer, K. (2021). Temperature increase and frost decrease driving upslope elevational range shifts in Alpine grouse and hares. *Global Change Biology*, *27*(24), 6602–6614. https://doi.org/10.1111/gcb.15909

Seaborn, T., Griffith, D., Kliskey, A., & Caudill, C. C. (2021). Building a bridge between adaptive capacity and adaptive potential to understand responses to environmental change. *Global Change Biology*, *27*(12), 2656–2668. https://doi.org/10.1111/gcb.15579

Sedlacek, J., Cortés, A. J., Wheeler, J., Bossdorf, O., Hoch, G., Klápště, J., ... & Van Kleunen, M. (2016). Evolutionary potential in the Alpine: Trait heritabilities and performance variation of the dwarf willow *Salix herbacea* from different elevations and microhabitats. *Ecology and Evolution*, *6*(12), 3940–3952. https://doi.org/10.1002/ece3.2171

Seebacher, F., White, C. R., & Franklin, C. E. (2015). Physiological plasticity increases resilience of ectothermic animals to climate change. *Nature Climate Change*, *5*(1), 61–66. https://doi.org/10.1038/nclimate2457

Shelomi, M. (2012). Where are we now? Bergmann's rule sensu lato in insects. *The American Naturalist*, *180*(4), 511–519. https://doi.org/10.1086/667595

Singer, M. C. (2017). Shifts in time and space interact as climate warms. *Proceedings of the National Academy of Sciences of the United States of America*, *114*(49), 12848–12850. https://doi.org/10.1073/pnas.1718334114

Stanley, S. M. (1988). Paleozoic mass extinctions; shared patterns suggest global cooling as a common cause. *American Journal of Science*, *288*(4), 334–352. https://doi.org/10.2475/ajs.288.4.334

Steffen, W., Rockström, J., Richardson, K., Lenton, T. M., Folke, C., Liverman, D., ... & Schellnhuber, H. J. (2018). Trajectories of the Earth System in the Anthropocene. *Proceedings of the National Academy of Sciences*, *115*(33), 8252–8259. https://doi.org/10.1073/pnas.181014111

Taberlet, P., Fumagalli, L., Wust-Saucy, A. G., & Cosson, J. F. (1998). Comparative phylogeography and postglacial colonization routes in Europe. *Molecular Ecology*, *7*(4), 453–464. https://doi.org/10.1046/j.1365-294x.1998.00289.x

Tafani, M., Cohas, A., Bonenfant, C., Gaillard, J. M., & Allainé, D. (2013). Decreasing litter size of marmots over time: A life history response to climate change? *Ecology*, *94*(3), 580–586. https://doi.org/10.1890/12-0833.1

Teplitsky, C., Mills, J. A., Alho, J. S., Yarrall, J. W., & Merilä, J. (2008). Bergmann's rule and climate change revisited: Disentangling environmental and genetic responses in a wild bird population. *Proceedings of the National Academy of Sciences, 105*(36), 13492–13496. https://doi.org/10.1073/pnas.0800999105

Thomas, C. D., Bodsworth, E. J., Wilson, R. J., Simmons, A. D., Davies, Z. G., Musche, M., & Conradt, L. (2001). Ecological and evolutionary processes at expanding range margins. *Nature, 411*, 577–581. https://doi.org/10.1038/35079066

Thomas, C. D., Cameron, A., Green, R. E., Bakkenes, M., Beaumont, L. J., Collingham, Y. C., ... & Williams, S. E. (2004). Extinction risk from climate change. *Nature, 427*, 145–148. https://doi.org/10.1038/nature02121

Thuiller, W., Lavorel, S., & Araújo, M. B. (2005). Niche properties and geographical extent as predictors of species sensitivity to climate change. *Global Ecology and Biogeography, 14*(4), 347–357. https://doi.org/10.1111/j.1466-822X.2005.00162.x

Tian, L., & Benton, M. J. (2020). Predicting biotic responses to future climate warming with classic ecogeographic rules. *Current Biology, 30*(13), R744–R749. https://doi.org/10.1016/j.cub.2020.06.003

Tingley, M. W., Koo, M. S., Moritz, C., Rush, A. C., & Beissinger, S. R. (2012). The push and pull of climate change causes heterogeneous shifts in avian elevational ranges. *Global Change Biology, 18*(11), 3279–3290. https://doi.org/10.1111/j.1365-2486.2012.02784.x

Trewick, S. A. (2001b). Identity of an endangered grasshopper (Acrididae: *Brachaspis*): Taxonomy, molecules and conservation. *Conservation Genetics, 2*, 233–243. https://doi.org/10.1023/A:10122 63717279

Trewick, S. A. (2008). DNA barcoding is not enough: Mismatch of taxonomy and genealogy in New Zealand grasshoppers (orthoptera: Acrididae). *Cladistics, 24*(2), 240–254. https://doi.org/10.1111/j.1096-0031.2007.00174.x

Trewick, S. A., & Bland, K. (2012). Fire and slice: Palaeogeography for biogeography at New Zealand's North Island/South Island juncture. *Journal of the Royal Society of New Zealand, 42*(3), 153–183. https://doi.org/10.1080/03036758.2010.549493

Trewick, S. A., Koot, E. M., & Morgan-Richards, M. (2023). Māwhitiwhiti Aotearoa: Phylogeny and synonymy of the silent alpine grasshopper radiation of New Zealand

(Orthoptera: Acrididae). *Zootaxa*, 5383(2), 225–241. https://doi.org/10.11646/zootaxa.5383.2.7

Trewick, S. A. & Morris, S. (2008). *Diversity and Taxonomic Status of Some New Zealand Grasshoppers.* Science & Technical Publishing Department of Conservation. https://www.doc.govt.nz/globalassets/documents/science-and-technical/drds290.pdf

Trewick, S. A., Wallis, G. P., & Morgan-Richards, M. (2000). Phylogeographical pattern correlates with Pliocene mountain building in the alpine scree weta (orthoptera, Anostostomatidae). *Molecular Ecology*, *9*(6), 657–666. https://doi.org/10.1046/j.1365-294x.2000.00905.x

Trewick, S. A., Wallis, G. P., & Morgan-Richards, M. (2011). The invertebrate life of New Zealand: A phylogeographic approach. *Insects*, *2*(3), 297–325. https://doi.org/10.3390/insects203 0297

Tziperman, E., & Gildor, H. (2003). On the mid-Pleistocene transition to 100-kyr glacial cycles and the asymmetry between glaciation and deglaciation times. *Paleoceanography*, *18*(1), 1001. https://doi.org/10.1029/2001pa000627

Vinton, A. C., Gascoigne, S. J., Sepil, I., & Salguero-Gómez, R. (2022). Plasticity's role in adaptive evolution depends on environmental change components. *Trends in Ecology & Evolution*, *37*(12), 1067–1078. https://doi.org/10.1016/j.tree.2022.08.008

Walther, G. R., Post, E., Convey, P., Menzel, A., Parmesan, C., Beebee, T. J., Fromentin, J. M., Hoegh-Guldberg, O., & Bairlein, F. (2002). Ecological responses to recent climate change. *Nature*, *416*, 389. https://doi.org/10.1038/416389a

Warren, R., Price, J., Graham, E., Forstenhaeusler, N., & VanDerWal, J. (2018). The projected effect on insects, vertebrates, and plants of limiting global warming to 1.5°C rather than 2°C. *Science*, *360*(6390), 791–795. https://doi.org/10.1126/science.aar364

Warren, R., VanDerWal, J., Price, J., Welbergen, J. A., Atkinson, I., Ramirez-Villegas, J., ... & Lowe, J. (2013). Quantifying the benefit of early climate change mitigation in avoiding biodiversity loss. *Nature Climate Change*, *3*(7), 678–682. https://doi.org/10.1038/nclimate1887

Whitman, D. W. (2008). The significance of body size in the Orthoptera: A review. *Journal of Orthoptera research*, *17*(2), 117–134. https://doi.org/10.1665/1082-6467-17.2.117

Wilson, R. J., Gutiérrez, D., Gutiérrez, J., Martínez, D., Agudo, R., & Monserrat, V. J. (2005). Changes to the elevational limits and extent of species ranges associated with climate change. *Ecology Letters*, *8*(11), 1138–1146. https://doi.org/10.1111/j.1461-0248.2005.00824.x

Wu, C. H., Holloway, J. D., Hill, J. K., Thomas, C. D., Chen, I. C., & Ho, C. K. (2019). Reduced body sizes in climate-impacted Borneo moth assemblages are primarily explained by range shifts. *Nature Communications*, *10*, 4612. https://doi.org/10.1038/s41467-019-12655-y

Zachos, J., Pagani, M., Sloan, L., Thomas, E., & Billups, K. (2001). Trends, rhythms, and aberrations in global climate 65 Ma to present. *Science, 292*(5517), 686–693. https://doi.org/10.1126/science.105941

“And as the snow melted from the bases of the mountains, the arctic forms would seize on the cleared and thawed ground, always ascending higher and higher, as the warmth increased, whilst their brethren were pursuing their northern journey.”

(Darwin, 1859, p. 367)

Sigaus australis, a grassland/herbfield-dwelling grasshopper within the New Zealand alpine radiation. Camp Stream, Craigieburn Forest Park, South Island.

Chapter Two

Global warming leads to habitat loss and genetic erosion of alpine biodiversity

MASSEY UNIVERSITY
TE KUNENGA KI PŪREHUROA
UNIVERSITY OF NEW ZEALAND

GRADUATE RESEARCH SCHOOL

STATEMENT OF CONTRIBUTION
DOCTORATE WITH PUBLICATIONS/MANUSCRIPTS

We, the student and the student's main supervisor, certify that all co-authors have consented to their work being included in the thesis and they have accepted the student's contribution as indicated below in the Statement of Originality.

Student name:	Fabio Leonardo Meza Joya
Name and title of main supervisor:	Steven A. Trewick
In which chapter is the manuscript/published work?	Chapter 2

Describe the contribution that the student and members of the supervisory team have made to the manuscript/published work:[1]

Conceptualization and data collection: Fabio Leonardo Meza-Joya, Steven A. Trewick and Mary Morgan-Richards; Data curation and analysis: Fabio Leonardo Meza-Joya; Visualization: Fabio Leonardo Meza-Joya and Steven A. Trewick; Writing – original draft: Fabio Leonardo Meza-Joya; Writing – review and editing: Steven A. Trewick and Mary Morgan-Richards; Funding acquisition and supervision: Steven A. Trewick and Mary Morgan-Richards.

Please select one of the following three options:

- (●) The manuscript/published work is published or in press

  Please provide the full reference of the research output:

  Meza-Joya. F. L., Morgan-Richards, M., Koot, E. M., & Trewick, S. A. (2023). Global warming leads to habitat loss and genetic erosion of alpine biodiversity. Journal of Biogeography, 50, 961–975. https://doi.org/10.1111/jbi.14590

- ( ) The manuscript is currently under review for publication

  Please provide the name of the journal:

- ( ) It is intended that the manuscript will be published, but it has not yet been submitted to a journal

Student's signature:	Fabio Leonardo Meza Joya — Digitally signed by Fabio Leonardo Meza Joya Date: 2024.01.02 14:46:21 +13'00'	Main supervisor's signature:	Digitally signed by Steve Trewick Date: 2024.01.09 10:36:32 +13'00'

This form should be placed at the beginning of each relevant thesis chapter.

[1] Refer to the Massey University Publishing and Authorship guidelines (OneMassey for staff, Stream for students) and/ or Contributor Roles Taxonomy (CRediT) guidelines for guidance.

Abstract

Aim: Species living on steep environmental gradients are expected to be especially sensitive to global climate change, but little is known about the factors influencing their responses to contemporary warming. Here, we investigate the influence of climate on the biogeography of three alpine species with overlapping ranges.

Location: Te Waipounamu (South Island) Aotearoa–New Zealand.

Taxon: Endemic alpine adapted Catantopinae grasshoppers.

Methods: We used niche modelling to estimate and project the potential niche of three focal species under past and future climate scenarios. Vulnerability assessments were performed using niche factor analyses. Demographic trends and phylogeographic structure were investigated using samples from 15 mountain tops to generate mitochondrial DNA haplotype networks and population genetic statistics.

Results: Niche models and genetic data suggest suitable habitat for all three alpine species was more widespread and contiguous in the past than today. Demographic analyses indicate in situ survival rather than post-Pleistocene colonisation of current habitat. Population structuring and genetic divergence suggest that mountain uplift during the Pliocene and environmental barriers during Pleistocene glacial and interglacial stages shaped contemporary population structure of each species. Although geographically overlapping, niche analyses suggest these alpine species are not ecologically identical, each showing distinct responses to environmental change, but all will lose intraspecific diversity through population extinction.

Main Conclusions: Climatic, biological and geophysical factors controlled population structuring of three cold-adapted species during the Pleistocene with a legacy of spatially separate intraspecific lineages. Ecological niche models for each species emphasise distinct combinations of environmental proxies, but all are expected to experience severe habitat reduction during climate warming. Increased global temperatures drive available habitat to higher elevation resulting in population contractions, range shifts, habitat fragmentation, local extinctions and genetic impoverishment. Despite alpine species not being ecologically identical, we predict all mountain biota will lose significant genetic diversity due to global warming.

Keywords: alpine species, Aotearoa New Zealand, biogeographic barriers, climate change, environmental envelope, habitat availability

Introduction

Across the biogeographic spectrum, species range shifting (usually poleward and upward) has been proposed as a general ecological response to contemporary planetary heating (Bellard et al., 2012; Chen et al., 2011; Freeman et al., 2018; Lenoir & Svenning, 2015; Walther et al., 2002). In keeping with inferences of variable prehistoric range shifts gleaned from phylogeographic (e.g. Taberlet et al., 1998) and fossil data (e.g. Lyons, 2003), contemporary range changes show considerable disparity in response pattern and rate (Chen et al., 2011; Lenoir et al., 2010; Moritz & Agudo, 2013). Critically, studies of past range shifts usually deal with much larger time-scales than we now know are relevant to extant populations (IPCC, 2022). Variation among species range shifts likely reflects the extent to which a species is exposed to climate change across its range, its phenotypic and genetic diversity and the capacity of local populations to disperse into newly available habitat (Bellard et al., 2012; Moritz & Agudo, 2013; Rinnan & Lawler, 2019).

The elevational gradient on mountains results in a decrease in mean air temperature with increasing elevation due to reduced atmospheric pressure. This means that vulnerability to global climate change is expressed over a narrow spatial scale, and recent analyses indicate a nonlinear relationship with enhanced rates of warming at high elevation (MRI, 2015). In addition, the extent of alpine habitat tends to be attenuated with elevation due to the shape of mountains (Pauli & Halloy, 2019). Therefore, the upward shift of alpine populations also isolates them in progressively smaller and more scattered high-elevation habitat patches (Chinn & Chinn, 2020; Galbreath et al., 2009; Gifford & Kozak, 2012), leading to population fragmentation, local extinction of intraspecific lineages and loss of intraspecific diversity (e.g. Pavlova et al., 2017; Rehnus et al., 2018; Rizvanovic et al., 2019).

Past climate change, and in particular Plio–Pleistocene climate cycling is inferred to have imposed changes in habitat availability for populations, hallmarked by latitudinal range shifts of warm climate species documented in Europe and North America (Davis & Shaw, 2001). Cold adapted species experienced analogous changes in fortune culminating in retreat of habitat at the start of the present interglacial as warming forced optimal climatic envelopes to higher elevation and latitude (e.g. Carmelet-Rescan et al., 2021; Endo et al., 2015; Galbreath et al., 2009; Trewick et al., 2000), a trend that

continues today at an increased rate (Bellard et al., 2012; Chen et al., 2011; Freeman et al., 2018; Walther et al., 2002). In contrast, during glacial phases, cold-adapted organisms could have experienced population and range expansion and connectivity via valley corridors (Carmelet-Rescan et al., 2021; Endo et al., 2015; Hewitt, 2004; Trewick et al., 2000), although valleys can also act as barriers (Trewick et al., 2000).

The dynamics of alpine glaciers reflect regional and temporal differences in precipitation, temperature and orography and models of palaeoglacier dynamics reflect this (Groos et al., 2021; James et al., 2019). During the last glacial maximum (LGM) on Kā Tiritiri o te Moana (Southern Alps) of Aotearoa (New Zealand), montane glaciers with as much as 6800 km3 of ice covered up to 30% of Te Waipounamu (South Island; James et al., 2019), but do not appear to have formed extensive ice fields overtopping mountain peaks. Instead, glaciers were predominantly valley-constrained (James et al., 2019; Figure 1). If there was sufficient snow melt on peaks during the glacial summer, it is plausible that an alpine-adapted biota persisted through glacial stages on nunataks of the Southern Alps. Although originally proposed for Scandinavia (Dahl, 1987), the nunatak hypothesis is relevant to New Zealand biogeography as it was not directly influenced by polar ice and associated periglacial climate (Gowan et al., 2021). Today vegetation grows directly beside active montane glaciers and in some cases even on the edge of the ice itself (Fickert et al., 2022), and this appears to have been the case during glacials (e.g. Marra & Thackray, 2010; Moar, 1980; Vandergoes et al., 2008).

The configuration of Pleistocene glaciers in the Southern Alps (Figure 1) allowed the persistence of plant and animal populations on mountain tops, supporting high, spatially structured intraspecific genetic diversity in alpine habitats (e.g. Carmelet-Rescan et al., 2021; Trewick et al., 2000; Trewick & Wallis, 2001). As the degree of population isolation in the past underpins the distribution of variation today, the biodiversity consequences of future climate change are implicated. Here, we investigated whether environmental processes driving distributional changes among endemic sympatric flightless alpine grasshoppers (Orthoptera: Acrididae) resulted in similar phylogeographic outcomes in separate species. This monophyletic group radiated before Pleistocene climate cycling began (Koot et al., 2020), so their current distributions could reveal responses to glacial and interglacial conditions (e.g. Carmelet-Rescan et al., 2021). We couple phylogeography, ecological niche modelling and climatic niche comparisons

to investigate how climate change across the latitudinal and elevational gradients of the Southern Alps influences three endemic, alpine grasshopper species with overlapping ranges that span 670 linear km.

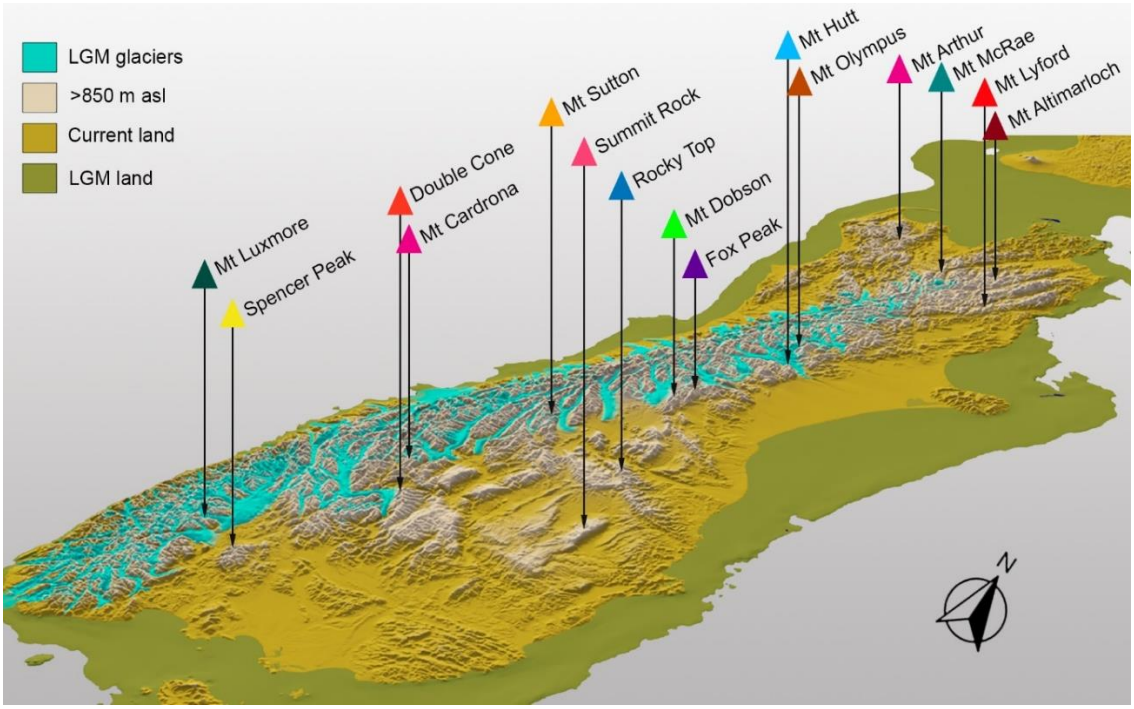

Figure 1. Oblique three-dimensional projection of South Island, New Zealand depicting inferred land extent, topography and glaciation during the last glacial maximum of the Pleistocene (after James et al., 2019). Sampling locations on 15 mountains, for grasshopper specimens used for genetic analyses (*Brachaspis nivalis*, *Paprides nitidus* and *Sigaus australis*), are indicated. Map projection: NZGD2000, with vertical scale emphasised for clarity.

Ecological niche modelling and niche factor analyses provide information about vulnerability of potential habitat based on climate proxies, and genetic data allow inference of past population connectivity that likely reflects local environmental traits. We sampled grasshoppers at 15 mountain tops spanning the latitudinal gradient (~4.5°) of the Southern Alps and proximity to LGM glaciers (Figure 1). We expect that glacial stages generally allowed range expansion compared to interglacials, but propose that the pattern of glaciation would tend to isolate populations in the west more than those to the east given the thickness and extent of glaciers in the Southern Alps during LGM (Figure 1). The latitudinal gradient of the Southern Alps is expected to result in cooler conditions to the south compared to the north, and this correlates with the elevation of the forest–

alpine transition that tends to be higher in the north and lower in the south of New Zealand (Wardle, 2008). If, as we expect, LGM conditions influenced the spatial distribution of intraspecific diversity, then anthropogenic warming over the next 50 years could result in uneven genetic erosion even among sympatric and closely related species.

Materials and Methods

Taxon sampling

We surveyed populations of *Brachaspis nivalis* (Hutton), *Paprides nitidus* Hutton and *Sigaus australis* (Hutton) on 15 mountain tops in Southern Alps, spanning the documented range of each species (Figure 1). Grasshoppers were collected during summer when they are active (December to March 2015–2020) and frozen before being preserved in 95% ethanol. Species were identified using morphological traits (e.g. pronotum margin, subgenital plate, and epiproct) following Bigelow (1967).

Ecological niche modelling

To estimate and project the potential niche of each focal species, we acquired location records with geodetic datum WGS84 for 14 endemic New Zealand grasshopper species, spanning 1967–2016 (Koot et al., 2022). Additional records were retrieved from recent collections by the Phoenix group (http://evolv es.massey.ac.nz), including target-group absences (Mateo et al., 2010). Duplicates were removed ensuring one data point per pixel (~1 km^2 habitat). A fundamental assumption of niche models is that species' current ranges are in equilibrium: matching the full extent of environmental conditions so they can persist indefinitely (Sax et al., 2013; Soberón & Peterson, 2005). This assumption might be void if occupancy is subject to anthropogenic land-use change (e.g. Carmelet-Rescan et al., 2021; Koot et al., 2022; Trewick, 2008). Mismatches between niche and range arise when individuals of a species can survive but not persist through time in places where environmental conditions exceed those realised in their native ranges (Sax et al., 2013). To minimise the influence of non-climatic, anthropogenic activity (Faurby & Araújo, 2018), we filtered presence records from areas unavailable to grasshoppers before humans reached Aotearoa about 800 years ago (Wilmshurst et al., 2008). Here, tall forest (Leathwick et al., 2004) was incompatible with native temperate grasshoppers

(Sivyer et al., 2018; Figure S1.1). The resulting database consisted of 1138 site records, including 80 presences for *B. nivalis*, 65 for *P. nitidus* and 187 for *S. australis* representing the native realised niche of these species (Figure S1.2; Table S1.1).

For potential niche proxies, we accessed 19 bioclimatic variables (averaged from 1960 to 1990) from WorldClim v1.4 (http://www.world clim.org; Hijmans et al., 2005) for three periods (MIROC-ESM global climate model): current (averaged from 1960 to 1990), past (LGM ~22 kyr) and future (averaged from 2061 to 2080). Two future global warming scenarios were projected: a greenhouse gas stabilisation pathway (RCP4.5) and a high concentration pathway (RCP8.5), with mean temperature increases in New Zealand of at least 1.4°C (RCP4.5) and 3.0°C (RCP8.5) by 2090 (New Zealand Ministry for the Environment, 2018). We included four additional variables describing geodiversity (soil type) and topography (slope, aspect and roughness), which are important for plant growth and treeline position in New Zealand (Case & Buckley, 2015; Wardle, 1965), and might be constraints on grasshopper habitat availability (Carmelet-Rescan et al., 2021; Koot et al., 2022). All layers were at 30 arc-seconds resolution (~1 km2), except LGM layers which were at 2.5 arc minutes (~5 km2). Layer files were cropped to the extent of New Zealand (Latitudes: −49, −32; Longitudes: 165, 180), which represents the potential accessible area for these species during the relevant time period (Soberón & Peterson, 2005) since New Zealand's major islands were connected during Pleistocene glacial phases (Trewick & Bland, 2012). Selection of relevant variables used the R (R Core Team, 2019) package 'fuzzySim' v.3.0 (Barbosa, 2015) such that variables retained for modelling did not show multicollinearity (VIF < 3; Table S1.2). Data processing used QGIS v.3.16.1 (QGIS Development Team, 2020).

To estimate the environmental niche for each grasshopper, we used three methods to build ensemble models: Generalised Boosting, Random Forest and Maximum Entropy. The best set of tuneable hyperparameters was inferred using the R package 'SDMtune' v.1.1.4 (Vignali et al., 2020) with the most relevant predictors (Tables S1.3 and S1.4). We refitted final models in the R package 'Biomod2' v.3.4.6 (Thuiller et al., 2020), using the most relevant predictors and the best performing parameters through a spatial-blocking cross-validation approach (Figure S1.3) with the R package 'blockCV' v.2.1.1 (Valavi et al., 2019). Five runs were completed for each modelling method, resulting in 15 models per species. We assessed the performance of individual models with the True

Skill Statistic (TSS) and area under the curve values (AUC) of receiver operator characteristic (ROC) curves. Models with TSS and AUC values > 0.8 were retained for building the final ensemble forecast output using a weighted average approach. Spatial projections under current conditions (1960–1990) were generated using the final mean-weighted ensemble models (EMmw). Variable importance for the final EMmw was calculated by applying the weightings used for the ensemble forecasting to the variable importance scores for individual models, summing values by variable and then dividing by the number of modelling methods applied.

Extrapolation risk associated with modelling past and future projections was assessed through a multivariate environmental similarity surface (MESS) analysis (Elith et al., 2010) using the R package 'dismo' v1.3-3 (Hijmans et al., 2020). To designate areas as suitable or not suitable, binary projections for each period (past, current and future) were generated from the final EMmw models using the cut-off value that maximised the proportion of presences and absences correctly predicted by the model. Output values higher than the predetermined threshold were considered 'presences'; otherwise, 'absences'. Binary vectors were used to estimate range metrics for past, present and future projections. Past (LGM) vectors were disaggregated to correspond with a 30-arc sec resolution using the R package 'raster' v.3.4-5 (Hijmans, 2020). Range change analyses were implemented using the *RangeSize* function in the R package 'Biomod2' v.3.4.6 (Thuiller et al., 2020) and QGIS.

Niche factor analyses

We used ecological-niche factor analyses (ENFA; Hirzel et al., 2002) to quantify two different aspects of each species' niche: (1) marginality, a measure of the position of a species' niche in the available environmental space (i.e. the global area), and (2) specialisation, a metric of the size of a species' niche relative to the global area (Hirzel et al., 2002; Rinnan & Lawler, 2019). The higher the marginality, the greater the ecological distance of habitat occupied by a species from the average habitat available; the higher the specialisation, the narrower a species niche (Hirzel et al., 2002). We also estimated three metrics reflecting different aspects of the species' potential responses to climate change: (1) sensitivity, a measure of a species persistence ability given the climatic conditions of its habitat; (2) exposure, a metric of the extent to which a species will experience climate change across its range; and (3) vulnerability, a measure of a

species susceptibility to climate change given its sensitivity and exposure. In general, the higher the sensitivity of a species, the narrower the climatic niche it inhabits; the higher its exposure, the greater the departure of its habitat from current to future climate; and the higher its vulnerability, the more susceptible to climate change (Rinnan & Lawler, 2019). We used the binary vector resulting from our niche modelling as a proxy for the current ranges of the grasshopper species. The global study area was defined as the combined range of the three species (Rinnan & Lawler, 2019), that is, the extent of the South Island. To determine the global climatic conditions, we used the subset of climate variables used for niche modelling, as they are not strongly correlated and are important in predicting suitable environments for these grasshoppers. Analyses in this section were conducted using the R package 'CENFA' v.1.1.0 (Rinnan, 2018).

DNA extraction, sequencing and alignment

Whole genomic DNA was extracted from leg muscle of 155 specimens (*B. nivalis* = 61, *P. nitidus* = 94) using a solvent-free Proteinase K and salting out method (Sunnucks & Hales, 1996) as described by Sivyer et al. (2018). DNA samples were subject to PCR amplification of the mitochondrial NADH-dehydrogenase 2 (ND2) gene under standard conditions, using the primers HopND2_147F and HopND2_1286R (Carmelet-Rescan et al., 2021). In these grasshoppers, ND2 has a higher capacity to accumulate haplotype diversity when compared with the commonly analysed COI locus (Carmelet-Rescan et al., 2021). Cycle sequencing reactions used BigDye Terminator v.3.1 (Life Technologies) with signal capture on an ABI-3500 Genetic Analyser (Life Technologies), and resulting sequences were edited and aligned in Geneious R10 (Kearse et al., 2012). Published DNA sequence data for *S. australis* (*n* = 132) were included (Carmelet-Rescan et al., 2021).

Population genetic structure

Genealogical relationships among ND2 haplotypes were inferred with haplotype median-joining (Bandelt et al., 1999) networks in PopART v.1.7 (Leigh & Bryant, 2015). Statistical support for distinct mitochondrial lineages was evaluated with a Bayesian phylogenetic analysis in MrBayes v.3.2.6 (Ronquist et al., 2012) with *Alpinacris crassicauda* Bigelow as the outgroup taxon (Koot et al., 2020). The best partition scheme for all three codon positions was HKY + Γ (LnL = −2379.62; BIC = 5664.86) as inferred

using PartitionFinder v.2.1.1 (Lanfear et al., 2017). Analyses used four chains on two runs for 10^6 generations, with sampling frequency of 10^3 generations and a burn-in of 0.10. Convergence of the posterior distribution parameters was examined by monitoring the effective sample size (ESS > 800) and trace plots in Tracer v1.6 (Rambaut et al., 2018). Pairwise genetic distances between populations were estimated using Mega X (Kumar et al., 2018) based on the Kimura 2-parameter (K2P; Kimura, 1980) and Tamura-Nei (TN; Tamura & Nei, 1993) models with a bootstrap procedure (1,000 replicates).

Matrilineal genetic variability was estimated in population samples ($n \geq 5$) using DnaSP v.5.10 (Librado & Rozas, 2009) to compute haplotype diversity (h), which represents the probability that two randomly sampled alleles are different (Nei & Tajima, 1981), and nucleotide diversity (π), which is defined as the average number of nucleotide differences per site between two sequences (Nei, 1987). Pairwise Φ_{ST} values (Excoffier et al., 1992) were computed in Arlequin v.3.5.2.2 (Excoffier & Lischer, 2010) to infer mtDNA differentiation among population samples, and a significance statistic permuted using 10,000 replicates. To identify whether the predicted loss of suitable habitat under climate change could result in changes of extant genetic diversity, we identified which of our sampled populations could be lost under warming scenarios and estimated haplotype diversity (h) and nucleotide diversity (π), excluding sequence data from those locations.

Historical demography was inferred based on the observed mismatch distribution under the constant population size model using DnaSP. A smooth, unimodal distribution is expected when populations have undergone recent demographic expansion, while multimodal and ragged distributions suggest a stable population (Rogers & Harpending, 1992). Harpending's raggedness index (Harpending, 1994) was used to evaluate the fit of the observed distribution to the constant population size model, and its statistical significance was assessed with 10,000 coalescence simulations. A significant index indicates a stable population typically showing 'ragged', multimodal mismatch (Harpending, 1994). Tajima's D (Tajima, 1989), Fu's F_S (Fu, 1997) and Ramos-Onsins' R_2 (Ramos-Onsins & Rozas, 2002) neutrality tests were performed in DnaSP to detect departures from the mutation–drift equilibrium indicative of population size changes. Statistical significance was assessed with 10,000 coalescence simulations. Significantly negative Fu's F_S and Tajima's D values and significantly positive R_2 values were taken as evidence of recent population expansion (Galbreath et al., 2009).

Results

Ecological niche modelling

Ensemble models showed high predictability, with average AUC scores of 0.966 for *B. nivalis*, 0.981 for *P. nitidus* and 0.978 for *S. australis*. True-positive rate (i.e. percentage of presences correctly predicted) and true-negative rate (i.e. percentage of absences correctly predicted) of predictions were also high, above 92.50% and 90.62%, respectively, for all species (Table S1.5). Evaluation scores for individual models indicated good to excellent performance (Figure S1.4). Temperature-related predictors had the largest influence on the environmental envelope estimated for all species. Annual mean temperature was in all cases the most important predictor variable (importance score > 70% in all cases), but the proximate importance of the other variables differed (Figure S1.5).

Current predictions support a wide distribution of *B. nivalis* (9,720 km^2) and *P. nitidus* (12,757 km^2) throughout the northern portion of the Southern Alps, while *S. australis* is predicted to have a wide distribution (16,651 km^2) across the southern half of South Island (Figure 2; Figure S1.6). Past projections indicate, for all three species, areas of suitable climate were less fragmented and more widespread during the LGM than today: 14,205 km^2 for *B. nivalis*, 20,441 km^2 for *P. nitidus* and 45,545 km^2 for *S. australis*. Areas of strict extrapolation for past conditions occur mainly in the southern portion of the Southern Alps, within the native distributional range of *S. australis* (Figure 2). Accounting for areas of strict extrapolation reduced inferred suitable area for this species during the LGM by 21% to 35,763 km^2. Suitable habitat for this species is predicted to have existed in North Island during past glacial periods, but *S. australis* is not found there (Koot et al., 2022). In general, our models showed a good performance in predicting the extent of deep valley glaciers during the LGM (Figure S1.6).

For all species, future projections indicate that the spatial distribution of suitable conditions will move poleward and upslope, in most cases accompanied by dramatic area reductions (Figure 2; Figure S1.7). Suitable habitat for *B. nivalis* and *P. nitidus* is expected to undergo a southward shift under future scenarios, with progressive contraction of their current northern ranges. Habitat loss with respect to current habitat, however, is projected to be more severe for *B. nivalis* (RCP4.5 = 62% loss and RCP8.5

= 0.75% loss) than for *P. nitidus*, where even a slight increase was predicted under the most optimistic climate change scenario (RCP4.5 = 5% gain and RCP8.5 = 20% loss). Suitable habitat for *S. australis* is expected to undergo marked reduction under future climate change, with increasing patchiness and eventual loss of most native environmental space (RCP4.5 = 80% loss and RCP8.5 = 90% loss). Areas of strict extrapolation for future conditions occur mostly across the lowlands of northern South Island, which are outside the projected suitable areas for the species (Figure 2).

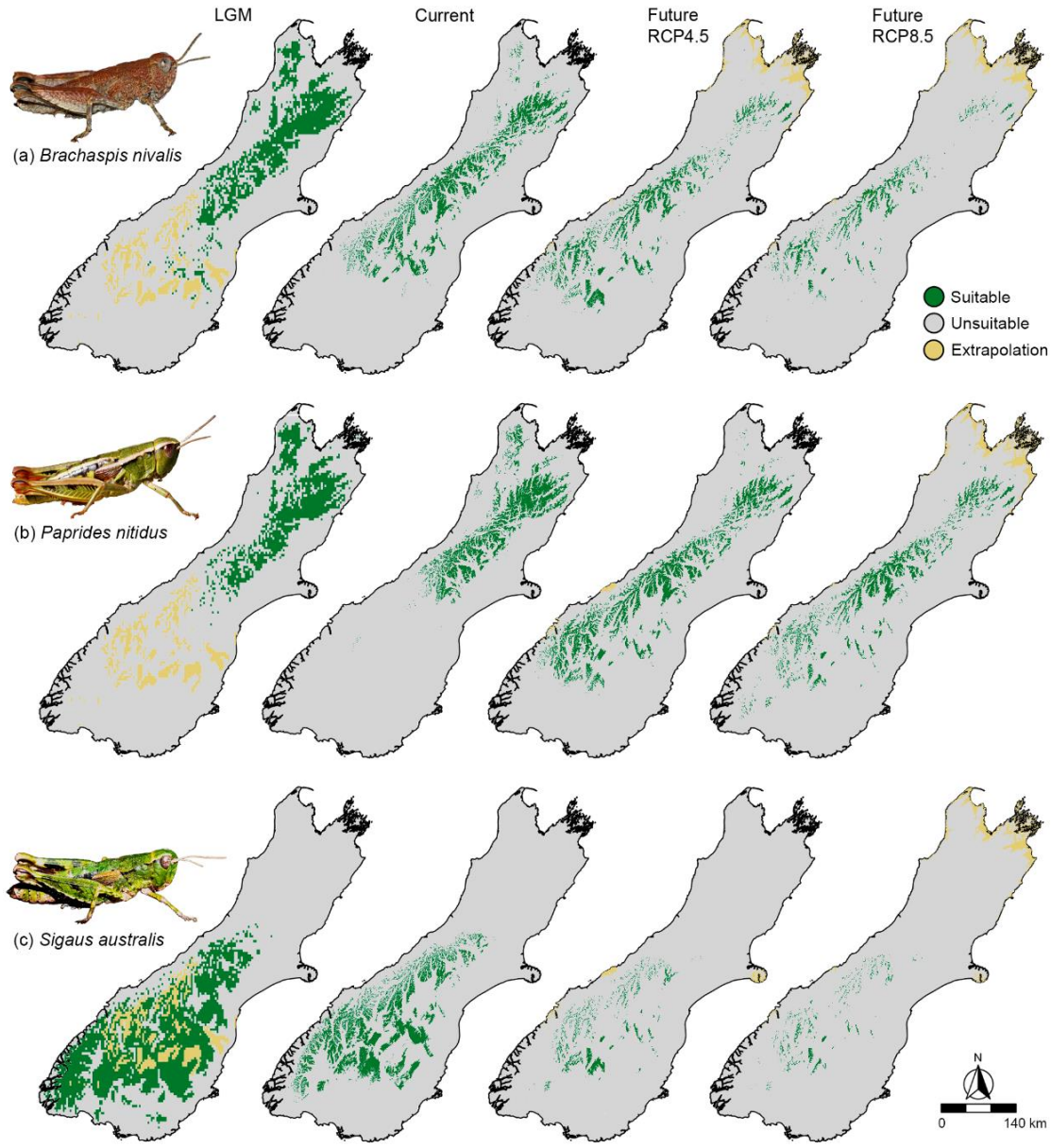

Figure 2. Predicted shifts in the suitable niche space for (a) *Brachaspis nivalis* (cut-off = 354.5), (b) *Paprides nitidus* (cut-off = 209.5) and (c) *Sigaus australis* (cut-off = 462.5) in South Island,

New Zealand under past (LGM), current and two future scenarios. Areas of strict extrapolation indicate climate conditions that differ from those in the calibration area used to develop the model. Map projection: NZGD2000.

Niche factor analyses

Specialisation was higher for *B. nivalis* (*S* = 3.208) and *P. nitidus* (*S* = 2.672) than for *S. australis* (*S* = 2.171), suggesting that these two species have narrower climate niches, hence, more specialised environmental requirements. Marginality values were similar for all species (*B. nivalis* = 2.172, *S. australis* = 2.176 and *P. nitidus* = 1.974), indicating that they inhabit environments substantially different from the mean climate conditions in South Island. Deviations from current climatic conditions are expected to be most pronounced for these species under the RCP8.5 scenario, as indicated by higher departure values than the RCP4.5 scenario. In general, *B. nivalis* had the greatest vulnerability while *S. australis* had the highest departure under future conditions (Table S1.6). These species are most sensitive to mean temperature of driest quarter and isothermality (*B. nivalis* and *P. nitidus*); and annual mean temperature and precipitation seasonality (*S. australis*). Moderate departures in mean temperature of driest quarter resulted in increased vulnerability for *B. nivalis* and *P. nitidus*, while substantial deviations in annual mean temperature and precipitation seasonality led to increased vulnerability for *S. australis* (Table S1.7).

Predicted spatial ranges of the three grasshopper species consistently exhibit high departures from current conditions in almost every variable under both climate change scenarios (Table S1.7). Areas with moderate to high exposure values typically coincide with the most vulnerable current native habitat for all species. For *B. nivalis*, this appears in the northeast (Marlborough and Kaikōura) and southeast (Mackenzie and Waitaki) mountains. For *P. nitidus*, areas of moderate to high vulnerability are scattered across the north (Marlborough) and central west of its current suitable envelope. The most vulnerable current native habitat for *S. australis* appears along the western mountains (Westland) and margins of Central Otago. Areas with low vulnerability to climate change are on the periphery of the central distributions of each species (Figure 3).

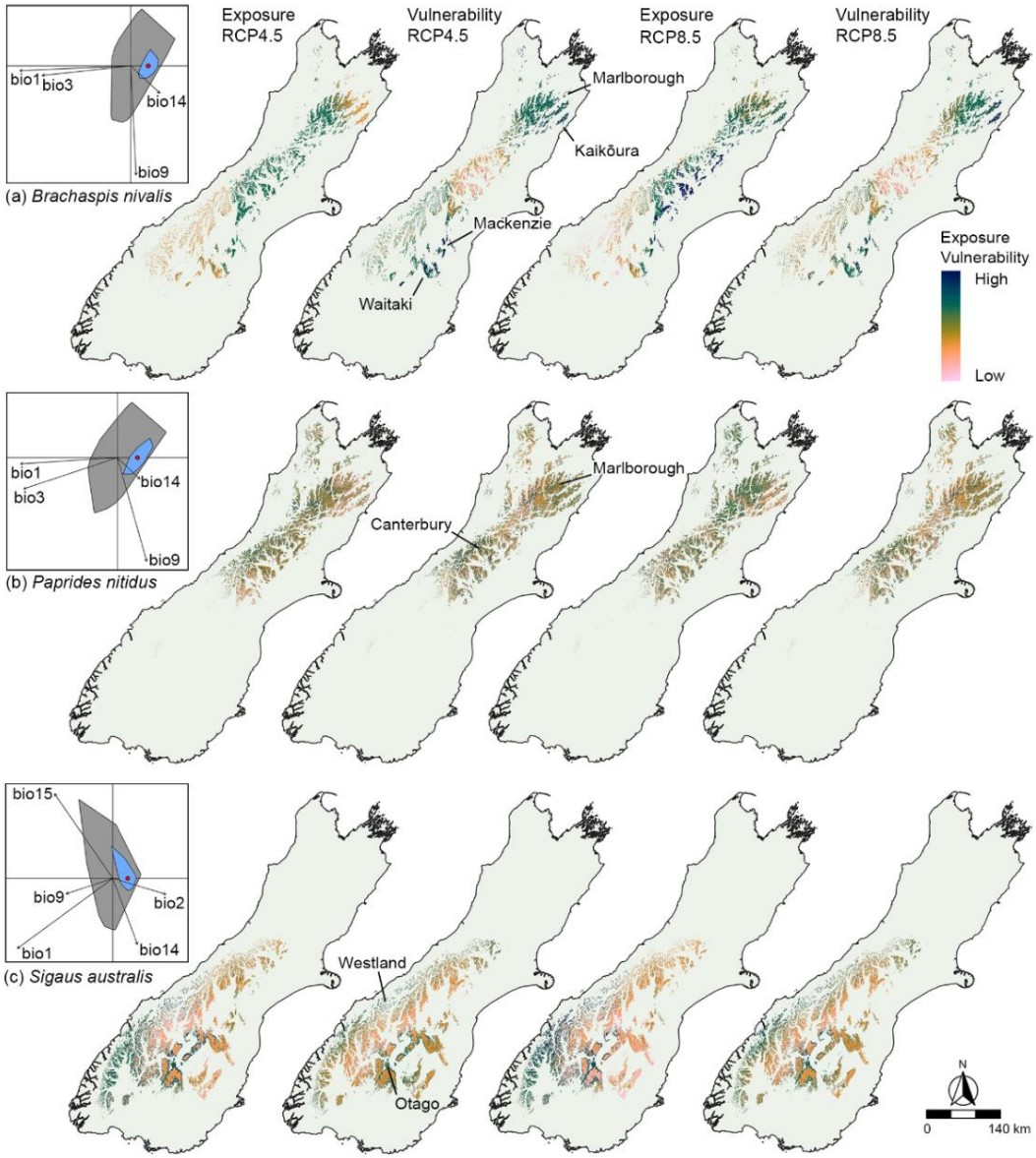

Figure 3. Future climatic exposure and vulnerability across the current native ranges of (a) *Brachaspis nivalis*, (b) *Paprides nitidus* and (c) *Sigaus australis* in South Island, New Zealand under two future climate scenarios. Insets show the suitable space (blue) within the available background (grey) across the marginality (x) and specialization (y) axes. Red dots correspond to the centroid of the used habitat and arrows are the projections of the environmental variables: annual mean temperature (bio1), annual mean diurnal range (bio2), isothermality (bio3), mean temperature of driest quarter (bio9), precipitation of driest month (bio14) and precipitation seasonality (bio15). Map projection: NZGD2000.

Population genetic structure

Mitochondrial DNA protein-coding gene ND2 sequences were obtained from 155 individuals. A 708 bp alignment with missing data for some sequences was used for Bayesian phylogenetic analyses. Trimming missing data for other analyses produced an

unambiguous aligned region of 603 bp containing 163 unique mtDNA haplotypes detected among the 287 individuals (Table S2.1): 39 in *B. nivalis* (n = 61), 55 in *P. nitidus* (n = 94) and 69 in *S. australis* (n = 132; data from Carmelet-Rescan et al., 2021). Haplotype networks and phylogenetic analyses revealed significant spatial genetic structure in all three grasshopper species (Figure 4). In all species, each haplotype was unique to a single mountain population sample; no haplotypes were shared among mountain samples.

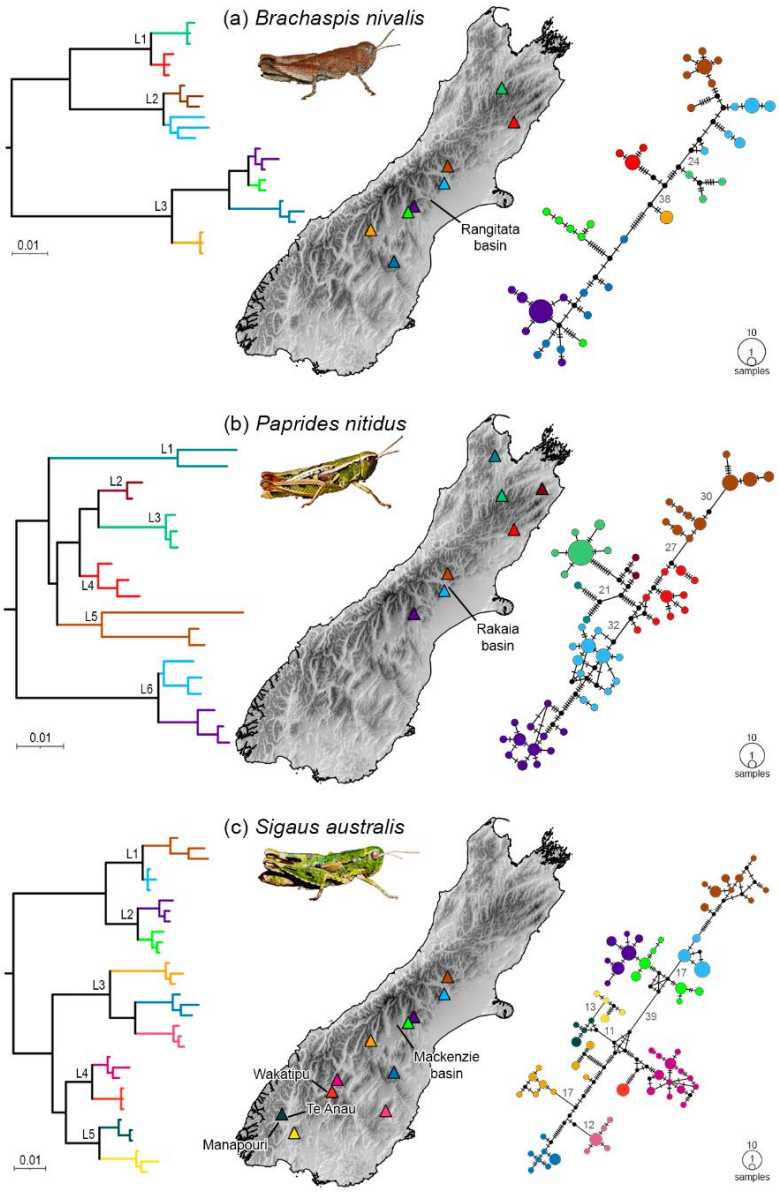

Figure 4. Mountains in South Island, New Zealand, sampled for genetic analyses of (a) *Brachaspis nivalis*, (b) *Paprides nitidus* and (c) *Sigaus australis*. Phylogenetic (left) and genealogical relationships (right) among major ND2 lineages for the studied species. Each

mountain location has a different colour as shown on map and used to code haplotypes by sample location; the same colours are used for each of the three sympatric species. In the networks, > 10 inferred substitutions between haplotypes are shown in numbers. For visualisation purposes, only the most common ND2 haplotypes are shown in the phylogenetic trees. See Figure S2.1 for the complete information on relationships and node support. Map projection: NZGD2000.

Phylogenetic analyses of ND2 haplotypes recovered three well-supported major lineages (posterior probabilities ≥ 0.95) for *B. nivalis*, five for *S. australis* and six for *P. nitidus* (Figure 4). Most lineages presented well-supported subdivisions reflecting intermediate levels of geographic structure; however, shallow divisions were generally not well resolved. Median-joining haplotype networks for each species showed similar clustering patterns as those produced by phylogenetic analyses (Figure 4; Figure S2.1). Pairwise Φ_{ST} showed large and significant departures from zero among populations, indicating little gene flow among mountain populations ($\Phi_{ST} > 0.409$; $p < 0.001$; Tables S2.2–S2.4). The most similar haplotypes among population samples were seen at Mt Fox and Mt Dobson (*B. nivalis* and *S. australis*), and Mt Fox and Mt Hutt (*P. nitidus*). Phylogeographic splits correlate with the north–south orientation of the Southern Alps for all species and average genetic distances among the deepest intraspecific lineages exceeded 10.3% (K2P) and 10.8% (TN). Within lineage distances were on average lower than 7.0% (K2P) and 7.5% (TN) in northern lineages, and below 6.2% (K2P) and 6.5% (TN) in southern lineages (Tables S2.2–S.2.4).

The level of genetic polymorphism in the ND2 matrilineal marker was similar in all three grasshoppers (Table S2.5). Haplotype diversity (h) and nucleotide diversity (π) values were marginally higher in the species with the largest sample sizes; *S. australis* (h = 0.984; $\pi = 0.066$), compared to *P. nitidus* ($h = 0.972$; $\pi = 0.055$) and *B. nivalis* ($h = 0.964$; $\pi = 0.057$). Mismatch distributions for each grasshopper species were multimodal, suggesting large, sustained populations. Neutrality statistics (D, F_S and R_2) of the drift–mutation equilibrium were non-significant, supporting the hypothesis of stable population sizes for all three species. Values of Harpending's r lacked statistical significance for all species. Taken together, these results (mismatch graphs and neutrality tests) were consistent with constant population size (Table S2.6), except for the Mt McRae population of *P. nitidus*, for which population expansion was indicated by the results from mismatch distributions and neutrality test.

To illustrate the potential for intraspecific genetic erosion, we projected current niche models onto future climate scenarios and identified local population extinction that would result in loss of some components of sampled genetic diversity (Figure 5; Table S2.7). A substantial proportion of our sampled haplotypes will be lost in the warmest scenario (RCP8.5): up to 36% for *B. nivalis* and 49% for *S. australis*. Similarly, sampled nucleotide diversity (π) would reduce by 14% for *B. nivalis* and 10% for *S. australis*. Results for *P. nitidus* suggest limited loss of genetic diversity, but the populations predicted to be lost for this species were under-sampled in our analyses (n = 2).

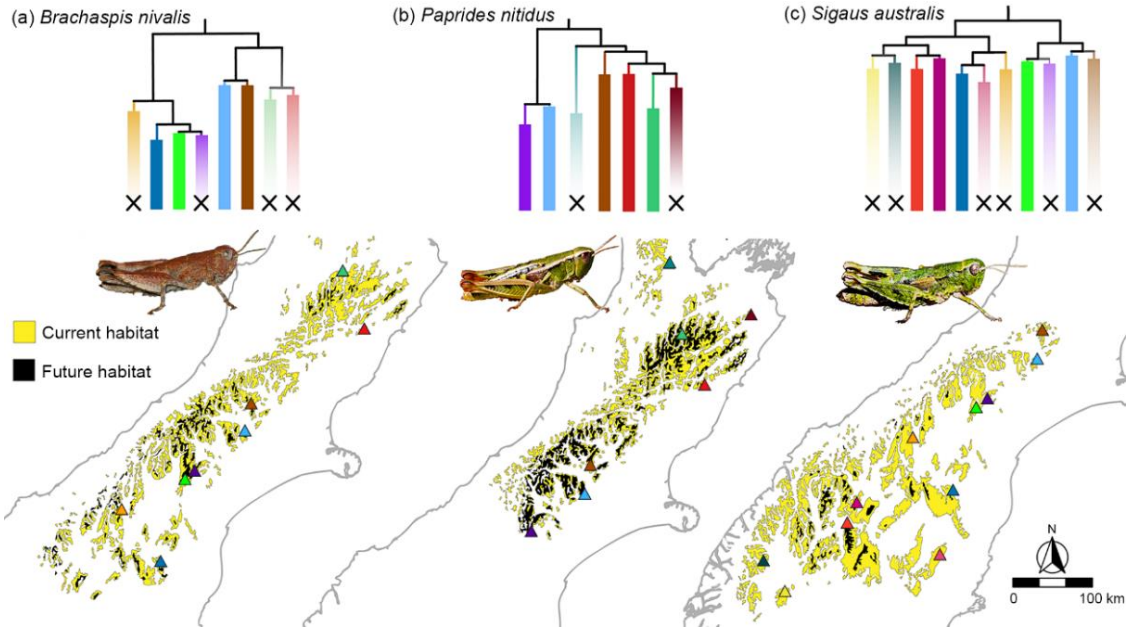

Figure 5. Predicted shifts in suitable native area and sampled intraspecific diversity for (a) *Brachaspis nivalis*, (b) *Paprides nitidus* and (c) *Sigaus australis* in South Island, New Zealand, under the warmest climate scenario (RCP8.5). Faded lineages in the phylogenies correspond to populations expected to be lost (X) under global warming. Colours for sampling locations as in Figure 1. Map projection: NZGD2000.

Discussion

Montane environments have distinctive ecological characteristics and specialised biology that are sensitive to global climate change (Ikeda, 2022). As in the Andes (Hazzi et al., 2018), Himalayas (Muellner-Riehl, 2019) and European Alps (Schönswetter & Schneeweiss, 2019), Pleistocene climate cycles in New Zealand promoted dramatic

changes in the distribution of alpine habitat (Newnham et al., 1999) and cold-adapted organisms are inferred to have attained larger distributions during lengthy glacial periods by tracking suitable environments (Carmelet-Rescan et al., 2021; Trewick, 2001a; Trewick et al., 2000, 2011). We developed niche models to examine this in detail for three sympatric alpine grasshoppers in the Southern Alps and found their habitat was more extensive and contiguous during the LGM than today. Consistent with this, we found high intraspecific genetic diversity in these grasshoppers across their spatial ranges. As high genetic diversity is indicative of large, persistent population size (Charlesworth, 2009; Morgan-Richards et al., 2017), we can infer that the alpine adapted grasshoppers maintained dense populations through the Pleistocene. Similar high intraspecific diversity is known from other New Zealand alpine insects including wētā (King et al., 2020; Trewick et al., 2000) and stoneflies (McCulloch et al., 2009). Deep gene trees with major lineages of each grasshopper species in allopatry suggest long-term extrinsic barriers partitioning large populations.

Cold-adapted species worldwide are inferred to have experienced range contraction as temperatures increased after the LGM (e.g. Guerrina et al., 2022; Ikeda, 2022; Muellner-Riehl, 2019; Trewick et al., 2011). This is the situation for the flightless, alpine grasshoppers studied here (see also Koot et al., 2022), where postglacial contraction of alpine conditions isolated their populations to mountain ridges and summits, retaining or emphasising existing population segregation (e.g. Carmelet-Rescan et al., 2021; Trewick, 2001b). Associated with this contraction of open alpine habitat is the increased elevation of closed, forest habitat with a timberline (Wardle, 1965) forming a strong natural barrier to dispersal. Population genetics and niche modelling indicate that current grasshopper populations are not derived from a few glacial refugia but represent numerous populations that persisted in situ through the Pleistocene (e.g. Carmelet-Rescan et al., 2021; Trewick, 2001a). The high levels of mtDNA genetic diversity and partitioning of genetic variation among populations is consistent with large populations accumulating mtDNA diversity through many glacial stages that together represent the dominant environmental conditions (~80% of past 800 ka) of the Pleistocene (PIWG, 2016).

In all three grasshopper species, deep intraspecific splits are associated with population samples arrayed along the north–south orientation of the Southern Alps (Figure 4). The most divergent clusters of each species are broadly concordant in the central region of

South Island implying a similar process and timing of divergence, but locations are not identical: the Rangitata (*B. nivalis*), Rakaia (*P. nitidus*) and Mackenzie basins (*S. australis*). Similar phylogeographic structure is known from other alpine animals in the Southern Alps (e.g. Hill et al., 2009; King et al., 2020; Trewick, 2001a; Trewick et al., 2000; Weston & Robertson, 2015), but these might reflect lineage sorting at different times (Trewick et al., 2011). The grasshoppers considered here each encompassed more than 10% sequence divergence (see also Trewick, 2001b, 2008), which for comparison, is an order of magnitude greater than found in well-studied *Chorthippus* grasshoppers across Europe (e.g. Lunt et al., 1998). Whereas phylogeographic structure in *Chorthippus* and other animals in western Europe reflect postglacial population expansion (Hewitt, 2000; Schmitt, 2007), divergence within the New Zealand species plausibly originated early in the establishment of alpine habitat in the Southern Alps (~3–5 Mya).

For many alpine animals, valleys represent barriers between populations if they contain inhospitable habitat that cannot be traversed (Figure 6). Forest, during interglacials, and ice, during glacials, are both likely to impede range shifts and gene flow among populations of flightless grasshoppers (Trewick et al., 2000). Thus, although shallower lineage splits (0.8%–2.6%) were associated with intraspecific grasshopper samples from adjacent mountains (e.g. *B. nivalis* and *S. australis* on Fox Peak and Mt Dobson, and *P. nitidus* on Mt Hutt and Fox Peak), valley habitat might override geographic distance as the main evolutionary driver. For example, gene flow was apparently more restricted among southern populations of *S. australis* that exhibit genetic divergence greater than 3.1% (e.g. Mt Cardrona, Double Cone, Mt Luxmore and Mt Spencer; see also Carmelet-Rescan et al., 2021; Trewick, 2008). Deep incised glacial lakes (e.g. Te Anau, Wakatipu, Manapouri) appear to have limited genetic exchange between these nearby populations of *S. australis* (e.g. Trewick, 2001b; Trewick et al., 2000). Similarly, lineage sharing in *P. nitidus* on Mt Hutt and Fox Peak (~70 km apart) but not between the closer (~30 km) Mt Hutt and Mt Olympus populations implies isolation that could be explained by glaciers (Figure 1). Deeply split genetic lineages in all three grasshoppers correlate with LGM glaciers and proglacial lakes (Sutherland et al., 2019) and strongly suggest that these were extrinsic barriers to grasshopper populations that persisted on nunataks (Figure 1) as proposed for alpine scree wētā in this landscape (Trewick et al., 2000). Nevertheless, in central South Island, the low lying, eastern Canterbury Plains developed

from glacial alluvial outwash and likely provided opportunities for grasshopper range shifts during glacials.

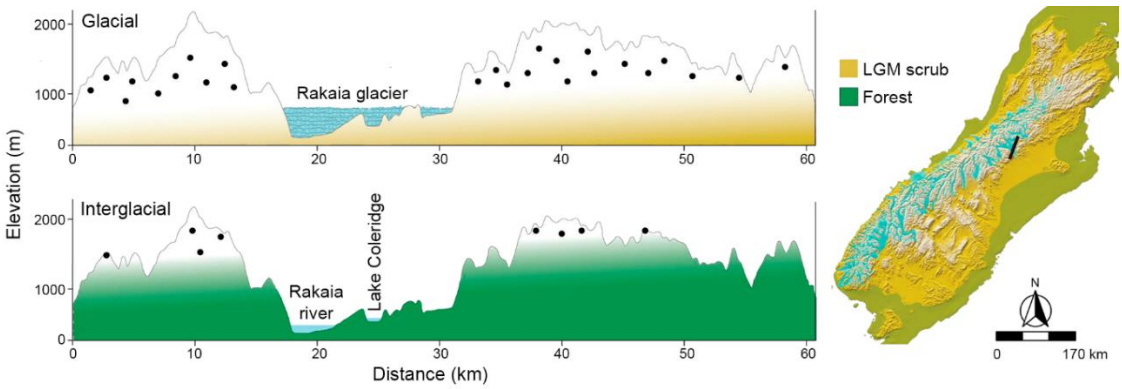

Figure 6. Valley habitats form dispersal barriers for flightless, alpine-adapted grasshoppers (black dots), where they contain montane glaciers during Pleistocene glacials, or dense forest during interglacials. The elevation profile represents a south-west section of the Southern Alps across the Rakaia (black line on map). Population segregation hypothesis for glacial conditions (top) and interglacial conditions (bottom). Map projection: NZGD2000.

Projecting forward and considering current climate change trends makes it clear that habitat availability for mountaintop species in the enhanced, protracted, anthropogenic 'interglacial' currently developing around the globe (PIWG, 2016) will further diminish. If niche stability, conservatism and saturation operate, we can expect further contraction and emphasised population reduction and fragmentation (Freeman et al., 2018). However, upward range shift and/or shrinkage will occur at species-specific rates, implying non-identical responses to change among these grasshoppers, dependent on intrinsic features of each species (e.g. niche specialisation and ecological preferences) and uneven climate departures across their ranges under future conditions. Here, differences in the distribution of current habitat led to different projected habitat availability which in turn signals species-specific patterns of genetic erosion (Figure 5). Range loss under the worst-case scenario (RCP8.5) is predicted to be least for *P. nitidus* (20%), and substantially more for B. *nivalis* (75%) and *S. australis* (90%), but all three are likely to lose diversity because lineages are associated with distinct regions along the latitudinal gradient. Thus, a Pleistocene history of spatial isolation will culminate in local extinction. Future latitudinal tracking of climatically suitable habitat, as predicted by niche models (Figure 2), is unlikely to result in opportunities for these flightless

grasshoppers; their limited capacity for long-range dispersal between habitat patches is evident from their phylogeography.

Temperature variation is a key predictor of these species' distributions and vulnerability patterns, but distinct bioclimatic factors suggest that the grasshopper species are subject to microhabitat segregation despite overlapping ranges. Likewise, deviations from current climatic conditions are projected to vary across the Southern Alps, and so strongly influence potential responses to global warming. Climate variables contributing to models are, however, better considered as proxies for combinations of environmental conditions and may not themselves be the direct drivers of species ranges, and correlative niche modelling and niche-factor analyses neglect other ecological processes shaping species' niches such as biotic interactions and population dynamics (e.g. Freeman et al., 2018; Suttle et al., 2007). Species of New Zealand alpine grasshopper co-occur throughout their ranges (Bigelow, 1967; Trewick & Morris, 2008) and interact with other biotic and abiotic elements that likely affect their ability to persist under environmental change (Thompson & Fronhofer, 2019). Accounting for these interactions might improve model predictions but gathering such data is challenging and the pace of environmental change may be overwhelming.

The existence of localised peripheral populations of these three flightless grasshoppers in non-alpine habitats (Trewick & Morris, 2008) suggests some capacity for survival in alternative conditions that enables range-shift into adjacent, novel habitat arising from anthropogenic activity (e.g. Sivyer et al., 2018). However, this opportunity relies on additional anthropogenic activity (removal of natural lowland forest vegetation) generating corridors from the alpine zone. As such, range adjustments into exotic habitat probably have only brief viability as lowland populations are likely to have low genetic diversity, small population size, diminished population cohesion (e.g. Pavlova et al., 2017; Rehnus et al., 2018; Rizvanovic et al., 2019), and might experience lag-extinction effects (e.g. Sax et al., 2013). Novel, anthropogenic open habitats are at high risk from continued land-use change (e.g. Koot et al., 2022; Sivyer et al., 2018), are dominated by exotic plants, and their derived species assemblages are in disequilibrium (Blonder et al., 2015), subject to invasive predators and weeds (e.g. Smith et al., 2007). Location and taxon-specific introgression (e.g. Dowle et al., 2014; Morgan-Richards et al., 2021) will influence the evolutionary potential of populations in new locations.

Despite its relatively small land area, the persistence of many populations throughout the Pleistocene has yielded much higher intraspecific diversity in these New Zealand insects than typically encountered in the Northern Hemisphere. As a result, genetic erosion of alpine biodiversity by anthropogenic global climate change will be especially intense. An optimistic view is that biodiversity decline will be countered by evolution (Catullo et al., 2019). Whether populations of flightless, alpine grasshopper shift their range up mountains as they track dwindling suitable habitat, or find dispersal corridors to exotic habitats, we know fragmentation leads to small populations with reduced adaptive potential (Willi et al., 2006) that are unlikely to have the genotypic scope to respond to natural selection arising directly from rapid climate change and other anthropogenic threats (Bowler et al., 2020). Despite alpine species not being ecologically identical, we expect loss of genetic diversity for all alpine biota due to global warming.

Acknowledgements

We are grateful to the New Zealand Department of Conservation for granting access and approval to collect from the Conservation Estate (Authorisation 49878-RES). We thank the ski fields and managers who allowed us to access field sites. David Carmelet-Rescan provided valuable niche modelling advice. Edward Trewick did 3D rendering for Figure 1 with QGIS (www.qgis.org) and Blender (www.blend er.org). This research was assisted by a grant from the Miss E. L. Hellaby Indigenous Grasslands Research Trust (awarded to EMK) and a doctoral scholarship from Massey University (awarded to FLMJ). Open access publishing facilitated by Massey University, as part of the Wiley-Massey University agreement via the Council of Australian University Librarians.

References

Bandelt, H. J., Forster, P., & Röhl, A. (1999). Median-joining networks for inferring intraspecific phylogenies. *Molecular Biology and Evolution*, *16*(1), 37–48. https://doi.org/10.1093/oxfordjournals.molbev.a026036

Barbosa, A. M. (2015). fuzzySim: Applying fuzzy logic to binary similarity indices in ecology. *Methods in Ecology and Evolution*, *6*(7), 853–858. https://doi.org/10.1111/2041-210X.12372

Bellard, C., Bertelsmeier, C., Leadley, P., Thuiller, W., & Courchamp, F. (2012). Impacts of climate change on the future of biodiversity. *Ecology Letters*, *15*(4), 365–377. https://doi.org/10.1111/j.1461-0248.2011.01736.x

Bigelow, R. S. (1967). *The grasshoppers (Acrididae) of New Zealand*. University of Canterbury Publications.

Blonder, B., Nogués-Bravo, D., Borregaard, M. K., Donoghue II, J. C., Jørgensen, P. M., Kraft, N. J., ... & Enquist, B. J. (2015). Linking environmental filtering and disequilibrium to biogeography with a community climate framework. *Ecology*, *96*(4), 972–985. https://doi.org/10.1890/14-0589.1

Bowler, D. E., Bjorkman, A. D., Dornelas, M., Myers-Smith, I. H., Navarro, L. M., Niamir, A., ... & Bates, A. E. (2020). Mapping human pressures on biodiversity across the planet uncovers anthropogenic threat complexes. *People and Nature*, *2*(2), 380–394. https://doi.org/10.1002/pan3.10071

Carmelet-Rescan, D., Morgan-Richards, M., Koot, E. M., & Trewick, S. A. (2021). Climate and ice in the last glacial maximum explain patterns of isolation by distance inferred for alpine grasshoppers. *Insect Conservation and Diversity*, *14*(5), 568–581. https://doi.org/10.1111/icad.12488

Case, B. S., & Buckley, H. L. (2015). Local-scale topoclimate effects on treeline elevations: A country-wide investigation of New Zealand's southern beech treelines. *PeerJ*, *3*, e1334. https://doi.org/10.7717/peerj.1334

Catullo, R. A., Llewelyn, J., Phillips, B. L., & Moritz, C. C. (2019). The potential for rapid evolution under anthropogenic climate change. *Current Biology*, *29*(19), R996–R1007. https://doi.org/10.1016/j.cub.2019.08.028

Charlesworth, B. (2009). Effective population size and patterns of molecular evolution and variation. *Nature Reviews Genetics*, *10*, 195. https://doi.org/10.1038/nrg2526

Chen, I. C., Hill, J. K., Ohlemüller, R., Roy, D. B., & Thomas, C. D. (2011). Rapid range shifts of species associated with high levels of climate warming. *Science*, *333*(6045), 1024–1026. https://doi.org/10.1126/science.1206432

Chinn, W. G. H., & Chinn, T. J. H. (2020). Tracking the snow line: Responses to climate change by New Zealand alpine invertebrates. *Arctic, Antarctic, and Alpine Research*, *52*(1), 361–389. https://doi.org/10.1080/15230430.2020.1773033

Dahl, E. (1987). The nunatak theory reconsidered. *Ecological Bulletin, 38*, 77–94. https://www.jstor.org/stable/20112974

Davis, M. B., & Shaw, R. G. (2001). Range shifts and adaptive responses to quaternary climate change. *Science*, *292*(5517), 673–679. https://doi.org/10.1126/science.292.5517.673

Dowle, E. J., Morgan-Richards, M., & Trewick, S. A. (2014). Morphological differentiation despite gene flow in an endangered grasshopper. *BMC Evolutionary Biology*, *14*, 216. https://doi.org/10.1186/s12862-014-0216-x

Elith, J., Kearney, M., & Phillips, S. (2010). The art of modelling range-shifting species. *Methods in Ecology and Evolution*, *1*(4), 330–342. https://doi.org/10.1111/j.2041-210X.2010.00036.x

Endo, Y., Nash, M., Hoffmann, A. A., Slatyer, R., & Miller, A. D. (2015). Comparative phylogeography of alpine invertebrates indicates deep lineage diversification and historical refugia in the Australian Alps. *Journal of Biogeography*, *42*(1), 89–102. https://doi.org/10.1111/jbi.12387

Excoffier, L., Smouse, P. E., & Quattro, J. M. (1992). Analysis of molecular variance inferred from metric distances among DNA haplotypes: Application to human mitochondrial DNA restriction data. *Genetics*, *131*(2), 479–491. https://doi.org/10.1093/genetics/131.2.479

Excoffier, L., & Lischer, H. E. (2010). Arlequin suite ver 3.5: A new series of programs to perform population genetics analyses under Linux and Windows. *Molecular Ecology Resources*, *10*(3), 564–567. https://doi.org/10.1111/j.1755-0998.2010.02847.x

Faurby, S., & Araújo, M. B. (2018). Anthropogenic range contractions bias species climate change forecasts. *Nature Climate Change*, *8*, 252–256. https://doi.org/10.1038/s41558-018-0089-x

Fickert, T., Friend, D., Molnia, B., Grüninger, F., & Richter, M. (2022). Vegetation ecology of debris-covered glaciers (DCGs)—site conditions, vegetation patterns and implications for DCGs serving as quaternary cold-and warm-stage plant refugia. *Diversity*, *14*(2), 114. https://doi.org/10.3390/d14020114

Freeman, B. G., Lee-Yaw, J. A., Sunday, J. M., & Hargreaves, A. L. (2018). Expanding, shifting and shrinking: The impact of global warming on species' elevational distributions. *Global Ecology and Biogeography*, *27*(11), 1268–1276. https://doi.org/10.1111/geb.12774

Fu, Y. X. (1997). Statistical tests of neutrality of mutations against population growth, hitchhiking and background selection. *Genetics*, *147*(2), 915–925. https://doi.org/10.1093/genetics/147.2.915

Galbreath, K. E., Hafner, D. J., & Zamudio, K. R. (2009). When cold is better: Climate-driven elevation shifts yield complex patterns of diversification and demography in an alpine specialist (American pika, *Ochotona princeps*). *Evolution*, *63*(11), 2848–2863. https://doi.org/10.1111/j.1558-5646.2009.00803.x

Gifford, M. E., & Kozak, K. H. (2012). Islands in the sky or squeezed at the top? Ecological causes of elevational range limits in montane salamanders. *Ecography*, *35*(3), 193–203. https://doi.org/10.1111/j.1600-0587.2011.06866.x

Gowan, E. J., Zhang, X., Khosravi, S., Rovere, A., Stocchi, P., Hughes, A. L., ... & Lohmann, G. (2021). A new global ice sheet reconstruction for the past 80 000 years. *Nature communications*, *12*, 1199. https://doi.org/10.1038/s41467-021-21469-w

Groos, A. R., Akçar, N., Yesilyurt, S., Miehe, G., Vockenhuber, C., & Veit, H. (2021). Nonuniform Late Pleistocene glacier fluctuations in tropical Eastern Africa. *Science Advances*, *7*(11), eabb6826. https://doi.org/10.1126/sciadv.abb6826

Guerrina, M., Theodoridis, S., Minuto, L., Conti, E., & Casazza, G. (2022). First evidence of post-glacial contraction of Alpine endemics: Insights from *Berardia subacaulis* in the European Alps. *Journal of Biogeography*, *49*(1), 79–93. https://doi.org/10.1111/jbi.14282

Harpending, H. C. (1994). Signature of ancient population growth in a low-resolution mitochondrial DNA mismatch distribution. *Human Biology*, *66*, 591–600. http://www.jstor.org/stable/41465371

Hazzi, N. A., Moreno, J. S., Ortiz-Movliav, C., & Palacio, R. D. (2018). Biogeographic regions and events of isolation and diversification of the endemic biota of the tropical Andes. *Proceedings of the National Academy of Sciences*, *115*(31), 7985–7990. https://doi.org/10.1073/pnas.1803908115

Hewitt, G. (2000). The genetic legacy of the Quaternary ice ages. *Nature*, 405, 907–913. https://doi.org/10.1038/35016000

Hewitt, G. M. (2004). Genetic consequences of climatic oscillations in the Quaternary *Philosophical Transactions of the Royal Society B: Biological Sciences*, *359*(1442), 183–195. https://doi.org/10.1098/rstb.2003.1388

Hijmans, R. J., Cameron, S. E., Parra, J. L., Jones, P. G. & Jarvis, A. (2005). Very high resolution interpolated climate surfaces for global land areas. *International Journal of Climatology*, *25*(15), 1965–1978. https://doi.org/10.1002/joc.1276

Hijmans, R. J. (2020). Raster: Geographic data analysis and modeling. https://cran.r-project.org/package=raster

Hijmans, R. J., Phillips, S., Leathwick, J., & Elith, J. (2020). Dismo: Species distribution modeling. https://cran.r-project.org/package=dismo

Hill, K. B. R., Simon, C., Marshall, D. C., Chambers, G. K., & McDowall, R. (2009). Surviving glacial ages within the biotic gap: Phylogeography of the New Zealand cicada *Maoricicada campbelli*. *Journal of Biogeography*, *36*(4), 675–692. https://doi.org/10.1111/j.1365-2699.2008.02036.x

Hirzel, A. H., Hausser, J., Chessel, D., & Perrin, N. (2002). Ecological-niche factor analysis: How to compute habitat-suitability maps without absence data? *Ecology*, *83*(7), 2027–2036. https://doi.org/10.1890/0012-9658(2002)083[2027:ENFAHT]2.0.CO;2

Ikeda, H. (2022). Decades-long phylogeographic issues: Complex historical processes and ecological factors on genetic structure of alpine plants in the Japanese Archipelago. *Journal of Plant Research*, *135*, 191–201. https://doi.org/10.1007/s10265-022-01377-w

IPCC (2022). *Climate change 2022: Impacts, adaptation, and vulnerability*. Cambridge University Press.

James, W. H. M., Carrivick, J. L., Quincey, D. J. & Glasser, N. F. (2019). A geomorphology based reconstruction of ice volume distribution at the Last Glacial Maximum across the Southern Alps of New Zealand. *Quaternary Science Reviews*, *219*, 20–35. https://doi.org/10.1016/j.quascirev.2019.06.035

Kearse, M., Moir, R., Wilson, A., Stones-Havas, S., Cheung, M., Sturrock, S., ... & Thierer, T. (2012). Geneious Basic: An integrated and extendable desktop software platform for the organization and analysis of sequence data. *Bioinformatics*, *28*(12), 1647–1649. https://doi.org/10.1093/bioinformatics/bts199

Kimura, M. (1980). A simple method for estimating evolutionary rate of base substitutions through comparative studies of nucleotide sequences. *Journal of Molecular Evolution*, *16*, 111–120. https://doi.org/10.1007/BF01731581

King, K. J., Lewis, D. M., Waters, J. M., & Wallis, G. P. (2020). Persisting in a glaciated landscape: Pleistocene microrefugia evidenced by the tree wētā *Hemideina maori* in

central South Island, New Zealand. *Journal of Biogeography*, *47*(11), 2518–2531. https://doi.org/10.1111/jbi.13953

Koot, E. M., Morgan-Richards, M., & Trewick, S. A. (2020). An alpine grasshopper radiation older than the mountains, on Kā Tiritiri o te Moana (Southern Alps) of Aotearoa (New Zealand). *Molecular Phylogenetics and Evolution*, *147*, 106783. https://doi.org/10.1016/j.ympev.2020.106783

Koot, E. M., Morgan-Richards, M., Trewick, S. A. (2022). Climate change and alpine adapted insects: Modelling environmental envelopes of a grasshopper radiation. *Royal Society Open Science*, *9*, 211596. https://doi.org/10.1098/rsos.211596

Kumar, S., Stecher, G., Li, M., Knyaz, C., & Tamura, K. (2018). MEGA X: Molecular Evolutionary Genetics Analysis across computing platforms. *Molecular Biology and Evolution*, *35*(6), 1547–1549. https://doi.org/10.1093/molbev/msy096

Lanfear, R., Frandsen, P. B., Wright, A. M., Senfeld, T. & Calcott, B. (2017). PartitionFinder 2: New methods for selecting partitioned models of evolution for molecular and morphological phylogenetic analyses. *Molecular Biology and Evolution*, *34*(3), 772–773. https://doi.org/10.1093/molbev/msw260

Leathwick, J. R., McGlone, M. S., & Walker, S. (2004). *New Zealand's potential vegetation pattern*. Manaaki Whenua Press.

Leigh, J. W., & Bryant, D. (2015). PopArt: Full-feature software for haplotype network construction. *Methods in Ecology and Evolution*, *6*, 1110–1116. https://doi.org/10.1111/2041-210X.12410

Lenoir, J., Gégout, J. C., Guisan, A., Vittoz, P., Wohlgemuth, T., Zimmermann, N. E., ... & Svenning, J. C. (2010). Going against the flow: Potential mechanisms for unexpected downslope range shifts in a warming climate. *Ecography*, *33*(2), 295–303. https://doi.org/10.1111/j.1600-0587.2010.06279.x

Lenoir, J., & Svenning, J. C. (2015). Climate-related range shifts—A global multidimensional synthesis and new research directions. *Ecography*, *38*(1), 15–28. https://doi.org/10.1111/ecog.00967

Librado, P., & Rozas, J. (2009). DnaSP v5: A software for comprehensive analysis of DNA polymorphism data. *Bioinformatics*, *25*(11), 1451–1452. https://doi.org/10.1093/bioinformatics/btp187

Lunt, D. H., Ibrahim, K. M., & Hewitt, G. M. (1998). mtDNA phylogeography and postglacial patterns of subdivision in the meadow grasshopper *Chorthippus*

parallelus. *Heredity*, 80(5), 633–641. https://doi.org/10.1046/j.1365-2540.1998.00311.x

Lyons, S. K. (2003). A quantitative assessment of the range shifts of Pleistocene mammals. *Journal of Mammalogy*, *84*(2), 385–402. https://doi.org/10.1644/1545-1542(2003)084<0385:AQAOTR>2.0.CO;2

Marra, M. J., & Thackray, G. D. (2010). Glacial forest refugium in Howard Valley, South Island, New Zealand. *Journal of Quaternary Science*, *25*(3), 309–319. https://doi.org/10.1002/jqs.1339

Mateo, R. G., Croat, T. B., Felicísimo, A. M. & Muñoz, J. (2010). Profile or group discriminative techniques? Generating reliable species distribution models using pseudo-absences and target-group absences from natural history collections. *Diversity and Distributions*, *16*(1), 84–94. https://doi.org/10.1111/j.1472-4642.2009.00617.x

McCulloch, G. A., Wallis, G. P. & Waters, J. M. (2009). Do insects lose flight before they lose their wings? Population genetic structure in subalpine stoneflies. *Molecular Ecology*, *18*(19), 4073–4087. https://doi.org/10.1111/j.1365-294X.2009.04337.x

Ministry for the Environment. (2018). *Climate change projections for New Zealand.* Ministry for the Environment Publications. https://environment.govt.nz/assets/Publications/Files/Climate-change-projections-2nd-edition-final.pdf

Moar, N. T. (1980). Late Otiran and early Aranuian grassland in central South Island. *New Zealand Journal of Ecology*, *3*, 4–12. http://www.jstor.org/stable/24052001

Moritz, C., & Agudo, R. (2013). The future of species under climate change: Resilience or decline? *Science*, *341*(6145), 504–508. https://doi.org/10.1126/science.1237190

Morgan-Richards, M., Bulgarella, M., Sivyer, L., Dowle, E. J., Hale, M., McKean, N. E. & Trewick, S. A. (2017). Explaining large mitochondrial sequence differences within a population sample. *Royal Society Open Science*, *4*, 170730. https://doi.org/10.1098/rsos.170730

Morgan-Richards, M., Vilcot, M., & Trewick, S. A. (2021). Lack of assortative mating might explain reduced phenotypic differentiation where two grasshopper species meet. *Journal of Evolutionary Biology*, *35*(4), 509–519. https://doi.org/10.1111/jeb.13879

Mountain Research Initiative EDW Working Group. (2015). Elevation-dependent warming in mountain regions of the world. *Nature Climate Change*, 5, 424–430. https://doi.org/10.1038/nclimate2563

Muellner-Riehl, A. N. (2019). Mountains as evolutionary arenas: Patterns, emerging approaches, paradigm shifts, and their implications for plant phylogeographic research in the Tibeto-Himalayan region. *Frontiers in Plant Science*, *10*, 195. https://doi.org/10.3389/fpls.2019.00195

Newnham, R. M., Lowe, D. J., & Williams, P. W. (1999). Quaternary environmental change in New Zealand: A review. *Progress in Physical Geography*, *23*, 567–610. https://doi.org/10.1177/030913339902300406

Nei, M. (1987). *Molecular Evolutionary Genetics*. Columbia University Press. https://doi.org/10.1002/ajpa.1330750317

Nei, M., & Tajima, F. (1981). Genetic drift and estimation of effective population size. *Genetics*, *98*(3), 625–640. https://doi.org/10.1093/genetics/98.3.625

Past Interglacials Working Group of PAGES. (2016). Interglacials of the last 800,000 years. *Reviews of Geophysics*, *54*, 162–219. https://doi.org/10.1002/2015RG000482

Pauli, H., & Halloy, S. (2019). *High mountain ecosystems under climate change*. Oxford University Press. https://doi.org/10.1093/acrefore/9780190228620.013.764

Pavlova, A., Beheregaray, L. B., Coleman, R., Gilligan, D., Harrisson, K. A., Ingram, B. A., ... & Sunnucks, P. (2017). Severe consequences of habitat fragmentation on genetic diversity of an endangered Australian freshwater fish: A call for assisted gene flow. *Evolutionary Applications*, *10*(6), 531–550. https://doi.org/10.1111/eva.12484

QGIS Development Team. (2020). QGIS: A free and open source geographic information system. Retrieved from http://qgis.osgeo.org

R Core Team. (2019). R: A language and environment for statistical computing. Retrieved from https://www.r-project.org

Rambaut, A., Drummond, A. J., Xie, D., Baele, G. & Suchard, M. A. (2018). Posterior summarisation in Bayesian phylogenetics using Tracer 1.7. *Systematic Biology*, *67*(5), 901–904. https://doi.org/10.1093/sysbio/syy032

Ramos-Onsins, S. E., & Rozas, J. (2002). Statistical properties of new neutrality tests against population growth. *Molecular Biology and Evolution*, *19*(12), 2092–2100. https://doi.org/10.1093/oxfordjournals.molbev.a004034

Rehnus, M., Bollmann, K., Schmatz, D. R., Hackländer, K., & Braunisch, V. (2018). Alpine glacial relict species losing out to climate change: The case of the fragmented mountain hare population (*Lepus timidus*) in the Alps. *Global Change Biology*, *24*(7), 3236–3253. https://doi.org/10.1111/gcb.14087

Rinnan, D. S. (2018). Cenfa: Climate and ecological niche factor analysis. https://cran.r-project.org/package=cenfa

Rinnan, D. S., & Lawler, J. (2019). Climate-niche factor analysis: A spatial approach to quantifying species vulnerability to climate change. *Ecography*, *42*(9), 1494–1503. https://doi.org/10.1111/ecog.03937

Rizvanovic, M., Kennedy, J. D., Nogués-Bravo, D., & Marske, K. A. (2019). Persistence of genetic diversity and phylogeographic structure of three New Zealand forest beetles under climate change. *Diversity and Distributions*, *25*(1), 142–153. https://doi.org/10.1111/ddi.12834

Rogers, A. R., & Harpending, H. (1992). Population growth makes waves in the distribution of pairwise genetic differences. *Molecular Biology and Evolution*, *9*(3), 552–569. https://doi.org/10.1093/oxfordjournals.molbev.a040727

Ronquist, F., Teslenko, M., van der Mark, P., Ayres, D. L., Darling, A., Höhna, S., ... & Huelsenbeck, J. P. (2012). MrBayes 3.2: Efficient Bayesian phylogenetic inference and model choice across a large model space. *Systematic Biology*, *61*(3), 539–542. https://doi.org/10.1093/sysbio/sys029

Sax, D. F., Early, R., & Bellemare, J. (2013). Niche syndromes, species extinction risks, and management under climate change. *Trends in Ecology & Evolution*, *28*(9), 517–523. https://doi.org/10.1016/j.tree.2013.05.010

Schmitt, T. (2007). Molecular biogeography of Europe: Pleistocene cycles and postglacial trends. *Frontiers in Zoology*, 4, 11. https://doi.org/10.1186/1742-9994-4-11

Schönswetter, P., & Schneeweiss, G. M. (2019). Is the incidence of survival in interior Pleistocene refugia (nunataks) underestimated? Phylogeography of the high mountain plant *Androsace alpina* (Primulaceae) in the European Alps revisited. *Ecology and evolution*, *9*(7), 4078–4086. https://doi.org/10.1002/ece3.5037

Sivyer, L., Morgan-Richards, M., Koot, E. & Trewick, S. A. (2018). Anthropogenic cause of range shifts and gene flow between two grasshopper species revealed by environmental modelling, geometric morphometrics and population genetics. *Insect Conservation and Diversity*, *11*, 415–434. https://doi.org/10.1111/icad.12289

Smith, D. H., Wilson, D. J., Moller, H., Murphy, E. C., & van Heezik, Y. (2007). Selection of alpine grasslands over beech forest by stoats (*Mustela erminea*) in montane southern New Zealand. *New Zealand Journal of Ecology*, *31*(1), 88–97. https://www.jstor.org/stable/24058130

Soberón, J., & Peterson, A. T. (2005). Interpretation of models of fundamental ecological niches and species' distributional areas. *Biodiversity Informatics*, *2*, 1–10. https://doi.org/10.17161/bi.v2i0.4

Sunnucks, P., & Hales, D. F. (1996). Numerous transposed sequences of mitochondrial cytochrome oxidase I–II in aphids of the genus *Sitobion* (Hemiptera: Aphididae). *Molecular Biology and Evolution*, *13*(3), 510–524. https://doi.org/10.1093/oxfordjournals.molbev.a025612

Sutherland, J. L., Carrivick, J. L., Shulmeister, J., Quincey, D. J., & James, W. H. (2019). Ice-contact proglacial lakes associated with the last glacial maximum across the Southern Alps, New Zealand. *Quaternary Science Reviews*, *213*, 67–92. https://doi.org/10.1016/j.quascirev.2019.03.035

Suttle, K. B., Thomsen, M. A., & Power, M. E. (2007). Species interactions reverse grassland responses to changing climate. *Science*, *315*(5812), 640–642. https://doi.org/10.1126/science.1136401

Taberlet, P., Fumagalli, L., Wust-Saucy, A. G., & Cosson, J. F. (1998). Comparative phylogeography and postglacial colonization routes in Europe. *Molecular Ecology*, *7*(4), 453–464. https://doi.org/10.1046/j.1365-294x.1998.00289.x

Tajima, F. (1989). Statistical method for testing the neutral mutation hypothesis by DNA polymorphism. *Genetics*, *123*(3), 585–595. https://doi.org/10.1093/genetics/123.3.585

Tamura, K. B., & Nei, M. (1993) Estimation of the number of nucleotide substitutions in the control region of mitochondrial DNA in humans and chimpanzees. *Molecular Biology and Evolution*, *10*(3), 512–526. https://doi.org/10.1093/oxfordjournals.molbev.a040023

Thuiller, W., Georges, D., Engler, R., & Breiner, F. (2020). Biomod2: Ensemble platform for species distribution modelling. https://cran.r-project.org/package=biomod2

Thompson, P. L., & Fronhofer, E. A. (2019). The conflict between adaptation and dispersal for maintaining biodiversity in changing environments. *Proceedings of the National Academy of Sciences*, *116*(42), 21061–21067. https://doi.org/10.1073/pnas.1911796116

Trewick, S. A. (2001a). Scree weta phylogeography: Surviving glaciation and implications for Pleistocene biogeography in New Zealand. *New Zealand Journal of Zoology*, *28*(3), 291–298. https://doi.org/10.1080/03014223.2001.9518271

Trewick, S. A. (2001b). Identity of an endangered grasshopper (Acrididae: *Brachaspis*): taxonomy, molecules and conservation. *Conservation Genetics*, *2*, 233–243. https://doi.org/10.1023/A:1012263717279

Trewick, S. A. (2008). DNA Barcoding is not enough: Mismatch of taxonomy and genealogy in New Zealand grasshoppers (Orthoptera: Acrididae). *Cladistics*, *24*(2), 240–254. https://doi.org/10.1111/j.1096-0031.2007.00174.x

Trewick, S. A., & Bland, K. (2012). Fire and slice: Palaeogeography for biogeography at New Zealand's North Island/South Island juncture. *Journal of the Royal Society of New Zealand*, *42*(3), 153–183. https://doi.org/10.1080/03036758.2010.549493

Trewick, S. A. & Morris, S. (2008). *Diversity and Taxonomic Status of Some New Zealand Grasshoppers.* Science & Technical Publishing Department of Conservation. https://www.doc.govt.nz/globalassets/documents/science-and-technical/drds290.pdf

Trewick, S. A., & Wallis, G. P. (2001). Bridging the "beech–gap": New Zealand invertebrate phylogeography implicates Pleistocene glaciation and Pliocene isolation. *Evolution*, *55*(11), 2170–2180. https://doi.org/10.1111/j.0014-3820.2001.tb00733.x

Trewick, S. A., Wallis, G. P., & Morgan-Richards, M. (2000). Phylogeographical pattern correlates with Pliocene mountain building in the alpine scree weta (Orthoptera, Anostostomatidae). *Molecular Ecology*, *9*(6), 657–666. https://doi.org/10.1046/j.1365-294x.2000.00905.x

Trewick, S. A., Wallis, G. P., & Morgan-Richards, M. (2011). The invertebrate life of New Zealand: A phylogeographic approach. *Insects*, *2*(3), 297–325. https://doi.org/10.3390/insects2030297

Valavi, R., Elith, J., Lahoz-Monfort, J. J., & Guillera-Arroita, G. (2019). BlockCV: An r package for generating spatially or environmentally separated folds for k-fold cross-validation of species distribution models. *Methods in Ecology and Evolution*, *10*, 225–232. https://doi.org/10.1111/2041-210x.13107

Vandergoes, M. J., Dieffenbacher-Krall, A. C., Newnham, R. M., Denton, G. H., & Blaauw, M. (2008). Cooling and changing seasonality in the southern Alps, New

Zealand during the Antarctic cold reversal. *Quaternary Science Reviews*, *27*(5–6), 589–601. https://doi.org/10.1016/j.quascirev.2007.11.015

Vignali, S., Barras, A. G., Arlettaz, R., & Braunisch, V. (2020). SDMtune: An R package to tune and evaluate species distribution models. *Ecology and Evolution*, *10*(20), 11488–11506. https://doi.org/10.1002/ece3.6786

Walther, G. R., Post, E., Convey, P., Menzel, A., Parmesan, C., Beebee, T. J., ... & Bairlein, F. (2002). Ecological responses to recent climate change. *Nature*, *416*, 389. https://doi.org/10.1038/416389a

Wardle, P. (1965). A comparison of alpine timber lines in New Zealand and North America. *New Zealand Journal of Botany*, *3*(2), 113–135. https://doi.org/10.1080/0028825X.1965.10876989

Wardle, P. (2008). New Zealand Forest to Alpine Transitions in Global Context. *Arctic, Antarctic, and Alpine Research*, *40*, 240–249. https://doi.org/10.1657/1523-0430(06-066)[WARDLE]2.0.CO;2

Weston, K. A., & Robertson, B. C. (2015). Population structure within an alpine archipelago: Strong signature of past climate change in the New Zealand rock wren (*Xenicus gilviventris*). *Molecular Ecology*, *24*(18), 4778–4794. https://doi.org/10.1111/mec.13349

Willi, Y., Van Buskirk, J., & Hoffmann, A. A. (2006). Limits to the adaptive potential of small populations. *Annual Review of Ecology, Evolution, and Systematics*, *37*, 433–458. https://doi.org/10.1146/annurev.ecolsys.37.091305.110145

Wilmshurst, J. M., Anderson, A. J., Higham, T. F., & Worthy, T. H. (2008). Dating the late prehistoric dispersal of Polynesians to New Zealand using the commensal Pacific rat. *Proceedings of the National Academy of Sciences*, *105*(22), 7676–7680. https://doi.org/10.1073/pnas.0801507105

Supporting Information

Appendix 1. This appendix contains additional information about niche analyses methods and results.

Table S1.1. Summary of the presence and absence data used in the niche modelling analysis, including the number of presence and absence points used to define the current and native realised niche, and the number of presence points falling outside the native range of each species. Target-group absences (Mateo et al., 2010) indicate sites where searches have revealed other Orthoptera and allied organisms (e.g. cicadas and cockroaches), but not the species modelled here.

Species	Realised niche				Presences outside the native range
	Current presences	Current absences	Native presences	Native absences	
Brachaspis nivalis	104	1,034	80	1,058	24
Paprides nitidus	83	1,055	65	1,073	18
Sigaus australis	263	875	187	951	76

Table S1.2. Climatic predictor variables initially investigated for ecological niche modelling (bio1–bio19). We included four additional variables describing geodiversity (soil type) and topography (slope, aspect, and roughness) derived from a fundamental soil layer and a digital elevation model obtained from the New Zealand Land Resource Information System portal (https://lris.scinfo.org.nz). Soil data was simplified from 72 to 20 major classes (e.g. Guisan et al., 2017). Variable selection was carried out using the *multGLM* function in the R package 'fuzzySim' v.3.0 (Barbosa 2015), which implements a stepwise selection procedure considering correlations among variables, false discovery rate, and parsimony. We also appraised the ecological relevance of selected variables favouring those expected to reflect a more direct influence on occurrences of these grasshopper species (e.g. temperature attributes: Carmelet-Rescan et al., 2021; Koot et al., 2022). Variables retained for final modelling depicting their final Variance Inflation Factor (VIF) value. Variable type is shown (dyn = dynamic, sta = static, con = continuous, cat = categorical).

Code	**Description**	**Variable**	***Brachaspis nivalis***	***Paprides nitidus***	***Sigaus australis***
bio1	Annual mean temperature (°C)	dyn, con	3.5587	2.3569	1.5307
bio2	Annual mean diurnal range (°C)	dyn, con	-	-	1.2284
bio3	Isothermality (%)	dyn, con	1.6952	1.7934	-
bio4	Temperature seasonality (SD, °C)	dyn, con	-	-	-
bio5	Max temperature of warmest month (°C)	dyn, con	-	-	-
bio6	Min temperature of coldest month (°C)	dyn, con	-	-	-
bio7	Temperature annual range (°C)	dyn, con	-	-	-
bio8	Mean temperature of wettest quarter (°C)	dyn, con	-	-	-
bio9	Mean temperature of driest quarter (°C)	dyn, con	2.8630	2.2475	2.8112
bio10	Mean temperature of warmest quarter	dyn, con	-	-	-
bio11	Mean temperature of coldest quarter (°C)	dyn, con	-	-	-
bio12	Annual precipitation (mm)	dyn, con	-	-	-
bio13	Precipitation of wettest month (mm)	dyn, con	-	-	-
bio14	Precipitation of driest month (mm)	dyn, con	1.1042	1.0759	1.1113
bio15	Precipitation seasonality (CV, %)	dyn, con	-	-	1.3506
bio16	Precipitation of wettest quarter (mm)	dyn, con	-	-	-
bio17	Precipitation of driest quarter (mm)	dyn, con	-	-	-
bio18	Precipitation of warmest quarter (mm)	dyn, con	-	-	-
bio19	Precipitation of coldest quarter (mm)	dyn, con	-	-	-
slope	Slope (°)	sta, con	-	-	-
asp	Aspect (°)	sta, con	-	-	-
rough	Roughness (°)	sta, con	-	-	-
soil	Soil type (class)	sta, cat	-	-	-

Table S1.3. As methods used to build ensemble models (Generalised Boosting Model, Random Forest, and Maximum Entropy) are susceptible to algorithm configuration (Hallgren et al., 2019), we sought the best set of tuneable hyperparameters using the R package 'SDMtune' v.1.1.4 (Vignali et al., 2021). Optimised models using the best performing hyperparameters showed a higher performance when compared to default models as indicated by AUC values. Model performance was estimated by randomly splitting our data into training (80%) and testing (20%) datasets. The training dataset was further split into three random folds to perform cross-validation. Evaluation metric on the training (AUC_{TRAIN}) and the test (AUC_{TEST}) datasets as the arithmetic mean across all cross-validation folds are shown.

Algorithm	**Default model**		**Optimised model**	
	AUC_{TRAIN}	**AUC_{TEST}**	**AUC_{TRAIN}**	**AUC_{TEST}**
Brachaspis nivalis				
Generalised Boosting Model	0.9353	0.8615	0.9686	0.9194
Random Forest	0.9998	0.8742	0.9999	0.9097
Maximum Entropy	0.9370	0.8934	0.9388	0.9297
Paprides nitidus				
Generalised Boosting Model	0.9598	0.9309	0.9854	0.9477
Random Forest	0.9998	0.9282	0.9998	0.9340
Maximum Entropy	0.9347	0.9297	0.9606	0.9371
Sigaus australis				
Generalised Boosting Model	0.9384	0.8551	0.9872	0.9389
Random Forest	0.9999	0.8877	0.9999	0.9378
Maximum Entropy	0.9505	0.8849	0.9561	0.9329

Table S1.4. List of tuneable hyperparameter tested using the R package 'SDMtune' v.1.1.4 (Vignali et al., 2021), indicating the best performing parameters used for refitting the final models for each species. Default values as implemented in the R package 'Biomod2' v.3.4.6 (Thuiller *et al*. 2020). The meaning of each tuneable hyperparameter can be found in the respective package documentation. Feature classes for Maximum Entropy are (l) linear, (q) quadratic, (p) product, and (h) hinge.

Algorithm	**Tuneable options**	**Default**	**Settings tested**	**Best performing parameters**		
				Brachaspis nivalis	***Paprides nitidus***	***Sigaus australis***
Generalised Boosting Model	number of trees	2500	750, 1250, 2500, 5000	750	2500	1250
	interaction depth	7	1, 3, 7, 10	10	7	7
	shrinkage	0.001	0.0005, 0.001, 0.002, 0.004	0.0005	0.001	0.004
	bag fraction	0.50	0.25, 0.50, 0.75, 1	0.5	0.75	0.75
Random Forest	# sampled variables	sqrt(#var)	1, 1.5, 2, 2.5, 3, 3.5, 4	3	3	2
	number of trees	500	250, 500, 1000, 2000	1000	1000	1000
	size of terminal nodes	5	1, 5, 10, 15, 20	15	5	20
Maximum Entropy	feature classes	lqpht	l, lq, lh, lqp, lqph, lqpht	lqph	lqpht	lh
	Regularisation multiplier	1	0.1, 0.5, 1, 1.5, 2, 2.5, 3	1.5	1	1

Table S1.5. The final mean-weighted ensemble models (EMmw) showed a high performance as indicated by their receiver operating characteristic (AUC), true positive rate, and true negative rate values. Cut-off values for generating binary maps are shown.

Species	AUC	Cut-off	True positive rate	True negative rate
Brachaspis nivalis	0.966	354.5	92.50	90.62
Paprides nitidus	0.981	209.5	100.00	90.85
Sigaus australis	0.978	462.5	93.58	91.69

Table S1.6. Contrasting sensitivity scores from niche factor analysis for New Zealand alpine grasshoppers *Brachaspis nivalis*, *Paprides nitidus*, and *Sigaus australis* under two climate change scenarios (RCP4.5 and 8.5). Bold values indicate the coefficients with the highest magnitude in each column. Departure reflects the extent to which a species will experience climate change (from current conditions) across its range and vulnerability reflects a species susceptibility to climate change.

Species	Sensitivity	RCP4.5		RCP8.5	
		Departure	Vulnerability	Departure	Vulnerability
Brachaspis nivalis	**3.208**	0.972	**1.940**	1.402	**1.980**
Paprides nitidus	2.672	0.973	1.777	1.485	1.830
Sigaus australis	2.171	**1.546**	1.667	**1.907**	1.689

Table S1.7. Significant CNFA factors for the studied species showing sensitivity, departure, and vulnerability factors under future climate scenarios (RCPs 4.5 and 8.5). Bioclimate variables are listed in decreasing magnitude of the coefficients of vulnerability. Bold values indicate the two coefficients with the largest magnitude in each column. The amount of specialisation in each CNFA factor is in parentheses.

Climate variable	**Marginality**	**Specialization 1**	**Specialization 2**	**Sensitivity**	**RCP 4.5**		**RCP 8.5**	
					Departure	**Vulnerability**	**Departure**	**Vulnerability**
Brachaspis nivalis	(14.41%)	(54.04%)	(25.20%)					
Mean temperature of driest quarter	0.08	**-0.97**	-0.36	**18.51**	**0.50**	**5.26**	**0.67**	**5.55**
Annual mean temperature	**-1.74**	-0.04	**0.58**	7.03	**0.73**	**3.48**	**1.13**	**3.87**
Isothermality	**-1.39**	-0.08	**-0.73**	**8.61**	0.37	3.44	0.49	3.58
Precipitation of driest month	0.46	**-0.24**	0.06	7.03	0.18	2.88	0.01	2.67
Paprides nitidus	(21.13%)	(44.54%)	(23.37%)					
Mean temperature of driest quarter	0.38	**-0.94**	0.29	**10.07**	0.42	**3.78**	**0.67**	**4.10**
Isothermality	**-1.20**	**-0.28**	**0.71**	**8.23**	**0.44**	**3.45**	0.64	**3.67**
Annual mean temperature	**-1.24**	-0.06	**-0.63**	5.51	**0.75**	3.10	**1.16**	3.45
Precipitation of driest month	0.29	-0.19	-0.13	4.74	0.12	2.30	0.01	2.19
Sigaus australis	(31.59%)	(45.85%)	(14.02%)					
Annual mean temperature	-1.54	**-0.54**	-	**6.95**	**0.68**	**3.41**	**1.06**	**3.78**
Precipitation seasonality	**-0.94**	**0.65**	-	**6.38**	0.67	**3.38**	0.91	**3.61**
Mean temperature of driest quarter	-0.75	-0.12	-	2.59	**1.19**	2.38	**1.30**	2.44
Precipitation of driest month	0.40	-0.51	-	5.10	0.21	2.48	0.02	2.28
Annual mean diurnal range	**0.86**	-0.12	-	4.34	0.15	2.23	0.06	2.15

Figure S1.1. Aotearoa New Zealand showing vegetation cover changes since the arrival of humans (Leathwick et al., 2004). Tall forest vegetation before humans reached Aotearoa about 800 years ago (Wilmshurst et al., 2008) was incompatible with native alpine grasshopper occupancy (Sivyer et al., 2018).

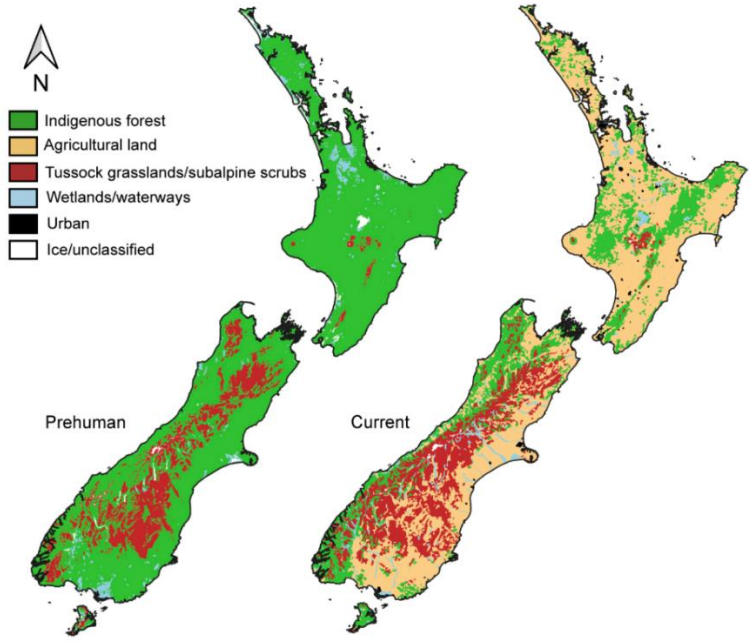

Figure S1.2. Occurrence data for New Zealand grasshoppers at 1,138 locations used in ecological niche modelling. Grasshopper niches were modelled based on their native distributions in naturally occurring open habitats, representing the native realised niche of these species: (a) *Brachaspis nivalis* (80 presences, 1,058 absences), (b) *Paprides nitidus* (65 presences, 1,073 absences), and (c) *Sigaus australis* (187 presences, 951 absences). (d) Locations where the focal species were not found during searches (i.e., absences).

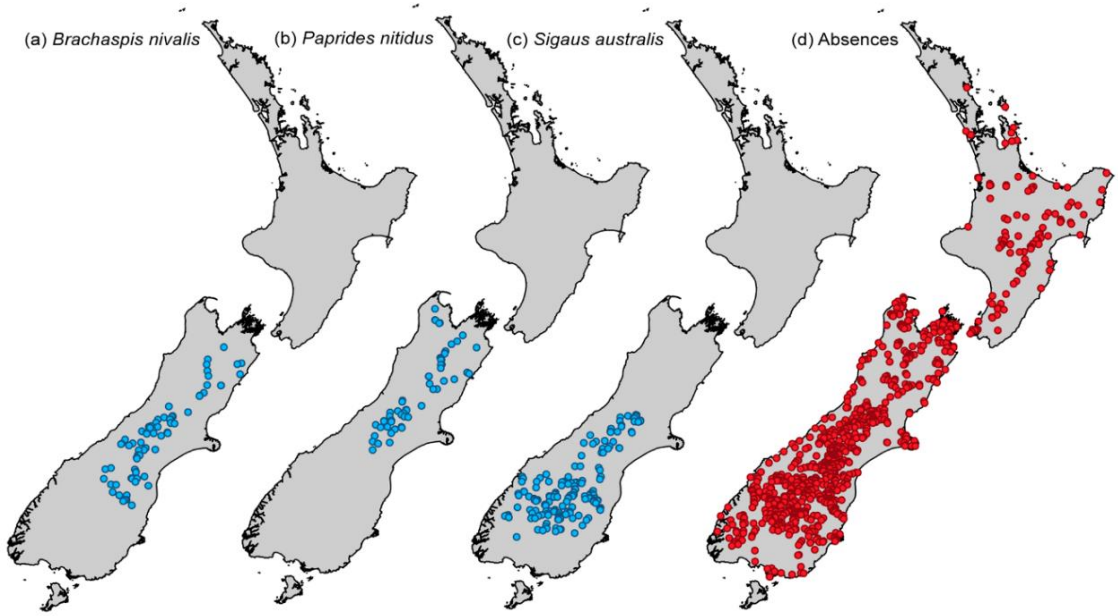

Figure S1.3. Spatial block arrangement of presence-absence data for one of the five folds used for modelling the ecological niche of *Brachaspis nivalis*, *Paprides nitidus*, and *Sigaus australis*. We we divided our study region into 34 equal-sized square blocks (~150 × 150 km), using the R package 'blockCV' v.2.1.1 (Valavi et al., 2019). The optimal block size was determined based on 10,000 sample points to estimate the effective autocorrelation range of all predictor variables. The blocks were allocated into five folds for cross-validation, each containing a similar number of presence and absence records.

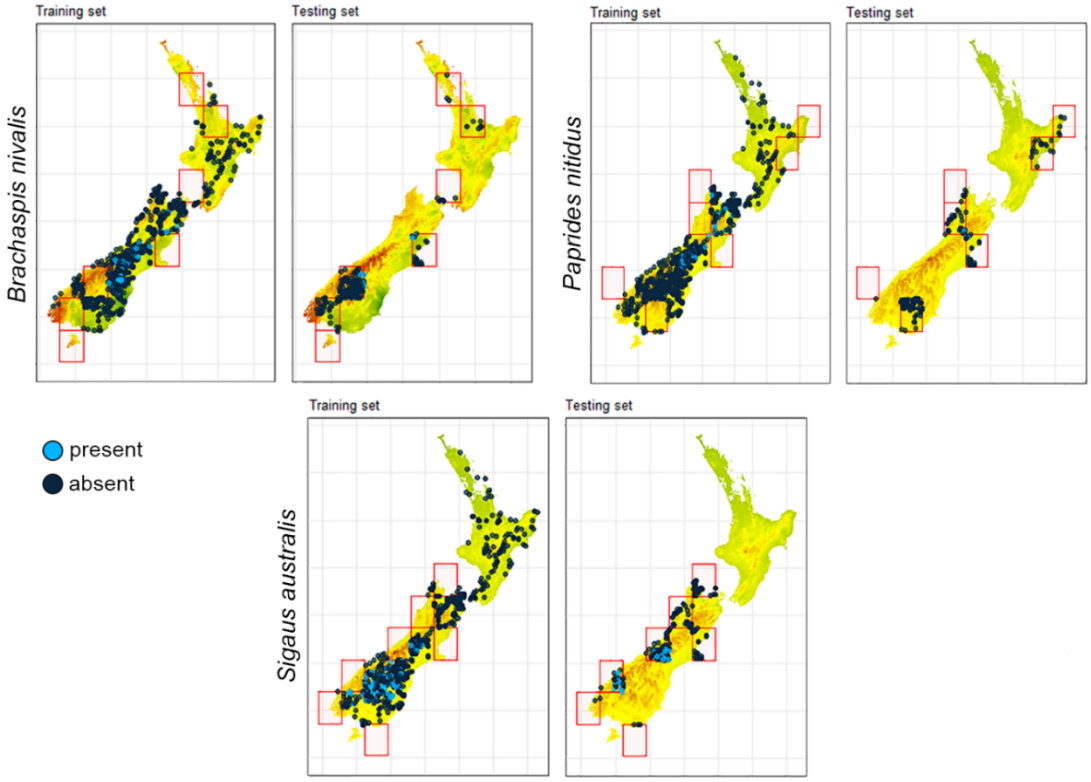

Figure S1.4. Individual models showed good to excellent predictive performance as indicated by their Receiver Operating Characteristic (ROC) and True Skill Statistic (TSS). Generalised Boosting Model (GBM), Random Forest (RF), and Maximum Entropy (MaxEnt).

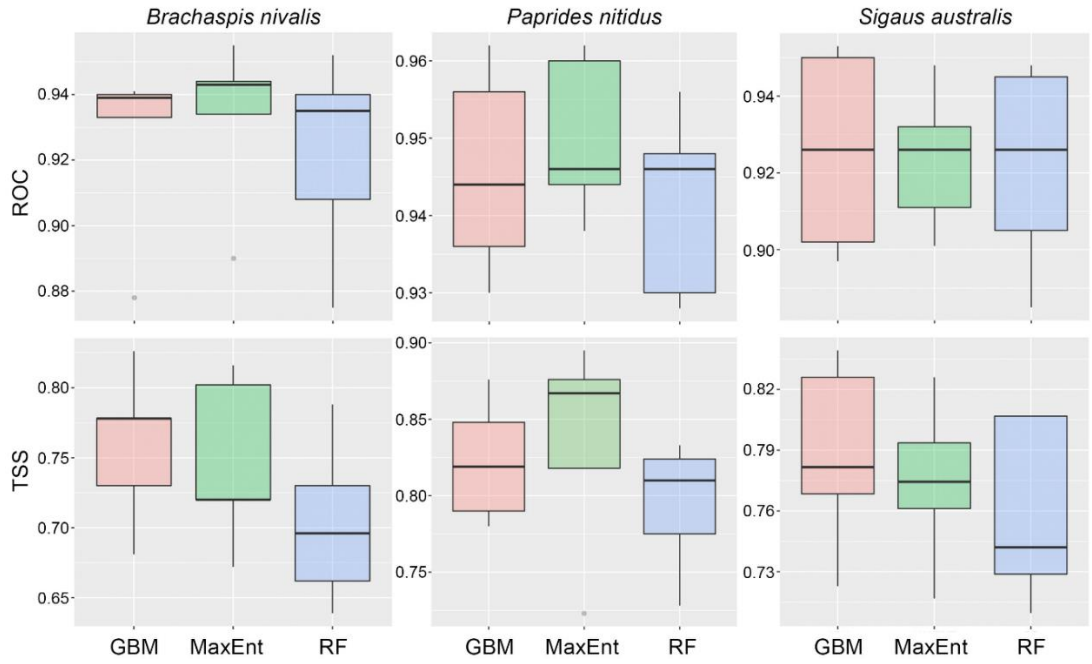

Figure S1.5. Temperature related predictors had the most significant influence on the environmental envelope estimated for all species. Variable importance scores for individual models were calculated by subtracting the mean correlation score of each predictor from 1, with scores closest to 1 indicating highly important variables. Variable importance scores and confidence bars (95%) are reported as percentages of total probability scores for the final mean-weighted ensemble models (EMmw). Variable codes as in Table S1.2.

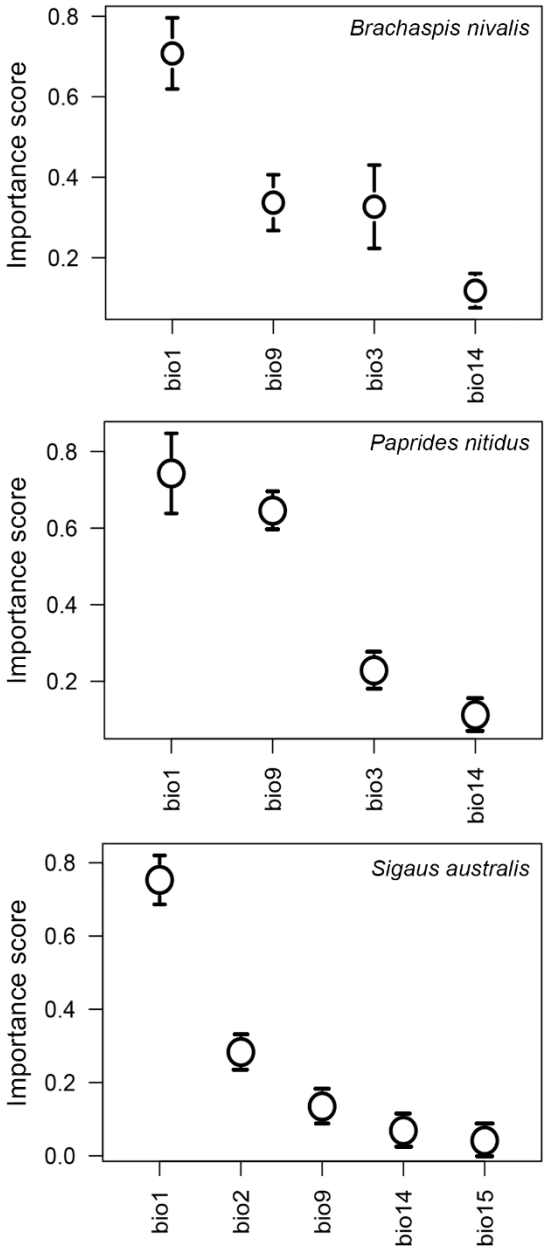

Figure S1.6. Potential niche spaces predicted for *Brachaspis nivalis*, *Paprides nitidus*, and *Sigaus australis* using the final mean-weighted ensemble models (EMmw). Predictions during the LGM show the inferred land extension (LGM–no ice) and areas covered by valley glaciers (LGM–ice) after James et al. (2019).

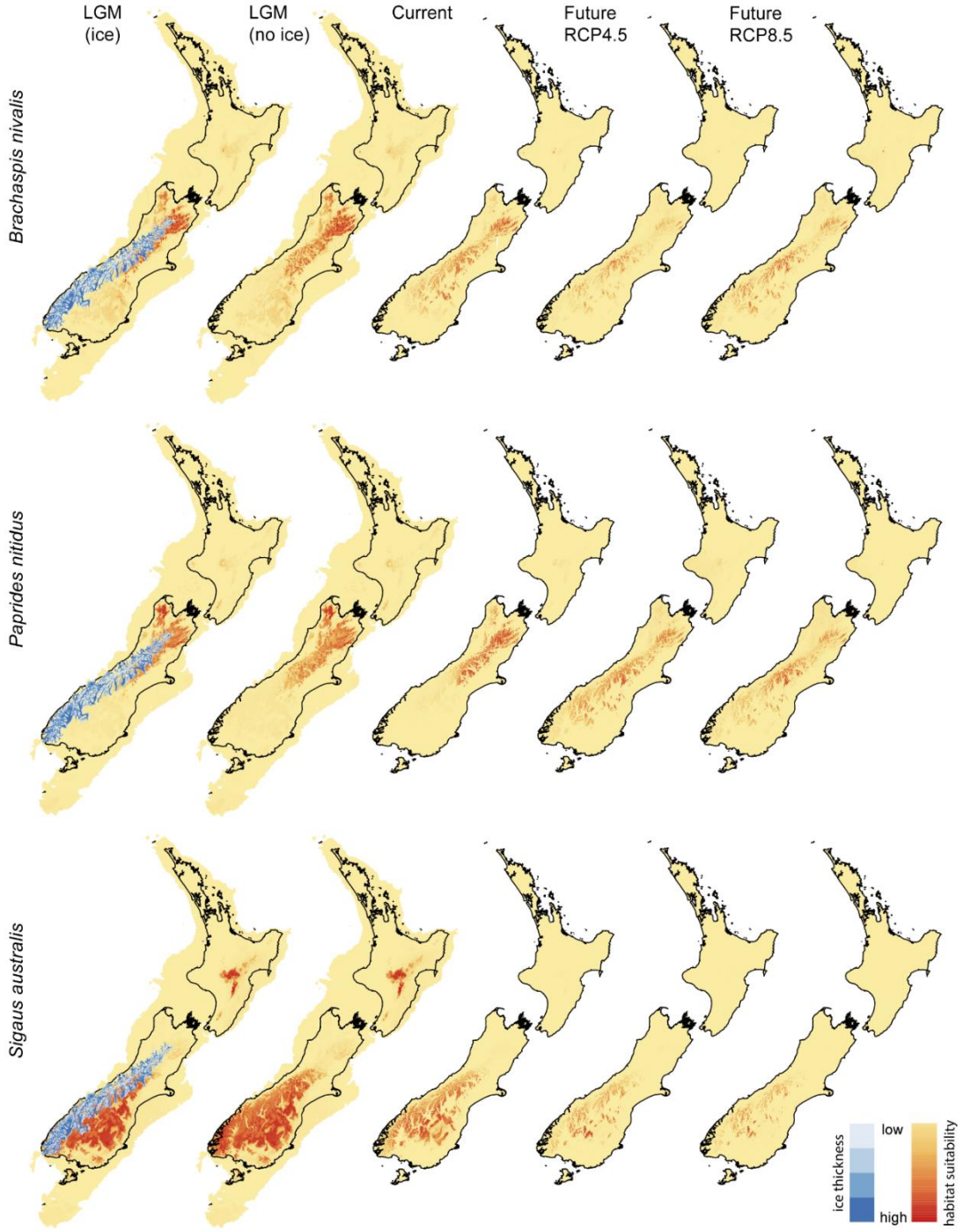

Figure S1.7. Predicted shifts of suitable native habitat in latitude (°), elevation (m), and size (km^2) under future climate scenarios (RCPs 4.5 and 8.5) for *Brachaspis nivalis*, *Paprides nitidus*, and *Sigaus australis*.

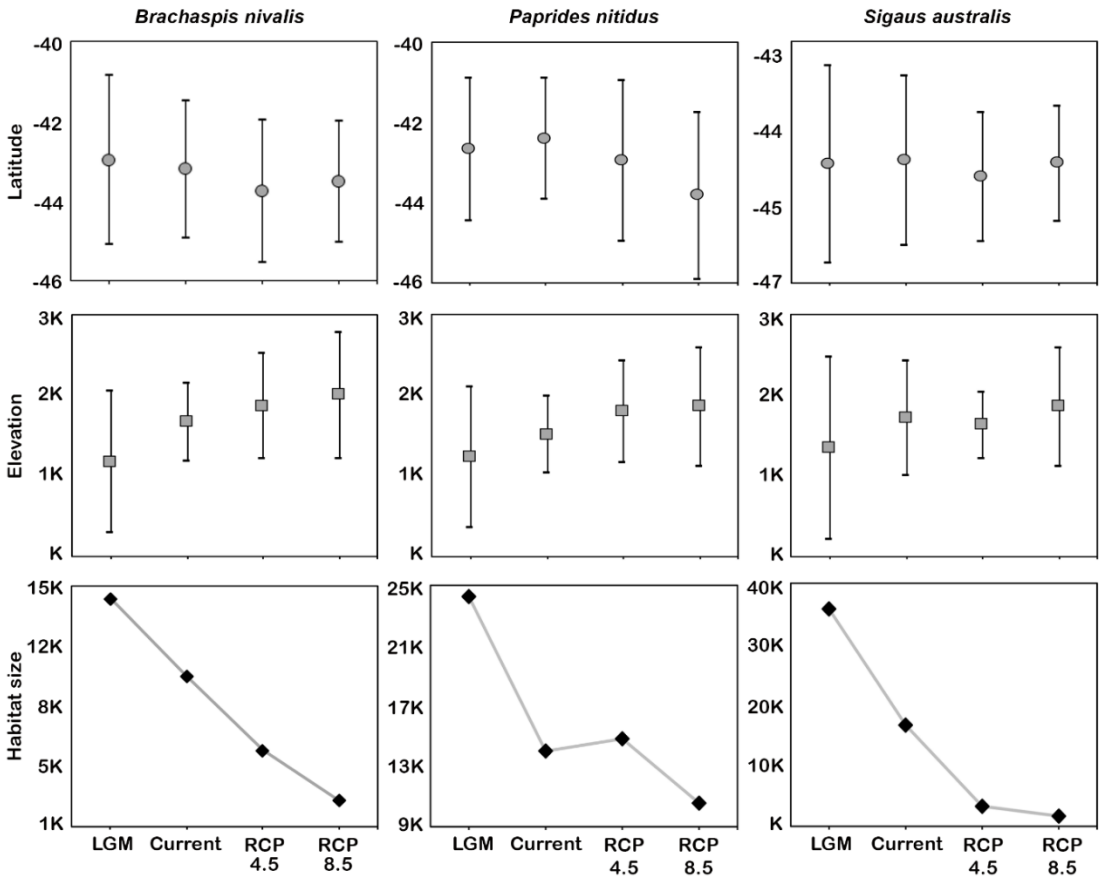

Supplementary references not included in the main text

Guisan, A., Thuiller, W., & Zimmermann, N. E. (2017). *Habitat suitability and distribution models*. Cambridge University Press. https://doi.org/10.1017/9781139028271

Hallgren, W., Santana, F., Low-Choy, S., Zhao, Y., & Mackey, B. (2019). Species distribution models can be highly sensitive to algorithm configuration. *Ecological Modelling*, *408*, 108719. https://doi.org/10.1016/j.ecolmodel.2019.108719

Appendix 2. This appendix contains additional information about molecular and genetic methods and results.

Table S2.1. Grasshopper mountain populations sampled for genetic analyses showing the number of individuals and geographic information.

Mountain	Site	Number of individuals			Latitude	Longitude	Elevation (m)
		Brachaspis nivalis	***Paprides nitidus***	***Sigaus australis***			
Mt Arthur	Around Flora Hut	-	2	-	-41.198	172.713	~1,340
Mt Altimarloch	-	-	2	-	-41.753	173.775	~1,662
Mt McRae	Rainbow Ski Area	6	19	-	-41.869	172.865	1,462–1,830
Mt Lyford	Mt Lyford Alpine Resort	3	13	-	-42.446	173.141	~1,468
Mt Olympus	Mt Olympus Ski Area	10	22	15	-43.188	171.605	1,660–1,825
Mt Hutt	Mt Hutt Ski Area	11	19	16	-43.495	171.537	1,450–1625
Fox Peak	Fox Peak Ski Area	16	17	20	-43.855	170.810	1,340–1700
Mt Dobson	Mt Dobson Ski Area	6	-	13	-43.946	170.658	1,700
Mt Sutton	Ohau Ski Field	3	-	13	-44.225	169.783	1,406
Rocky Top	Awakino Ski Field	6	-	10	-44.780	170.320	1,923
Mt Cardrona	Cardrona Alpine Resort	-	-	20	-44.877	168.953	1,190–1,890
Double Cone	The Remarkables Ski Area	-	-	5	-45.057	168.808	1,877
Mt Luxmore	Around Kepler Track	-	-	6	-45.386	167.585	1,386
Summit Rock	-	-	-	9	-45.422	170.072	1,290
Spencer Peak	-	-	-	5	-45.716	167.852	1,548
Total individuals		**61**	**94**	**132**			

Table S2.2. Pairwise Φ_{ST} showed significant genetic differentiation among populations ($n \geq 5$) of *Brachaspis nivalis* (A). Estimates of evolutionary divergence based on mean pairwise ND2 mtDNA genetic distances suggest an ancient divergence between northern and southern lineages (B). Kimura 2-parameter (lower left) and Tamura-Nei model (upper right). The rate variation among sites was modelled with a gamma distribution (shape parameter = 1).

(A) Pairwise Φ_{ST} values

	Mt Dobson	Rocky Top	Mt Olympus	Fox Peak	Mt Hutt	Mt McRae
Mt Dobson	-					
Rocky Top	0.520	-				
Mt Olympus	0.931	0.927	-			
Fox Peak	0.409	0.785	0.969	-		
Mt Hutt	0.914	0.908	0.544	0.957	-	
Mt McRae	0.939	0.938	0.947	0.980	0.916	-

(B) Pairwise genetic distances

	Mt McRae	Mt Altimarloch	Mt Olympus	Mt Hutt	Fox Peak	Mt Dobson	Mt Sutton	Rocky Top
Mt McRae	-	0.021	0.075	0.076	0.128	0.122	0.094	0.129
Mt Altimarloch	0.020	-	0.055	0.060	0.132	0.126	0.099	0.129
Mt Olympus	0.070	0.053	-	0.013	0.118	0.115	0.102	0.111
Mt Hutt	0.071	0.057	0.013	-	0.120	0.117	0.104	0.113
Fox Peak	0.116	0.118	0.109	0.111	-	0.008	0.030	0.021
Mt Dobson	0.111	0.113	0.106	0.108	0.008	-	0.027	0.021
Mt Sutton	0.087	0.091	0.093	0.096	0.029	0.026	-	0.030
Rocky Top	0.115	0.115	0.102	0.105	0.021	0.021	0.029	-

Table S2.3. Pairwise Φ_{ST} showed significant genetic differentiation among populations ($n \geq 5$) of *Paprides nitidus* (A). Estimates of evolutionary divergence based on mean pairwise ND2 mtDNA genetic distances suggest an ancient divergence between northern and southern lineages (B). Kimura 2-parameter (lower left) and Tamura-Nei model (upper right). The rate variation among sites was modelled with a gamma distribution (shape parameter = 1).

(A) Pairwise Φ_{ST} values

	Mt Olympus	Fox Peak	Mt Hutt	Mt McRae	Mt Lyford
Mt Olympus	-				
Fox Peak	0.803	-			
Mt Hutt	0.778	0.817	-		
Mt McRae	0.736	0.969	0.955	-	
Mt Lyford	0.615	0.913	0.894	0.863	-

(B) Pairwise genetic distances

	Mt Arthur	Mt Altimarloch	Mt McRae	Mt Lyford	Mt Olympus	Mt Hutt	Fox Peak
Mt Arthur	-	0.062	0.074	0.069	0.098	0.110	0.109
Mt Altimarloch	0.060	-	0.024	0.024	0.065	0.073	0.086
Mt McRae	0.070	0.024	-	0.036	0.072	0.085	0.097
Mt Lyford	0.066	0.024	0.035	-	0.063	0.072	0.082
Mt Olympus	0.091	0.062	0.069	0.061	-	0.098	0.114
Mt Hutt	0.104	0.071	0.081	0.070	0.094	-	0.026
Fox Peak	0.104	0.082	0.092	0.079	0.108	0.025	-

Table S2.4. Pairwise Φ_{ST} showed significant genetic differentiation among populations ($n \geq 5$) of *Sigaus australis* (A). Estimates of evolutionary divergence based on mean pairwise ND2 mtDNA genetic distances suggest an ancient divergence between northern and southern lineages (B). Kimura 2-parameter (lower left) and Tamura-Nei model (upper right). The rate variation among sites was modelled with a gamma distribution (shape parameter = 1).

(A) Pairwise Φ_{ST} values

	Mt Olympus	Fox Peak	Mt Cardrona	Mt Hutt	Mt Sutton	Summit Rock	Spencer Peak	Mt Luxmore	Rocky Top	Mt Dobson	Double Cone
Mt Olympus	0.000										
Fox Peak	0.920	0.000									
Mt Cardrona	0.944	0.957	0.000								
Mt Hutt	0.825	0.941	0.961	0.000							
Mt Sutton	0.810	0.841	0.724	0.825	0.000						
Summit Rock	0.956	0.975	0.940	0.978	0.604	0.000					
Spencer Peak	0.934	0.965	0.900	0.968	0.632	0.952	0.000				
Mt Luxmore	0.941	0.968	0.905	0.974	0.621	0.964	0.844	0.000			
Rocky Top	0.941	0.963	0.920	0.962	0.577	0.914	0.921	0.933	0.000		
Mt Dobson	0.853	0.477	0.927	0.867	0.778	0.941	0.913	0.916	0.920	0.000	
Double Cone	0.950	0.974	0.839	0.981	0.635	0.980	0.936	0.965	0.949	0.926	0.000

(B) Pairwise genetic distances

	Mt Olympus	Mt Hutt	Fox Peak	Mt Dobson	Mt Sutton	Rocky Top	Mt Cardrona	Double Cone	Mt Luxmore	Summit Rock	Spencer Peak
Mt Olympus		0.027	0.066	0.061	0.140	0.127	0.134	0.132	0.152	0.126	0.131
Mt Hutt	0.026		0.050	0.045	0.126	0.099	0.123	0.119	0.128	0.121	0.127
Fox Peak	0.063	0.048		0.011	0.133	0.120	0.120	0.123	0.146	0.119	0.132
Mt Dobson	0.059	0.044	0.011		0.132	0.114	0.117	0.118	0.144	0.112	0.126
Mt Sutton	0.128	0.117	0.121	0.120		0.056	0.072	0.076	0.059	0.073	0.082
Rocky Top	0.116	0.094	0.110	0.105	0.054		0.069	0.068	0.043	0.069	0.073
Mt Cardrona	0.123	0.114	0.110	0.108	0.070	0.066		0.025	0.079	0.054	0.058
Double Cone	0.121	0.112	0.113	0.110	0.073	0.066	0.025		0.085	0.054	0.055
Summit Rock	0.138	0.119	0.133	0.132	0.057	0.042	0.076	0.082		0.082	0.088
Mt Luxmore	0.115	0.111	0.111	0.104	0.070	0.065	0.052	0.053	0.079		0.031
Spencer Peak	0.119	0.117	0.122	0.116	0.079	0.071	0.057	0.054	0.084	0.031	

Table S2.5. Summary statistics (± standard deviation) for mountain populations of New Zealand alpine grasshoppers ($n \geq 5$) based mitochondrial ND2 sequence data. Sample size (*n*), number of observed haplotypes (N_h), number of polymorphic sites (S), haplotype diversity (*h*), and nucleotide diversity (π). Bold values indicate the largest coefficients of genetic variation. No polymorphisms in the data (-).

Species	**Population**	***n***	**N_h**	**S**	***h***	**π**
Brachaspis	Mt McRae	6	3	3	0.6000 ± 0.0007	0.0017 ± 0.0007
	Mt Olympus	10	7	12	0.8670 ± 0.0115	0.0042 ± 0.0019
	Mt Hutt	11	6	11	0.8550 ± 0.0850	0.0072 ± 0.0014
	Fox Peak	16	6	8	0.6170 ± 0.0182	0.0020 ± 0.0008
	Mt Dobson	6	6	12	**1.0000 ± 0.0960**	0.0084 ± 0.0014
	Rocky Top	6	6	16	**1.0000 ± 0.0960**	**0.0102 ± 0.0960**
	Species	61	39	101	0.9640 ± 0.0140	0.0571 ± 0.0019
Paprides nitidus	Mt McRae	19	6	6	0.5380 ± 0.1330	0.0014 ± 0.0004
	Mt Lyford	13	10	18	**0.9490 ± 0.0510**	0.0091 ± 0.0012
	Mt Olympus	22	11	40	0.9090 ± 0.0370	**0.0298 ± 0.0021**
	Mt Hutt	19	12	14	0.9240 ± 0.0420	0.0050 ± 0.0013
	Fox Peak	17	12	12	**0.9490 ± 0.0370**	0.0038 ± 0.0008
	Species	94	55	123	0.9720 ± 0.0090	0.0553 ± 0.0014
Sigaus australis	Mt Olympus	15	9	14	0.9140 ± 0.0520	0.0068 ± 0.0013
	Mt Hutt	16	6	5	0.8000 ± 0.0680	0.0022 ± 0.0004
	Fox Peak	20	10	9	0.8790 ± 0.0520	0.0030 ± 0.0005
	Mt Dobson	13	7	14	0.8720 ± 0.0670	0.0093 ± 0.0014
	Mt Sutton	13	9	47	**0.9490 ± 0.0420**	**0.0347 ± 0.0060**
	Rocky Top	10	7	10	0.8670 ± 0.1070	0.0044 ± 0.0010
	Mt [illegible]	20	13	14	0.9420 ± 0.0340	0.0050 ± 0.0006
	Double [illegible]	5	1	0	-	-
	Mt Luxmore	6	4	4	0.8000 ± 0.1720	0.0031 ± 0.0007
	Summit [illegible]	9	5	5	0.7220 ± 0.1590	0.0021 ± 0.0007
	Spencer	5	4	7	0.9000 ± 0.1610	0.0063 ± 0.0013
	Species	13	69	133	**0.9840 ± 0.0030**	**0.0660 ± 0.0011**

Table S2.6. Demographic statistics for mountain populations of New Zealand alpine grasshoppers ($n \geq 5$) based on mtDNA ND2 sequence data were in most cases consistent with the hypothesis of constant population size. Sample size (*n*), mismatch distribution shape (Mismatch), Harpending's raggedness index (*r*), Tajima's *D*, Fu's *Fs*, and Ramos-Onsins and Roza's R_2. Significance is given within parentheses with significant values denoted in bold ($p < 0.05$ except for *Fs* where $p < 0.02$). No polymorphisms in the data (-).

Species	Lineage	*n*	Mismatch	*r*	*D*	*Fs*	R_2	Expansion
Brachaspis nivalis	Mt McRae	6	skewed bimodal	**0.062 (0.000)**	**-1.233 (0.000)**	-0.190 (0.283)	0.255 (0.614)	No
	Mt Olympus	10	bimodal	0.208 (0.818)	**-1.796 (0.010)**	-2.511 (0.084)	0.169 (0.555)	No
	Mt Hutt	11	bimodal	0.088 (0.388)	0.655 (0.793)	0.362 (0.584)	0.188 (0.773)	No
	Fox Peak	16	skewed bimodal	0.071 (0.279)	**-1.811 (0.015)**	-2.122 (0.131)	0.126 (0.323)	No
	Mt Dobson	6	multimodal	0.177 (0.622)	-0.275 (0.432)	-2.814 (0.054)	0.127 (0.068)	No
	Rocky Top	6	bimodal	0.116 (0.292)	-0.771 (0.253)	-1.773 (0.072)	0.261 (0.868)	No
	Species	61	multimodal	0.007 (0.282)	2.080 (0.998)	-1.224 (0.410)	0.168 (0.976)	No
Paprides nitidus	Mt McRae	19	skewed unimodal	0.061 (0.173)	**-1.693 (0.029)**	-2.986 (0.034)	**0.076 (0.002)**	Yes
	Mt Lyford	13	multimodal	0.086 (0.578)	-2.220 (0.451)	-2.670 (0.094)	0.123 (0.228)	No
	Mt Olympus	22	bimodal	0.030 (0.439)	2.488 (0.999)	3.666 (0.925)	0.221 (0.998)	No
	Mt Hutt	19	skewed bimodal	0.074 (0.493)	-0.893 (0.199)	**-5.484 (0.012)**	0.095 (0.106)	No
	Fox Peak	17	skewed bimodal	0.115 (0.660)	-1.358 (0.080)	**-8.231 (<0.001)**	0.098 (0.093)	No
	Species	94	multimodal	0.004 (0.087)	1.288 (0.929)	-4.031 (0.220)	0.134 (0.926)	No
Sigaus australis	Mt Olympus	15	multimodal	0.149 (0.810)	-0.439 (0.366)	-1.956 (0.171)	0.147 (0.306)	No
	Mt Hutt	16	skewed unimodal	0.100 (0.322)	-0.361 (0.404)	-1.796 (0.138)	0.128 (0.287)	No
	Fox Peak	20	skewed unimodal	0.071 (0.319)	-1.006 (0.148)	-5.162 (**0.007**)	0.089 (0.067)	No
	Mt Dobson	13	multimodal	0.036 (0.096)	0.992 (0.876)	0.564 (0.630)	0.190 (0.860)	No
	Mt Sutton	13	multimodal	0.042 (0.462)	1.698 (0.977)	2.162 (0.841)	0.219 (0.985)	No
	Rocky Top	10	skewed unimodal	0.039 (0.053)	-1.089 (0.147)	-2.386 (0.079)	0.120 (0.083)	No
	Mt Cardrona	20	skewed unimodal	0.050 (0.288)	-0.892 (0.192)	**-6.781 (0.004)**	0.094 (0.111)	No
	Double Cone	5	-	-	-	-	-	-
	Mt Luxmore	6	skewed bimodal	0.200 (0.339)	0.355 (0.662)	-0.625 (0.351)	0.191 (0.262)	No
	Summit Rock	9	skewed unimodal	**0.054 (0.045)**	-1.294 (0.077)	-1.886 (0.095)	0.142 (0.092)	No
	Spencer Peak	5	skewed bimodal	0.250 (0.496)	0.913 (0.752)	0.051 (0.506)	0.225 (0.518)	No
	Species	132	multimodal	0.003 (0.066)	1.673 (0.957)	-4.445 (0.241)	0.139 (0.965)	No

Table S2.7. Predicted shifts in suitable native area (Km^2) and sampled intraspecific diversity (± standard deviation) for three endemic, alpine grasshoppers *Brachaspis nivalis*, *Paprides nitidus*, and *Sigaus australis* under two future climate scenarios (RCP4.5 and RCP8.5). Number of populations (n_p), sample size (n_s), number of observed haplotypes (N_h), haplotype diversity (h), and nucleotide diversity (π).

Climate scenario	Area	n_p	n_s	N_h	h	π
Brachaspis nivalis						
Current	9,720	8	61	39	0.9640 ± 0.0140	0.0571 ± 0.0019
Future (RCP4.5)	5,411	6	42	29	0.9730 ± 0.0120	0.0556 ± 0.0031
Future (RCP8.5)	2,482	4	33	25	0.9730 ± 0.0160	0.0486 ± 0.0044
Paprides nitidus						
Current	12,757	7	94	55	0.9720 ± 0.0090	0.0553 ± 0.0014
Future (RCP4.5)	13,369	6	92	53	0.9700 ± 0.0090	0.0544 ± 0.0013
Future (RCP8.5)	10,169	5	90	51	0.9690 ± 0.0100	0.0546 ± 0.0013
Sigaus australis						
Current	16,651	11	132	69	0.9840 ± 0.0030	0.0660 ± 0.0011
Future (RCP4.5)	3,293	5	62	37	0.9750 ± 0.0080	0.0588 ± 0.0008
Future (RCP8.5)	1,684	5	64	34	0.9700 ± 0.0080	0.0596 ± 0.0011

FigureS2.1. Phylogenetic trees for (a) *Brachaspis nivalis*, (b) *Paprides nitidus*, and (c) *Sigaus australis*. For convenience, identical sequences were excluded from the analyses. Only nodes with strong support are labelled (posterior probability ≥ 95). Nodes with maximum support (1.00) are indicated with an asterisk. Terminals are coloured according to the sampling locations in Figure 1.

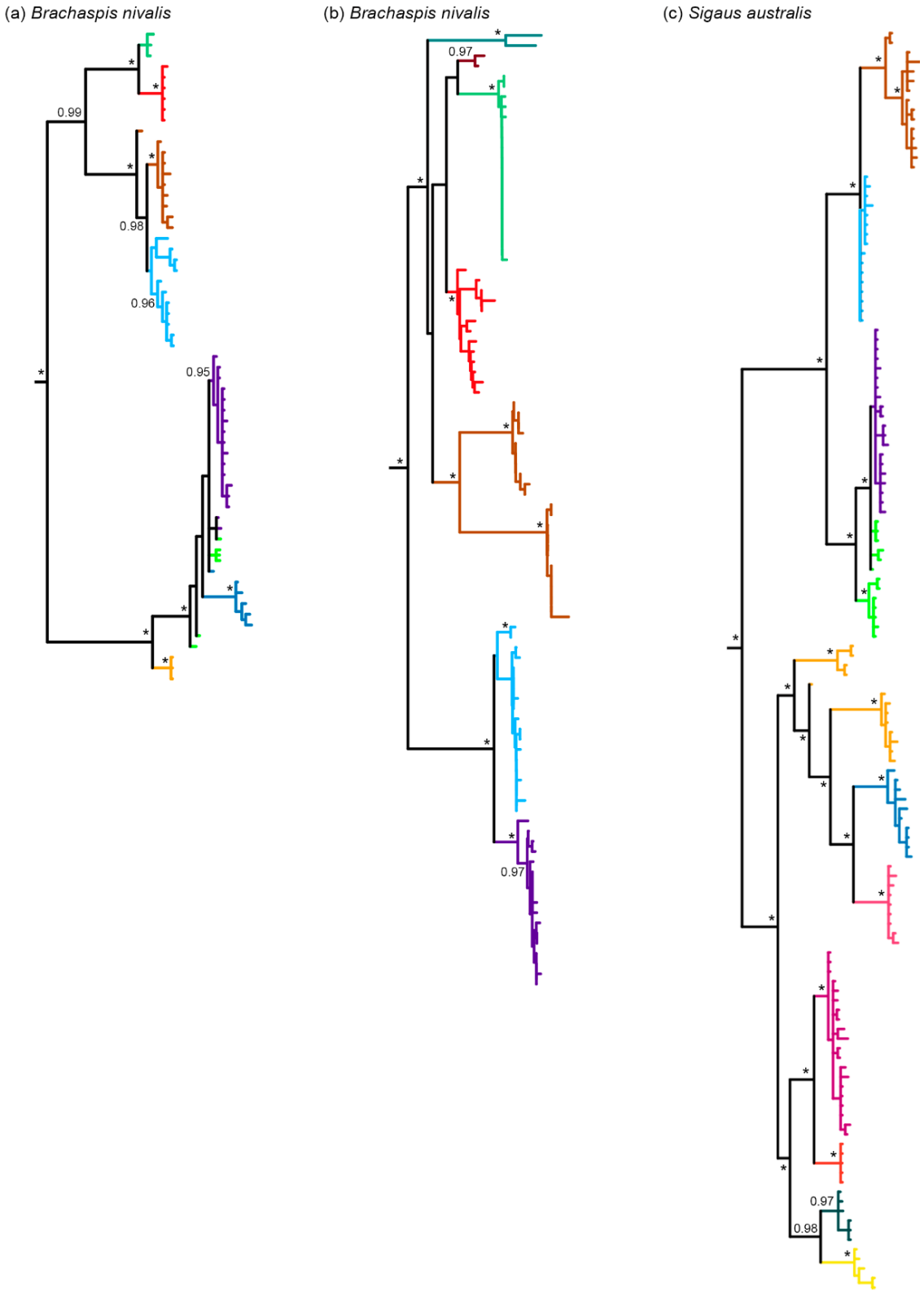

“One of the most common charges against body size relationships is that they have sacrificed precision to achieve generality.... This is true; a statistical description is always less precise (and more general) than the individual members of the data set.”

(Peters, 1983, p. 5)

Paprides nitidus, a grassland/herbfield-dwelling grasshopper within the New Zealand alpine radiation. Temple Basin, Arthur’s Pass National Park, South Island.

Chapter Three

Relationships among body size components of three flightless New Zealand grasshopper species (Orthoptera, Acrididae) and their ecological applications

MASSEY UNIVERSITY
TE KUNENGA KI PŪREHUROA
UNIVERSITY OF NEW ZEALAND

GRADUATE RESEARCH SCHOOL

STATEMENT OF CONTRIBUTION
DOCTORATE WITH PUBLICATIONS/MANUSCRIPTS

We, the student and the student's main supervisor, certify that all co-authors have consented to their work being included in the thesis and they have accepted the student's contribution as indicated below in the Statement of Originality.

Student name:	Fabio Leonardo Meza Joya
Name and title of main supervisor:	Steven A. Trewick
In which chapter is the manuscript/published work?	Chapter 3

Describe the contribution that the student and members of the supervisory team have made to the manuscript/published work:[1]

Conceptualization: Fabio Leonardo Meza-Joya, Steven A. Trewick and Mary Morgan-Richards; Data collection, curation and analysis: Fabio Leonardo Meza-Joya; Visualization and writing – original draft: Fabio Leonardo Meza-Joya; Writing – review and editing: Steven A. Trewick and Mary Morgan-Richards; Funding acquisition: Fabio Leonardo Meza-Joya, Steven A. Trewick and Mary Morgan-Richards; Supervision: Steven A. Trewick and Mary Morgan-Richards.

Please select one of the following three options:

- (●) The manuscript/published work is published or in press

  Please provide the full reference of the research output:

  Meza-Joya, F. L., Morgan-Richards, M., & Trewick, S. A. (2022). Relationships among body size components of three flightless New Zealand grasshopper species (Orthoptera, Acrididae) and their ecological applications. Journal of Orthoptera Research, 31(1), 91–103. https://doi.org/10.3897/jor.31.79819

- ( ) The manuscript is currently under review for publication

  Please provide the name of the journal:

- ( ) It is intended that the manuscript will be published, but it has not yet been submitted to a journal

Student's signature:	Fabio Leonardo Meza Joya — Digitally signed by Fabio Leonardo Meza Joya Date: 2024.01.02 14:53:32 +13'00'	Main supervisor's signature:	Digitally signed by Steve Trewick Date: 2024.01.09 10:37:03 +13'00'

This form should be placed at the beginning of each relevant thesis chapter.

[1] Refer to the Massey University Publishing and Authorship guidelines (OneMassey for staff, Stream for students) and/ or Contributor Roles Taxonomy (CRediT) guidelines for guidance.

Abstract

Body size is perhaps the most fundamental property of an organism and is central to ecology at multiple scales, yet obtaining accurate estimates of ecologically meaningful size metrics, such as body mass, is often impractical. Allometric scaling and mass-to-mass relationships have been used as alternative approaches to model the expected body mass of many species. However, models for predicting body size in key herbivorous insects, such as grasshoppers, exist only at the family level. To address this data gap, we collected empirical body size data (hind femur length and width, pronotum length, live fresh mass, ethanol-preserved mass, and dry mass) from 368 adult grasshoppers of three flightless species at Hamilton Peak, Southern Alps, New Zealand. We examined the relationships among body size components across all species using linear and non-linear regression models. Femur length and preserved mass were robust predictors of both fresh mass and dry mass across all species; however, regressions using preserved mass as a predictor always showed higher predictive power than those using femur length. Based on our results, we developed species-specific statistical linear mixed-effects models to estimate the fresh and dry masses of individual grasshoppers from their preserved mass and femur length. Including sex as an additional co-variate increased model fit in some cases but did not produce better estimates than traditional mass-to-mass and allometric scaling regressions. Overall, our results showed that two easy-to-measure, unambiguous, highly repeatable, and non-destructive size measures (i.e. preserved mass and femur length) can predict, to an informative level of accuracy, fresh and dry body mass across three flightless grasshopper species. Knowledge about the relationships between body dimensions and body mass estimates in these grasshoppers has several important ecological applications, which are discussed.

Keywords: allometric scaling, body mass, linear body dimension, mass-to-mass relationships, predictive models

Introduction

Organism body size is one of the most important axes in ecology, as it is related to nearly all biological processes, from individual performance to ecosystem function (Whitman, 2008; Chown & Gaston, 2010). In insects, body size is closely linked to physiological rates (e.g. metabolic and growth), life-history traits (e.g. longevity and fecundity), and ecological attributes, such as abundance, range size, and dispersal (Peters, 1983; Siemann et al., 1996; Whitman, 2008; Chown & Gaston, 2010; Ehnes et al., 2011; Stevens et al., 2012). Moreover, arthropod body size is central to the contribution of individuals and communities to key ecosystem processes and services, such as decomposition, carbon cycling, primary productivity, pollination, predation, and herbivory (Cízek, 2005; Barnes et al., 2018; Kendall et al., 2019). Therefore, changes in the body size of a taxon reflect changes in resources that may cascade across all levels of biological organization. For example, body size differences are usually associated with individual survival and fecundity, and changes in body size might alter ecological processes, including trophic interactions, plant-animal interactions, and food web connectivity (Peters, 1983; Stang et al., 2009; DeLong et al., 2015; Horne et al., 2018).

Adult body size in Orthoptera is generally expressed in terms of length and mass, each of which is controlled by both genetic and environmental factors that operate through molecular and physiological mechanisms (Nijhout, 2003; Whitman, 2008; Chown & Gaston, 2010). Although length and mass are often correlated, each captures a different aspect of an organism's size and is subject to different selective pressures during an organism's lifespan (Gaston & Blackburn, 2000). Insect structural body size (e.g. length dimensions) is determined during development by gene–environment interactions, whereas adult body mass additionally varies through time depending on environmental factors, for example, reproductive phase and nutritional status (Whitman, 2008; Chown & Gaston, 2010; Knapp & Knappová, 2013). Despite this fact, body mass- and linear-based estimates are often used interchangeably as measures of adult body size in ecological research (Chown & Gaston, 2010). Decisions on the body size measure used in a particular study should be made cautiously and considering the research question and species (Gaston & Blackburn, 2000; Moretti et al., 2017).

Body mass is the most meaningful size metric, as it is directly linked with metabolic rate and is affected by environmental conditions (Gaston & Blackburn, 2000; Sohlström et

al., 2018). Therefore, fresh (live) mass is preferred to relate body size to a range of functional and ecological attributes, such as metabolism, movement, and abundance (e.g. Chown & Steenkamp, 1996; Meehan, 2006; Ehnes et al., 2011; Hirt et al., 2017). In some instances, however, dry mass is recorded to estimate, for example, organism biomass, since variation from water content is reduced (e.g. Sage, 1982; Cressa, 1999; Sabo et al., 2002; Gilbert, 2011; Penell et al., 2018). While body mass is a useful predictive trait for many ecosystem processes, measuring individual arthropod body mass is a time-consuming and tedious process (Johnston & Cunjak, 1999; Eklöf et al., 2017; Sohlström et al., 2018; Kendall et al., 2019). Moreover, collection and storage methods often prevent the direct determination of mass estimates, especially when specimens are damaged (e.g. loss of appendages) or when subject to chemical preservation that causes unpredictable mass change (Johnston & Cunjak, 1999; Wetzel et al., 2005; Chown & Gaston, 2010; Moretti et al., 2017). As a result, most ecological studies on insects rely on more easily measured body dimensions (e.g. body length) as proxies for body size (Chown & Gaston, 2010). Many insect collections are composed of specimens preserved in ethanol, and these collections provide an important source of information about organismal change over time if we can convert preserved mass to biologically meaningful measures.

Allometric scaling rules applied to co-varying traits can be used to predict an organism's body mass based on an easy-to-obtain body length measurement, thus avoiding the use of problematic body mass estimators (Johnston & Cunjak, 1999; Moretti et al., 2017; Pennell et al., 2018; Kendall et al., 2019). Scaling equations have proven to be powerful tools for the prediction of body mass for a wide range of insect taxa based on different linear metrics (e.g. Rogers et al., 1977; Schoener, 1980; Johnston & Cunjak, 1999; Sabo et al., 2002; García-Barros, 2015; Kendall et al., 2019). These equations rely on regression parameters estimated for length–mass relationships, which are often subject to intersexual allometric differences (Hagen & Dupont, 2013; Kendall et al., 2019). Incorporating sexual size dimorphism data into scaling relationships, and thus their regression parameters, is crucial to overcome this limitation (e.g. Kendall et al., 2019). Despite the broad application of allometric scaling in ecological research, there are surprisingly few studies providing regression parameters for estimating the body mass of key herbivorous taxa, such as grasshoppers (but see Schoener, 1980; Sabo et al., 2002 for allometric equations at the ordinal level).

Short-horn grasshoppers (Orthoptera: Acrididae) are among the most diverse (> 6,700 described species) and ubiquitous fauna of grassland ecosystems around the world (Uvarov, 1966; Latchininsky et al., 2011; Song et al., 2018) contributing, in some cases, to more than half of the total above-ground arthropod biomass (Gillon, 1983; Song et al., 2018). The endemic short-horn grasshoppers of Aotearoa New Zealand occur widely, but are especially abundant in alpine habitats (Bigelow, 1967; Trewick, 2001; Trewick, 2008; Trewick & Morris, 2008; Koot et al., 2020). As major invertebrate herbivores in native grassland ecosystems (Batcheler, 1967; White, 1975), these grasshoppers might play a major role in structuring plant communities and regulating ecosystem function via plant productivity, competition, and nutrient cycling (Olff & Ritchie, 1998; Belovsky & Slade, 2000; Moretti et al., 2013; Deraison et al., 2015). Given the ecological importance of grasshoppers, the determination of allometric scaling relationships provides an opportunity to explore ecologically important traits and variations that are otherwise difficult to measure.

Body size data have been accumulated for New Zealand grasshoppers mostly as linear dimensions: hind femur length and width, and pronotum length (e.g. Batcheler, 1967; Staples, 1967; Bigelow, 1967; Mason, 1971; but see Dowle et al., 2014; Carmelet-Rescan et al., 2021). However, the suitability of these measures as predictors of body size and their relationship with other body mass estimates have not been tested. A key feature of grasshoppers is the use of jumping in locomotion and predator avoidance (Queathem, 1991), and this is especially true for flightless species such as those found in New Zealand. Therefore, the size of the hind jumping leg may be closely related to other size components and, thus, to overall body size. The marked sexual size dimorphism of most grasshoppers might compound intraspecific differences in the relationships among body size components. Here, we examined these relationships focusing on three brachypterous and flightless species of the endemic alpine radiation of Kā Tiritirio-te-moana, the Southern Alps (Bigelow, 1967; Trewick & Morris, 2008; Koot et al., 2020; Figure 1A–C): *Brachaspis nivalis* (Hutton, 1987), *Paprides nitidus* Hutton, 1987, and *Sigaus australis* (Hutton, 1987). First, we quantified the effects of short-term ethanol preservation by describing the weight change over 120 days. Then, we examined scaling ratios to assess the predictive power of preserved mass for both fresh and dry masses. We also analysed intraspecific length–mass relationships over an elevation gradient to account, at least partially, for environmental variation in body size. Based on our results,

we developed species-specific statistical models to estimate the fresh and dry mass of individual grasshoppers from their preserved mass and hind femur length. Overall, our models showed high predictive power such that body mass estimates derived from them can be used to test mechanistic hypotheses for shifts in morphological and ecological traits related to body size.

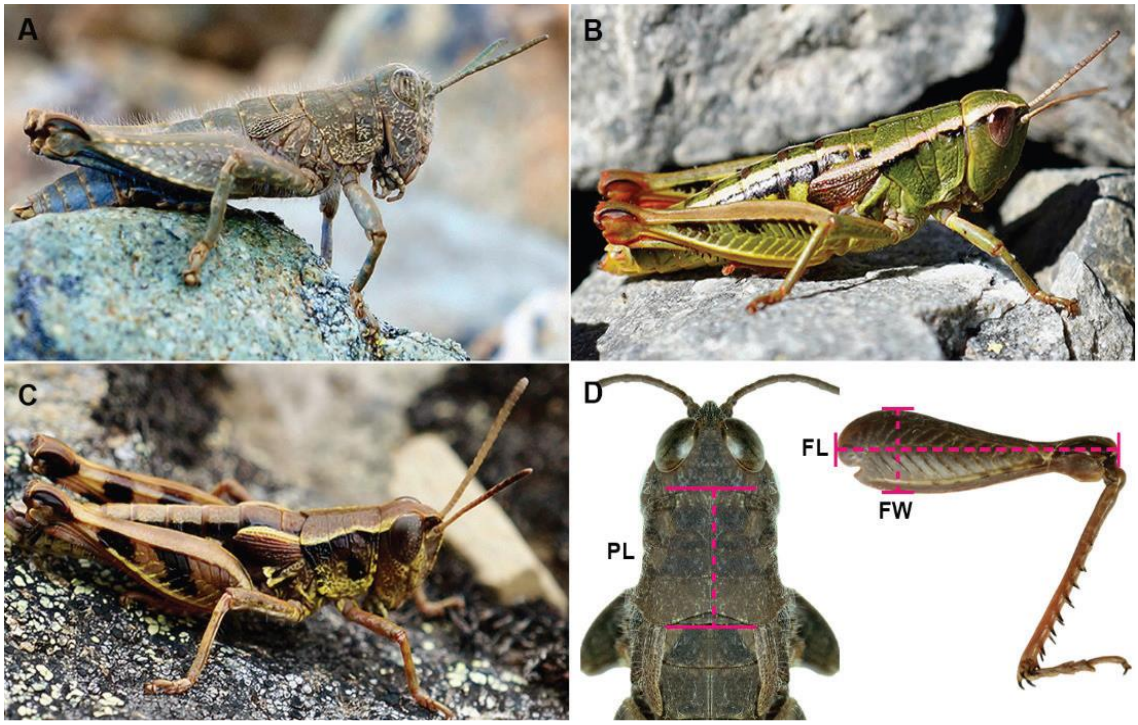

Figure 1. Adult endemic, brachypterous, and flightless grasshopper species from Hamilton Peak in the Southern Alps, New Zealand. A. *Brachaspis nivalis* female; B. *Paprides nitidus* female; C. *Sigaus australis* male; D. Body dimensions used as proxies of overall body size in this study: morphometric data were collected for hind femur length (FL), hind femur width (FW), and pronotum length (PL).

Materials and Methods

Specimen collection and measurements

A total of 368 complete adult specimens (no missing appendages) representing three grasshopper species (*B. nivalis* 61♂, 71♀; *P. nitidus* 73♂, 73♀; *S. australis* 42♂, 48♀) were collected on Hamilton Peak in the Craigieburn Range, New Zealand (-43.129, 171.688; WGS84). Sampling was done by hand, capturing grasshoppers disturbed by walking at five sites at ~100 m elevation intervals (BR1 to BR5) from 1,383 to 1,817 m asl, to capture as much local variation in body size as possible. Species and sex were

recorded from live specimens in the field and were later corroborated upon processing based on morphological features (e.g. body colour pattern, pronotum shape, and body shape and size) following Bigelow (1967). Maturity and sex were determined using the size and shape of the tegmina and terminalia (Bigelow, 1967).

Grasshoppers were weighed alive after cooling to 4°C, then frozen overnight before being preserved in 95% ethanol for DNA preservation. Specimens were weighed using a Sartorius Quintix35–1S digital scale (Sartorius Lab Instruments GmbH & Co, Goettingen, Germany) accurate to 0.001 g. We measured the left hind femur length (hereafter femur length) and width (hereafter femur width), and pronotum length of specimens (Figure 1D) using an Olympus SZX7 stereomicroscope with Olympus SC100 image capture and Olympus cellSens Dimension v1.6 software (Olympus Corporation, Tokyo, Japan). These measures were chosen because they are commonly used proxies for body size in grasshoppers (e.g. Bigelow, 1967; Mason, 1971; Harris et al., 2012; Yadav et al., 2018).

To quantify the effects of our preservation method on body mass estimates, we remeasured the body mass of all specimens after two and four months of storage in ethanol. Once all other measurements were completed, a random subsample of 50 specimens of each species (25 males and 25 females) were dried in an oven at 60°C for at least 96 h, until their mass ceased to change, and were then weighed. To assess measurement repeatability, we randomly selected five males and five females of each species and remeasured and reweighed them three times in random order.

Data analysis and model structures

Repeatability (R) was calculated independently for species and sexes with the R package rptR v.0.9.22 (Stoffel et al., 2017), using specimen as a grouping term. The ratio of intra-observer variance (i.e. R) was calculated as the among-group variance (VG) over the sum of group-level and within-group (residual) variance (VR): $R = VG / (VG + VR)$. Confidence intervals (95%) around repeatability values were estimated using 1,000 parametric bootstrap iterations. The effect of preservation in 95% ethanol on specimen body mass was examined by comparing the mass of individuals when live (fresh mass) and after ethanol preservation for two and four months. We also examined the frequency distributions of differences in body mass before and after preservation for each species.

As the shape of the size–frequency distribution was almost identical for both preserved states (Figure 2), we used a Wilcoxon signed-rank test to analyse overall and sex-specific differences between fresh mass and preserved mass after four months of preservation (hereafter preserved mass), pooling data from all species. For these analyses, a non-parametric approach was preferred, as mass difference between live and 4-month preserved specimens was not normally distributed when considered together. Statistical tests were implemented using the R package 'rstatix' v.0.7.0 (Kassambara, 2021).

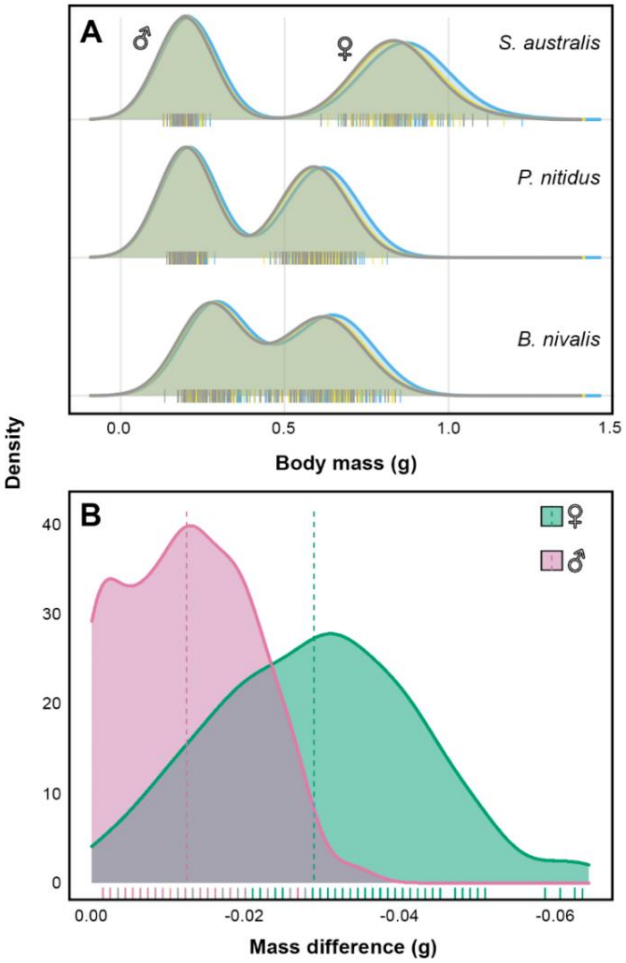

Figure 2. A. Density distributions of body mass in three flightless New Zealand grasshopper species when alive (turquoise) and after ethanol-preservation for two (dark yellow) and four months (black); B. The distribution of the difference in mass between live and 4-month preserved specimens pooled for all three species and partitioned by sex. Mean values for male (-0.012 g) and females (-0.029 g) are indicate by dashed lines. Marginal rug indicates individual observations of body mass.

We explored mass-to-mass ratios between ethanol preserved mass (after four months of preservation, PM), and both fresh mass (FM) and dry mass (DM) for each species, using model II regressions with standardized major axis (SMA) in the R package 'smart' v.3.4-8 (Warton et al., 2012). We performed SMA regressions by (i) including an intercept term (i.e., not forced through the origin) under the robust outlier option and (ii) assuming that changes in any body mass metric is reflected in the other metric, as measurements came from the same specimens (y = 0 when x = 0), and forcing the intercept through the origin (i.e. zero-intercept). We also tested for a common slope between sexes and among sites (i.e. elevation) with an ANCOVA-like test, using the slopes estimated in SMA regressions (Warton et al., 2012). Since preserved mass was closely related to the other measures of mass ($R^2 \geq 0.913$, $p < 0.001$; for additional details see Results), we specified a series of species-specific linear mixed-effects (LMM) models to predict FM and DM as a function of PM using the R package 'lme4' v.1.1-27.1 (Bates et al., 2015). This approach allowed us to account for sex- and site-specific differences in body mass by including sex as an additional fixed effect and as an interaction term with preserved mass, elevation as a random intercept, and preserved mass as a random slope.

We used ordinary least squares (OLS) regressions in R base (R Core Team, 2020) to compare body dimensions (femur length = FL, femur width = FW, and pronotum length = PL) as predictors of body mass components (i.e. FM and DM) using log-transformed data. For each species, we estimated and compared the slopes of fitted lines between sexes using the R package 'emmeans' v.1.6.2-1 (Lenth, 2021). As the strength of relationships varied between sexes and in some instances presented apparent deviations from linearity (see Results), we fitted sex-specific non-linear models (Knell, 2009) to analyse the shape of the scaling relationship. Five models were compared using Akaike's Information Criteria (AIC): (i) quadratic, (ii) logistic, (iii) four-parameter logistic, (iv) Weibull growth function, and (v) power function models. Models were fitted on untransformed variables (Packard, 2011) using R base and the R package 'aomisc' v.0.647 (Onofri, 2020). We chose femur length for the following analyses because it was highly correlated with all other body dimensions (Pearson's $R > 0.924$, $p < 0.001$) and easier to measure consistently, as indicated by our repeatability analysis (Figure S1.1, Table S1.1).

We further explored scaling relationships between FL and both FM and DM using model II regressions SMA including only an intercept term (i.e., not forced through the origin), as the femur length of adult insects does not change in response to changes in body mass (Whitman, 2008; Chown & Gaston, 2010; Bailey et al., 2020). We also specified LMMs using FL as a predictor of both FM and DM, using homologous model structures as defined previously for mass-to-mass modelling, to account for sex- and site-specific differences in trait variability. These approaches were chosen because sex-specific linear models generally performed as well as or better than non-linear models ($\Delta AIC \leq 1.95$), although when predicting dry mass for females of *B. nivalis*, the quadratic model performed slightly better than the linear model ($\Delta AIC = 2.61$). For model formulation, we used log-transformed values because static allometric relationships explored here are generally well-described by a power function ($y = ax^b$), which is linearized when log-transformed: $\ln(y) = \ln(\alpha) + \beta \times \ln(x) + e$, where y = dry mass, α = intercept, β = allometric coefficient, and x = linear size proxy.

The best-fitted models (both allometric and LMMs) were selected using Akaike's information criterion corrected for sample size (AICc) and Akaike weight (wi) using the R package 'AICcmodavg' v.2.3-1 (Mazerolle, 2020). Models with $\Delta AICc < 2$ were considered equally supported by the data, while models with $\Delta AICc > 2$ were considered to show substantial differences (Burnham & Anderson, 2002). The Akaike weight (wi) was interpreted as the probability that model i was the best model given all evaluated models and data available (Burnham & Anderson, 2002). For all models, the goodness of fit was examined by calculating conditional R^2 using the R package 'MUMIn' v.1.43.17 (Barton, 2020). The statistical significance of fixed and random effects was examined for the best-fitted models using the R package 'lmerTest' v.3.1-3 (Kuznetsova et al., 2017). Assumptions of model fit were met for all models as indicated by diagnostic plots of residuals.

Testing model accuracy

We predicted fresh and dry body mass for 368 grasshopper specimens using mass-to-mass ratios, scaling regressions, and parameters from the best-fitted LMMs. We then tested the relationship between measured and predicted values using model II regressions with a major axis approach using the R package 'lmodel2' v.1.7-3 (Legendre, 2018). This method is appropriate when comparing empirical observations to model predictions

(Legendre & Legendre, 2012). The statistical significance of relationships was tested using one-tailed permutation tests (with 1,000 permutations), and the strengths of the relationships were determined by model R^2 values. Observed relationships were also compared to the ideal $x = y$ association where estimated = measured by calculation of 95% confidence intervals around the estimated slope. The accuracy of our predictions was also estimated using the root-mean-square error (RMSE) between the observed and predicted values, using the R package 'Metrics' v.0.1.4 (Hamner & Frasco, 2018). All analyses were performed using R 4.0.3 (R Core Team, 2020).

Results

We found high measurement consistency (R > 0.970), although the degree of repeatability differed among body size proxies, species, and sexes, reflecting the relative size of the values (Figure S1.1, Table S1.1). The highest mean repeatability was recorded for the larger traits (femur length R = 0.9990 ± 0.0001 SD, preserved mass R = 0.9985 ± 0.0001 SD), the larger species (*B. nivalis* R = 0.9941 ± 0.0082 SD and *S. australis* R = 0.9941 ± 0.0094 SD compared to *P. nitidus* R = 0.9912 ± 0.0147 SD), and the larger sex (females R = 0.9953 ± 0.0068 SD compared to males R = 0.9907 ± 0.0148 SD). Overall, grasshopper specimens weighed significantly less after four months in ethanol than when they were alive (Wilcoxon's test $p < 0.001$; Figure 2A), although differences were small (4.606% ± 2.705 SD). On average, the larger female specimens lost more weight than the male specimens (Wilcoxon's test $p < 0.001$; Figure 2B; Figure S2.1 and S2.2).

There were strong and significant relationships between preserved mass (PM) and both fresh mass (FM, $R^2 \geq 0.997$, $p < 0.001$) and dry mass (DM, $R^2 \geq 0.913$, $p < 0.001$) in all species (Figure 3; Figure S3.1). No significant differences in slopes were indicated by the ANCOVA-like test for the two sexes, but site differences were found when predicting DM as a function of PM in *S. australis* (Table S3.1). Estimated ratios of preserved to fresh mass (mean ratio = 1.041 ± 0.005 SD) and preserved to dry mass (mean = 0.310 ± 0.008 SD) were similar for all species (Table 1). All LMMs including co-variables exhibited similar overall predictive power as judged by their fitting scores (Table 2). When predicting fresh mass as a function of preserved mass, the PM-only fixed-effect model incorporating site as a random effect (FM~PM+(1|Site)) outperformed other

models for all species, except *B. nivalis* (Table 2a). For this species, one of the models accounting for sexual dimorphism exceeded the baseline model (i.e. FM~PM+(1|Site)) in terms of AICc (ΔAICc = 3.47, Δwi = 0.54) but not R^2 (ΔR^2 = 0.001). In contrast, when predicting dry mass, one of the models accounting for sexual dimorphism and site differences (FM~PM+Sex+(PM|Site)) surpassed other models for all species (Table 1b) except *B. nivalis*. In this species, the PM-only fixed-effect model outperformed models including sex in terms of AICc (ΔAICc = 2.47, Δwi = 0.51) but not R^2 (ΔR^2 = 0.000). Fixed effects were significant in all best-fitted models (p > 0.001), yet the random effect (i.e. site) was only significant when predicting FM for *S. australis* (p > 0.001; Table S4.1). All LMMs outperformed the null models (i.e. FM~1+(1|Site) and DM~1+(1|Site)) in their predictive power (Table 2).

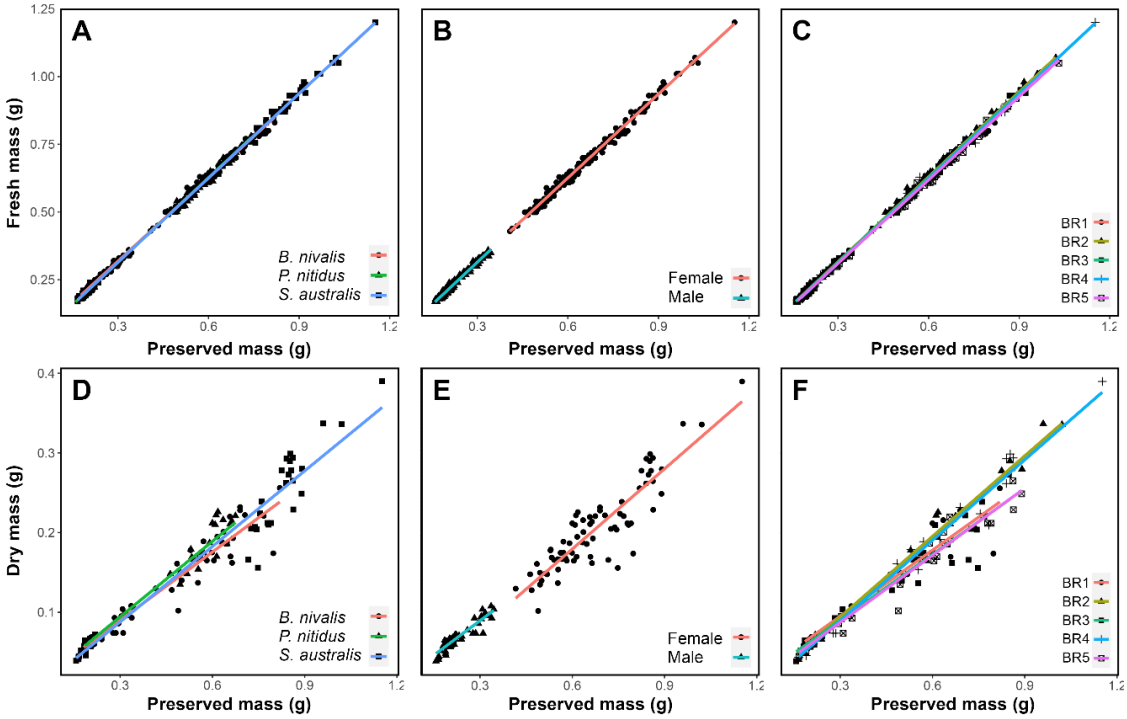

Figure 3. Mass-to-mass relationships in three flightless New Zealand grasshopper species showing the influence of elevation and sexual dimorphism. Fresh mass–preserved mass (A–C) and dry mass–preserved mass (D–F). Sample sites (BR1 to BR5) indicating five sites in ~100-m elevation intervals from 1,383 to 1,817 m asl. Lines represent the best-fit from standardized major axis regressions. Credible intervals are omitted for clarity. Some regression lines overlie each other.

Table 1. Mass-to-mass ratios for predicting both fresh and dry mass from preserved mass in three flightless New Zealand grasshopper species. Regression parameters based on standardized major axis regressions and their confidence intervals (95% CI) are shown.

Species	SMA	Intercept$_{(CI)}$	Slope$_{(CI)}$	R^2	*p*-value	Ratio
(a) Preserved mass to fresh mass (PM:FM)						
Brachaspis nivalis	0-intercept	0.000	1.045$_{(1.041, 1.050)}$	0.999	< 0.001	FM=1.045PM
Brachaspis nivalis	intercept	0.009$_{(0.004, 0.013)}$	1.030$_{(1.021, 1.039)}$	0.997	< 0.001	FM=1.030PM
Paprides nitidus	0-intercept	0.000	1.045$_{(1.041, 1.049)}$	0.999	< 0.001	FM=1.045PM
Paprides nitidus	intercept	0.000$_{(-0.003, 0.003)}$	1.045$_{(1.038, 1.052)}$	0.998	< 0.001	FM=1.045PM
Sigaus australis	0-intercept	0.000	1.042$_{(1.038, 1.045)}$	0.999	< 0.001	FM=1.042PM
Sigaus australis	intercept	0.002$_{(-0.001, 0.006)}$	1.039$_{(1.033, 1.045)}$	0.998	< 0.001	FM=1.039PM
(b) Preserved mass to dry mass (PM:DM)						
Brachaspis nivalis	0-intercept	0.000	0.296 $_{(0.286, 0.306)}$	0.986	< 0.001	DM=0.296P
Brachaspis nivalis	intercept	-0.004 $_{(-0.014, 0.005)}$	0.308 $_{(0.289, 0.330)}$	0.913	< 0.001	DM=0.308P
Paprides nitidus	0-intercept	0.000	0.316 $_{(0.308, 0.323)}$	0.993	< 0.001	DM=0.316P
Paprides nitidus	intercept	0.001 $_{(-0.004, 0.006)}$	0.310 $_{(0.297, 0.324)}$	0.969	< 0.001	DM=0.310P
Sigaus australis	0-intercept	0.000	0.308 $_{(0.298, 0.319)}$	0.987	< 0.001	DM=0.308P
Sigaus australis	intercept	-0.009 $_{(-0.019, 0.001)}$	0.321 $_{(0.304, 0.338)}$	0.959	< 0.001	DM=0.321P

Table 2. Model selection showing the best-fitted models (AICc in bold) for predicting both fresh mass and dry mass from preserved mass in three New Zealand flightless grasshopper species. Abbreviations: K = number of parameters, AICc = Akaike's information criterion corrected for sample size, wi = Akaike weight, LL = Log-Likelihood, R^2 = marginal R^2. Model parameters of the best-fitting models (ΔAICc < 2) used for predictions are shown in Supporting Information Appendix 5.

Species	Model formulae	K	AICc	ΔAICc	wi	LL	R^2
(a) fresh mass (FM) as a function of preserved mass (PM)							
Brachaspis	FM~PM+Sex+(1|Site)	5	**-808.58**	0.00	0.66	409.53	0.997
nivalis	FM~PM+Sex+(PM|Site)	7	**-807.01**	1.57	0.23	410.96	0.997
	FM~PM*Sex+(1|Site)	6	-806.38	2.20	0.22	409.53	0.997
	FM~PM+(1|Site)	4	-805.11	3.47	0.12	406.71	0.996
	FM~1+(1|Site)	3	-64.11	744.47	0.00	35.15	0.112
Paprides	FM~PM+(1|Site)	4	**-937.02**	0.00	0.67	472.65	0.998
nitidus	FM~PM+Sex+(1|Site)	5	-934.87	2.14	0.23	472.65	0.998
	FM~PM*Sex+(1|Site)	6	-933.26	3.75	0.10	472.93	0.998
	FM~PM+Sex+(PM|Site)	7	-931.53	5.49	0.04	473.17	0.998
	FM~1+(1|Site)	3	-35.70	901.31	0.00	20.94	0.000
Sigaus	FM~PM+(1|Site)	4	**-566.34**	0.00	0.50	288.35	0.999
australis	FM~PM+Sex+(1|Site)	5	**-565.69**	0.65	0.36	287.41	0.999
	FM~PM*Sex+(1|Site)	6	-563.69	2.65	0.13	288.20	0.999
	FM~PM+Sex+(PM|Site)	7	-561.04	5.31	0.03	288.20	0.999
	FM~1+(1|Site)	3	69.40	635.75	0.00	-31.56	0.000

(b) dry mass (DM) as a function of preserved mass (PM)							
Brachaspis	DM~PM+(1|Site)	4	**-259.16**	0.00	0.73	134.03	0.915
nivalis	DM~PM+Sex+(1|Site)	5	-256.70	2.47	0.21	134.03	0.915
	DM~PM*Sex+(1|Site)	6	-254.14	5.02	0.06	134.05	0.915
	DM~PM+Sex+(PM|Site)	7	-251.39	7.77	0.01	134.03	0.915
	DM~1+(1|Site)	3	-139.34	119.82	0.00	72.93	0.000
Paprides	DM~PM+Sex+(PM|Site)	7	**-300.56**	0.00	0.67	158.65	0.981
nitidus	DM~PM+Sex+(1|Site)	5	-298.31	2.25	0.22	154.85	0.976
	DM~PM*Sex+(1|Site)	6	-296.03	4.53	0.07	155.02	0.976
	DM~PM+(1|Site)	4	-294.75	5.81	0.04	151.83	0.972
	DM~1+(1|Site)	3	-125.73	174.83	0.00	66.13	0.000
Sigaus	DM~PM+Sex+(PM|Site)	7	**-258.46**	0.00	0.59	137.53	0.979
australis	DM~PM+Sex+(1|Site)	5	**-257.21**	1.25	0.31	134.27	0.974
	DM~PM*Sex+(1|Site)	6	-254.85	3.62	0.10	134.38	0.974
	DM~PM+(1|Site)	4	-241.01	17.46	0.00	124.94	0.964
	DM~1+(1|Site)	3	-78.24	180.22	0.00	42.38	0.000

As expected, there was a strong and significant correlation (Pearson's $R \leq 0.893$, $p < 0.001$) among all body size measures, with pairwise comparisons involving femur length (FL) having the highest correlation coefficients (Pearson's $R > 0.924$, $p < 0.001$; Figure S5.1). All body dimensions exhibited strong and significant linear relationships with both fresh mass ($R^2 \geq 0.938$, $p < 0.001$) and dry mass ($R^2 \geq 0.887$, $p < 0.001$), although the strength of these relationships differed between sexes and, in some cases, appeared nonlinear (Figure S5.2 and S5.3). Differences in slopes between sexes were subtle for all species, and a significant difference was only detected when predicting FM in the function of pronotum length (PL) for *S. australis* ($p = 0.007$, Table S5.1 and S5.2). Comparisons of sex-specific models showed that, in most cases, linear models performed as well as or better than alternative non-linear models. However, slight deviation from linearity was detected when predicting DM for female *B. nivalis*, where an allometric quadratic model performed marginally better than a linear model for females ($\Delta AIC = 2.61$), although both models were comparable for males ($\Delta AIC = 1.88$). Scaling relationships between body mass estimates and femur length were generally well-described by a power function (Table S6.1). The coefficients from SMA regressions were similar for all species when scaling the relationship between FL and both FM and DM (Table 3; Figure 4). Most LMMs including co-variables displayed comparable overall predictive ability as judged by their fitting scores (Table 4). In general, models accounting for sexual dimorphism outperformed other models for all species, although

in a few cases, parameters from equally supported baseline models (e.g. FL-only fixed-effect, ΔAICc < 2) led to more accurate body mass predictions (Table 4). Fixed effects were significant in all best-fitted models (in all cases $p > 0.001$, but $p = 0.048$ when predicting fresh mass for *B. nivalis*), but the random effect (i.e. site) was not significant for any model ($p > 0.001$; Table S4.2). All formulated LMMs outperformed the null models (i.e. ln(FM)~1+(1|Site) and ln(DM)~1+(1|Site)) in their predictive power.

Table 3. Length–mass scaling coefficients for predicting both fresh and dry mass from femur length in three flightless New Zealand grasshopper species. Regression parameters based on standardized major axis regressions and their confidence intervals (95% CI) are shown.

Species	Model formulae	Intercept$_{(CI)}$	Slope$_{(CI)}$	R^2	*p*-value
(a) fresh mass (FM) as a function of femur length (FL)					
Brachaspis nivalis	ln(FM)~ln(FL)	-7.754$_{(-7.937, -7.571)}$	2.696$_{(2.625, 2.768)}$	0.965	< 0.001
Paprides nitidus	ln(FM)~ln(FL)	-8.914$_{(-9.085, -8.743)}$	3.090$_{(3.024, 3.157)}$	0.976	< 0.001
Sigaus australis	ln(FM)~ln(FL)	-9.584$_{(-9.783, -9.385)}$	3.315$_{(3.241, 3.391)}$	0.982	< 0.001
(b) dry mass (DM) as a function of femur length (FL)					
Brachaspis nivalis	ln(DM)~ln(FL)	-9.234 $_{(-9.747, -8.721)}$	2.778$_{(2.585, 2.986)}$	0.898	< 0.001
Paprides nitidus	ln(DM)~ln(FL)	-10.077$_{(-10.504, -9.650)}$	3.071$_{(2.908, 3.242)}$	0.953	< 0.001
Sigaus australis	ln(DM)~ln(FL)	-11.423$_{(-11.919, -10.927)}$	3.539$_{(3.357, 3.731)}$	0.939	< 0.001

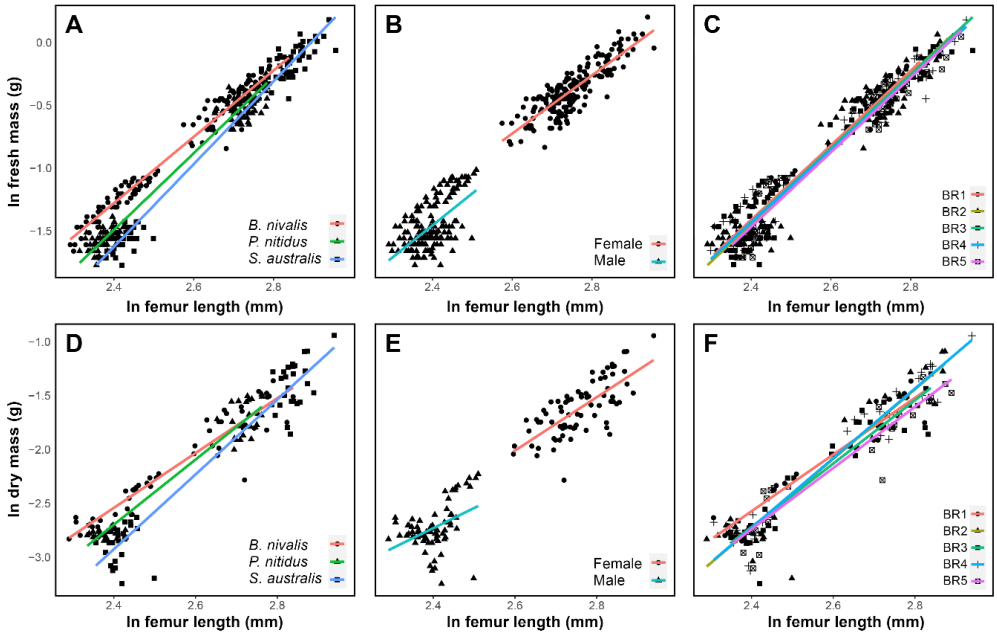

Figure 4. Length-to-mass relationships in three flightless New Zealand grasshopper species showing the influence of elevation and sexual dimorphism. Fresh mass–femur length (A–C) and

dry mass–femur length (D–F). Length–mass relationships are shown on natural logarithmic axes (ln). Sample sites (BR1 to BR5) indicating five sites in ~100-m elevation intervals from 1,383 to 1,817 m asl. Lines represent the best-fit from standardized major axis regressions. Credible intervals are omitted for clarity. Some regression lines overlie each other.

Table 4. Model selection showing the best-fitted models (AICc in bold) for predicting both fresh mass and dry mass from femur length in three flightless New Zealand grasshopper species. Abbreviations: K = number of parameters, AICc = Akaike's information criterion corrected for sample size, wi = Akaike weight, LL = Log-Likelihood, R^2 = marginal R^2. Model parameters of the best-fitting models (ΔAICc < 2) used for predictions are shown in Supporting Information Appendix 5.

Species	Model formulae	K	AICc	ΔAICc	wi	LL	R^2
(a) fresh mass (FM) as a function of femur length (FL)							
Brachaspis	ln(FM)~ln(FL)*Sex+(1|Site)	6	**-284.34**	0.00	0.44	148.51	0.968
nivalis	ln(FM)~ln(FL)+Sex+(ln(FL)|Site)	7	**-283.44**	0.90	0.28	149.18	0.969
	ln(FM)~ln(FL)+Sex+(1|Site)	5	**-283.22**	1.12	0.25	146.85	0.967
	ln(FM)~ln(FL)+(1|Site)	4	-278.56	5.78	0.02	143.44	0.965
	ln(FM)~1+(1|Site)	3	149.94	434.28	0.00	-71.88	0.111
Paprides	ln(FM)~ln(FL)+(1|Site)	4	**-328.73**	0.00	0.64	169.58	0.976
nitidus	ln(FM)~ln(FL)+Sex+(1|Site)	5	**-327.15**	1.58	0.29	169.88	0.981
	ln(FM)~ln(FL)*Sex+(1|Site)	6	-324.43	4.30	0.07	169.62	0.981
	ln(FM)~ln(FL)+Sex+(ln(FL)|Site)	7	-296.49	32.24	0.00	152.38	0.981
	ln(FM)~1+(1|Site)	3	247.53	576.26	0.00	-120.68	0.000
Sigaus	ln(FM)~ln(FL)+Sex+(1|Site)	5	**-180.21**	0.00	0.65	95.46	0.987
australis	ln(FM)~ln(FL)+(1|Site)	4	**-178.53**	1.68	0.28	95.77	0.982
	ln(FM)~ln(FL)*Sex+(1|Site)	6	-175.85	4.36	0.07	95.61	0.987
	ln(FM)~ln(FL)+Sex+(ln(FL)|Site)	7	-156.20	24.01	0.00	82.34	0.987
	ln(FM)~1+(1|Site)	3	204.43	384.63	0.00	-99.07	0.000
(b) dry mass (DM) as a function of femur length (FL)							
Brachaspis	ln(DM)~ln(FL)+(1|Site)	4	**-45.22**	0.00	0.48	27.05	0.904
nivalis	ln(DM)~ln(FL)+Sex+(1|Site)	5	**-44.42**	0.80	0.32	27.89	0.902
	ln(DM)~ln(FL)*Sex+(1|Site)	6	-43.14	2.08	0.17	28.55	0.904
	ln(DM)~ln(FL)+Sex+(FL|Site)	7	-39.14	6.08	0.02	27.90	0.903
	ln(DM)~1+(1|Site)	3	66.45	111.67	0.00	-29.96	0.000
Paprides	ln(DM)~ln(FL)+Sex+(1|Site)	5	**-69.02**	0.00	0.53	40.21	0.962
nitidus	ln(DM)~ln(FL)*Sex+(1|Site)	6	**-68.45**	0.57	0.40	41.23	0.964
	ln(DM)~ln(FL)+(1|Site)	4	**-67.97**	1.05	0.03	35.94	0.955
	ln(DM)~ln(FL)+Sex+(ln(FL)|Site)	7	-63.98	5.04	0.04	40.13	0.963
	ln(DM)~1+(1|Site)	3	85.46	154.48	0.00	-39.46	0.000
Sigaus	ln(DM)~ln(FL)+(1|Site)	4	**-28.96**	0.00	0.65	18.93	0.955
australis	ln(DM)~ln(FL)+Sex+(1|Site)	5	-26.75	2.21	0.21	19.06	0.955
	ln(DM)~ln(FL)+Sex+(ln(FL)|Site)	7	-24.78	4.19	0.08	20.72	0.960
	ln(DM)~ln(FL)*Sex+(1|Site)	6	-24.27	4.70	0.06	19.11	0.956
	ln(DM)~1+(1|Site)	3	120.31	149.28	0.00	-56.90	0.000

We found that predicted body mass (both fresh and dry mass) was significantly correlated with empirical measurements; however, using PM as a predictor led to the most accurate estimates (Figure 5). In all cases, the relationship between estimated and measured body mass was not significantly different from a 1:1 relationship, with > 89% of the variation explained (Table 5). The range of prediction error (RMSE) was near identical for body mass predictions obtained from mass-to-mass ratios, scaling regressions, and LMMs. When using PM as a predictor, FM estimates from PM:FM ratios were marginally more accurate than those from LMMs (RMSE = 0.011 g and 0.012 g, respectively). In contrast, LMMs were slightly more accurate than PM:DM ratios when predicting DM (RMSE = 0.014 g and 0.017 g, respectively). However, the range of prediction error was considerably higher when using FL as a predictor. For FM estimates, predictions based on SMA scaling relationships were marginally more accurate than those from LMMs (RMSE = 0.048 g and 0.050 g, respectively), but when predicting DM, prediction errors were identical using both methods (RMSE = 0.025 g).

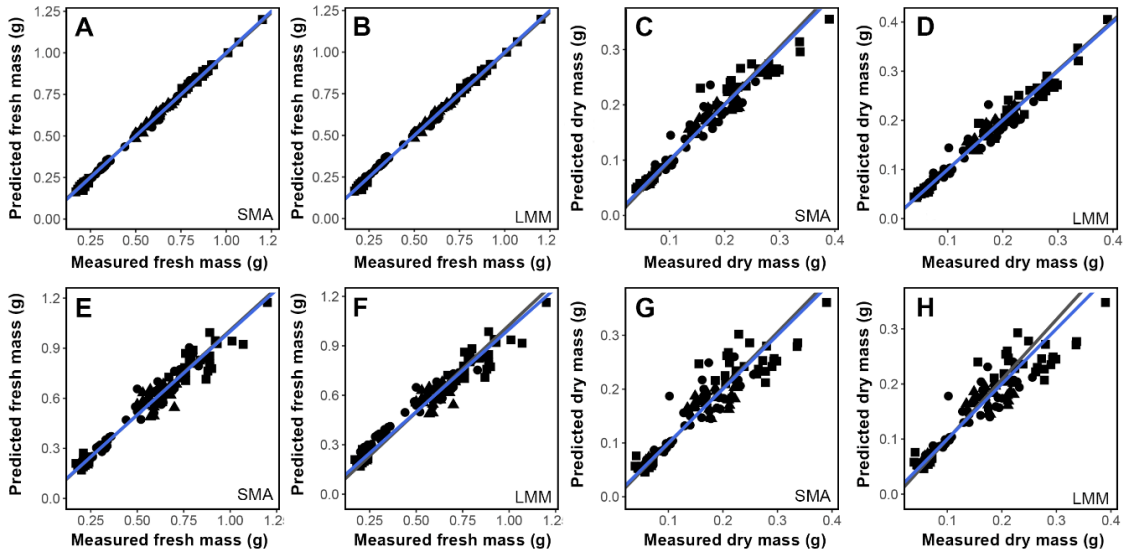

Figure 5. High predictability observed when comparing measured and predicted body mass using type-II linear regression with a major axis approach. Predictions based on preserved mass (A–D) and femur length (E–H) pooling data from three flightless New Zealand grasshopper species: *Brachaspis nivalis* (pink circles), *Paprides nitidus* (green triangles), and *Sigaus australis* (blue squares). The expected x = y relationship is shown in dashed black line, and the observed is shown in solid grey line. Predictions from standardized major axis regressions (SMA) and linear mixed-effects models (LMM) are shown. Note that in most cases fitting lines overlap.

Table 5. Details of statistical models (type II linear regression with a Major Axis) testing the relationships between predicted and measured body mass in three flightless New Zealand grasshopper species. Predictions are based on mass-to-mass ratios and scaling parameters from standardized major axis regressions (SMA) and linear mixed-effects models (LMM). The R^2 values, estimated intercept, and slope (95% confidence intervals) are given.

Model	Sample size	R^2	Intercept$_{(CI)}$	Slope$_{(CI)}$	*p*-value
(a) Preserved mass to fresh mass					
PM:FM ratio	368	0.998	0.004$_{(0.002–0.006)}$	0.993 $_{(0.989–0.998)}$	< 0.001
LMM	368	0.998	-0.004$_{(-0.006–-0.002)}$	1.005 $_{(1.004–1.010)}$	< 0.001
(b) Preserved mass to dry mass					
PM:DM ratio	150	0.957	-0.006$_{(-0.011–0.001)}$	1.035 $_{(1.000–1.071)}$	< 0.001
LMM	150	0.958	-0.004$_{(-0.009–0.001)}$	1.032 $_{(0.997–1.068)}$	< 0.001
(c) femur length to fresh mass					
SMA	368	0.965	-0.006 $_{(-0.021–0.009)}$	1.013 $_{(0.982–1.045)}$	< 0.001
LMM	368	0.963	-0.031 $_{(-0.048–-0.016)}$	1.056 $_{(1.023–1.091)}$	< 0.001
(d) femur length to dry mass					
SMA	150	0.898	-0.004$_{(-0.013–0.002)}$	1.034 $_{(0.979–1.092)}$	< 0.001
LMM	150	0.901	-0.009$_{(-0.018–0.002)}$	1.088 $_{(1.031–1.148)}$	< 0.001

Discussion

A key source of variation in morphological traits is measurement repeatability, which is inherently related to the statistical power of analyses based on those measurements (Bailey & Byrnes, 1990; Wylde & Bonduriansky, 2021). We found the highest repeatability for larger traits compared to smaller traits (e.g. femur length vs. femur width), and the larger sex (female vs. male) when pooling values for all size proxies and species. The effect of sex on repeatability was less clear when considering individual traits, suggesting that repeatability depends on other factors such as species size, trait size, and their interactions rather than sex alone. As noted by Bigelow (1967), measurement repeatability in the studied grasshoppers decreases in traits with rounded boundaries (e.g. femur width), and in traits with margins highly variable in shape (e.g. pronotum length). In addition, the orientation of specimens to the focal plane of the microscope can result in parallax error, especially for small structures that are difficult to measure (Wylde & Bonduriansky, 2021). Larger traits (e.g. femur length), were measured with relatively little error compared to smaller features (femur width and pronotum length) that were subject to more parallax error. Repeatability was also higher for the larger body mass measures (fresh and preserved mass) compared to dry specimens

(dry mass), which had small values that were sensitive to variation in humidity. Dried specimens become slightly hydrated during weighing, resulting in increased errors in measurement. Body length is a widely used linear metric, but we found it unreliable in grasshoppers, as abdomen size varied considerably with body condition, including reproductive state (Hochkirch & Gröning, 2008; García-Navas et al., 2017). Moreover, the extent of telescoping abdominal segments (Bigelow, 1967) and distortion during preservation are additional sources of measurement error (García-Barros, 2015).

Collecting and storing insects in chemical fluids, such as ethanol, has the potential to alter their body mass (Moretti et al., 2017; Penell et al., 2018), thus limiting their use in ecological studies that require accurate body mass data (Leuven et al., 1985; Chown & Gaston, 2010). We found that the weight loss of 95% ethanol-preserved specimens was largely restricted to the first two months of preservation after which weight stabilized, and only minimal differences were recorded (Figure S2.1). The high ethanol concentration (i.e. 95%) used here to also protect DNA could explain these results, as it would speed the leaching of water from tissues. Studies of aquatic insects show similar responses, with weight loss mostly limited to the first four weeks after preservation (e.g. Stanford, 1973; Leuven et al., 1985; Cressa, 1999; Wetzel et al., 2005). The degree of weight loss during preservation is a function of specimen size, which probably explains different responses to preservation of sexes. In absolute terms (g), larger specimens (females) lost more mass than smaller ones (males), yet the proportional difference (%) was negligible (Figure S2.2). These results agree with previous studies (e.g. Wetzel et al., 2005; Paxton, 2013); however, additional factors, such as surface area–volume ratio, environmental conditions, and concentration and volume of preservative, may also influence the leaching process (Leuven et al., 1985; Paxton, 2013).

Studies of the mass-to-mass relationships of terrestrial insects are scarce (e.g. Edwards, 1996; Penell et al., 2018). Here, we found that preserved mass was a prime predictor of body mass across all three grasshopper species, especially when predicting fresh mass (Tables 1, 2). Inter-individual differences during the drying process seemed to challenge model accuracy and fit when predicting dry mass. Visual inspection of dry mass–preserved mass regressions indicates unexplained size-related variance, meaning higher residual error in large individuals across all species. This suggests that inter-individual differences in body composition (e.g. water, carbohydrates, protein, and fat content) and

condition (nutritional and reproductive status) may be important factors explaining such variance.

The choice of a robust linear size trait is an important consideration for accurate mass estimates when applying allometric scaling regressions (Gaston & Blackburn, 2000; Moretti et al., 2017). Here, we showed that femur length strongly correlates with other body dimensions and body mass measures in all three grasshopper species, having by itself a high predictive power when estimating body mass at the species level, especially when predicting fresh mass (Tables 3 and 4). Femur length has previously been shown to have a linear relationship to body length in one of these species, which is in turn linearly related to body mass (Batcheler, 1967). However, in all cases, body mass predictions based on preserved mass were substantially more accurate (Table 5), with prediction errors < 0.018 g (against < 0.050 g for predictions based on femur length). Thus, it seems sensible to use preserved mass as a predictor when basic knowledge of the effects of preservation method on body mass is available. Otherwise, femur length is the metric to be used, as more than 90% of the variance in body mass was described by this trait in all cases (Tables 3, 4). The addition of alternative body dimensions during the modelling process would result in marginal improvement of prediction accuracy but would substantially increase the time needed for processing samples (e.g. Sohlström et al., 2018).

As expected, sex was sometimes retained as an informative predictor of body mass when used in addition to or as an interaction with femur length. This is not surprising given that adult females of these grasshopper species are approximately three times as heavy as adult males. Including sex generally increased model fit (Tables 2 and 4); however, its inclusion did not produce better estimates than traditional mass-to-mass and allometric scaling regressions (Table 5; Figure 5). Similar allometric relationships have been found in bees and hoverflies (Kendall et al., 2019) where sex was influential in the fit of the models but not in their predictive power. Likewise, the use of sex-specific regressions did not produce better mass estimates than simple regressions for European spiders (Penell et al., 2018). Although the use of models accounting for sexual size dimorphisms is desirable, it seems that, at least for our dataset, general regressions led to better estimates than more complex models. While femur length was an accurate predictor of body mass across species, it became less reliable when comparing sexes within a given

species, which can be related to the fact that, contrary to body mass, femur length remains fixed throughout adult life. Adult body size variation in structural linear traits is affected by environmental factors during development (Davidowitz et al., 2004). Therefore, intraspecific changes in the average value of adult structural size traits will require changes in size and structure at the population level (Bailey et al., 2020).

The difficulty of accurately predicting intraspecific body size variation based on co-varying linear traits is not new. The lack of predictive power has previously been explained in terms of traits varying in response to environmental conditions during development (Hagen & Dupont, 2013; Kendall et al., 2019). Thus, decomposing a multidimensional trait, such as body size, into linear measures seems insufficient to capture intraspecific body size variation. Indeed, body size in the broadest sense is closely linked to the volume of an organism, which in linear terms is described by length, width, and height (Moretti et al., 2017; Sohlström et al., 2018). With this in mind, predictions based on models incorporating complementary morphological traits directly related to width and/or height (e.g. femur length in addition to pronotum width) would improve intraspecific body mass prediction accuracy, and thus the applicability of allometric scaling for exploring the ecological implications of widespread phenomena, such as sexual size dimorphism. Given that the sexes commonly respond differently to environmental shifts, a considerable amount of the unexplained intraspecific variation observed here may be related to sexual differences in body size plasticity (e.g. Stillwell et al., 2010).

The slope parameter β (power coefficient) of our femur length regressions ranged between 2.152 and 3.293 for fresh mass and between 2.544 and 3.425 for dry mass, thus being close to 3 as expected for animals with isometric growth (Suter & Stratton, 2011). These values are higher than those from pre-existing allometric models (Schoener, 1980) for tropical orthopterans ($\beta = 1.65–1.96$ for dry mass estimates), further supporting differences in slopes between insects from different climatic zones: tropical insects usually have smaller gradients than temperate ones (Schoener, 1980). Interestingly, the slopes of temperate grasshoppers from North America (Sabo et al., 2002) are around the lower limit of those reported here for New Zealand grasshoppers ($\beta = 2.274$ for dry mass estimates). However, regression parameters for North American grasshoppers were obtained using body length as a co-variable, thus preventing reliable comparison, as

allometric relationships often differ between traits. As noted above, the use of body length in allometric studies on grasshoppers is not recommended, as this trait is difficult to measure accurately, thus jeopardizing model predictive power. Therefore, we expect our regressions to be highly applicable to ecological studies on New Zealand grasshoppers.

One source of potential error in our models is intraspecific regional variation in body size. This limitation can be problematic because scaling relationships in terrestrial insects, and thus, their regression parameters, are likely to vary geographically if populations' body size evolve independently of one another depending on local conditions (e.g. Johnston & Cunjak, 1999; Sohlström et al., 2018; Kendall et al., 2019). New Zealand grasshoppers exhibit variations in body size among populations inhabiting elevational and latitudinal gradients (Bigelow, 1967; Staples, 1967; Mason, 1970). By including size data from specimens collected on an elevational gradient in our models, we expect to have improved model robustness and reduced, at least in part, the effects of geographic size variation on their predictive power (Figures 3 and 4). Variation in response to sampling season is expected to represent an additional source of error in our models, as average body size can change from year to year at the same site due to differences in environmental conditions (Bigelow, 1967). Therefore, the performance of our models could be affected when predicting mass estimates from individuals with size measures far outside the trait ranges reported here.

Ecological applications

Here we show that, for New Zealand grasshoppers, two easy-to-measure, non-destructive, and highly repeatable size estimates (i.e. preserved mass and femur length) are good predictors of other difficult-to-measure but ecologically meaningful size traits, such as fresh and dry mass. Many ecological disciplines typically require body mass data to relate body size to a range of ecological attributes. For example, body mass has been proposed as a suitable metric for testing ecogeographic patterns, such as Bergmann's rule (Blackburn et al., 1999). Since body mass is universally comparable, it is the metric of choice in macroecological studies interested in body size variation or size-dependent ecological processes (Gaston & Blackburn, 2000). Body size estimates for New Zealand grasshoppers are more frequently available as body size dimensions (but see Batcheler,

1967), making mass-to-mass and length–mass regression models useful for increasing our ability to further explore the ecological implications of body size.

Body mass estimates from scaling regressions have proven useful for studying aspects shaping arthropod communities including biomass production (e.g. Eklöf et al., 2017; Penell et al., 2018; Kinsella et al., 2020) and abundance (White et al., 2007). Traditionally, size–abundance relationships rely on fresh body mass of organisms (White et al., 2007; Sohlström et al., 2018), which is not available for most species. Thus, mass estimates from scaling regressions will alleviate this limitation. Given the apparent linear relationship between body size and consumption rate in the grasshopper species we examined (White, 1975), indirect body mass estimates from length–mass regressions could also be used to predict herbivore impact on plant communities. For example, grasshopper dry mass correlates negatively with plant biomass in the field (Moretti et al., 2013), providing a potential trait for predicting plant consumption (Deraison et al., 2014).

Recently, declines in body size have been proposed as a general response to anthropogenic climate change in both endothermic and ectothermic animals (Gardner et al., 2011). Examining trends in body size requires the use of consistent size measures, and unfortunately, data often come as different size proxies, thereby hindering comparisons (Bailey et al., 2020). Body mass estimates from scaling regressions have helped to overcome this limitation by providing a tool for making size metrics from different sources (e.g. museum specimens, published datasets, and fresh sampling) comparable, so that tests of body size responses to climate change and warming temperatures can be performed (e.g. Tseng et al., 2018). This approach has proven useful for studying the trends and drivers of the change in the biomass of flying insects over time and space (e.g. Macgregor et al., 2019; Kinsella et al., 2020) and can now be used to estimate the body mass of New Zealand grasshoppers from historical abundance datasets (e.g. White, 1975; White & Sedcole, 1991).

Acknowledgements

The authors thank Broken River Ski Area and its manager Dr Claire Newell, who allowed us access to the field site and the New Zealand Department of Conservation for granting collecting permits (Authorization Number: 49878-RES). We also acknowledge our field

partners: Mari Nakano, Evans Effah, and Andrea Clavijo. This research was supported by a grant from the Orthopterists' Society's Theodore J. Cohn Research Fund and a doctoral scholarship from Massey University (awarded to FLMJ). The manuscript was improved by constructive feedback from Derek Woller and Maria Celeste Scattolini.

References

Bailey, L. D., Kruuk, L. E., Allen, R., Clayton, M., Stein, J., & Gardner, J. L. (2020). Using different body size measures can lead to different conclusions about the effects of climate change. *Journal of Biogeography*, *47*(8), 1687–1697. https://doi.org/10.1111/jbi.13850

Bailey, R. C., & Byrnes, J. (1990). A new, old method for assessing measurement error in both univariate and multivariate morphometric studies. *Systematic Zoology*, *39*(2), 124–130. https://doi.org/10.2307/2992450

Barnes, A. D., Jochum, M., Lefcheck, J. S., Eisenhauer, N., Scherber, C., O'Connor, M. I., ... & Brose, U. (2018). Energy flux: The link between multitrophic biodiversity and ecosystem functioning. *Trends in Ecology & Evolution*, *33*(3), 186–197. https://doi.org/10.1016/j.tree.2017.12.007

Barton, K. (2020). MuMIn: Multi-model inference. https://cran.r-project.org/package=MuMIn

Batcheler, C. L. (1967). Preliminary observations of alpine grasshoppers in a habitat modified by deer and chamois. *Proceedings of the New Zealand Ecological Society*, *14*, 15–26. http://www.jstor.org/stable/24061274

Bates, D., Mächler, M., Bolker, B., & Walker, S. (2014). Fitting linear mixed-effects models using lme4. *Journal of Statistical Software, 67*, 1–48. https://doi.org/10.18637/jss.v067.i01

Belovsky, G. E., & Slade, J. B. (2000). Insect herbivory accelerates nutrient cycling and increases plant production. *Proceedings of the National Academy of Sciences of the United States of America*, *97*(26), 14412–14417. https://doi.org/10.1073/pnas.250483797

Bigelow R. S. (1967). *The Grasshoppers (Acrididae) of New Zealand*. University of Canterbury Publications.

Blackburn, T. M., Gaston, K. J., & Loder, N. (1999). Geographic gradients in body size: A clarification of Bergmann's rule. *Diversity and Distributions*, *5*(4), 165–174. https://doi.org/10.1046/j.1472-4642.1999.00046.x

Burnham, K. P. & Anderson, D. R. (2002). *Model Selection and Multimodel Inference: A Practical Information-Theoretic Approach*. Springer. https://doi.org/10.1007/b97636

Carmelet-Rescan D., Morgan-Richards M., Koot E. M., & Trewick S. A. (2021). Climate and ice in the last glacial maximum explain patterns of isolation by distance inferred for alpine grasshoppers. *Insect Conservation and Diversity*, 14, 568–581. https://doi.org/10.1111/icad.12488

Chown, S. L., & Gaston, K. J. (2010). Body size variation in insects: A macroecological perspective. *Biological Reviews*, *85*(1), 139–169. https://doi.org/10.1111/j.1469-185X.2009.00097.x

Chown, S. L., & Steenkamp, H. E. (1996). Body size and abundance in a dung beetle assemblage: Optimal mass and the role of transients. *African Entomology*, *4*(2), 203–212. https://hdl.handle.net/10520/AJA10213589_205

Cízek, L. (2005). Diet composition and body size in insect herbivores: Why do small species prefer young leaves? *European Journal of Entomology*, *102*(4), 675–681. https://doi.org/10.14411/eje.2005.096

Cressa, C. (1999). Dry mass estimates of some tropical aquatic insects. *Revista de Biología Tropical*, *47*(1–2), 133–141. https://doi.org/10.15517/rbt.v47i1-2.19062

Davidowitz, G., D'Amico, L. J., & Nijhout, H. F. (2004). The effects of environmental variation on a mechanism that controls insect body size. *Evolutionary Ecology Research*, *6*(1), 49–62. https://www.evolutionary-ecology.com/abstracts/v06/1643.html

DeLong, J. P., Gilbert, B., Shurin, J. B., Savage, V. M., Barton, B. T., Clements, C. F., ... & O'Connor, M. I. (2015). The body size dependence of trophic cascades. *The American Naturalist*, *185*(3), 354–366. https://doi.org/10.1086/679735

Deraison, H., Badenhausser, I., Börger, L., & Gross, N. (2015). Herbivore effect traits and their impact on plant community biomass: An experimental test using grasshoppers. *Functional Ecology*, *29*(5), 650–661. https://doi.org/10.1111/1365-2435.12362

Dowle, E. J., Morgan-Richards, M., & Trewick, S. A. (2014). Morphological differentiation despite gene flow in an endangered grasshopper. *BMC Evolutionary Biology*, *14*, 216. https://doi.org/10.1186/s12862-014-0216-x

Edwards, R. L. (1996). Estimating live spider weight using preserved specimens. *Journal of Arachnology*, *24*, 161–166. http://www.jstor.org/stable/3705952

Ehnes, R. B., Rall, B. C., & Brose, U. (2011). Phylogenetic grouping, curvature and metabolic scaling in terrestrial invertebrates. *Ecology Letters*, *14*(10), 993–1000. https://doi.org/10.1111/j.1461-0248.2011.01660.x

Eklöf, J., Austin, Å., Bergström, U., Donadi, S., Eriksson, B. D., Hansen, J., & Sundblad, G. (2017). Size matters: Relationships between body size and body mass of common coastal, aquatic invertebrates in the Baltic Sea. *PeerJ*, *5*, e2906. https://doi.org/10.7717/peerj.2906

García-Barros, E. (2015). Multivariate indices as estimates of dry body weight for comparative study of body size in Lepidoptera. *Nota Lepidopterologica*, *38*(1), 59–74. https://doi.org/10.3897/nl.38.8957

García-Navas, V., Noguerales, V., Cordero, P. J., & Ortego, J. (2017). Ecological drivers of body size evolution and sexual size dimorphism in short-horned grasshoppers (Orthoptera: Acrididae). *Journal of Evolutionary Biology*, *30*(8), 1592–1608. https://doi.org/10.1111/jeb.13131

Gardner, J. L., Peters, A., Kearney, M. R., Joseph, L., & Heinsohn, R. (2011). Declining body size: A third universal response to warming? *Trends in Ecology & Evolution*, *26*, 285–291. https://doi.org/10.1016/j.tree.2011.03.005

Gaston, K. J., & Blackburn, T. M. (2000). *Pattern and process in macroecology*. Blackwell Publishing. https://doi.org/10.1002/9780470999592

Gilbert, J. D. (2011). Insect dry weight: Shortcut to a difficult quantity using museum specimens. *Florida Entomologist*, *94*, 964–970. https://doi.org/10.1653/024.094.0433

Gillon Y. (1983). *The invertebrates of the grass layer*. In F. Bourliere (Eds.), *Ecosystems of the World 13: Tropical Savannas* (pp. 289–311). Elsevier.

Hagen, M., & Dupont, Y. L. (2013). Inter-tegular span and head width as estimators of fresh and dry body mass in bumblebees (*Bombus* spp.). *Insectes Sociaux*, *60*(2), 251–257. https://doi.org/10.1007/s00040-013-0290-x

Hamner B., Frasco M. (2018). Metrics: Evaluation metrics for machine learning. https://cran.r-project.org/package=Metrics

Harris, R., McQuillan, P., & Hughes, L. (2012). Patterns in body size and melanism along a latitudinal cline in the wingless grasshopper, *Phaulacridium vittatum*. *Journal of Biogeography*, *39*(8), 1450–1461. https://doi.org/10.1111/j.1365-2699.2012.02710.x

Hirt, M. R., Lauermann, T., Brose, U., Noldus, L. P., & Dell, A. I. (2017). The little things that run: A general scaling of invertebrate exploratory speed with body mass. *Ecology*, *98*, 2751–2757. https://doi.org/10.1002/ecy.2006

Hochkirch, A., & Gröning, J. (2008). Sexual size dimorphism in Orthoptera (sens. Str.): A review. *Journal of Orthoptera Research*, *17*(2), 189–196. https://doi.org/10.1665/1082-6467-17.2.189

Horne, C. R., Hirst, A. G., & Atkinson, D. (2018). Insect temperature-body size trends common to laboratory, latitudinal and seasonal gradients are not found across altitudes. *Functional Ecology*, *32*(4), 948–957. https://doi.org/10.1111/1365-2435.13031

Johnston, T. A., & Cunjak, R. A. (1999). Dry mass–length relationships for benthic insects: A review with new data from Catamaran Brook, New Brunswick, Canada. *Freshwater Biology*, *41*(4), 653–674. https://doi.org/10.1046/j.1365-2427.1999.00400.x

Kassambara A. (2021). rstatix: Pipe-friendly framework for basic statistical tests. https://cran.r-project.org/package=rstatix

Kendall, L. K., Rader, R., Gagic, V., Cariveau, D. P., Albrecht, M., Baldock, K. C., ... & Bartomeus, I. (2019). Pollinator size and its consequences: Robust estimates of body size in pollinating insects. *Ecology and Evolution*, *9*(4), 1702–1714. https://doi.org/10.1002/ece3.4835

Kinsella, R. S., Thomas, C. D., Crawford, T. J., Hill, J. K., Mayhew, P. J., & Macgregor, C. J. (2020). Unlocking the potential of historical abundance datasets to study biomass change in flying insects. *Ecology and Evolution*, *10*(15), 8394–8404. https://doi.org/10.1002/ece3.6546

Knapp, M., & Knappová, J. (2013). Measurement of body condition in a common carabid beetle, *Poecilus cupreus*: A comparison of fresh weight, dry weight, and fat content. *Journal of Insect Science*, *13*, 6. https://doi.org/10.1673/031.013.0601

Knell, R. J. (2009). On the analysis of non-linear allometries. *Ecological Entomology*, *34*(1), 1–11. https://doi.org/10.1111/j.1365-2311.2008.01022.x

Koot, E. M., Morgan-Richards, M., & Trewick, S. A. (2020). An alpine grasshopper radiation older than the mountains, on Kā Tiritiri o te Moana (Southern Alps) of Aotearoa (New Zealand). *Molecular Phylogenetics and Evolution*, 147, 106783. https://doi.org/10.1016/j.ympev.2020.106783

Kuznetsova, A., Brockhoff, P. B., & Christensen, R. H. B. (2017). lmerTest package: Tests in linear mixed effects models. *Journal of Statistical Software*, *82*(1), 1–26. https://doi.org/10.18637/jss.v082.i13

Latchininsky, A., Sword, G., Sergeev, M., Cigliano, M. M., & Lecoq, M. (2011). Locusts and grasshoppers: Behavior, ecology, and biogeography. *Psyche: A Journal of Entomology*, *2011*, e578327. https://doi.org/10.1155/2011/578327

Legendre P. (2018). lmodel2: Model II regression. https://cran.r-project.org/package=lmodel2

Legendre P., & Legendre L. F. J. (2012). *Numerical ecology*. Elsevier.

Lenth R. V. (2021). emmeans: Estimated marginal means, aka Least–Squares means. https://cran.r-project.org/package=emmeans

Leuven, S. E. W., Brock, C. M., & van Druten, H. A. M. (1985). Effects of preservation on dry- and ash-free dry weight biomass of some common aquatic macro-invertebrates. *Hydrobiology*, *127*, 151–159. https://doi.org/10.1007/BF00004193

MacGregor, C. J., Williams, J. H., Bell, J. R., & Thomas, C. D. (2019). Moth biomass increases and decreases over 50 years in Britain. *Nature Ecology and Evolution*, *3*, 1645–1649. https://doi.org/10.1038/s41559-019-1028-6

Mason P. C. (1971). *Alpine Grasshoppers (Orthoptera: Acrididae) in the Southern Alps of Canterbury, New Zealand*. [Doctoral thesis, University of Canterbury]. Science: Theses and Dissertations Collection. http://hdl.handle.net/10092/5531

Mazerolle M. J. (2020). AICcmodavg: Model selection and multimodel inference based on (Q)AIC(c). https://cran.r-project.org/package=AICcmodavg

Meehan, T. D. (2006). Mass and temperature dependence of metabolic rate in litter and soil invertebrates. *Physiological and Biochemical Zoology*, *79*(5), 878–884. https://doi.org/10.1086/505997

Moretti, M., de Bello, F., Ibanez, S., Fontana, S., Pezzatti, G. B., Dziock, F., ... & Lavorel, S. (2013). Linking traits between plants and invertebrate herbivores to track functional effects of land-use changes. *Journal of Vegetation Science*, *24*(5), 949–962. https://doi.org/10.1111/jvs.12022

Moretti, M., Dias, A. T., De Bello, F., Altermatt, F., Chown, S. L., Azcárate, F. M., ... & Berg, M. P. (2017). Handbook of protocols for standardized measurement of terrestrial invertebrate functional traits. *Functional Ecology*, *31*(3), 558–567. https://doi.org/10.1111/1365-2435.12776

Nijhout, H. F. (2003). The control of body size in insects. *Developmental Biology*, *261*, 1–9. https://doi.org/10.1016/S0012-1606(03)00276-8

Olff, H., & Ritchie, M. E. (1998). Effects of herbivores on grassland plant diversity. *Trends in Ecology & Evolution*, *13*(7), 261–265. https://doi.org/10.1016/S0169-5347(98)01364-0

Onofri A. (2020). aomisc: Statistical methods for the agricultural sciences. https://cran.r-project.org/package=aomisc

Packard, G. C. (2011). Unanticipated consequences of logarithmic transformation in bivariate allometry. *Journal of Comparative Physiology B*, *181*(6), 841–849. https://doi.org/10.1007/s00360-011-0565-3

Paxton M. (2013). *Preservation effects on common macroinvertebrates of the Intermountain West*. [Undergraduate honors thesis, Utah State University]. Undergraduate Honors Capstone Projects. https://digitalcommons.usu.edu/honors/640

Penell, A., Raub, F., & Höfer, H. (2018). Estimating biomass from body size of European spiders based on regression models. *The Journal of Arachnology*, *46*(3), 413–419. https://doi.org/10.1636/JoA-S-17-044.1

Peters R. H. (1983) *The Ecological Implications of Body Size*. Cambridge University Press. https://doi.org/10.1017/CBO9780511608551

Queathem, E. (1991). The ontogeny of grasshopper jumping performance. *Journal of Insect Physiology*, *37*(2), 129–138. https://doi.org/10.1016/0022-1910(91)90098-K

R Core Team. (2020). R: A language and environment for statistical computing. Retrieved from https://www.r-project.org

Rogers, L. E., Buschbom, R. L., & Watson, C. R. (1977). Length-weight relationships of shrub-steppe invertebrates. *Annals of the Entomological Society of America*, *70*(1), 51–53. https://doi.org/10.1093/aesa/70.1.51

Sabo, J. L., Bastow, J. L., & Power, M. E. (2002). Length–mass relationships for adult aquatic and terrestrial invertebrates in a California watershed. *Journal of the North American Benthological Society*, *21*(2), 336–343. https://doi.org/10.2307/1468420

Sage, R. D. (1982). Wet and dry-weight estimates of insects and spiders based on length. *American Midland Naturalist*, *108*(2), 407–411. https://doi.org/10.2307/2425505

Schoener, T. W. (1980). Length–weight regressions in tropical and temperate forest–understory insects. *Annals of the Entomological Society of America*, *73*(1), 106–109. https://doi.org/10.1093/aesa/73.1.106

Siemann, E., Tilman, D., & Haarstad, J. (1996). Insect species diversity, abundance and body size relationships. *Nature*, *380*, 704–706. https://doi.org/10.1038/380704a0

Sohlström, E. H., Marian, L., Barnes, A. D., Haneda, N. F., Scheu, S., Rall, B. C., ... & Jochum, M. (2018). Applying generalized allometric regressions to predict live body mass of tropical and temperate arthropods. *Ecology and Evolution*, *8*(24), 12737–12749. https://doi.org/10.1002/ece3.4702

Song, H., Mariño–Pérez, R., Woller, D. A., & Cigliano, M. M. (2018). Evolution, diversification, and biogeography of grasshoppers (Orthoptera: Acrididae). *Insect Systematics and Diversity*, *2*(4), 1–25. https://doi.org/10.1093/isd/ixy008

Stanford, J. A. (1973). A centrifuge method for determining live weights of aquatic insect larvae, with a note on weight loss in preservative. *Ecology*, *54*(2), 449–451. https://doi.org/10.2307/1934356

Stang, M., Klinkhamer, P. G., Waser, N. M., Stang, I., & Van der Meijden, E. (2009). Size-specific interaction patterns and size matching in a plant–pollinator interaction web. *Annals of Botany*, *103*(9), 1459–1469. https://doi.org/10.1093/aob/mcp027

Staples D. J. (1967). *Colour and Size Variation within a Population of Brachaspis collinus (Hutton) (Orthoptera: Acrididae)*. [Undergraduate honors thesis, University of Canterbury]. Science: Theses and Dissertations Collection. https://hdl.handle.net/10092/101128

Stevens, V. M., Trochet, A., Van Dyck, H., Clobert, J., & Baguette, M. (2012). How is dispersal integrated in life histories: A quantitative analysis using butterflies. *Ecology Letters*, *15*(1), 74–86. https://doi.org/10.1111/j.1461-0248.2011.01709.x

Stillwell, R. C., Blanckenhorn, W. U., Teder, T., Davidowitz, G., & Fox, C. W. (2010). Sex differences in phenotypic plasticity affect variation in sexual size dimorphism in insects: From physiology to evolution. *Annual Review of Entomology*, *55*(1), 227–245. https://doi.org/10.1146/annurev-ento-112408-085500

Stoffel, M. A., Nakagawa, S., & Schielzeth, H. (2017). rptR: Repeatability estimation and variance decomposition by generalized linear mixed-effects models. *Methods in Ecology and Evolution*, *8*(11), 1639–1644. https://doi.org/10.1111/2041-210X.12797

Suter, R. B., & Stratton, G. E. (2011). Does allometric growth explain the diminutive size of the fangs of *Scytodes* (Araneae: Scytodidae)? *The Journal of Arachnology*, *39*(1), 174–177. http://www.jstor.org/stable/23048798

Trewick, S. A. (2001). Identity of an endangered grasshopper (Acrididae: *Brachaspis*): Taxonomy, molecules and conservation. *Conservation Genetics*, *2*, 233–243. https://doi.org/10.1023/A:1012263717279

Trewick, S. A. (2008). DNA Barcoding is not enough: Mismatch of taxonomy and genealogy in New Zealand grasshoppers (Orthoptera: Acrididae). *Cladistics*, 24(2), 240–254. https://doi.org/10.1111/j.1096–0031.2007.00174.x

Trewick S. A., & Morris S. (2008). *Diversity and Taxonomic Status of Some New Zealand Grasshoppers*. Science & Technical Publishing Department of Conservation, Wellington. https://www.doc.govt.nz/globalassets/documents/science–and–technical/drds290.pdf

Tseng, M., Kaur, K. M., Soleimani Pari, S., Sarai, K., Chan, D., Yao, C. H., ... & Fograscher, K. (2018). Decreases in beetle body size linked to climate change and warming temperatures. *Journal of Animal Ecology*, 87(3), 647–659. https://doi.org/10.1111/1365-2656.12789

Uvarov B. P. (1966). *Grasshoppers and Locusts*. Cambridge University Press.

Warton, D. I., Duursma, R. A., Falster, D. S., & Taskinen, S. (2012). smatr 3–an R package for estimation and inference about allometric lines. *Methods in Ecology and Evolution*, *3*(2), 257–259. https://doi.org/10.1111/j.2041–210X.2011.00153.x

Wetzel, M. A., Leuchs, H., & Koop, J. H. (2005). Preservation effects on wet weight, dry weight, and ash-free dry weight biomass estimates of four common estuarine macro-invertebrates: No difference between ethanol and formalin. *Helgoland Marine Research*, *59*(3), 206–213. https://doi.org/10.1007/s10152-005-0220-z

White, E. G. (1975). A survey and assessment of grasshoppers as herbivores in the South Island alpine tussock grasslands of New Zealand. *New Zealand Journal of Agricultural Research*, *18*(1), 73–85. https://doi.org/10.1080/00288233.1975.10430390

White, E. G., & Sedcole, J. R. (1991). A 20-year record of alpine grasshopper abundance, with interpretations for climate change. *New Zealand Journal of Ecology*, *15*(2), 139–152. http://www.jstor.org/stable/24053567

White, E. P., Ernest, S. K. M., Kerkhoff, A. J., & Enquist, B. J. (2007). Relationships between body size and abundance in ecology. *Trends in Ecology & Evolution*, *22*(6), 323–330. https://doi.org/10.1016/j.tree.2007.03.007

Whitman, D. W. (2008). The significance of body size in the Orthoptera: A review. *Journal of Orthoptera Research*, *17*(2), 117–134. https://doi.org/10.1665/1082-6467-17.2.117

Wylde, Z., & Bonduriansky, R. (2021). A comparison of two methods for estimating measurement repeatability in morphometric studies. *Ecology and Evolution*, 11(2), 763–770. https://doi.org/10.1002/ece3.7032

Yadav, S., Stow, A. J., Harris, R. M., & Dudaniec, R. Y. (2018). Morphological variation tracks environmental gradients in an agricultural pest, *Phaulacridium vittatum* (Orthoptera: Acrididae). *Journal of Insect Science*, *18*(6), 13. https://doi.org/10.1093/jisesa/iey121

Supporting Information

Appendix 1. Measurement repeatability based on repeated measures of body size traits from the same specimens in three New Zealand grasshopper species.

Figure S1.1. Estimates of trait repeatability (R) by body size proxy, species, and sex. Abbreviations: femur length (FL), femur width (FW), pronotum length (PL), dry mass (DM), fresh mass (FM), and preserved mass (PM). White points indicate mean values.

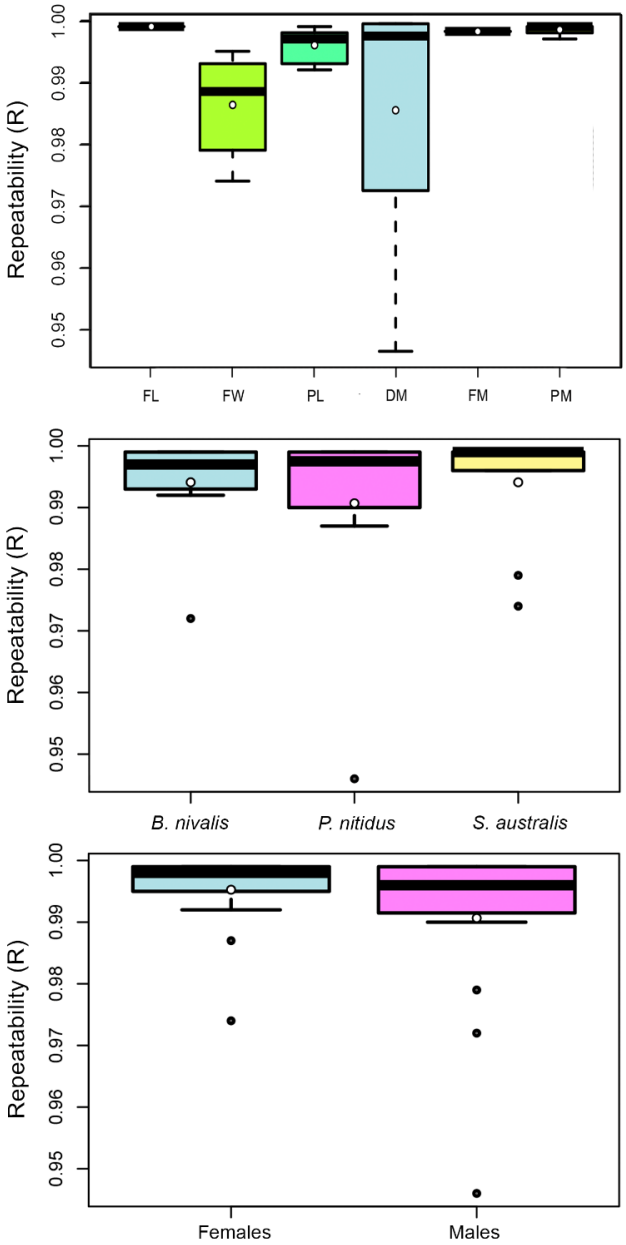

Table S1.1. Estimates of trait repeatability (R) by sex showing standard errors (SE) and 95% confidence intervals (95% CI). Trait range and mean (± standard deviation, SD) are provided. Trait: femur length (FL), femur width (FW), pronotum length (PL), preserved mass (PM), and dry mass (DM).

Trait	Species	Sex	Range	Mean ± SD	R ± SE	95% CI
FL	*B. nivalis*	M	9.88–12.30	11.112 ± 0.664	0.999 ± 0.002	0.994–1.000
FL	*B. nivalis*	F	13.13–17.10	14.989 ± 0.884	0.999 ± 0.005	0.988–0.999
FL	*P. nitidus*	M	10.11–11.34	10.761 ± 0.250	0.999 ± 0.007	0.985–0.999
FL	*P. nitidus*	F	14.19–16.18	15.298 ± 0.459	0.999 ± 0.004	0.988–0.999
FL	*S. australis*	M	10.55–12.17	11.214 ± 0.366	0.999 ± 0.004	0.992–1.000
FL	*S. australis*	F	15.95–19.21	17.291 ± 0.687	0.999 ± 0.007	0.991–1.000
FW	*B. nivalis*	M	3.01–3.76	3.354 ± 0.188	0.995 ± 0.020	0.964–0.999
FW	*B. nivalis*	F	3.86–4.92	4.367 ± 0.241	0.993 ± 0.020	0.948–0.998
FW	*P. nitidus*	M	2.75–3.18	2.981 ± 0.088	0.990 ± 0.024	0.929–0.998
FW	*P. nitidus*	F	3.82–4.49	4.120 ± 0.134	0.987 ± 0.035	0.891–0.997
FW	*S. australis*	M	2.91–3.46	3.229 ± 0.113	0.979 ± 0.057	0.834–0.995
FW	*S. australis*	F	4.44–5.24	4.826 ± 0.179	0.974 ± 0.062	0.776–0.994
PL	*B. nivalis*	M	3.49–4.65	4.195 ± 0.271	0.996 ± 0.017	0.961–0.999
PL	*B. nivalis*	F	4.88–6.51	5.577 ± 0.374	0.992 ± 0.017	0.942–0.998
PL	*P. nitidus*	M	3.96–4.67	4.338 ± 0.141	0.993 ± 0.028	0.936–0.998
PL	*P. nitidus*	F	5.01–6.67	6.020 ± 0.330	0.998 ± 0.005	0.984–0.999
PL	*S. australis*	M	3.22–4.19	3.799 ± 0.192	0.999 ± 0.004	0.988–0.999
PL	*S. australis*	F	5.66–6.70	6.163 ± 0.236	0.998 ± 0.007	0.984–0.999
DM	*B. nivalis*	M	0.059–0.108	0.081 ± 0.016	0.972 ± 0.056	0.815–0.994
DM	*B. nivalis*	F	0.102–0.256	0.178 ± 0.038	0.998 ± 0.009	0.981–0.999
DM	*P. nitidus*	M	0.058–0.067	0.062 ± 0.002	0.946 ± 0.138	0.477–0.991
DM	*P. nitidus*	F	0.135–0.226	0.182 ± 0.028	0.999 ± 0.001	0.995–1.000
DM	*S. australis*	M	0.039–0.072	0.057 ± 0.009	0.996 ± 0.006	0.982–0.999
DM	*S. australis*	F	0.156–0.390	0.253 ± 0.056	0.999 ± 0.002	0.993–1.000
FM	*B. nivalis*	M	0.191–0.360	0.285 ± 0.045	0.999 ± 0.001	0.997–1.000
FM	*B. nivalis*	F	0.429–0.832	0.636 ± 0.096	0.999 ± 0.001	0.998–1.000
FM	*P. nitidus*	M	0.173–0.251	0.208 ± 0.015	0.999 ± 0.001	0.993–1.000
FM	*P. nitidus*	F	0.500–0.779	0.618 ± 0.062	0.999 ± 0.001	0.992–1.000
FM	*S. australis*	M	0.173–0.240	0.207 ± 0.019	0.999 ± 0.001	0.994–1.000
FM	*S. australis*	F	0.641–1.198	0.877 ± 0.109	0.999 ± 0.001	0.991–1.000
PM	*B. nivalis*	M	0.178–0.345	0.270 ± 0.051	0.999 ± 0.001	0.997–1.000
PM	*B. nivalis*	F	0.408–0.819	0.609 ± 0.105	0.998 ± 0.001	0.989–0.999
PM	*P. nitidus*	M	0.160–0.230	0.197 ± 0.008	0.999 ± 0.001	0.996–1.000
PM	*P. nitidus*	F	0.463–0.741	0.579 ± 0.058	0.997 ± 0.001	0.987–0.999
PM	*S. australis*	M	0.166–0.235	0.195 ± 0.018	0.999 ± 0.001	0.994–0.999
PM	*S. australis*	F	0.633–1.152	0.831 ± 0.103	0.999 ± 0.001	0.991–1.000

Appendix 2. Effect of the preservation method (i.e., 95% ethanol) on body mass by comparing mass estimates between live (fresh mass) and preserved states (preserved mass after two and four months of preservation) in three New Zealand grasshopper species.

Figure S2.1. Shrinkage in body mass by species over two-month (A–B) and between two-month and four-month preservation period (C–D). White points indicate mean values.

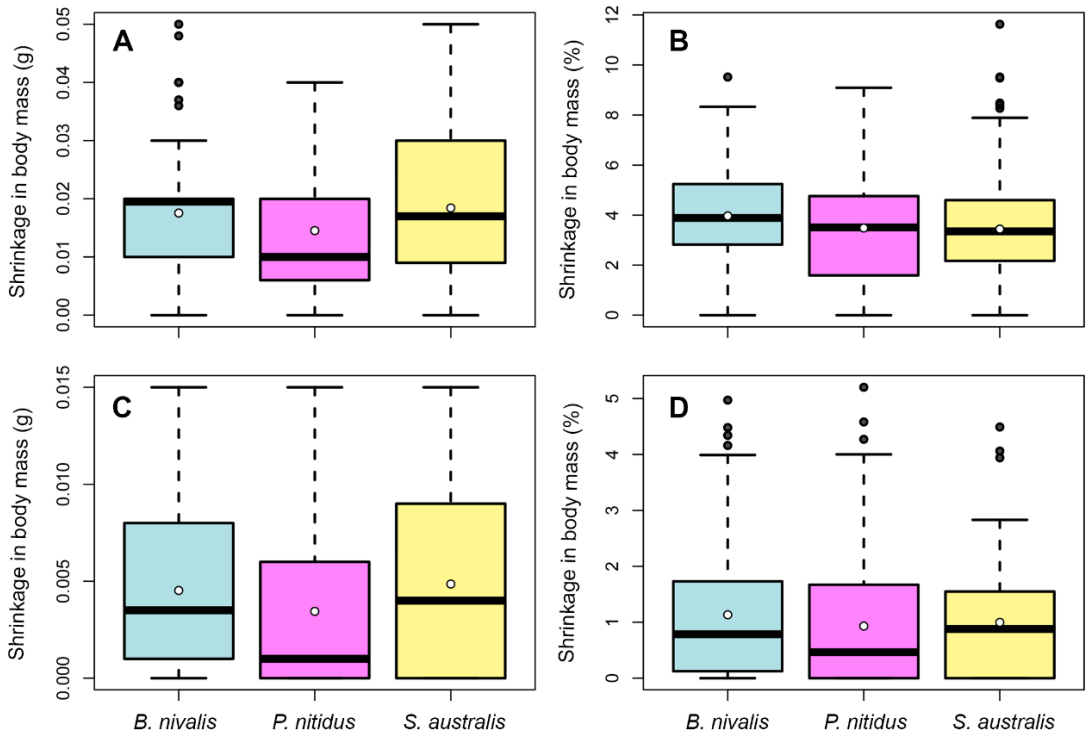

Figure S2.2. Shrinkage in body mass by sex over two-month (A–B) and between two-month and four-month preservation period (C–D). White points indicate mean values.

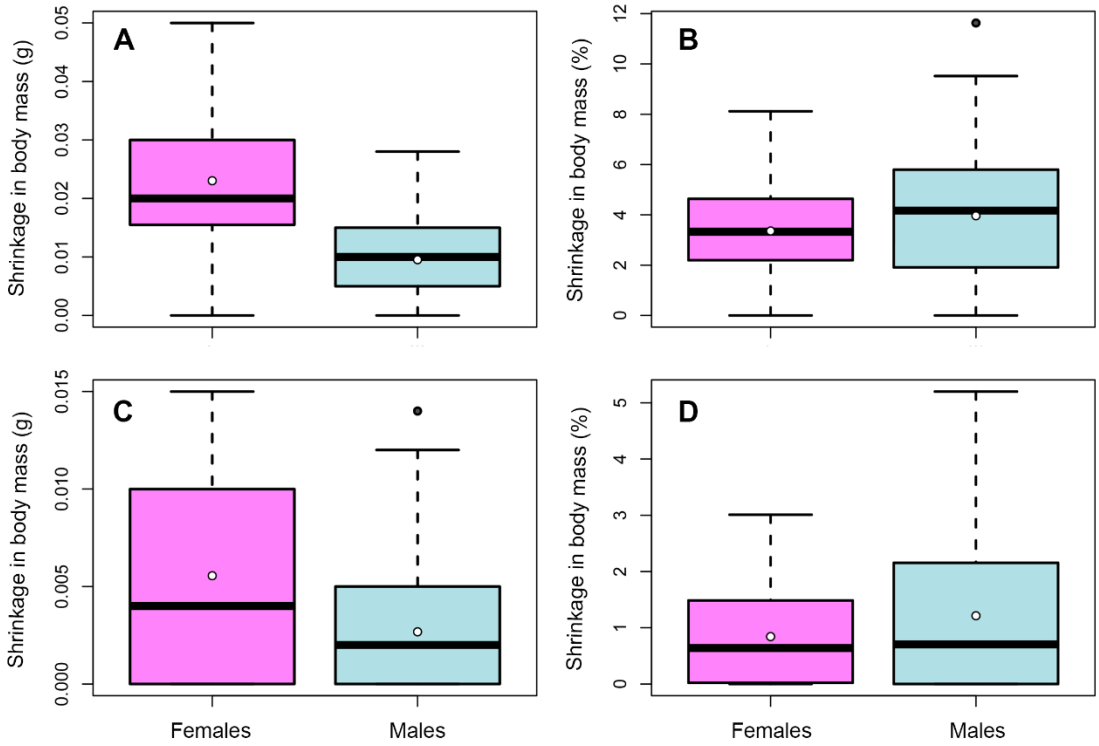

Appendix 3. Intraspecific relationships between preserved mass and both fresh and dry mass in three New Zealand grasshopper species.

Figure S3.1. Relationships between fresh mass and preserved mass (left panels) and dry mass and preserved mass (right panels). The dotted black lines represent the linear equation from standardized major axis regressions including an intercept term (i.e., not forced through the origin) and using the robust outlier option.

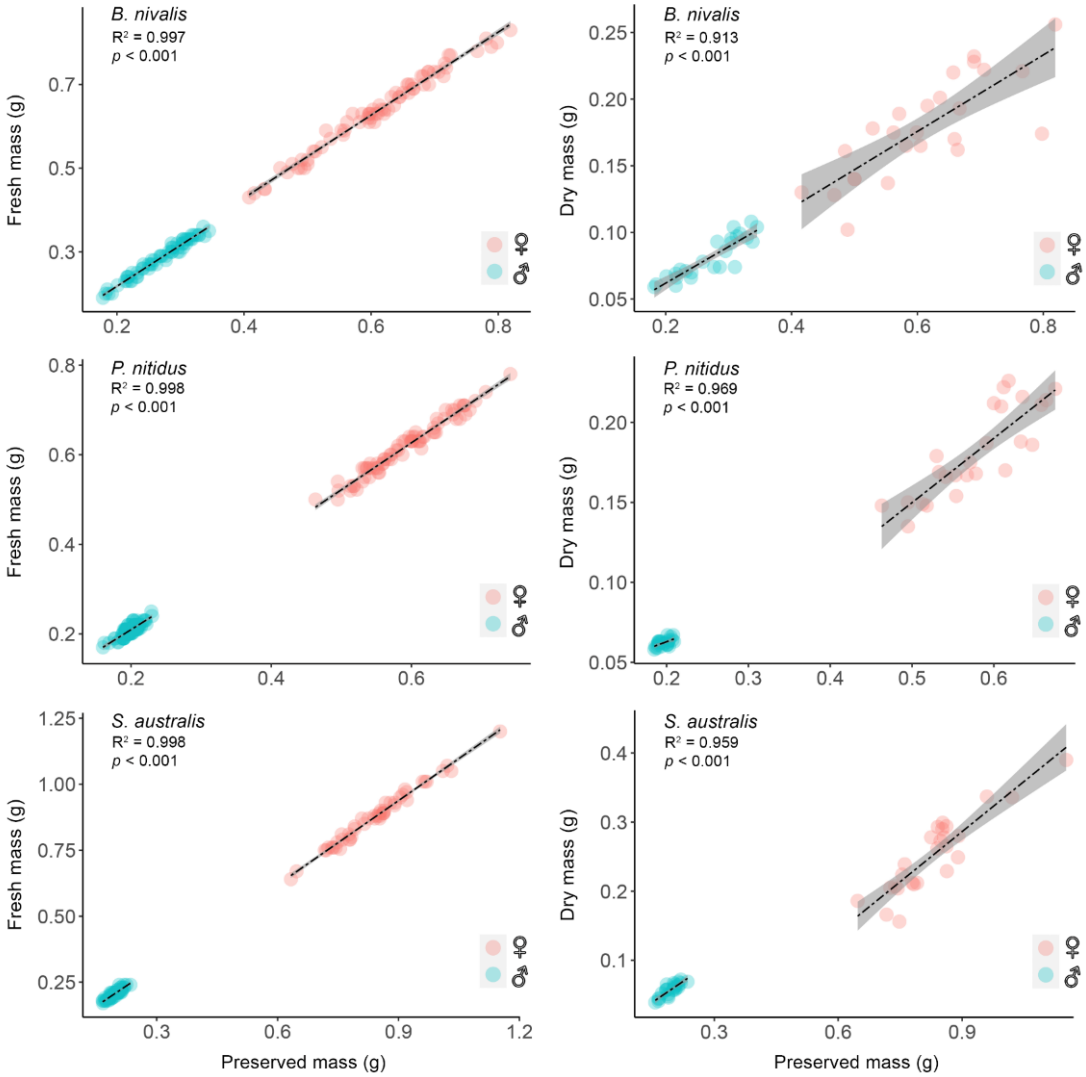

Table S3.1. Slope comparisons between sexes and among sites using an ANCOVA-like test with the slopes estimated by standardized major axis regressions. Likelihood ratio statistics (LRs), degrees of freedom, and *p*-values are shown.

Species	**Group**	**LRs**	**df**	***p*-value**
(a) fresh mass as a function of preserved mass				
Brachaspis nivalis	Sex	0.048	1	0.826
	Site	7.811	4	0.099
Paprides nitidus	Sex	1.117	1	0.291
	Site	3.361	4	0.499
Sigaus australis	Sex	0.547	1	0.460
	Site	3.590	4	0.309
(b) dry mass as a function of preserved mass				
Brachaspis nivalis	Sex	1.143	1	0.285
	Site	3.278	4	0.512
Paprides nitidus	Sex	3.787	1	0.052
	Site	8.654	4	0.070
Sigaus australis	Sex	0.865	1	0.352
	Site	17.79	4	< 0.001

Appendix 4. Regression parameters for the best-fitted linear mixed-effect models for body mass prediction based on preserved mass (Table 2) and femur length (Table 4) in three New Zealand grasshopper species.

Table S4.1. Parameters for body mass predictions based on body preserved mass (see Table 2). Standard deviations (SD) and standard errors (SE) for estimated slopes (β) and intercepts (α) are given. Abbreviations: The asterisks indicate significance levels of the regression parameters (*** indicates $p < 0.001$; ** indicates $p < 0.01$).

Species	Model formulae	Random effects		Fixed effects			
		α_{Site} (SD)	β_{PM} (SD)	Residual (SD)	α (SE)	β_{PM} (SE)	β_{Sex} (SE)
(a) fresh mass (FM) as a function of preserved mass (PM)							
B. nivalis	FM~PM+Sex+(1|Site)	2.760^{-6} (0.002)	N/A	1.106^{-4} (0.011)	0.030 (0.008)***	0.995 (0.013)***	-0.0124 (0.005)**
P. nitidus	FM~PM+(1|Site)	2.374^{-6} (0.002)	N/A	9.262^{-5} (0.001)	0.001 (0.002)	1.042 (0.004)***	N/A
S. australis	FM~PM+(1|Site)	2.870^{-5} (0.005)***	N/A	8.982^{-5} (0.009)	0.002 (0.003)	1.038 (0.003)***	N/A
(b) dry mass (DM) as a function of preserved mass (PM)							
B. nivalis	DM~PM+(1|Site)	0.000 (0.000)	N/A	0.001 (0.016)	0.004 (0.006)	0.287 (0.013)***	N/A
P. nitidus	DM ~PM+Sex+(PM|Site)	9.868^{-6} (0.003)	3.541^{-4} (0.003)	7.663^{-5} (0.009)	-0.052 (0.019)**	0.403 (0.033)***	0.035 (0.012)**
S. australis	DM ~PM+Sex+(PM|Site)	2.993^{-5} (0.005)	4.939^{-4} (0.022)	2.320^{-4} (0.015)	-0.103 (0.028)***	0.426 (0.035)***	0.077 (0.021)***

Table S4.2. Parameters for body mass predictions as a function of femur length (see Table 4). Standard deviations (SD) and standard errors (SE) for estimated slopes (β) and intercepts (α) are given. Abbreviations: The asterisks indicate significance levels of the regression parameters (*** indicates $p < 0.001$; * indicates $p < 0.05$).

Species	**Model formulae**	**Random effects**		**Fixed effects**			
		α_{Site} (SD)	**Residual (SD)**	**α (SE)**	**B_{FL} (SE)**	**β_{Sex} (SE)**	**$\beta_{FL:Sex}$ (SE)**
(a) fresh mass (FM) as a function of femur length (FL)							
B. nivalis	ln(FM)~ln(FL)*Sex+(1|Site)	6.28^{-20} (2.51^{-10})	6.065^{-3} (7.788^{-2})	-6.289 (0.429)***	2.152 (0.159)***	-1.176 (0.588)*	0.422 (0.230)
P. nitidus	ln(FM)~ln(FL)+(1|Site)	0.000 (0.000)	0.007 (0.085)	-8.813 (0.101)***	3.051 (0.004)***	N/A	N/A
S. australis	ln(FM)~ln(FL)+(1|Site)	0.000 (0.000)	0.009 (0.097)	-9.528 (3.293)***	3.293 (0.047)***	N/A	N/A
(a) dry mass (DM) as a function of femur length (FL)							
B. nivalis	ln(DM)~ln(FL)+(1|Site)	0.000 (0.000)	0.020 (0.141)	-8.646 (0.311)***	2.544 (0.121)***	N/A	N/A
P. nitidus	ln(DM)~ln(FL)+(1|Site)	0.000 (0.000)	0.014 (0.116)	-9.947 (0.242)***	3.021 (0.095)***	N/A	N/A
S. australis	ln(DM)~ln(FL)+(1|Site)	0.002 (0.049)	0.026 (0.161)	-11.123 (0.282)***	3.425 (0.106)***	N/A	N/A

Appendix 5. Relationships between mass estimates (g) and body dimensions (mm) in three New Zealand grasshopper species.

Figure S5.1. Pairwise correlation coefficients between body size metrics (i.e., femur length = FL, femur width = FW, pronotum length = PL, dry mass = DM, fresh mass = FM, and preserved mass = PM) for *B. nivalis* (blue), *P. nitidus* (green), and *S. australis* (grey). Measures are in mm. Significant ($p < 0.001$) correlations are denoted by ***.

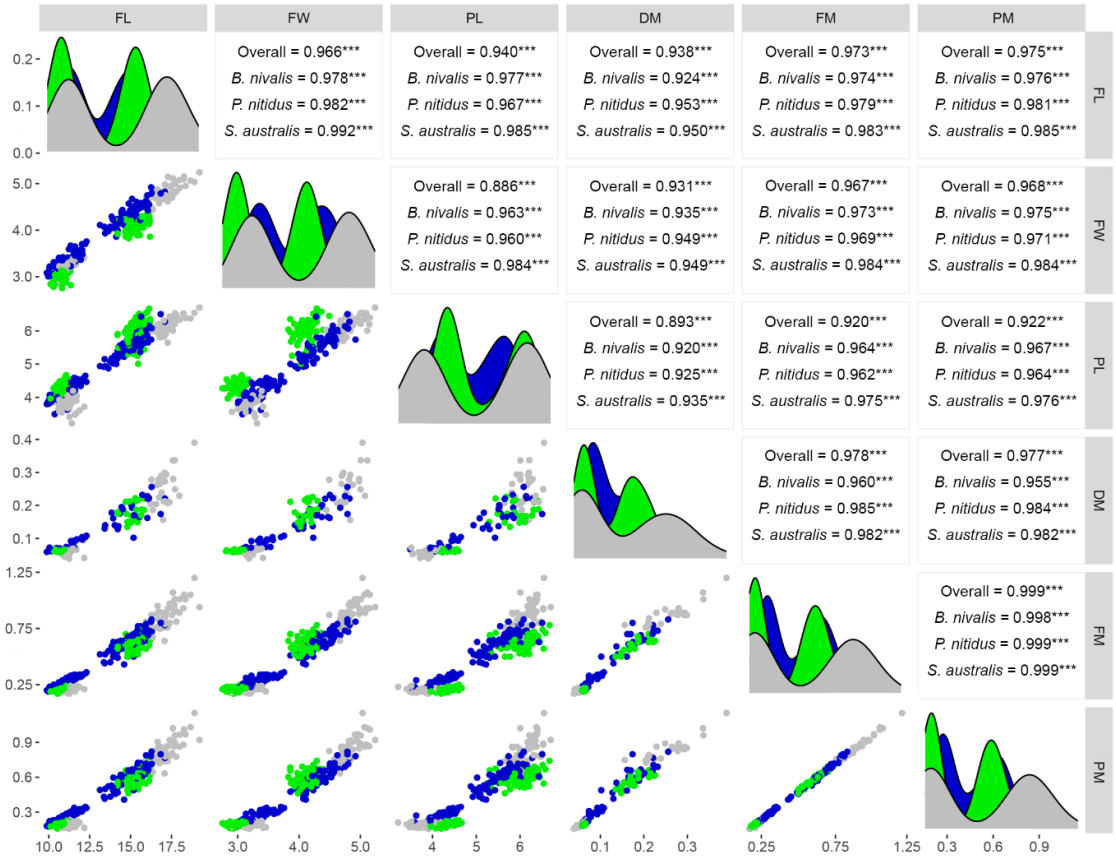

Figure S5.2. Relationships between fresh mass and femur length (left panels), femur width (center panels) length, and pronotum length (right panels) based on OLS regressions. The dotted black lines represent the linear regression with grey-shaded area denoting the 95% confidence intervals.

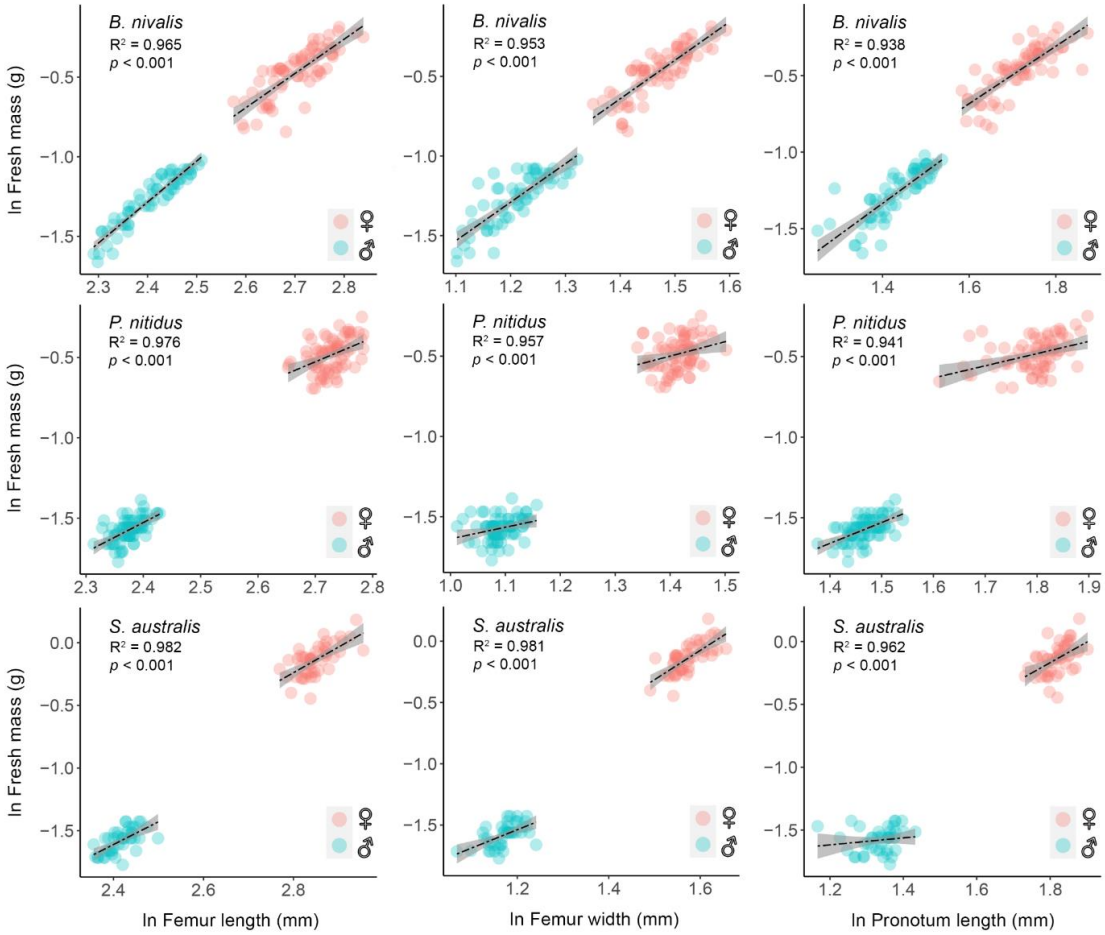

Figure S5.3. Relationships between dry mass and femur length (left panels), femur width (center) length, and pronotum length (right panels) based on OLS regressions. The dotted black lines represent the linear regression with grey-shaded area denoting the 95% confidence intervals.

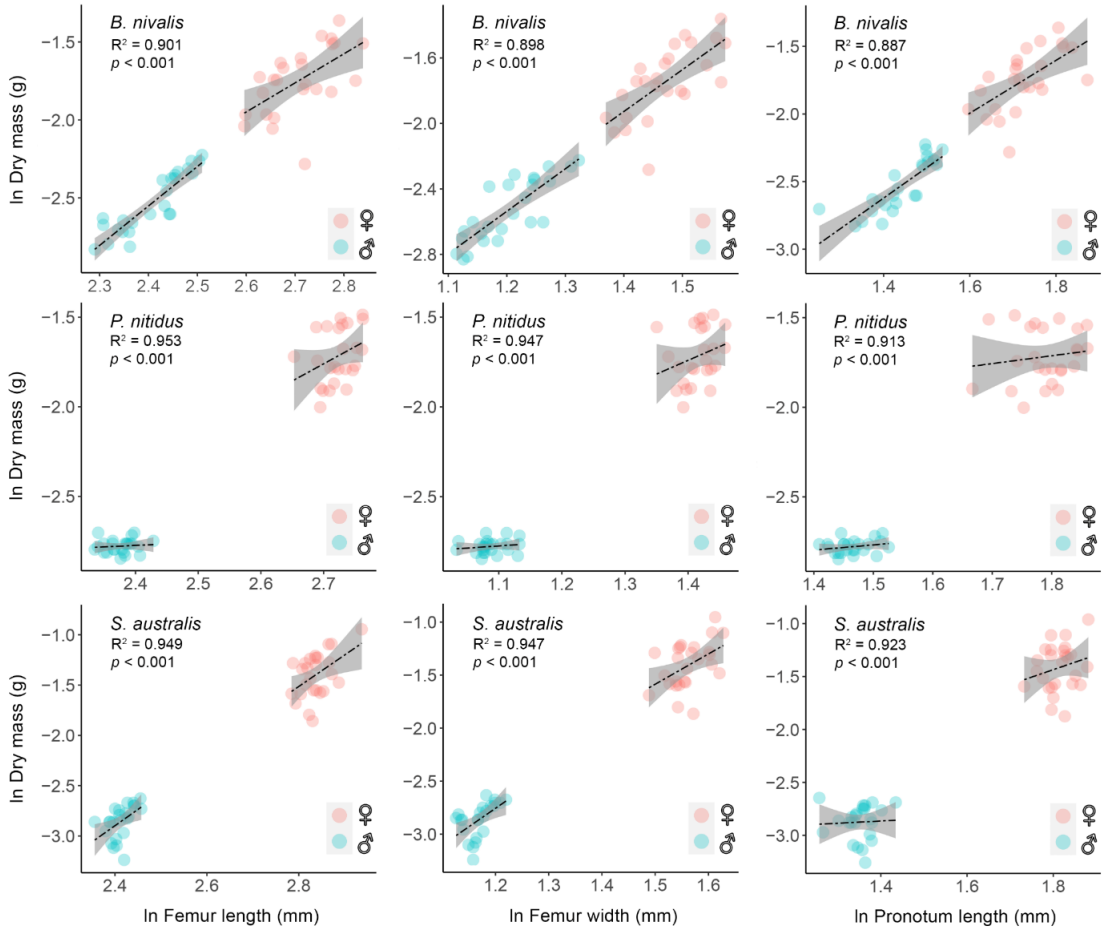

Table S5.1. Slope comparisons between sexes within species based on OLS regressions of fresh mass and body dimensions. Standard errors (SE), degrees of freedom (df), and 95% confidence intervals (95% CI) are shown. Significance (*p*-values) for pairwise slope comparison from Tukey's tests are given between brackets.

Species	**Sex**	**Slope**	**SE**	**df**	**95% CI**
(a) fresh mass as a function of femur length					
Brachaspis nivalis	♀	0.163	0.012	127	0.139–0.187
(p = 0.073)	♂	0.195	0.013	127	0.170–0.221
Paprides nitidus	♀	0.115	0.023	143	0.069–0.160
(p = 0.496)	♂	0.141	0.030	143	0.081–0.200
Sigaus australis	♀	0.141	0.022	86	0.098–0.185
(p = 0.669)	♂	0.126	0.029	86	0.069–0.183
(b) fresh mass as a function of femur width					
Brachaspis nivalis	♀	0.621	0.050	127	0.522–0.721
(p = 0.994)	♂	0.621	0.053	127	0.517–0.725
Paprides nitidus	♀	0.251	0.086	143	0.080–0.421
(p = 0.709)	♂	0.202	0.096	143	0.013–0.392
Sigaus australis	♀	0.585	0.081	86	0.424–0.746
(p = 0.071)	♂	0.363	0.091	86	0.183–0.543
(c) fresh mass as a function of pronotum length					
Brachaspis nivalis	♀	0.380	0.035	127	0.312–0.449
(p = 0.447)	♂	0.419	0.038	127	0.344–0.494
Paprides nitidus	♀	0.145	0.031	143	0.083–0.207
(p = 0.099)	♂	0.250	0.055	143	0.142–0.358
Sigaus australis	♀	0.324	0.076	86	0.173–0.475
(p = 0.007)	♂	0.056	0.060	86	-0.064–0.176

Table S5.2. Slope comparisons between sexes within species based on OLS regressions of dry mass and body dimensions. Standard errors (SE), degrees of freedom (df), and 95% confidence intervals (95% CI) are shown. Significance (*p*-values) for pairwise slope comparison from Tukey's tests are given between brackets.

Species	**Sex**	**Slope**	**SE**	**df**	**95% CI**
(a) dry mass as a function of femur length					
Brachaspis nivalis	♀	0.142	0.032	46	0.077–0.208
(*p* = 0.275)	♂	0.193	0.033	46	0.128–0.259
Paprides nitidus	♀	0.147	0.063	45	0.020–0.274
(*p* = 0.174)	♂	0.013	0.074	45	-0.136–0.161
Sigaus australis	♀	0.220	0.073	46	0.073–0.368
(*p* = 0.953)	♂	0.227	0.104	46	0.018–0.435
(b) dry mass as a function of femur width					
Brachaspis nivalis	♀	0.663	0.123	46	0.416–0.910
(*p* = 0.949)	♂	0.674	0.121	46	0.430–0.918
Paprides nitidus	♀	0.430	0.237	45	-0.048–0.909
(*p* = 0.298)	♂	0.068	0.249	45	-0.433–0.569
Sigaus australis	♀	0.707	0.232	46	0.240–1.170
(*p* = 0.716)	♂	0.861	0.349	46	0.157–1.560
(c) dry mass as a function of pronotum length					
Brachaspis nivalis	♀	0.395	0.088	46	0.218–0.572
(*p* = 0.621)	♂	0.457	0.086	46	0.284–0.629
Paprides nitidus	♀	0.085	0.091	45	-0.099–0.268
(*p* = 0.870)	♂	0.056	0.147	45	-0.240–0.351
Sigaus australis	♀	0.042	0.212	46	-0.383–0.468
(*p* = 0.438)	♂	0.279	0.217	46	-0.157–0.715

Appendix 6. Non-linear models fitted to describe intraspecific allometric relationships between mass estimates (FM and DM) and femur length (FL) in three New Zealand grasshopper species.

Table S6.1. Model selection for intraspecific allometric relationships. Best-fitting models based on AIC (ΔAIC < 2) values are shown in bold.

Species	Sex	Model	df	AIC	ΔAIC
(a) fresh mass as a function of femur length					
Brachaspis nivalis	♀	**logistic**	**3**	**-202.06**	**0.00**
		linear	**3**	**-201.86**	**0.20**
		Power function	**3**	**-201.30**	**0.76**
		quadratic	**3**	**-201.03**	**1.03**
		4-parameter logistic	4	-200.02	2.04
		Weibull growth function	5	-198.20	3.86
	♂	**quadratic**	**4**	**-335.51**	**0.00**
		4-parameter logistic	**5**	**-333.62**	**1.89**
		linear	**3**	**-333.56**	**1.95**
		Power function	3	-328.23	7.28
		logistic	3	27.31	362.82
		Weibull growth function	3	27.31	362.82
Paprides nitidus	♀	**Power function**	**3**	**-429.81**	**0.00**
		linear	**3**	**-429.59**	**0.22**
		quadratic	**4**	**-429.57**	**0.24**
		4-parameter logistic	**5**	**-429.16**	**0.65**
		logistic	3	-15.60	414.21
		Weibull growth function	3	-15.60	414.21
	♂	**quadratic**	**4**	**-213.28**	**0.00**
		4-parameter logistic	**5**	**-213.22**	**0.06**
		Power function	**3**	**-212.42**	**0.86**
		linear	**3**	**-212.26**	**1.02**
		logistic	**3**	**-211.98**	**1.30**
		Weibull growth function	3	-211.43	2.05
Sigaus australis	♀	**4-parameter logistic**	**5**	**-228.30**	**0.00**
		quadratic	**4**	**-228.29**	**0.01**
		linear	**3**	**-227.84**	**0.46**
		Power function	**3**	**-227.58**	**0.72**
		logistic	3	-6.86	221.44
		Weibull growth function	3	-6.86	221.44
	♂	**Power function**	**3**	**-100.63**	**0.00**
		linear	**3**	**-100.48**	**0.15**
		4-parameter logistic	**5**	**-100.01**	**0.62**
		quadratic	**4**	**-98.76**	**1.87**
		Weibull growth function	3	-93.13	7.50
		logistic	3	-31.63	69.00

(b) dry mass as a function of femur length					
Brachaspis nivalis	♀	**quadratic**	**4**	**-179.17**	**0.00**
		4-parameter logistic	**5**	**-178.62**	**0.55**
		Power function	**3**	**-177.32**	**1.85**
		linear	3	-176.56	2.61
		Weibull growth function	3	-146.79	32.38
		logistic	3	-47.78	131.39
	♂	**linear**	**3**	**-99.63**	**0.00**
		Power function	**3**	**-99.54**	**0.09**
		quadratic	**4**	**-97.75**	**1.88**
		4-parameter logistic	5	-96.08	3.55
		logistic	3	-8.19	91.44
		Weibull growth function	3	-8.19	91.44
Paprides nitidus	♀	**linear**	**3**	**-217.20**	**0.00**
		Power function	**3**	**-217.19**	**0.01**
		quadratic	**4**	**-216.16**	**1.04**
		4-parameter logistic	5	-212.88	4.32
		Weibull growth function	3	-207.04	10.16
		logistic	3	-59.17	158.03
	♂	**Power function**	**3**	**-106.36**	**0.00**
		linear	**3**	**-106.29**	**0.07**
		quadratic	**4**	**-105.70**	**0.66**
		4-parameter logistic	5	-103.62	2.74
		logistic	3	-7.82	98.54
		Weibull growth function	3	-7.82	98.54
Sigaus australis	♀	**quadratic**	**4**	**-159.95**	**0.00**
		linear	**3**	**-158.59**	**1.36**
		Power function	**3**	**-158.57**	**1.38**
		4-parameter logistic	5	-156.54	3.41
		logistic	3	-65.41	98.54
		Weibull growth function	3	-65.41	98.54
	♂	**Power function**	**3**	**-80.59**	**0.00**
		logistic	**3**	**-80.54**	**0.05**
		linear	**3**	**-80.15**	**0.44**
		quadratic	**4**	**-79.52**	**1.07**
		4-parameter logistic	5	-77.57	3.02
		Weibull growth function	3	9.47	90.06

“Those forms which possess in some considerable degree the character of species, but which are so closely similar to some other forms, or are so closely linked to them by intermediate gradations, that naturalists do not like to rank them as distinct species, are in several respects the most important for us.”

(Darwin, 1859, p. 47)

Sigaus piliferus, the sole grasshopper within the New Zealand alpine radiation endemic to North Island. Taranaki Falls, Tongariro National Park, North Island.

Chapter Four

Phenotypic and genetic divergence in a cold-adapted grasshopper may lead to lineage-specific responses to rapid climate change

MASSEY UNIVERSITY
TE KUNENGA KI PŪREHUROA
UNIVERSITY OF NEW ZEALAND

GRADUATE RESEARCH SCHOOL

STATEMENT OF CONTRIBUTION
DOCTORATE WITH PUBLICATIONS/MANUSCRIPTS

We, the student and the student's main supervisor, certify that all co-authors have consented to their work being included in the thesis and they have accepted the student's contribution as indicated below in the Statement of Originality.

Student name:	Fabio Leonardo Meza Joya
Name and title of main supervisor:	Steven A. Trewick
In which chapter is the manuscript/published work?	Chapter 4

Describe the contribution that the student and members of the supervisory team have made to the manuscript/published work:[1]

Conceptualization and data collection: Fabio Leonardo Meza-Joya, Steven A. Trewick and Mary Morgan-Richards; Data curation and analysis: Fabio Leonardo Meza-Joya; Visualization and writing – original draft: Fabio Leonardo Meza-Joya; Writing – review and editing: Steven A. Trewick and Mary Morgan-Richards; Funding acquisition: Fabio Leonardo Meza-Joya, Steven A. Trewick and Mary Morgan-Richards; Supervision: Steven A. Trewick and Mary Morgan-Richards.

Please select one of the following three options:

- ○ The manuscript/published work is published or in press
  Please provide the full reference of the research output:
- ◉ The manuscript is currently under review for publication
  Please provide the name of the journal:
  Diversity & Distributions
- ○ It is intended that the manuscript will be published, but it has not yet been submitted to a journal

Student's signature:	Fabio Leonardo Meza Joya — Digitally signed by Fabio Leonardo Meza Joya Date: 2024.01.02 15:00:17 +13'00'	Main supervisor's signature:	Digitally signed by Steve Trewick Date: 2024.01.09 10:37:35 +13'00'

This form should be placed at the beginning of each relevant thesis chapter.

[1] Refer to the Massey University Publishing and Authorship guidelines (OneMassey for staff, Stream for students) and/ or Contributor Roles Taxonomy (CRediT) guidelines for guidance.

Abstract

Aim: Species responses to global warming will depend on intraspecific diversity, yet studies of factors governing biogeographic patterns of variability are scarce. Here, we investigate the evolutionary processes underlying genetic and phenotypic diversity in the flightless and cold-adapted grasshopper *Sigaus piliferus*, and project its suitable space in time.

Location: Te Ika-a-Māui Aotearoa—North Island of New Zealand.

Methods: We used mitochondrial sequences to investigate population connectivity and demographic trends using phylogeographic tools and neutrality statistics. Body size and pronotum shape were used to document phenotypic variation using naïve clustering. We used niche metrics to assess intraspecific niche variation, and niche modelling to investigate suitability under past and future scenarios. Genotype-phenotype-environment associations were explored using multiple matrix regressions with randomization.

Results: Niche models and genetic data suggest suitable space for this grasshopper was more restricted during glacial than interglacial stages. Genealogical relationships among ND2 haplotypes revealed a deep north-south split partly concordant with phenotypic and niche variation. Demographic analyses depict a general situation of population expansion, yet varied levels of genetic diversity were observed. Genotype-phenotype-environment analyses indicate a link between climate and body size differentiation, but not pronotal shape. Niche projections predict severe habitat reduction due to climate warming.

Main conclusions: The current distribution and intraspecific diversity of *S. piliferus* reflect complex biogeographical scenarios consistent with Quaternary climates and volcanism. Phenotypic divergence in body size appears adaptive, but the same may not apply to pronotum shape. Current levels of genetic and phenotypic variation suggest adaptive potential, yet the pace of anthropogenic warming over the next 50 years could result in small populations that may collapse before adapting. Differences in niche features between diverging intraspecific lineages suggest distinct responses to climate change, and this has implications for prioritising conservation actions and management strategies.

Keywords: adaptation, conservation, genetic drift, intraspecific variation, Quaternary climates and volcanism, range shifts

Introduction

Understanding the forces shaping intraspecific variability is a keystone in evolutionary biogeography and conservation, providing important insights on the factors determining biotic responses to environmental changes (Seaborn et al., 2021). Spatial patterns of intraspecific variation reflect the influence of past environmental fluctuations leading to divergent evolutionary trajectories (Gillespie & Roderick, 2014; Grant & Grant, 2017; Hewitt, 2004). Quaternary climates, and in particular late glacial stages, were major drivers of biogeographic reorganisation around the world (Davis & Shaw, 2001; Hewitt, 2004; Steward et al., 2010), and it is apparent that the effects of Pleistocene climate change on biota covaried with latitude, topography, and intrinsic species traits such as dispersal behaviour and ecological preferences (Byrne, 2008; Davis & Shaw, 2001; Đurović et al., 2020; Hewitt, 2004; Stewart et al., 2010). Polar ice cap extension and retreat in the Northern Hemisphere in inferred to be a key driver of population range shifts in many species, whereas Southern Hemisphere landscapes were little effected in this way (Byrne, 2008; Carmelet-Rescan et al., 2021; Meza-Joya et al., 2023; Trewick et al., 2000). Conditions during glacial phases appear to have promoted range expansion of cold-adapted biota, especially in regions less affected by polar ice sheet such as mountains in the tropics (Hewitt, 2004), the Japanese Alps (Ikeda & Setoguchi, 2007), and Southern Alps in New Zealand (Trewick et al., 2000). These range shifts shaped distinct genetic and phenotypic variants upon which deterministic (e.g. selection) and stochastic forces (e.g. genetic drift) acted to mould modern patterns of intraspecific diversity (Gillespie & Roderick, 2014; Grant & Grant, 2017; Hewitt, 2004).

The New Zealand Southern Alps (Kā Tiritiri o te Moana) dominate the South Island landscape, climate and to a large extent biogeography, but North Island, New Zealand (Te Ika-a-Māui, Aotearoa) has a different and geologically younger landscape. Here the study of biogeographic partitioning has to consider the extensive geophysical remodelling that was coincident with Plio-Pleistocene climate shifts (Figure 1). Most of southern North Island emerged as land since Late Pliocene (3 Mya) and late Pleistocene land connection bridging may have allowed exchange of terrestrial biota between the main islands (Trewick & Bland, 2012). Rapid uplift of the southern North Island axial ranges during Pleistocene (~1 Mya) generated heterogeneous environments (Trewick & Bland, 2012) that appear to have stimulated lineage diversification (Heenan & McGlone,

2013; Marshall et al., 2012; Prebble et al., 2021). More recent sea straits (~450 kyr) may have partitioned terrestrial populations but gene flow was possible during lowered sea levels of the later glaciations (Trewick & Bland, 2012; Trewick et al., 2017). Repeated and lengthy Pleistocene glacial phases (Rother et al., 2014), drove vegetation turnover that may have repeatedly reshaped animal biogeography (e.g. Trewick et al., 2000). In particular a shift between forest during warmer stages and alpine-like scrub grassland during cooler, drier phases (McGlone, 1985). Volcanism in the centre of the island promoted vicariant processes (Trewick et al., 2011), and genetic data indicate intraspecific secondary contacts in the area (Shepherd et al., 2022), and instances of hybridisation have been detected between cytogenetically divergent populations of the tree wētā *Hemideina thoracica* (Morgan-Richards et al., 2000).

Here we examine drivers of intraspecific diversity in *Sigaus piliferus* Hutton (Orthoptera: Acrididae), the sole North Island representative of an endemic New Zealand radiation of flightless, cold-adapted grasshoppers (Koot et al., 2022). According to fossil calibrated phylogenetic analysis this species diverged from a common ancestor with the larger high-alpine *Sigaus villosus* Salmon ~14 Mya (17–11 Mya) during the Middle Miocene (Koot et al., 2020), so its current patchy and relatively low latitude distribution could reflect responses to late Neogene geoclimatic conditions. Like its South Island counterparts, *S. piliferus* is common in alpine areas, but unlike them, it also naturally occurs in sub-alpine habitats, where it seems to be rare and subject to local population extinction over the last 80 years (Trewick & Morris, 2008). As expected of a small, flightless endemic insect (Koot et al., 2022), this species displays apparent phenotypic (Bigelow, 1967) and genotypic (Trewick & Morris, 2008) spatial structure, that suggest a combination of restricted gene flow and local selective pressures. The absence of near relatives of *S. piliferus* in North Island and ability of this species to inhabit alpine and non-alpine ecosystems is suggestive of ecological flexibility and/or adaption to alternative conditions.

Integration of genetic, phenotypic, and climatic data provides a robust framework to investigate possible drivers of local adaptation and to identify populations that require conservation resources to avoid loss of evolutionary potential (Dowle et al., 2015; Merilä & Hendry, 2014; Mullen et al., 2009). Genetic analyses using mitochondrial sequences provide information about the influence of palaeo-geophysical changes on population

connectivity and demography, and correlation with morphological variation. Ecological niche models allow us to infer persistence and vulnerability of suitable environmental space through time based on climate proxies. Observations from other cold-adapted New Zealand grasshoppers (e.g. Carmelet-Rescan et al., 2021; Meza-Joya et al., 2023) suggest *S. piliferus* was probably compatible with glacial climates, hence we expect cold stages to have allowed population expansion compared to interglacials. By exploring genetic, phenotypic and environmental associations we estimate the relative role of genetic drift and selection on patterns of phenotypic differentiation across this species range. The active geophysical history of North Island must have been influential for the genetic (Trewick & Morris, 2008) and morphological (Bigelow, 1967) differentiation observed in populations of this species, so we would expect both deterministic and stochastic evolutionary processes to explain current patterns of intraspecific divergence. If as expected, past climates influenced the spatial distribution of intraspecific diversity in this grasshopper, then anthropogenic warming during this century will also influence surviving diversity.

Materials and Methods

Sample collection and DNA extraction

We collected *Sigaus piliferus* from 33 locations spanning its documented range (Figure 1; Table S1.1). Most specimens came from elevations above 1000 m, but lower elevation populations were also identified and sampled. Grasshoppers were collected during summer when they were active (December to March 2004–2022) and frozen before being preserved in 95% ethanol. Taxonomic identification, sex, and maturity were determined based on morphological traits (Bigelow, 1967). Whole genomic DNA was extracted from leg muscle of 186 specimens (Table S1.1) using a solvent-free Proteinase K and salting-out method (Trewick & Morgan-Richards, 2005). Extracted DNA was amplified by PCR for the mitochondrial protein-coding NADH-dehydrogenase 2 (ND2) gene under standard conditions, using the primers HopND2_147F and HopND2_1286R (Carmelet-Rescan et al., 2021). This marker has a higher capacity to accumulate haplotype diversity in these grasshoppers than the commonly analysed COI locus (Carmelet-Rescan et al., 2021). Sequencing reactions used BigDye Terminator v.3.1 (Life Technologies) with

signal capture on an ABI-3730xl System (ThermoFisher). DNA sequences were edited and aligned in GENEIOUS vR10 (Kearse et al., 2012).

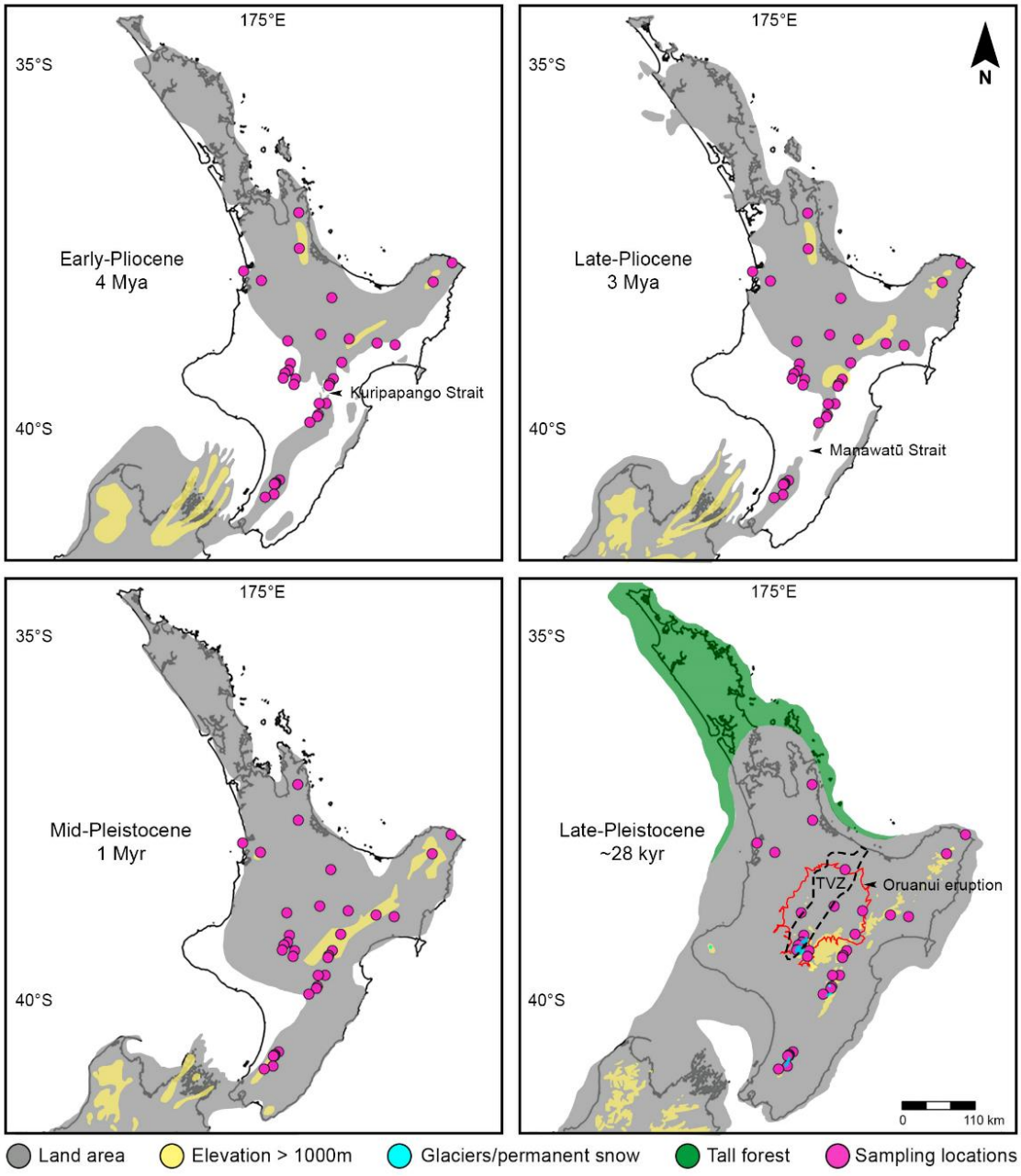

Figure 1. North Island, New Zealand palaeogeography against the modern coastline, indicating major geophysical features since late Pliocene time. Tectonic uplift (Trewick & Bland, 2012), lowered sea level (~28 kyr; Rother et al., 2014) and continuous forests contraction at the last glacial phase (Newnham et al., 2013), with area affected by widespread pyroclastic flow from Oruanui eruption in the Taupō Volcanic Zone (TVZ) at ~25.5 kyr (Wilson, 2001). Sampling of *Sigaus piliferus* location names are available in Table S1.1. Map projection: NZGD2000.

Population genetic structure and demography

Genealogical relationships among ND2 haplotypes were inferred using a statistical parsimony network algorithm implemented in POPART 1.7 (Leigh and Bryant, 2015). Statistical support for distinct mitochondrial lineages was evaluated with a Bayesian phylogenetic analysis in MRBAYES 3.2.6 (Ronquist et al., 2012) with *Sigaus villosus* as outgroup taxon (Koot et al., 2020). The analysis used four chains on two runs for 20^6 generations, with sampling frequency of 20^3 generations and a burn-in of 0.10. Pairwise genetic distances between population samples were estimated using MEGA X (Kumar et al., 2018) based on the Kimura 2-parameter (K2P; Kimura, 1980) and Tamura-Nei (TN; Tamura & Nei, 1993) models with 1,000 bootstrap replicates. We used spatial Principal Component Analysis (sPCA) in the R (R Core Team, 2022) package 'adegenet' 2.1.3 (Jombart, 2008) to examine non-random spatial patterns of genetic variability. Spatial distances were based on the K nearest neighbours method (K = 25), which allowed possible connections at regional scale, and statistical significance was assessed using an Eigenvalue test (Montano & Jombart, 2017) with 10,000 permutations. We tested for genetic differentiation among the identified sPCA genetic clusters using an AMOVA with the R package 'poppr' 2.9.3 (Kamvar et al., 2014) with 10,000 permutations.

Matrilineal DNA variability in population samples ($n > 5$) was estimated using DNASP 5.10 (Librado & Rozas, 2009) to compute haplotype (h) and nucleotide diversity (π). Pairwise Φ_{ST} values (Excoffier et al., 1992) were computed to test genetic differentiation among populations with the R package 'haplotypes' 1.1.2 (Aktas, 2020) with 10,000 replicates. Historical demography was inferred using mismatch distributions under the constant population size model with DNASP. The fit of the observed distribution to the null model was evaluated using the Harpending's r raggedness index (Harpending, 1994). We also calculated three neutrality statistics to detect departures from the mutation–drift equilibrium indicative of population size change under the assumption of locus neutrality: Tajima's D (Tajima, 1989), Fu's F_S (Fu, 1997) and Ramos-Onsins' R_2 (Ramos-Onsins & Rozas, 2002). Statistical significance ($P < 0.05$ except for Fs where $P < 0.02$) was evaluated with 10,000 simulations. The correlation between pairwise genetic (Φ_{ST}) and topographically-corrected geographic distances (km) derived using the R package 'TopoDistance' 0.3.7 (Wang, 2020), was studied using a Mantel test with 10,000 permutations in the R package 'ade4' v1.7–17 (Bougeard & Dray, 2018).

Morphological variation

We applied traditional and geometric morphometrics to test for congruent patterns between phenotypic and genetic variation (Figure S2.1). For our traditional approach, four non-independent body dimensions (hind femur length, FL; hind femur width, FW; pronotum length, PL; pronotum width, PW) and two ratios (FL/FW and PW/PL) were recorded from 156 adult grasshoppers (n = 100♀, 56♂; Table S2.1) using an Olympus SZX7 stereomicroscope with Olympus SC100 image capture and Olympus cellSens Dimension v1.6 software (Olympus Corporation, Japan). These metrics were chosen as they are not arbitrarily affected by preservation (Bigelow, 1967), correlate with body mass (Meza-Joya et al., 2022), and informative of phenotypic variation in *S. piliferus* (Bigelow, 1967). For the geometric method we digitalised 14 landmarks around the dorsal perimeter of the pronotum on images from 161 adult grasshoppers (n = 101♀, 60♂; Table S2.2) using TPSDIG2 2.29 (Rohlf, 2015). This structure is informative for analysing size-independent shape variation in New Zealand alpine grasshoppers (Carmelet-Rescan et al., 2021). Images were taken using a Canon EOS 600D with EF100 mm f2.8 USM macro lens (Canon Inc., Japan) mounted on a vertical stand (Kaiser Fototechnik, Germany). A Generalized Procrustes Analysis (GPA) was applied to remove non-shape variation from the dataset using the R package 'geomorph' 4.0.0 (Adams et al., 2020). Repeatability analyses indicated any technical measurement error was biologically negligible (Figure S2.2).

Preliminary analyses showed the studied traits are sexually dimorphic in this grasshopper (Figure S2.3) and thus, only females were analysed hereafter due to better sample size and more homogeneous geographic sampling compared to males. We modelled the most likely number of morphological clusters within our datasets (size and shape) without prior information on specimen origin using Gaussian mixture modelling with the R package 'Mclust' 5.0.2 (Scrucca et al., 2016). For the traditional approach, analyses considered the total dataset (i.e. four metrics and two ratios), while geometric data clustering was computed using meaningful components from a Principal components analyses (PCA) on size-uncorrected Procrustes coordinates (i.e. PC1). Exploratory multivariate models with PERMANOVA design with 10,000 permutations (shape ~ log(centroid size) indicated size influence on shape was minimal (R^2 = 0.041, P = 0.0004) and classification performance increases when using shape and size at the same time

rather than only shape (see Mitteroecker & Schaefer, 2022). Canonical variate analyses (CVA) with 10,000 permutations were conducted in the R package 'Morpho' 2.9 (Schlager, 2016) to investigate the degree of dissimilarity between model-based groups using the Mahalanobis distance (Md) with Bonferroni adjusted *P* value (Klingenberg, 2013).

Ecological niche modelling

To estimate and project the potential niche of *S. piliferus* we compiled a presence-absence database (geodetic datum WGS84) including data for 14 related, endemic New Zealand grasshopper species, spanning 1967 to 2016 (Koot et al., 2022), plus recent sample collections and verified, high resolution observations (uncertainty <1km^2) from iNaturalist NZ (https://inaturalist.nz). We also included target-group absences (Mateo et al., 2010) consisting of sites where sampling effort has produced other Orthoptera (Gryllidae and Tettigoniidae), but not *S. piliferus*. Duplicate records were removed ensuring one datum per pixel (i.e. ~1 km^2 habitat area). The resulting database consisted of 1,188 site records, including 1,053 absences and 135 presences, representing the realised niche of *S. piliferus* (Figure S3.1).

As potential niche proxies we used 19 bioclimatic layers from WorldClim v1.4 for five periods (MIROC-ESM and NCAR-CCSM climate models): last interglacial at ~120–140 kyr (LIG), last glacial maximum at ~28 kyr (LGM), mid-Holocene at ~6 kyr (MH), current (1960–1990), and future (2061–2080). We projected two future scenarios with mean temperature increases of 1.4 °C (RCP4.5) and 3.0 °C (RCP8.5) in New Zealand by 2090 (Ministry for the Environment, 2018). Additional variables capturing geodiversity and topographic traits were discarded early in the variable selection process (Table S3.1). Layer files were at 30 arc-seconds resolution (~1 km^2), except LGM which was at 2.5 arc minutes (~5 km^2). All layers were cropped to the extent of New Zealand, which represents the potential accessible area for the species during the relevant time period given land connections between major islands of the archipelago during Pleistocene glacial phases (Trewick & Bland, 2012). Layer processing used QGIS 3.16.1 (QGIS Development Team, 2020). To reduce multicollinearity we selected a subset of five independent and ecologically informative variables (Table S3.1) using the R package 'fuzzySim' 3.0 (Barbosa, 2015).

Three modelling methods were used (Generalised Boosting, Random Forest, and Maximum Entropy) with settings optimised by testing alternative hyperparameters (Tables S3.2 and S3.3) with the R package 'SDMtune' 1.1.4 (Vignali et al., 2021). Final models were refitted using the most relevant environmental predictors and the best performing hyperparameters in the R package 'biomod2' 3.4.6 (Thuiller et al., 2020), through a spatial-blocking cross-validation approach (Figure S3.2) with the R package 'blockCV' 2.1.1 (Valavi et al., 2019). Five runs were completed for each modelling method, resulting in 15 individual models. Model performance was evaluated using the area under the receiver operator characteristic curve (AUC) and true skill statistic (TSS). Models with high predictive power (TSS and AUC > 0.9; Figure S3.3) were ensembled using a weighted mean approach (EMmw), and variable importance for the EMmw (Figure S3.4) estimated (Fletcher et al., 2016). Time projections were generated using the EMmw and binary (presence/absence) maps were built using the cut-off value that maximised the rate of presences and absences correctly predicted. Extrapolation risk was assessed through a multivariate environmental similarity surface (MESS) analysis (Elith et al., 2010) with the R package 'dismo' 1.3-3 (Hijmans et al., 2020).

Climate niche analyses

We assessed niche differentiation within *S. piliferus* using a principal component analysis (PCA) approach (Broennimann et al., 2017), as implemented in the R package 'ecospat' 3.5.1 (Di Cola et al., 2017) with 5,000 random points across North Island to summarise the climate space available for each mtDNA lineage. Niche overlap between lineages was calculated using a corrected version of the Schoener's *D* index (Di Cola et al., 2017), which ranges from 0 (no overlap) to 1 (total overlap) of climate space. We used the niche similarity test (Warren et al., 2008) to assess whether the observed *D* values were more (i.e. niche conservatism) or less similar (i.e. niche divergence) than expected by chance using 1,000 permutations. We quantified niche marginality (*M*) and specialisation (*S*) for each lineage with the R package 'CENFA' 1.1.0 (Rinnan, 2018). The higher the marginality, the more the niche deviates from the mean climate conditions and the higher the specialisation, the narrower the niche (Hirzel et al., 2002). This analysis used the actual presence data and the climatic background was represented by the subset of climate variables used for niche modelling (Table S3.1), as they are not strongly correlated and are important for predicting this grasshopper climate envelope.

Genotype-phenotype-environment associations

We used multiple matrix regression with randomization (MMRR) to explore genotype-phenotype-environment associations among populations of *S. piliferus*. For this, we built pairwise Euclidean distances for body size (FL, FW, PL, and PW) with the R package 'vegan' 2.5-7 (Oksanen et al., 2020), and pronotum shape with the R package 'Geomorph' using a PERMANOVA design with 10,000 iterations (shape ~ population). Euclidian distances for the subset of variables used for niche modelling (Table S3.1) plus mean annual temperature (hereafter temperature) were estimated using the R package 'Stats' 4.0.3 (R Core Team, 2022), as they are expected to capture climate-related factors influential for phenotypic variation in orthopterans (e.g. Whitman, 2008). Elevation was excluded as it was highly correlated with temperature (r = 0.808, P = 0.001). Pairwise ND2 Φ_{ST} and topographically-corrected geographic distances (km) were used as proxies of genetic and geographic variation (see above). We performed MMRRs with 10,000 permutations in the R package 'PopGenReport' 3.0.7 (Adamack & Gruber, 2014). We fitted separate models to assess the effects of geography, climate, and genetic divergence on body size and then in pronotum shape differentiation. We used a backward elimination procedure to retain the most informative variables to be included in the final models by fitting a starting model with all explanatory variables, and then removing iteratively those with the lowest contribution to the model (i.e. highest p-value) until only significant variables remained (P < 0.05). Analyses were conducted considering 27 population samples for which we had genetic and phenotypic data.

Results

Population genetic structure and demography

We obtained a 747 bp alignment of mitochondrial ND2 sequences for 186 individual *Sigaus piliferus* (Table S1.1). The analysed fragment exhibited an A+T bias (A+T content = 0.752, G+C content = 0.248) as is typical for insects (Trewick & Morgan-Richards, 2005). The aligned ND2 sequences rendered an unambiguous region with 47 amino acid substitutions and 155 polymorphic nucleotide sites, comprising 91 haplotypes.

Genealogical relationships based on a parsimony haplotypic network revealed a deep north-south phylogeographic split either side of the Manawatū Basin (Figure 2). The southern lineage included 32 samples from five locations in the Tararua Range, while the northern lineage comprised 154 samples from 25 locations (Table S1.1). These deepest lineages were separated by 42 mutational steps and average genetic distances between 9.6% (TN) and 9.7% (K2P). Mean within-lineage distance were 2.0% (K2P and TN) in the north, and 1.1% (K2P and TN) in the south (Figure S1.1). The more widespread northern lineage had some geographic structure, the most salient separating most samples from Kaimai Range and other populations by 36 mutational steps (6.8% TN; 6.9% K2P). This general structure was retrieved by our phylogeny (posterior probabilities > 0.95), yet shallow divisions were not resolved (Figures 2 and S1.2). Most haplotypes were private (95.5%), and the most common haplotypes (30 and 31), separated by two mutational steps, were found in population samples from central North Island (maximum geographic distance ~135 km). The sPCA Eigenvalue test supported global (P = 0.0001) but no local structure (P = 0.9999), consistent with a weak signature of isolation by distance over the entire species range (r = 0.385, P = 0.0001) and no regional patterns: north (r = −0.006, P = 0.5426) and south (r = −0.454, P = 0.8728). Interpolation of the most informative sPCA axis (17.9% of variance explained) revealed two major regions with distinct genetic diversity (north and south) in agreement with the structure recovered by our haplotype network and phylogenetic tree (Figure 2). AMOVA indicated this partition accounts for 79.92% of total genetic variability, with significant differentiation between north and south lineages (P = 0.001).

The examined mtDNA ND2 fragment showed high haplotype diversity (h = 0.965 ± 0.007) and moderate nucleotide diversity (π = 0.038 ± 0.003) within *S. piliferus*. Haplotype diversity was marginally higher in the southern lineage (0.984 ± 0.012 vs. 0.950 ± 0.009) but nucleotide diversity was almost two times more in the northern lineage (0.020 ± 0.002 vs. 0.011 ± 0.002), likely reflecting the influence of unequal sample sizes (northern = 154 vs. southern = 32 samples). When examining population samples (n > 5), haplotype diversity ranged from 0.011 to 0.861 and higher values were generally found in those from central North Island. In turn, nucleotide diversity ranged from 0.0003 to 0.0150 and values were generally higher at northernmost (Kaimai Range) and southernmost samples (Tararua Range), with differences reaching two orders of magnitude regardless of sample size (Table S1.2). Genetic differentiation among

population samples was found to be moderate to strong and significant in most cases (Φ_{ST} > 0.459, P < 0.05; Figure S1.3), consistent with limited gene flow.

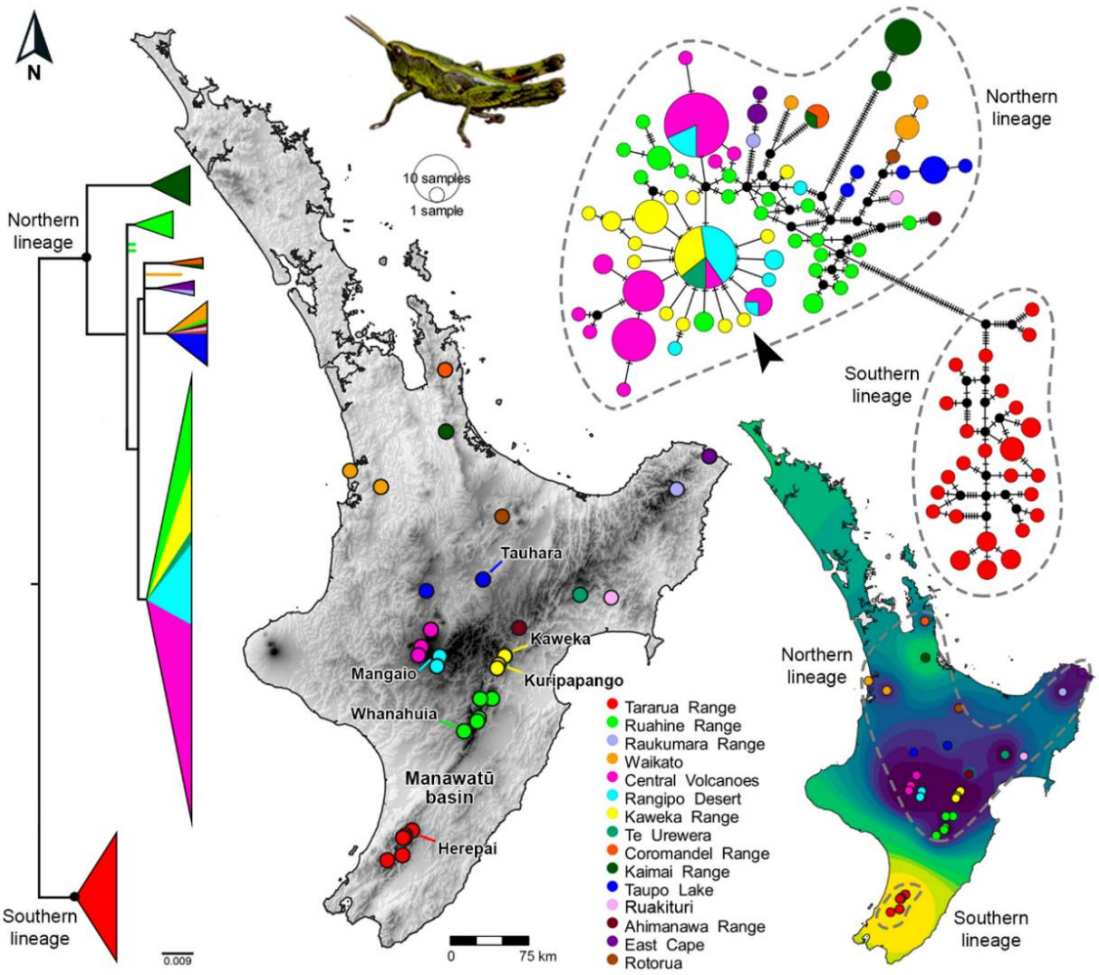

Figure 2. Relief map of North Island, New Zealand with sampling locations for genetic analyses of *Sigaus piliferus* (coloured by geographic region). Phylogenetic (left) and genealogical (right top) relationships among mtDNA ND2 haplotypes revealed a deep north–south phylogeographic split and phylogeographic structure among northern populations. This major structure was supported by interpolation of the first global axis of a spatial PCA (right bottom). A star-like pattern of haplotype diversity (black arrowhead) was apparent in the Central Plateau area. Collapsed phylogenetic clades (posterior probability ≥ 95) are shown as triangles with colours indicating the proportion of terminals per geographic region (complete information on relationships and node support are available in Figure S1.2). Populations with statistical support for demographic expansion are shown. Map projection: NZGD2000.

Mismatch distributions for the whole dataset and the two main lineages were multimodal, a signature of demographic equilibrium. Tajima's D and Ramos-Onsins & Rozas' R_2

values agreed with the inference of population stability, however, Fu's *Fs* test was significantly negative for the whole dataset (−18.143, $P = 0.026$) and both lineages (northern = −20.120, $P = 0.011$; southern = −11.631, $P = 0.003$), implying an excess of alleles as expected from recent population expansion. This inference was supported by non-significant Harpending's *r* values in all cases. When analysing individual population samples ($n > 5$), compelling statistical support for expansion was found for five populations in central North Island and nearby areas: Tauhara, Mangaio, Kaweka, Kuripapango, and Whanahuia (Figure 2; Table S1.3). The star shape of the haplotypic network including these populations is indicative of recent population expansion (Figure 2). Statistical support for demographic expansion was also found for one south population sample (Herepai), others fitted the model of constant population size (Figure 2; Table S1.3).

Morphological variation

Phenotypic clustering (size and shape) comprising two overlapping morphological clusters was broadly consistent with the major genetic partitions (Figure 3). The best-fitted Gaussian model for linear size (ellipsoidal, equal shape; BIC = −879.84) mostly overlay the two major lineages of the molecular analyses (22 misassignments, 88% accuracy; Figure 3a). In general, females in lower latitudes/elevations (north) have larger femora and pronota than those in higher latitudes/elevations (south), although misclassifications were evident in the central area. Shape variation was only loosely associated with major genetic structure (40 misassignments, 60% accuracy; Figure 3b) as depicted by the best-fitted Gaussian model (univariate, equal variance model; BIC = −302.89). Overall, females in the north tend to have more triangular and waisted pronota than those in the south. Canonical variate analyses showed significant differentiation between inferred Gaussian clusters, although the signal was stronger for size (Md = 3.37, $P < 0.0001$, classification accuracy = 98%) than for shape (Md = 1.89, $P < 0.0001$, classification accuracy = 86%).

Ecological niche modelling

Evaluation scores for individual models indicated good to excellent performance (Figure S3.3), and the ensemble model had high predictability, with a mean AUC score of 0.996. Sensitivity (i.e. fraction of presences correctly predicted) and specificity (i.e. fraction of

absences correctly predicted) were also high, 100% and 99.6%, respectively. The cut-off threshold that maximised the proportion of presences and absences correctly predicted by the model was 488.5. Precipitation and temperature related variables had the largest influence on the suitable envelope estimated for *S. piliferus*. Precipitation seasonality, precipitation of driest month, and mean temperature of driest quarter were the most important predictor variables (importance score ≥ 25% in all cases; Figure S3.4).

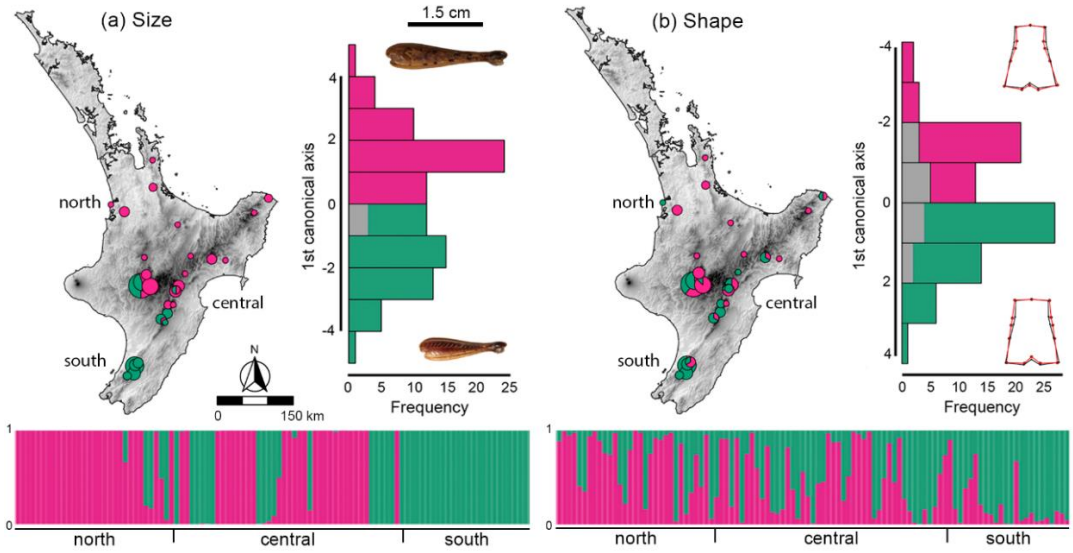

Figure 3. Relief maps of North Island, New Zealand showing the spatial distribution of phenotypic assignment inferred by Gaussian clustering for adult female *Sigaus piliferus* based on body size (a) and pronotum shape (b). Pies represent population samples scaled by the number of individuals in each cluster. Phenotypic mixing is apparent in the species' mid-range (central North Island). Stacked bar plots (bottom) show assignment probabilities to each morphological cluster for each individual arranged by latitude. Canonical variate frequencies (right) supported group clustering based on Gaussian modelling. Map projection: NZGD2000.

Current predictions closely matched the known range of *S. piliferus* throughout most elevated areas in North Island (19,723 km^2), except those in Taranaki and Northland districts, where the species has not been recorded (Figure 4; Figure S3.5). Considering extrapolation risk (Figure S3.6), hindcasts indicate suitable space was more extensive and connected during interglacial (LIG = 21,448 km^2 and MH = 13,776 km^2) than glacial periods (LGM = 6,868 km^2). North Island habitat space at the last interglacial was predicted to be similar to current predictions, whereas much less habitat was predicted at the LGM and this restricted to north (Coromandel–Kaimai ranges), northeast

(Raukumara Range) and south (west Tararua Range). Climate warming during the mid-Holocene pushed suitable conditions upslope, resulting in the loss of 36% of suitable space. Similarly, the suitable habitat envelope is expected to move poleward and upward under future warming scenarios (Figure 5; Figure S3.5). After accounting for extrapolation risk (Figure S3.6), habitat loss was predicted to be more severe under the most pessimistic climatic scenario (RCP 8.5 = 7,930 km^2 vs. RCP 4.5 = 10,139 km^2), but in all cases involves loss of at least half of the current suitable space (RCP 4.5 = 49% and RCP 8.5 = 60%) and extensive fragmentation.

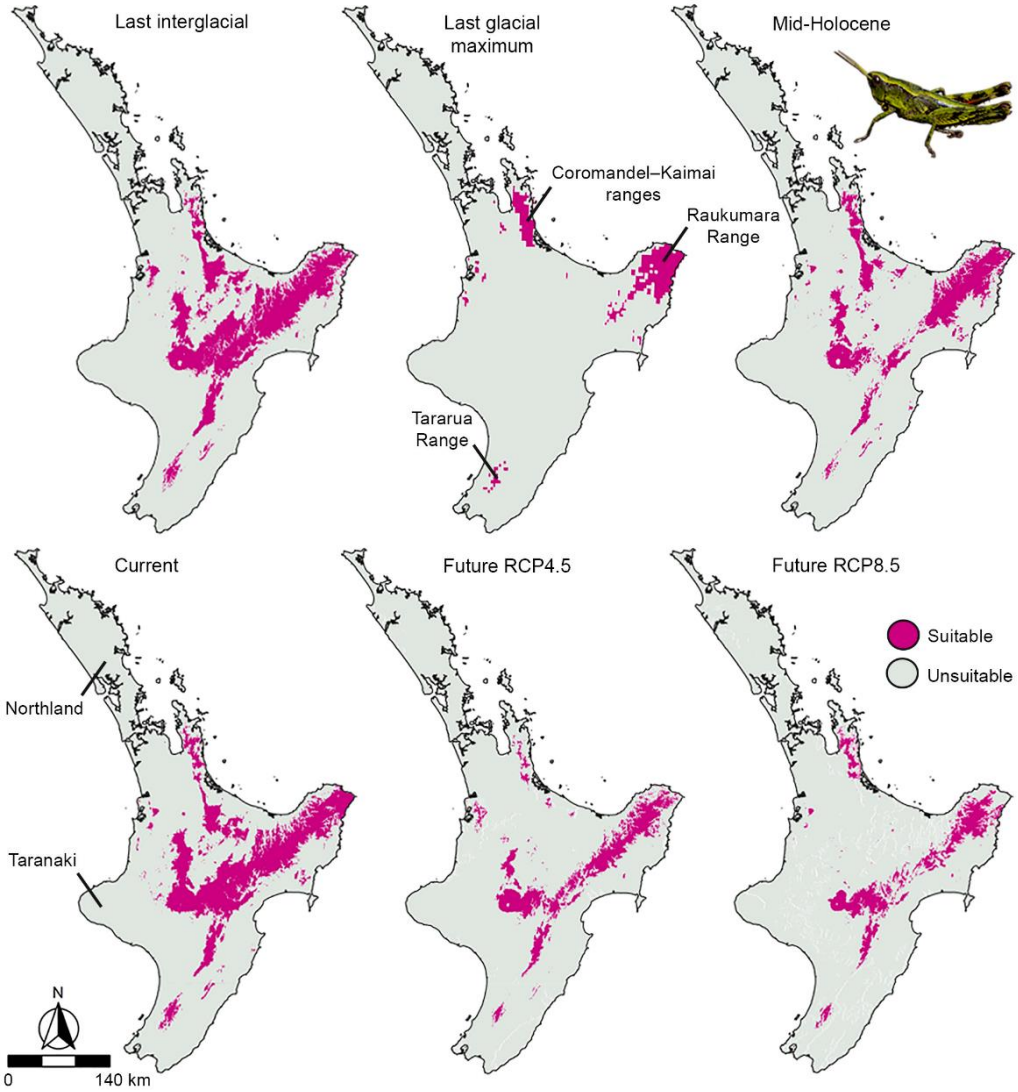

Figure 4. Predicted suitable niche space for *Sigaus piliferus* (cut-off = 488.5) in North Island, New Zealand during three past epochs (last interglacial, last glacial maximum, and mid-Holocene), current time, and two future scenarios (RCP 4.5 and RCP 8.5). Map projection: NZGD2000.

Climate niche analyses

The first two axes of the PCA based on five climate variables (Table S3.1) across the whole study area, explained 48.93% and 21.82% of the total environmental variance, respectively (Figure 5a). Niche segregation between mtDNA lineages was closely related to the first PCA axis, which had a strong negative relation with mean temperature of wettest and driest quarter (-0.95 and -0.88, respectively). Niche overlap was minimal (D = 0.107), indicating these lineages have non-equivalent niches. Despite this, we found evidence of niche conservatism as the similarity test indicated that niches were significantly more similar than expected by chance in both reciprocal directions: southern–northern (P = 0.045) and northern–southern comparisons (P = 0.048). No evidence of niche divergence was detected in any direction from the climate model ($P \geq$ 0.885). Niche specialisation and marginality were higher for the southern (S = 13.895, M = 3.993) than for the northern lineage (S = 1.673, M = 3.538), indicating that populations in the south have narrower climate niches that greatly differ from the average climate conditions in the island, hence, more specialised climate requirements.

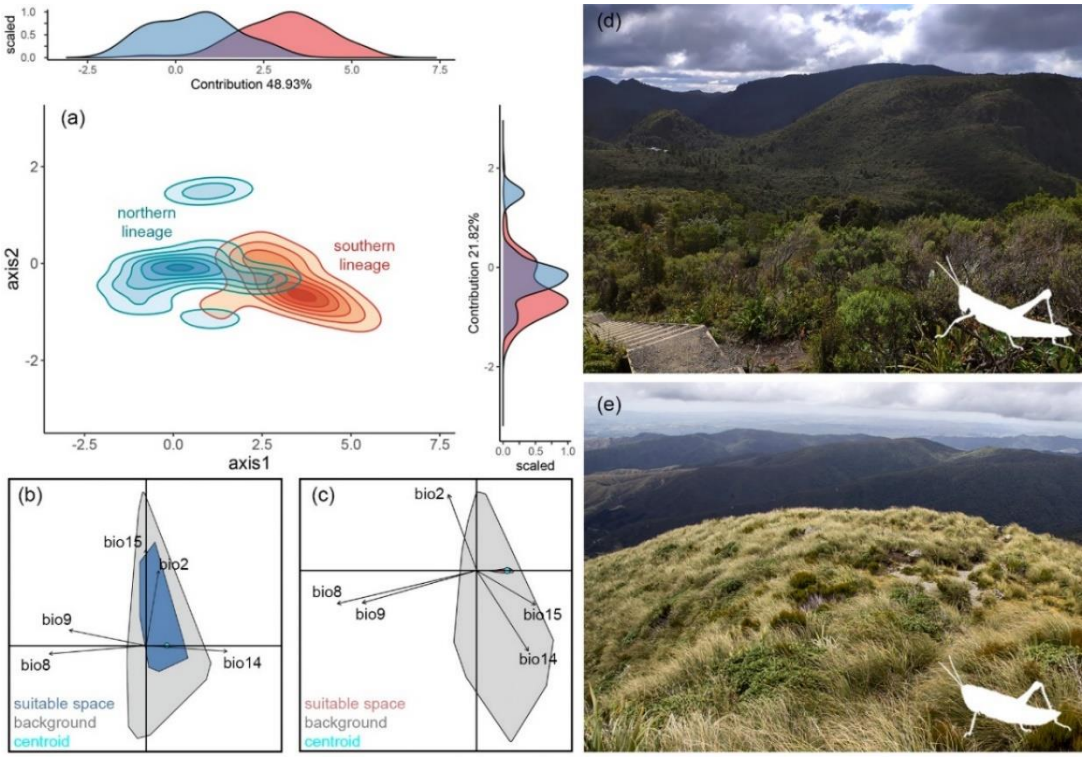

Figure 5. Distinct niche and habitat features for grasshopper lineages within *Sigaus piliferus*. Niche overlap along the first two axes of a principal component analysis on five climatic variables

(see Table S3.1) indicates limited niche sharing (a); top and right plots show the density distribution along each axis. Suitable space within the available background across the marginality (x) and specialization (y) axes for the northern (b) and southern lineage (c); the centroids of the used space and the projections of the predictors are shown. Grasshoppers within the northern lineage (d) typically occur in montane woody vegetation (e.g. The Pinnacles, Coromandel Range), while those within the southern lineage (e) are found on open alpine grasslands (e.g. Herepai Peak, Tararua Range). Silhouettes indicate the typical morphology of grasshoppers (to the same scale) found in each type of habitat.

Genotype-phenotype-environment associations

The examined environmental factors explain a moderate amount of body size divergence in *S. piliferus*, but not patterns of pronotal shape differentiation (Table 1). The best-fitted model for body size (R^2 = 0.424, P < 0.0001) indicated divergence was significantly positively affected by temperature (β = 0.377, P < 0.001), diurnal range (β = 0.375, P = 0.003), and to a minor degree geographic distance (β = 0.202, P = 0.034), and negligible yet negative effects were found for precipitation seasonality and temperature of wettest quarter (Table 1; Figure S4.1). In contrast, the best-fitted model for pronotum shape (R^2 = 0.070, P = 0.0024) showed only geographic distance had a weak significantly positive effect on shape differentiation (β = 0.004, P = 0.002), but the low explanatory power of this model indicates biological irrelevance. Genetic distance was removed earlier during the backward elimination procedure, indicating no association between genetic and both body size and pronotum shape divergence.

Table 1. Final multiple matrix regression with randomization models obtained through backward stepwise selection procedure indicating factors contributing to phenotypic differentiation among populations of *Sigaus piliferus*. The regression coefficient (β) and p-value (*P*) for each explanatory variable are given.

Parameter	**Body size**		**Pronotum shape**	
	β	*P*	β	*P*
temperature	0.377	< 0.001	-	-
diurnal range	0.375	0.003	-	-
geographic distance	0.202	0.032	0.004	0.002
precipitation seasonality	−0.043	0.036	-	-
temperature of wettest quarter	−0.084	0.045	-	-
model adjusted R^2	0.424		0.070	
model *P*	< 0.0001		0.002	

Discussion

As in other mid to high-latitude regions in both hemispheres (e.g. Đurović et al., 2020; Endo et al., 2015; Ikeda & Setoguchi, 2007; Stewart et al., 2010), Pleistocene glacial phases allowed alpine conditions to flourish in New Zealand (McGlone, 1985; Heenan & McGlone, 2013), and cold-adapted organisms are inferred to have attained larger ranges and population sizes in response (Carmelet-Rescan et al., 2021; Meza-Joya et al., 2023; Trewick et al., 2000, 2011). We tested this expectation for the flightless, cold-adapted New Zealand grasshopper *Sigaus piliferus* but unexpectedly found a scenario consistent with reduced and fragmented habitat during glacial phases. Overlying this ecological response to changing climate we found evidence of demographic disruption from volcanic activity in the central part of the species' distribution.

Contraction of suitable space for *S. piliferus* at the last glacial maximum challenges expectations for an alpine specialist in this region where palaeoecological evidence indicates unglaciated alpine-like plant communities dominated the landscape (McGlone, 1985; Newnham et al., 2013). Suitable habitat for *S. piliferus* during the LGM was apparently restricted to the latitudinal limits of the current range (Figure 4), where distinct climate regimes prevailed (Drost et al., 2007). We suggest this hindcast reflects intraspecific niche variation that is consistent with our field observations of northern and southern populations (Figure 5). Climate based predictions for northern populations are more widely represented across the landscape, indicating the lineage expanded its thermal regimen towards increased warm tolerance compared to southern populations of *S. piliferus* and sibling species in South Island. In contrast, the southern populations show niche specialisation to a rarer habitat that is expected to be more vulnerable to future warming. These distinct niche features suggest variability in population-level response to climate change (e.g. Maguire et al., 2018) and could reinforce geographic isolation with future climate warming and promote ecological speciation (see Wiens & Graham, 2005).

Increased interglacial habitat for *S. piliferus* would have enabled the range shifting that is apparent from demographic inference of population expansion and weak or no signature of isolation-by-distance across this species' range. Extant populations from areas less affected by volcanism towards the edges of the range, represent compelling instances of postglacial expansion. Niche models indicate persistent suitability in the

north at the LGM (Coromandel–Kaimai ranges), and gradual contraction since then. This agrees with demographic inferences from the sole population sample ($n > 5$) from this region (Te Aroha) indicating population stability. In contrast, a fragmented LGM habitat in the south (Tararua Range) appears to have coalesced and we found demographic signatures of expansion in all populations ($n > 5$) from this region (Herepai, Arete Peak and Holdsworth) indicating recent expansion from few ancestors. These contrasting histories suggests populations at the range edges are critical for this species adaptive capacity. If these patterns also hold for future climate scenarios, the narrowly distributed southern lineage may be especially threatened.

Volcanism has been an important influence on North Island biogeography during the last two million years (Trewick & Bland, 2012). Stratigraphic features (Manville et al., 2009; Segschneider et al., 2002) and palynology (Wilmshurst & McGlone, 1996) indicate pyroclastic flow from the most recent Taupō super-eruption (~1.8 kyr, Wilson & Walker, 1985) mantled the landscape, destroyed vegetation and disrupted populations across the centre of the island (Morgan-Richards et al., 2000; Shepherd et al., 2022; Trewick et al., 2011). Together with continuous activity on the central volcanic plateau (Ngāuruhoe, Tongariro and Ruapehu volcanos) since ~0.28 Ma (Cronin et al., 1996; Trewick & Bland, 2012), vegetation loss and recovery (Wilmshurst & McGlone, 1996) would have been critical for herbivorous insect population dynamics. Volcanic destruction of forest in the central volcanic zone led to replacement by pioneer ferns and grasses (Wilmshurst & McGlone, 1996), and the resulting mosaic of open habitats could provide ecological opportunities for grasshopper populations to flourish.

Population recovery after repeated volcanism is typically characterised by recolonisation from diverse source populations outside the volcanic zone (Baranzelli et al., 2020; Muir et al., 2000; Osuna et al., 2020). Extant populations of *S. piliferus* in the central volcanic zone indicate decline followed by recent expansion. Intermediate mtDNA haplotype diversity (0.118–0.861) but low nucleotide diversity (0.0003–0.0034) suggest recent large populations derived from few ancestors and this is supported by characteristic star-like pattern of haplotype genealogy (Figure 2, arrowhead). Haplotype diversity in the area is an order of magnitude lower than found in related alpine grasshoppers in South Island that attained larger populations during glacial maxima (Carmelet-Rescan et al., 2021; Meza-Joya et al., 2023).

Deep lineages splits within *S. piliferus* (~9.7% ND2 sequence divergence) indicate a common maternal ancestor in the Pliocene (~5–2 Mya) when the North Island landscape was developing (Trewick & Bland, 2012). The deep genetic divergence between major lineages resembles that found in alpine Orthoptera in South Island (Carmelet-Rescan et al., 2021; Meza-Joya et al., 2023; Trewick, 2008; Trewick et al., 2000) and cold-adapted insects elsewhere (e.g. Borer et al., 2010; Endo et al., 2015; Martinez-Sañudo et al., 2022). However, the elevated topography in North Island is mostly younger (<1 Mya) and suggests that even divergent *S. piliferus* lineages such as that associated with the Kaimai range (~6.9%) have been associated with habitat that differs from most South Island grasshoppers. Beyond the central volcanic zone haplotype sharing was limited to two pairs of adjacent populations (Pinnacles–Te Aroha and Pirongia–Karioi).

In keeping with mtDNA signal for two main lineages (north and south) with a central zone of shallow mixing, we found phenotypic variation indicated two broad groups, north and south. Our morphometric data reveal morphological variance among grasshoppers in the central area (Figure 3), consistent with the high variation noted previously (Bigelow 1967). The co-occurrence of disparate (‘northern’ and ‘southern’) phenotypes in the central region may reflects mixing of nuclear genetics, a signal not detected with single locus mtDNA. At the northern and southern ends of the species distribution we found evidence of body size and shape divergence consistent with adaptive to local habitats. We suggest that mixed phenotypes in the central volcanic zone results from population disruption leading to reinvasion and disequilibrium. Future research using next-generation sequencing may improve our understanding of past evolutionary history and current trajectories in these populations, and this may be especially useful for conservation planning in these lineages.

The latitudinal and altitudinal gradient of North Island is expected to result in warmer conditions to the north (low latitude/elevation) compared to the south (away from the equator), and temperature is widely recognized as playing a key role in body size differentiation in orthopterans (Whitman, 2008). A tendency towards larger size at warmer, lower latitudes and elevations, is the most frequently reported pattern in Orthoptera and other insects (García-Navas et al., 2017a; Mousseau, 1997; Shelomi, 2012), and we found body size differentiation in *S. piliferus* was associated with temperature gradients. Phenotypic variation might also represent adaptation to other

environmental attributes such as vegetation type, that is itself linked to temperature and seasonality (Wardle, 1985). Contrary to observations of other New Zealand grasshoppers we found that *S. piliferus* at northern sites with montane woody vegetation (e.g. Coromandel–Kaimai ranges) were notable for their elongate bodies and long hind legs whereas those in southern open alpine grasslands (e.g. Tararua Range) have stout bodies and robust femora (Figure 5). This association of locomotory morphology with vegetation type has been documented in European grasshoppers (García-Navas et al., 2017b). Bigelow (1967), studying museum material, also noted that northern *S. piliferus* were the 'largest, longest-legged and most angular', but did not observe habitat vegetation.

The existence of two *S. piliferus* ecotypes suggests different responses to past and future environmental change. If niche stability and saturation operate, suitable space for *S. piliferus* is predicted to diminish during the intensified 'anthropogenic' interglacial now developing around the globe, and this will result in increased patchiness across its current range due to upward shifts. In keeping with this, loss of suitable space was also predicted at mid-Holocene, which was warmer than today. As temperatures increase, latitudinal tracking of suitable habitat space in North Island, as inferred for the more mountainous South Island, is unlikely (Koot et al., 2022). The extent of habitat loss and fragmentation predicted in North Island (49–60%) will likely cause extinction of populations with distinct genetic identities and thus genetic erosion (see Meza-Joya et al., 2023). While climatic model strongly predicts the realised niche of *S. piliferus*, variables used for modelling are proxies for drivers of this species range, and neglect the ecological factors setting range limits and responses to environmental shifts (Wiens et al., 2011). The existence of relict northern populations on the margins of exotic pine plantations suggest survival under alternative conditions is possible, but such silvicultural systems are in ecological disequilibrium, subject to invasive exotic pests (Crous et al., 2017), and may create population sinks or ecological traps for native biota (Pawson et al., 2010), threatening persistence on these grasshoppers.

Predicting species' fates under anthropogenic climate change remains a challenge due to uncertainties on how to characterise the adaptive capacity of biotic units across the population-species continuum and determine robust metrics for prioritising populations for conservation (Coates et al., 2018; Seaborn et al., 2021). By combining genetic,

phenotypic and niche differentiation metrics, we found evidence that local selection for adaptive phenotypes is the primary driver of diversification in *S. piliferus*, rather than neutral processes linked to drift or divergence time alone. The predicted upward shift of suitable space for southern populations (Tararua Ranges) during climate warming will further reinforce geographic isolation, and this might be an instance where anthropogenic climate change drives evolutionary divergence (see Wiens & Graham, 2005). Contrary to expectations of warming driving selection for smaller body size (Gardner et al., 2011), warming conditions seems to select for larger sizes in parts of this grasshopper system. This highlights the need to incorporate phenotypic data and functional genetics in studies of species response to climate change to gauge the rate and likely outcomes. Despite current levels of intraspecific diversity in *S. piliferus* indicating adaptive capacity, the rate of habitat loss predicted over the next 50 years of warming will lead to small and fragmented populations (Koot et al. 2022) with limited capability to adapt via contemporary evolution to the novel selective forces arising from rapid environmental pressures (Kardos et al., 2021; Radchuk et al., 2019; Willi et al., 2022).

Acknowledgements

We are grateful to the New Zealand Department of Conservation for granting access and approval to collect from the Conservation Estate (Authorization 49878-RES). David Carmelet provided valuable advice on shape analyses. We also acknowledge our field partners: Eliana Ramos and Mari Nakano. The R script for Figure 5a was kindly provided by Javier Fernández-López and Irene Villa-Machío. This research was supported by a grant from the Miss E. L. Hellaby Indigenous Grasslands Research Trust, a doctoral scholarship from Massey University and a Massey University Doctoral Conference Grant (awarded to FLMJ).

References

Adamack, A. T., & Gruber, B. (2014). PopGenReport: Simplifying basic population genetic analyses in R. *Methods in Ecology and Evolution*, *5*(4), 384–387. https://doi.org/10.1111/2041-210X.12158.

Adams, D. C., Collyer, M. L. & Kaliontzopoulou, A. (2020). Geomorph: Software for geometric morphometric analyses. https://cran.r-project.org/package=geomorph

Aktas, C. (2020). haplotypes: Manipulating DNA sequences and estimating unambiguous haplotype network with statistical parsimony. https://cran.r-project.org/package=haplotypes

Baranzelli, M. C., Cosacov, A., Rocamundi, N., Issaly, E. A., Aguilar, D. L., Camps, G. A., ... & Sérsic, A. N. (2020). Volcanism rather than climatic oscillations explains the shared phylogeographic patterns among ecologically distinct plant species in the southernmost areas of the South American Arid Diagonal. *Perspectives in Plant Ecology, Evolution and Systematics*, *45*, 125542. https://doi.org/10.1016/j.ppees.2020.125542

Barbosa, A. M. (2015). fuzzySim: Applying fuzzy logic to binary similarity indices in ecology. *Methods in Ecology and Evolution*, *6*(7), 853–858. https://doi.org/10.1111/2041-210X.12372

Bigelow, R. S. (1967). *The grasshoppers (Acrididae) of New Zealand*. University of Canterbury Publications.

Bougeard, S., & Dray, S. (2018). Supervised multiblock analysis in R with the ade4 package. *Journal of Statistical Software*, 86, 1–17. https://doi.org/10.18637/jss.v086.i01

Borer, M., Alvarez, N., Buerki, S., Margraf, N., Rahier, M., & Naisbit, R. E. (2010). The phylogeography of an alpine leaf beetle: Divergence within *Oreina elongata* spans several ice ages. *Molecular Phylogenetics and Evolution*, *57*(2), 703–709. https://doi.org/10.1016/j.ympev.2010.08.017

Broennimann, O., Fitzpatrick, M. C., Pearman, P. B., Petitpierre, B., Pellissier, L., Yoccoz, N. G., ... & Guisan, A. (2012). Measuring ecological niche overlap from occurrence and spatial environmental data. *Global Ecology and Biogeography*, *21*(4), 481–497. https://doi.org/10.1111/j.1466-8238.2011.00698.x

Byrne, M. (2008). Evidence for the multiple refugia at different time scales during Pleistocene climatic oscillations in southern Australia inferred from phylogeography. *Quaternary Science Reviews*, *27*(27–28), 2576–2585. https://doi.org/10.1016/j.quascirev.2008.08.032

Carmelet-Rescan, D., Morgan-Richards, M., Koot, E. M., & Trewick, S. A. (2021). Climate and ice in the last glacial maximum explain patterns of isolation by distance inferred for alpine grasshoppers. *Insect Conservation and Diversity*, *14*(5), 568–581. https://doi.org/10.1111/icad.12488

Coates, D. J., Byrne, M., & Moritz, C. (2018). Genetic diversity and conservation units: Dealing with the species-population continuum in the age of genomics. *Frontiers in Ecology and Evolution*, *6*, 165. https://doi.org/10.3389/fevo.2018.00165

Cronin, S. J., Neall, V. E., & Palmer, A. S. (1996). Geological history of the north-eastern ring plain of Ruapehu volcano, New Zealand. *Quaternary International*, *34*, 21–28. https://doi.org/10.1016/1040-6182(95)00066-6

Crous, C. J., Burgess, T. I., Le Roux, J. J., Richardson, D. M., Slippers, B., & Wingfield, M. J. (2017). Ecological disequilibrium drives insect pest and pathogen accumulation in non-native trees. *AoB Plants*, *9*(1), plw081. https://doi.org/10.1093/aobpla/plw081

Davis, M. B., & Shaw, R. G. (2001). Range shifts and adaptive responses to quaternary climate change. *Science*, *292*(5517), 673–679. https://doi.org/10.1126/science.292.5517.673

Di Cola, V., Broennimann, O., Petitpierre, B., Breiner, F. T., D'Amen, M., Randin, C., … & Guisan, A. (2017). Ecospat: An R package to support spatial analyses and modeling of species niches and distributions. *Ecography*, *40*(6), 774–787. https://doi.org/10.1111/ecog.02671

Dowle, E. J., Morgan-Richards, M., Brescia, F., & Trewick, S. A. (2015). Correlation between shell phenotype and local environment suggests a role for natural selection in the evolution of *Placostylus* snails. *Molecular Ecology*, *24*, 4205–4221. https://doi.org/10.1111/mec.13302

Drost, F., Renwick, J., Bhaskaran, B., Oliver, H., & McGregor, J. (2007). A simulation of New Zealand's climate during the Last Glacial Maximum. *Quaternary Science Reviews*, *26*, 2505–2525. https://doi.org/10.1016/j.quascirev.2007.06.005

Đurović, S. Z., Temunović, M., Niketić, M., Tomović, G., Schönswetter, P., & Frajman, B. (2021). Impact of Quaternary climatic oscillations on phylogeographic patterns

of three habitat-segregated *Cerastium* taxa endemic to the Dinaric Alps. *Journal of Biogeography*, *48*(8), 2022–2036. https://doi.org/10.1111/jbi.14133

Elith, J., Kearney, M., & Phillips, S. (2010). The art of modelling range-shifting species. *Methods in Ecology and Evolution*, *1*(4), 330–342. https://doi.org/10.1111/j.2041-210X.2010.00036.x

Endo, Y., Nash, M., Hoffmann, A. A., Slatyer, R., & Miller, A. D. (2015). Comparative phylogeography of alpine invertebrates indicates deep lineage diversification and historical refugia in the Australian Alps. *Journal of Biogeography*, *42*(1), 89–102. https://doi.org/10.1111/jbi.12387

Excoffier, L., Smouse, P. E., & Quattro, J. M. (1992). Analysis of molecular variance inferred from metric distances among DNA haplotypes: Application to human mitochondrial DNA restriction data. *Genetics*, *131*(2), 479–491. https://doi.org/10.1093/genetics/131.2.479

Fletcher, D. H., Gillingham, P. K., Britton, J. R., Blanchet, S., & Gozlan, R. E. (2016). Predicting global invasion risks: A management tool to prevent future introductions. *Scientific Reports*, *6*(1), 1–8. https://doi.org/10.1038/srep26316

Fu, Y. X. (1997). Statistical tests of neutrality of mutations against population growth, hitchhiking and background selection. *Genetics*, *147*(2), 915–925. https://doi.org/10.1093/genetics/147.2.915

García-Navas, V., Noguerales, V., Cordero, P. J., & Ortego, J. (2017a). Ecological drivers of body size evolution and sexual size dimorphism in short-horned grasshoppers (Orthoptera: Acrididae). *Journal of Evolutionary Biology*, *30*(8), 1592–1608. https://doi.org/10.1111/jeb.13131

García-Navas, V., Noguerales, V., Cordero, P. J., & Ortego, J. (2017b). Phenotypic disparity in Iberian short-horned grasshoppers (Acrididae): The role of ecology and phylogeny. BMC Evolutionary Biology, 17, 1–14. https://doi.org/10.1186/s12862-017-0954-7

Gardner, J. L., Peters, A., Kearney, M. R., Joseph, L., & Heinsohn, R. (2011). Declining body size: A third universal response to warming? *Trends in Ecology & Evolution*, *26*(6), 285–291. https://doi.org/10.1016/j.tree.2011.03.005

Gillespie, R. G., & Roderick, G. K. (2014). Geology and climate drive diversification. *Nature*, *509*, 297–298. https://doi.org/10.1038/509297a

Grant, B. R., & Grant, P. R. (2017). Watching speciation in action. *Science*, *355*, 910–911. https://doi.org/10.1126/science.aam6411

Harpending, H. C. (1994). Signature of ancient population growth in a low-resolution mitochondrial DNA mismatch distribution. *Human Biology*, *66*, 591–600. http://www.jstor.org/stable/41465371

Heenan, P. B., & McGlone, M. S. (2013). Evolution of New Zealand alpine and open-habitat plant species during the late Cenozoic. *New Zealand Journal of Ecology*, *37*(1), 105–113. http://www.jstor.org/stable/24060763

Hewitt, G. (2004). Genetic consequences of climatic oscillations in the Quaternary *Philosophical Transactions of the Royal Society B: Biological Sciences*, *359*(1442), 183–195. https://doi.org/10.1098/rstb.2003.1388

Hijmans, R. J., Phillips, S., Leathwick, J., & Elith, J. (2020). Dismo: Species distribution modeling. https://cran.r-project.org/package=dismo

Hirzel, A. H., Hausser, J., Chessel, D., & Perrin, N. (2002). Ecological-niche factor analysis: How to compute habitat-suitability maps without absence data? *Ecology*, *83*(7), 2027–2036. https://doi.org/10.1890/0012-9658(2002)083[2027:ENFAHT]2.0.CO;2

Ikeda, I., & Setoguchi, H. (2007). Phylogeography and refugia of the Japanese endemic alpine plant, *Phyllodoce nipponica* Makino (Ericaceae). *Journal of Biogeography*, *34*(1), 169–176. https://doi.org/10.1111/j.1365-2699.2006.01577.x

Jombart, T. (2008) adegenet: A R package for the multivariate analysis of genetic markers. *Bioinformatics*, *24*(11), 1403–1405. https://doi.org/10.1093/bioinformatics/btn129

Kamvar, Z. N., Tabima, J. F., & Grünwald, N. J. (2014). Poppr: An R package for genetic analysis of populations with clonal, partially clonal, and/or sexual reproduction. *PeerJ*, *2*, e281. https://doi.org/10.7717/peerj.281

Kardos, M., Armstrong, E. E., Fitzpatrick, S. W., Hauser, S., Hedrick, P. W., Miller, J. M., ... & Funk, W. C. (2021). The crucial role of genome-wide genetic variation in

conservation. *Proceedings of the National Academy of Sciences*, *118*(48), e2104642118. https://doi.org/10.1073/pnas.2104642118

Kearse, M., Moir, R., Wilson, A., Stones-Havas, S., Cheung, M., Sturrock, S., ... & Thierer, T. (2012). Geneious Basic: An integrated and extendable desktop software platform for the organization and analysis of sequence data. *Bioinformatics*, *28*(12), 1647–1649. https://doi.org/10.1093/bioinformatics/bts199

Kimura, M. (1980). A simple method for estimating evolutionary rate of base substitutions through comparative studies of nucleotide sequences. *Journal of Molecular Evolution*, *16*, 111–120. https://doi.org/10.1007/BF01731581

Koot, E. M., Morgan-Richards, M., & Trewick, S. A. (2020). An alpine grasshopper radiation older than the mountains, on Kā Tiritiri o te Moana (Southern Alps) of Aotearoa (New Zealand). *Molecular Phylogenetics and Evolution*, *147*, 106783. https://doi.org/10.1016/j.ympev.2020.106783

Koot, E. M., Morgan-Richards, M., Trewick, S. A. (2022). Climate change and alpine adapted insects: Modelling environmental envelopes of a grasshopper radiation. *Royal Society Open Science*, *9*, 211596. https://doi.org/10.1098/rsos.211596

Kumar, S., Stecher, G., Li, M., Knyaz, C., & Tamura, K. (2018). MEGA X: Molecular Evolutionary Genetics Analysis across computing platforms. *Molecular Biology and Evolution*, *35*(6), 1547–1549. https://doi.org/10.1093/molbev/msy096

Leigh, J. W., & Bryant, D. (2015). PopArt: Full-feature software for haplotype network construction. *Methods in Ecology and Evolution*, *6*, 1110–1116. https://doi.org/10.1111/2041-210X.12410

Librado, P., & Rozas, J. (2009). DnaSP v5: A software for comprehensive analysis of DNA polymorphism data. *Bioinformatics*, *25*(11), 1451–1452. https://doi.org/10.1093/bioinformatics/btp187

Manville, V., Segschneider, B., Newton, E., White, J. D. L., Houghton, B. F., & Wilson, C. J. N. (2009). Environmental impact of the 1.8 ka Taupo eruption, New Zealand: Landscape responses to a large-scale explosive rhyolite eruption. *Sedimentary Geology*, 220, 318–336. https://doi.org/10.1016/j.sedgeo.2009.04.017

Maguire, K. C., Shinneman, D. J., Potter, K. M., & Hipkins, V. D. (2018). Intraspecific niche models for Ponderosa pine (*Pinus ponderosa*) suggest potential variability in

population-level response to climate change. Systematic Biology, 67, 965–978. https://doi.org/10.1093/sysbi o/syy017

Martinez-Sañudo, I., Basso, A., Ortis, G., Marangoni, F., Stancher, G., & Mazzon, L. (2022). Strong genetic differentiation between fragmented alpine bush-cricket populations demands preservation of evolutionary significant units. *Insect Conservation and Diversity*, *15*(6), 752–762. https://doi.org/10.1111/icad.12601

Mateo, R. G., Croat, T. B., Felicísimo, A. M. & Muñoz, J. (2010). Profile or group discriminative techniques? Generating reliable species distribution models using pseudo-absences and target-group absences from natural history collections. *Diversity and Distributions*, *16*(1), 84–94. https://doi.org/10.1111/j.1472-4642.2009.00617.x

McDowall, R. M. (1996). Volcanism and freshwater fish biogeography in the northeastern North Island of New Zealand. *Journal of Biogeography*, *23*, 139–148. https://doi.org/10.1046/j.1365-2699.1996.00960.x

McGlone, M. S. (1985). Plant biogeography and the late Cenozoic history of New Zealand. *New Zealand Journal of Botany*, *23*, 723–749. https://doi.org/10.1080/0028825X.1985.10434240

Merilä, J., & Hendry, A. P. (2014). Climate change, adaptation, and phenotypic plasticity: The problem and the evidence. *Evolutionary Applications*, *7*, 1–14. https://doi.org/10.1111/eva.12137

Meza-Joya. F. L., Morgan-Richards, M., Koot, E. M., & Trewick, S. A. (2023). Global warming leads to habitat loss and genetic erosion of alpine biodiversity. *Journal of Biogeography*, *50*, 961–975. https://doi.org/10.1111/jbi.14590

Meza-Joya, F. L., Morgan-Richards, M., & Trewick, S. A. (2022). Relationships among body size components of three flightless New Zealand grasshopper species (Orthoptera, Acrididae) and their ecological applications. *Journal of Orthoptera Research*, *31*(1), 91–103. https://doi.org/10.3897/jor.31.79819

Millien, V., Kathleen Lyons, S., Olson, L., Smith, F. A., Wilson, A. B., & Yom-Tov, Y. (2006). Ecotypic variation in the context of global climate change: Revisiting the rules. *Ecology Letters*, *9*(7), 853–869. https://doi.org/10.1111/j.1461-0248.2006.00928.x

Ministry for the Environment. (2018). *Climate change projections for New Zealand.* Ministry for the Environment Publications. https://environment.govt.nz/assets/Publications/Files/Climate-change-projections-2nd-edition-final.pdf

Mitteroecker, P., & Schaefer, K. (2022). Thirty years of geometric morphometrics: Achievements, challenges, and the ongoing quest for biological meaningfulness. *American Journal of Biological Anthropology*, *178*, 181–210. https://doi.org/10.1002/ajpa.24531

Mousseau, T. A. (1997). Ectotherms Follow the Converse to Bergmann's Rule. *Evolution*, *51*(2), 630–632. https://doi.org/10.1111/j.1558-5646.1997.tb02453.x

Muir, C. C., Galdikas, B. M. F., & Beckenbach, A. T. (2000). mtDNA sequence diversity of orangutans from the islands of Borneo and Sumatra. *Journal of Molecular Evolution*, 51, 471–480. https://doi.org/10.1007/s002390010110

Montano, V., & Jombart, T. (2017). An Eigenvalue test for spatial principal component analysis. *BMC Bioinformatics*, *18*(1), 1–7. https://doi.org/10.1186/s12859-017-1988-y

Morgan-Richards, M., Trewick, S. A., & Wallis, G. P. (2000). Characterization of a hybrid zone between two chromosomal races of the weta *Hemideina thoracica* following a geologically recent volcanic eruption. *Heredity*, 85(6), 586–592. https://doi.org/10.1046/j.1365-2540.2000.00796.x

Mullen, L. M., Vignieri, S. N., Gore, J. A., & Hoekstra, H. E. (2009). Adaptive basis of geographic variation: Genetic, phenotypic and environmental differences among beach mouse populations. *Proceedings of the Royal Society B*, *276*(1674), 3809–3818. https://doi.org/10.1098/rspb.2009.1146

Newnham, R., McGlone, M., Moar, N., Wilmshurst, J., & Vandergoes, M. (2013). The vegetation cover of New Zealand at the last glacial maximum. *Quaternary Science Reviews*, *74*, 202–214. https://doi.org/10.1016/j.quascirev.2012.08.022.

Oksanen, J., Blanchet, F. G., Friendly, M., Kindt, R., Legendre, P., McGlinn, D., ... & Wagner, H. (2020). vegan: Community ecology package. https://cran.r-project.org/package=vegan

Opatova, V., & Arnedo, M. A. (2014). Spiders on a hot volcanic roof: Colonisation pathways and phylogeography of the Canary Islands endemic trap-door spider *Titanidiops canariensis* (Araneae, Idiopidae). *PLoS One*, *9*(12), e115078. https://doi.org/10.1371/journal.pone.0115078

Osuna, F., González, D., de los Monteros, A. E., & Guerrero, J. A. (2020). Phylogeography of the volcano rabbit (*Romerolagus diazi*): The evolutionary history of a mountain specialist molded by the climatic-volcanism interaction in the Central Mexican highlands. *Journal of Mammalian Evolution*, *27*(4), 745–757. https://doi.org/10.1007/s10914-019-09493-6

Past Interglacials Working Group of PAGES. (2016). Interglacials of the last 800,000 years. *Reviews of Geophysics*, *54*, 162–219. https://doi.org/10.1002/2015RG000482

Pawson, S. M., Ecroyd, C. E., Seaton, R., Shaw, W. B., & Brockerhoff, E. G. (2010). New Zealand's exotic plantation forests as habitats for threatened indigenous species. *New Zealand Journal of Ecology*, *34*(3), 342–355. http://www.jstor.org/stable/24060703

Prebble, J. G., Kennedy, E. M., Reichgelt, T., Clowes, C., Womack, T., Mildenhall, D. C., ... & Crouch, E. M. (2021). A 100 million year composite pollen record from New Zealand shows maximum angiosperm abundance delayed until Eocene. *Palaeogeography, Palaeoclimatology, Palaeoecology*, *566*, 110207. https://doi.org/10.1016/j.palaeo.2020.110207

QGIS Development Team. (2020). QGIS: A free and open source geographic information system. Retrieved from http://qgis.osgeo.org

R Core Team. (2022). R: A language and environment for statistical computing. Retrieved from https://www.r-project.org

Radchuk, V., Reed, T., Teplitsky, C., van de Pol, M., Charmantier, A., Hassall, C., ... & Kramer-Schadt, S. (2019). Adaptive responses of animals to climate change are most likely insufficient. *Nature communications*, *10*, 3109. https://doi.org/10.1038/s41467-019-10924-4

Ramos-Onsins, S. E., & Rozas, J. (2002). Statistical properties of new neutrality tests against population growth. *Molecular Biology and Evolution*, *19*(12), 2092–2100. https://doi.org/10.1093/oxfordjournals.molbev.a004034

Rinnan, D. S. (2018). Cenfa: Climate and ecological niche factor analysis. https://cran.r-project.org/package=cenfa

Rohlf, F. (2015). The Tps series of software. *Hystrix, 26*, 1–4. https://doi.org/10.4404/hystrix-26.1-11264

Rother, H., Fink, D., Shulmeister, J., Mifsud, C., Evans, M., & Pugh, J. (2014). The early rise and late demise of New Zealand's last glacial maximum. *Proceedings of the National Academy of Sciences*, *111*(32), 11630–11635. https://doi.org/10.1073/pnas.1401547111

Scrucca, L., Fop, M., Murphy, T. B., & Raftery, A. E. (2016). Mclust 5: Clustering, classification and density estimation using Gaussian finite mixture models. *The R Journal*, *8*(1), 289–317. https://doi.org/10.32614/RJ-2016-021

Seaborn, T., Griffith, D., Kliskey, A., & Caudill, C. C. (2021). Building a bridge between adaptive capacity and adaptive potential to understand responses to environmental change. *Global Change Biology*, *27*(12), 2656–2668. https://doi.org/10.1111/gcb.15579

Segschneider, B., Landis, C. A., Manville, V., White, J. D. L., & Wilson, C. J. N. (2002). Environmental response to a large, explosive rhyolite eruption: Sedimentology of post-1.8 ka pumice-rich Taupo volcaniclastics in the Hawke's Bay region, New Zealand. *Sedimentary Geology*, *150*, 275–299. https://doi.org/10.1016/S0037-0738(01)00200-7

Shelomi, M. (2012). Where are we now? Bergmann's rule sensu lato in insects. *The American Naturalist*, *180*(4), 511–519. https://doi.org/10.1086/667595

Shepherd, L., Simon, C., Langton-Myers, S., & Morgan-Richards, M. (2022). Insights into Aotearoa New Zealand's biogeographic history provided by the study of natural hybrid zones. *Journal of the Royal Society of New Zealand*. https://doi.org/10.1080/03036758.2022.2061020

Stewart, J. R., Lister, A. M., Barnes, I., & Dalén, L. (2010). Refugia revisited: Individualistic responses of species in space and time. *Proceedings of the Royal Society B: Biological Sciences*, *277*(1682), 661–671. https://doi.org/10.1098/rspb.2009.1272

Tajima, F. (1989). Statistical method for testing the neutral mutation hypothesis by DNA polymorphism. *Genetics*, *123*(3), 585–595. https://doi.org/10.1093/genetics/123.3.585

Tamura, K. B., & Nei, M. (1993) Estimation of the number of nucleotide substitutions in the control region of mitochondrial DNA in humans and chimpanzees. *Molecular Biology and Evolution*, *10*(3), 512–526. https://doi.org/10.1093/oxfordjournals.molbev.a040023

Thuiller, W., Georges, D., Engler, R., & Breiner, F. (2020). Biomod2: Ensemble platform for species distribution modelling. https://cran.r-project.org/package=biomod2

Trewick, S. A. (2008). DNA barcoding is not enough: Mismatch of taxonomy and genealogy in New Zealand grasshoppers (orthoptera: Acrididae). *Cladistics*, *24*(2), 240–254. https://doi.org/10.1111/j.1096-0031.2007.00174.x

Trewick, S. A., & Bland, K. (2012). Fire and slice: Palaeogeography for biogeography at New Zealand's North Island/South Island juncture. *Journal of the Royal Society of New Zealand*, *42*(3), 153–183. https://doi.org/10.1080/03036758.2010.549493

Trewick, S. A. & Morris, S. (2008). *Diversity and taxonomic status of some New Zealand grasshoppers.* Science & Technical Publishing Department of Conservation. https://www.doc.govt.nz/globalassets/documents/science-and-technical/drds290.pdf

Trewick, S. A., Pilkington, S., Shepherd, L. D., Gibb, G. C., & Morgan-Richards, M. (2017). Closing the gap: Avian lineage splits at a young, narrow seaway imply a protracted history of mixed population response. *Molecular Ecology*, *26*(20), 5752–5772. https://doi.org/10.1111/mec.14323

Trewick, S. A., Wallis, G. P., & Morgan-Richards, M. (2000). Phylogeographical pattern correlates with Pliocene mountain building in the alpine scree weta (Orthoptera, Anostostomatidae). *Molecular Ecology*, *9*(6), 657–666. https://doi.org/10.1046/j.1365-294x.2000.00905.x

Trewick, S. A., Wallis, G. P., & Morgan-Richards, M. (2011). The invertebrate life of New Zealand: A phylogeographic approach. *Insects*, *2*(3), 297–325. https://doi.org/10.3390/insects2030297

Valavi, R., Elith, J., Lahoz-Monfort, J. J., & Guillera-Arroita, G. (2019). BlockCV: An r package for generating spatially or environmentally separated folds for k-fold cross-validation of species distribution models. *Methods in Ecology and Evolution*, *10*, 225–232. https://doi.org/10.1111/2041-210x.13107

Vignali, S., Barras, A. G., Arlettaz, R., & Braunisch, V. (2020). SDMtune: An R package to tune and evaluate species distribution models. *Ecology and Evolution*, *10*(20), 11488–11506. https://doi.org/10.1002/ece3.6786

Wang, I. J. (2020). Topographic path analysis for modeling dispersal and functional connectivity: Calculating topographic distances using the topoDistance R package. *Methods in Ecology and Evolution*, *11*, 265–272. https://doi.org/10.1111/2041-210X.13317

Wardle, P. (1985). New Zealand timberlines. 3. A synthesis. *New Zealand Journal of Botany*, *23*(2), 263–271. https://doi.org/10.1080/0028825X.1985.10425330

Warren, D. L., Glor, R. E., & Turelli, M. (2008). Environmental niche equivalency versus conservatism: Quantitative approaches to niche evolution. *Evolution*, *62*(11), 2868–2883. https://doi.org/10.1111/j.1558-5646.2008.00482.x

Wiens, J. J. (2011). The niche, biogeography and species interactions. *Philosophical Transactions of the Royal Society B*, *366*, 2336–2350. https://doi.org/10.1098/rstb.2011.0059

Wiens, J. J. & Graham, C. H. (2005). Niche conservatism: Integrating evolution, ecology and conservation biology. *Annual Review of Ecology, Evolution, and Systematics*, *36*, 519– 539. https://doi.org/10.1146/annurev.ecolsys.36.102803.095431

Whitman, D. W. (2008). The significance of body size in the Orthoptera: A review. *Journal of Orthoptera Research*, *17*, 117–134. https://doi.org/10.1665/1082-6467-17.2.117

Willi, Y., Kristensen, T. N., Sgrò, C. M., Weeks, A. R., Ørsted, M., & Hoffmann, A. A. (2022). Conservation genetics as a management tool: The five best-supported paradigms to assist the management of threatened species. *Proceedings of the National Academy of Sciences*, *119*(1), e2105076119. https://doi.org/10.1073/pnas.2105076119

Wilmshurst, J. M., & McGlone, M. S. (1996). Forest disturbance in the central North Island, New Zealand, following the 1850 BP Taupo eruption. *The Holocene*, *6*(4), 399–411. https://doi.org/10.1177/095968369600600402

Supporting Information

Appendix 1. Supplementary information about molecular and genetic methods and results.

Table S1.1. Genetic sampling of *Sigaus piliferus* in North Island, New Zealand (ordered by latitude), showing the geographic region, number of individuals (*n*), latitude, longitude, and elevation (m).

Population	Region	*n*	Latitude	Longitude	Elevation
The Pinnacles	Coromandel Range	2	-37.047	175.716	729
Mt Te Aroha	Kaimai Range	10	-37.533	175.742	939
Te Araroa	East Cape	3	-37.639	178.359	40
Mt Karioi	Waikato	1	-37.861	174.799	696
Mt Hikurangi	Raukumara Range	1	-37.912	178.055	1435
Mt Pirongia	Waikato	4	-37.983	175.109	723
Lake Tikitapu	Rotorua	1	-38.189	176.327	423
Mt Tauhara	Taupo Lake	6	-38.690	176.159	1027–1080
Lake Waikaremoana	Te Urewera	3	-38.780	177.141	658–703
Ruakituri Valley	Ruakituri	1	-38.791	177.456	252
Pureora Forest Park	Taupo Lake	2	-38.795	175.590	760
Takarere Road	Ahimanawa Range	1	-39.061	176.541	619
Mt Tongariro, Ketetahi Track	Central Volcanoes	9	-39.099	175.648	1086–1258
Mt Ruapehu, Whakapapa Village	Central Volcanoes	17	-39.236	175.555	934–1603
Mt Kaweka	Kaweka Range	10	-39.288	176.405	1021–1608
Mt Ruapehu, Turoa Village	Central Volcanoes	24	-39.303	175.529	1241–1690
Military Ground, Mangaio Stream	Rangipo Desert	12	-39.307	175.746	1100
Mt Kuripapango	Kaweka Range	12	-39.358	176.344	678–1312
Ngaruroro Valley	Kaweka Range	4	-39.385	176.333	514–677
Military Ground, Lake Moawhango	Rangipo Desert	7	-39.386	175.721	934
Golden Crown	Ruahine Range	1	-39.626	176.295	1260
Corner Hut	Ruahine Range	2	-39.631	176.173	1193
Armstrong Saddle	Ruahine Range	3	-39.783	176.165	1368
Waipawa Saddle	Ruahine Range	4	-39.810	176.150	1362
Whanahuia Mountains	Ruahine Range	14	-39.891	176.019	1042–1427
Herepai Peak	Tararua Range	12	-40.687	175.516	1083
Mt Dundas	Tararua Range	2	-40.726	175.447	1460
Arete Peak	Tararua Range	10	-40.745	175.434	1289–1404
Mt Holdsworth	Tararua Range	6	-40.883	175.423	1285
Mt Hector	Tararua Range	2	-40.926	175.266	1160–1440

Table S1.2. Summary statistics (± standard deviation) of genetic variation among partial mitochondrial ND2 haplotypes for population samples (n > 5) of the New Zealand alpine grasshopper *Sigaus piliferus*, ordered by latitude. The translated ND2 alignment (249 sites) presented 47 amino acid substitutions at positions 9, 29, 37, 41, 42, 45, 62, 82, 84, 85, 97, 102, 103, 108, 110, 112, 113, 114, 118, 120, 121, 122, 134, 141, 148, 149, 174, 175, 176, 178, 180, 181, 187, 190, 191, 203, 208, 215, 221, 225, 227, 230, 231, 236, 238, 242, and 248. Sample size (n), number of observed haplotypes (N_h), number of polymorphic sites (S), haplotype diversity (h), and nucleotide diversity (π). Bold values indicate the largest coefficients of haplotype and nucleotide diversity. No polymorphisms in the data (-).

Population	**Lineage**	***n***	**N_h**	**S**	***h***	**π**
Te Aroha	North	10	3	52	0.5110±0.1640	**0.0150±0.0104**
Tauhara	North	6	3	2	0.6000±0.2150	0.0009±0.0004
Ketetahi	North	9	5	5	**0.8610±0.0870**	0.0029±0.0005
Whakapapa	North	17	2	2	0.1180±0.1010	0.0003±0.0003
Kaweka	North	10	5	5	0.6670±0.1630	0.0013±0.0005
Turoa	North	24	6	7	0.7030±0.0620	0.0017±0.0004
Mangaio	North	12	6	8	0.7580±0.1220	0.0022±0.0006
Kuripapango	North	12	6	10	0.7580±0.1220	0.0034±0.0010
Moawhango	North	7	3	4	0.7620±0.1150	0.0026±0.0006
Whanahuia	North	14	13	20	0.0111±0.0310	0.0112±0.0012
Herepai	South	12	10	14	**0.9550±0.0570**	0.0062±0.0010
Arete Peak	South	10	6	14	0.9110±0.0620	0.0067±0.0012
Holdsworth	South	6	5	11	0.9330±0.1220	**0.0074±0.0014**
Northern lineage	-	154	66	121	0.9500±0.0090	**0.0198±0.0021**
Southern lineage	-	32	25	49	**0.9840±0.0120**	0.0111±0.0015
Total dataset	-	186	91	155	0.9650±0.0070	0.0375±0.0027

Table S1.3. Summary of demographic statistics based on partial mitochondrial ND2 haplotypes for population samples ($n > 5$) of the New Zealand alpine grasshopper *Sigaus piliferus*, ordered by latitude. Sample size (*n*), mismatch distribution shape (Mismatch), Harpending's raggedness index (*r*), Tajima's *D*, Fu's *Fs*, and Ramos-Onsins and Roza's R_2. Significance is given within parentheses with significant values denoted in bold ($P < 0.05$ except for *Fs* where $P < 0.02$). A smooth, unimodal distribution is expected when populations have undergone recent demographic expansion, while multimodal and ragged distributions suggest a stable population (Rogers & Harpending, 1992). A significant *r* index indicates a stable population typically showing 'ragged', multimodal mismatch (Harpending, 1994). Significantly negative Fu's *Fs* and Tajima's *D* values and significantly positive R_2 values were taken as evidence of recent population expansion (Galbreath et al., 2009).

Population	**Lineage**	***n***	**Mismatch**	***r***	***D***	***Fs***	***R_2***	**Expansion**
Te Aroha	North	10	multimodal	0.485 (0.999)	**−1.911 (0.007)**	8.659 (0.998)	0.283 (1.000)	No
Tauhara	North	6	skewed unimodal	0.240 (0.237)	−1.132 (0.373)	**−0.858 (0.000)**	0.236 (0.254)	**Yes**
Ketetahi	North	9	skewed bimodal	0.107 (0.252)	0.753 (0.811)	−0.670 (0.361)	0.204 (0.694)	No
Whakapapa	North	17	skewed bimodal	0.806 (0.963)	**−1.504 (0.000)**	0.122 (0.586)	0.235 (0.872)	No
Kaweka	North	10	skewed unimodal	0.067 (0.127)	**−1.741 (0.000)**	−2.260 (0.068)	0.134 (0.098)	**Yes**
Turoa	North	24	skewed bimodal	0.127 (0.535)	−1.047 (0.148)	−1.313 (0.266)	0.085 (0.085)	No
Mangaio	North	12	skewed unimodal	**0.025 (0.012)**	**−1.572 (0.044)**	−1.924 (0.140)	0.115 (0.086)	**Yes**
Kuripapango	North	12	skewed bimodal	0.084 (0.357)	−0.933 (0.204)	−0.694 (0.360)	**0.108 (0.049)**	**Yes**
Moawhango	North	7	multimodal	0.782 (0.959)	0.797 (0.829)	1.222 (0.753)	0.238 (0.696)	No
Whanahuia	North	14	multimodal	0.027 (0.082)	1.356 (0.944)	**−5.035 (0.015)**	0.202 (0.945)	**Yes**
Herepai	South	12	multimodal	0.048 (0.186)	0.014 (0.547)	**−3.920 (0.019)**	0.144 (0.403)	**Yes**
Arete Peak	South	10	skewed bimodal	0.041 (0.085)	0.149 (0.597)	0.399 (0.548)	0.168 (0.549)	No
Holdsworth	South	6	bimodal	0.271 (0.704)	0.899 (0.833)	−0.175 (0.462)	0.225 (0.685)	No
Northern lineage	-	154	multimodal	0.009 (0.603)	−1.081 (0.123)	**−20.120 (0.011)**	0.058 (0.131)	**Yes**
Southern lineage	-	32	multimodal	0.016 (0.266)	−1.184 (0.102)	**−11.631 (0.003)**	0.076 (0.074)	**Yes**
Total dataset	-	186	multimodal	0.005 (0.402)	0.149 (0.649)	−18.143 (0.026)	0.089 (0.644)	No

Figure S1.1. Mean genetic distances (Kimura 2-parameter, lower left; Tamura-Nei, upper right) among population samples of *Sigaus piliferus* (ordered by latitude) suggest an ancient divergence between northern and southern lineages. The rate variation was modelled with gamma distribution = 1.

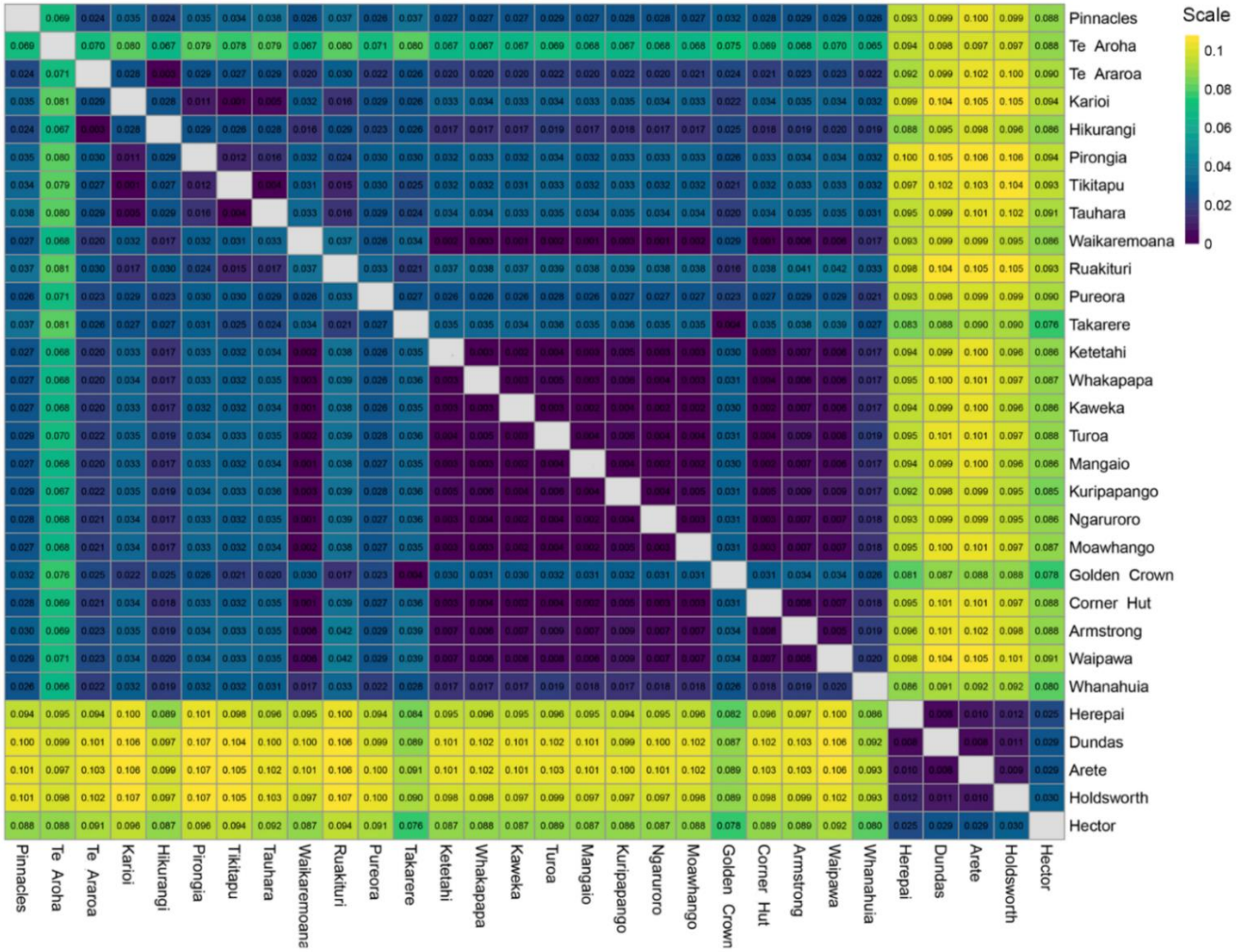

Figure S1.2. Bayesian phylogenetic tree for *Sigaus piliferus* based on mitochondrial ND2 sequences from 186 specimens. The best partition scheme (LnL = -2,978.36; BIC = 8,523.75) as inferred using PARTITIONFINDER v2.1.1 (Lanfear et al., 2017) contained two partitions for the data, each with a different evolutionary model: (ND2_pos1 and ND2_pos3 = HKY+G) (ND2_pos2 = HKY+I) (ND2_pos3). The analysis used four chains on two runs for 20^6 generations, with sampling frequency of 20^3 generations and a burn-in of 0.10. Convergence of the posterior distribution parameters was examined by monitoring the Effective Sample Size (ESS > 200) and trace plots in TRACER v1.6 (Rambaut et al., 2018). For visualisation purposes, only ingroup sequences are shown.

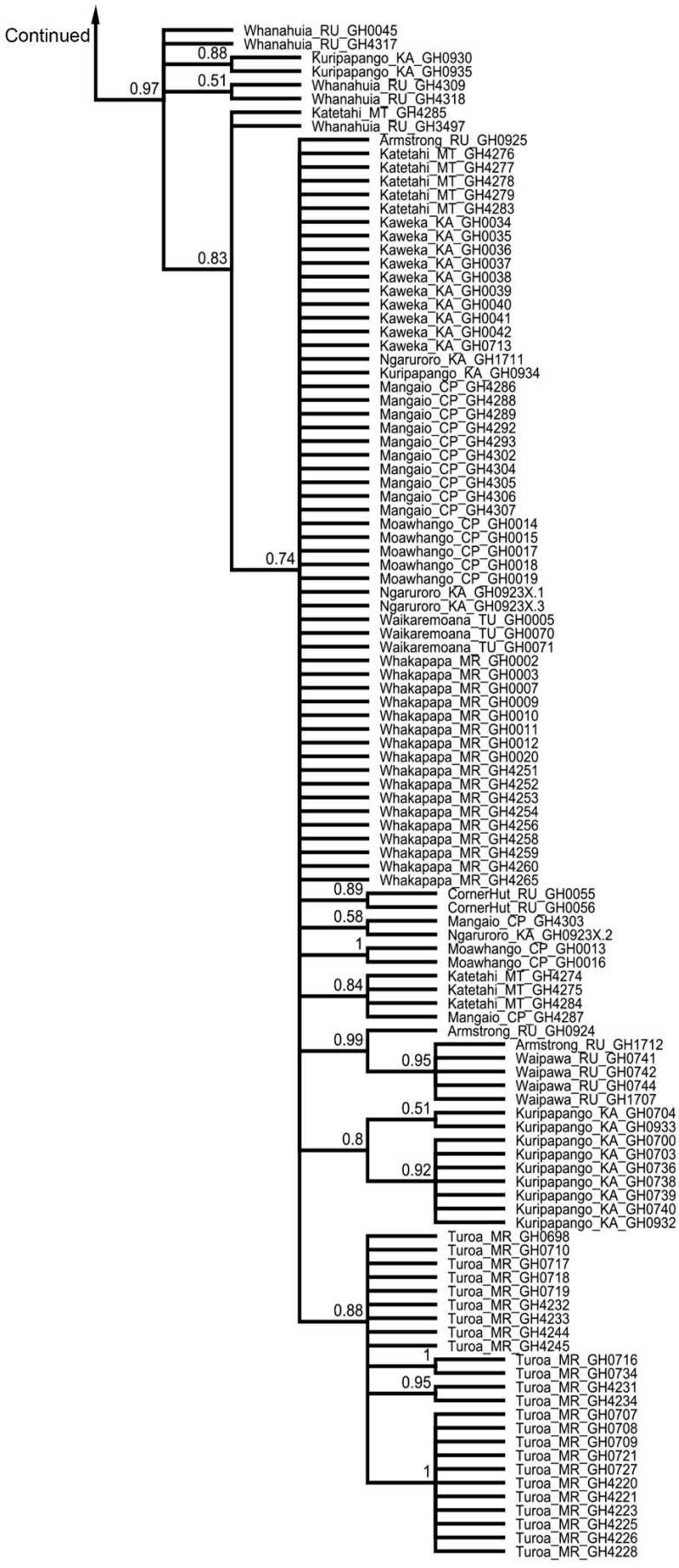
Continued
Whanahuia_RU_GH0045
Whanahuia_RU_GH4317
0.88
Kuripapango_KA_GH0930
Kuripapango_KA_GH0935
0.51
Whanahuia_RU_GH4309
0.97
Whanahuia_RU_GH4318
Katetahi_MT_GH4285
Whanahuia_RU_GH3497
Armstrong_RU_GH0925
Katetahi_MT_GH4276
Katetahi_MT_GH4277
Katetahi_MT_GH4278
Katetahi_MT_GH4279
Katetahi_MT_GH4283
Kaweka_KA_GH0034
Kaweka_KA_GH0035
Kaweka_KA_GH0036
0.83
Kaweka_KA_GH0037
Kaweka_KA_GH0038
Kaweka_KA_GH0039
Kaweka_KA_GH0040
Kaweka_KA_GH0041
Kaweka_KA_GH0042
Kaweka_KA_GH0713
Ngarururoro_KA_GH1711
Kuripapango_KA_GH0934
Mangaio_CP_GH4286
Mangaio_CP_GH4288
Mangaio_CP_GH4289
Mangaio_CP_GH4292
Mangaio_CP_GH4293
Mangaio_CP_GH4302
Mangaio_CP_GH4304
Mangaio_CP_GH4305
Mangaio_CP_GH4306
Mangaio_CP_GH4307
Moawhango_CP_GH0014
Moawhango_CP_GH0015
Moawhango_CP_GH0017
0.74
Moawhango_CP_GH0018
Moawhango_CP_GH0019
Ngarururoro_KA_GH0923X.1
Ngarururoro_KA_GH0923X.3
Waikaremoana_TU_GH0005
Waikaremoana_TU_GH0070
Waikaremoana_TU_GH0071
Whakapapa_MR_GH0002
Whakapapa_MR_GH0003
Whakapapa_MR_GH0007
Whakapapa_MR_GH0009
Whakapapa_MR_GH0010
Whakapapa_MR_GH0011
Whakapapa_MR_GH0012
Whakapapa_MR_GH0020
Whakapapa_MR_GH4251
Whakapapa_MR_GH4252
Whakapapa_MR_GH4253
Whakapapa_MR_GH4254
Whakapapa_MR_GH4256
Whakapapa_MR_GH4258
Whakapapa_MR_GH4259
Whakapapa_MR_GH4260
Whakapapa_MR_GH4265
0.89
CornerHut_RU_GH0055
CornerHut_RU_GH0056
0.58
Mangaio_CP_GH4303
Ngarururoro_KA_GH0923X.2
1
Moawhango_CP_GH0013
Moawhango_CP_GH0016
Katetahi_MT_GH4274
0.84
Katetahi_MT_GH4275
Katetahi_MT_GH4284
Mangaio_CP_GH4287
Armstrong_RU_GH0924
0.99
Armstrong_RU_GH1712
0.95
Waipawa_RU_GH0741
Waipawa_RU_GH0742
Waipawa_RU_GH0744
Waipawa_RU_GH1707
0.51
Kuripapango_KA_GH0704
Kuripapango_KA_GH0933
0.8
Kuripapango_KA_GH0700
Kuripapango_KA_GH0703
0.92
Kuripapango_KA_GH0736
Kuripapango_KA_GH0738
Kuripapango_KA_GH0739
Kuripapango_KA_GH0740
Kuripapango_KA_GH0932
Turoa_MR_GH0698
Turoa_MR_GH0710
Turoa_MR_GH0717
Turoa_MR_GH0718
Turoa_MR_GH0719
0.88
Turoa_MR_GH4232
Turoa_MR_GH4233
Turoa_MR_GH4244
Turoa_MR_GH4245
1
Turoa_MR_GH0716
Turoa_MR_GH0734
0.95
Turoa_MR_GH4231
Turoa_MR_GH4234
Turoa_MR_GH0707
Turoa_MR_GH0708
Turoa_MR_GH0709
Turoa_MR_GH0721
1
Turoa_MR_GH0727
Turoa_MR_GH4220
Turoa_MR_GH4221
Turoa_MR_GH4223
Turoa_MR_GH4225
Turoa_MR_GH4226
Turoa_MR_GH4228

Figure S1.3. Pairwise Φ_{ST} (upper left matrix) showed in most cases significant P-values (lower right matrix) of genetic differentiation among population samples of *Sigaus piliferus* (ordered by latitude).

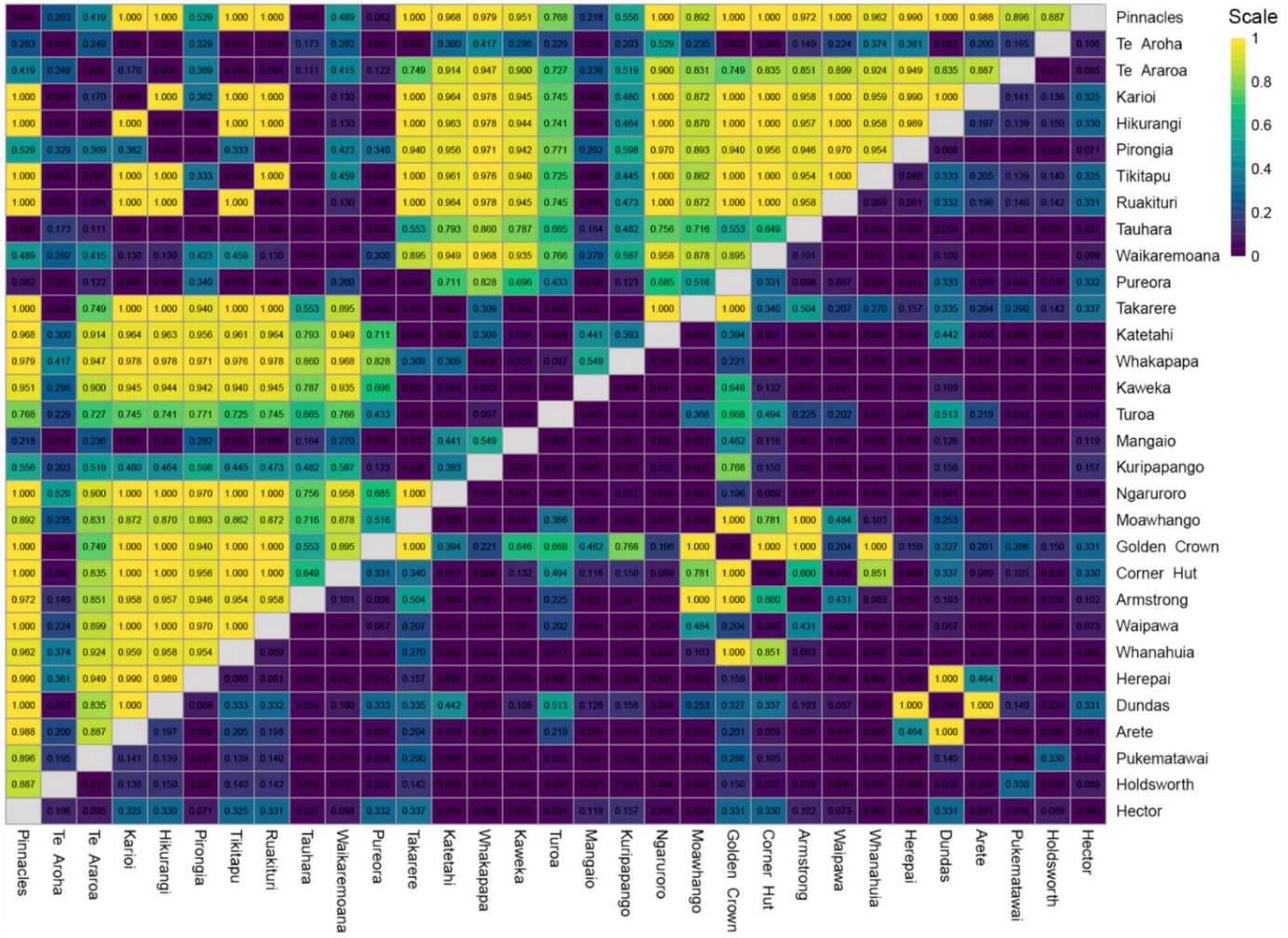

Appendix 2. Supplementary information about phenotypic analyses methods and results.

Table S2.1. Morphometric sampling of *Sigaus piliferus* in North Island, New Zealand (ordered by latitude), showing the geographic region, number of individuals by sex (*n*), latitude, longitude, and elevation (m).

Population	Region	*n*	Latitude	Longitude	Elevation
The Pinnacles	Coromandel Range	1♀	-37.047	175.716	729
Mt Te Aroha	Kaimai Range	2♀/1♂	-37.533	175.742	939
Te Araroa	East Cape	2♀/1♂	-37.639	178.359	40
Mt Karioi	Waikato	1♀	-37.861	174.799	696
Mt Hikurangi	Raukumara Range	1♀/1♂	-37.912	178.055	1435
Mt Pirongia	Waikato	3♀	-37.983	175.109	723
Lake Tikitapu	Rotorua	1♀	-38.189	176.327	423
Pukahunui Valley	Rotorua	1♀	-38.740	176.654	699
Lake Waikaremoana	Te Urewera	3♀	-38.780	177.141	658–703
Ruakituri Valley	Ruakituri	1♀	-38.791	177.456	252
Pureora Forest Park	Taupo Lake	1♀/1♂	-38.795	175.590	760
Takarere Road	Ahimanawa Range	1♀	-39.061	176.541	619
Mt Tongariro, Ketetahi Track	Central Volcanoes	3♀/6♂	-39.099	175.648	1086–1258
Mt Ruapehu, Whakapapa Village	Central Volcanoes	9♀/8♂	-39.236	175.555	934–1603
Mt Kaweka	Kaweka Range	4♀/2♂	-39.288	176.405	1021–1608
Mt Ruapehu, Turoa Village	Central Volcanoes	18♀/12♂	-39.303	175.529	1241–1690
Military Ground, Mangaio Stream	Rangipo Desert	8♀/11♂	-39.307	175.746	1100
Mt Kuripapango	Kaweka Range	2♀/2♂	-39.358	176.344	678–1312
Ngaruroro Valley	Kaweka Range	4♀	-39.385	176.333	514–677
Golden Crown	Ruahine Range	1♀	-39.626	176.295	1260
Corner Hut	Ruahine Range	2♀	-39.631	176.173	1193
Armstrong Saddle	Ruahine Range	3♀	-39.783	176.165	1368
Whanahuia Mountains	Ruahine Range	3♀/4♂	-39.891	176.019	1042–1427
Pohangina Saddle	Ruahine Range	1♀/1♂	-39.947	176.121	1402
Herepai Peak	Tararua Range	3♀	-40.687	175.516	1083
Mt Dundas	Tararua Range	4♀	-40.726	175.447	1460
Arete Peak	Tararua Range	10♀	-40.745	175.434	1289–1404
Mt Holdsworth	Tararua Range	5♀/2♂	-40.883	175.423	1285
Mt Hector	Tararua Range	2♀	-40.926	175.266	1160–1440

Table S2.2. Geometric morphometric sampling of *Sigaus piliferus* in North Island, New Zealand (ordered by latitude), showing the geographic region, number of individuals by sex (*n*), latitude, longitude, and elevation (m).

Population	Region	*n*	Latitude	Longitude	Elevation
The Pinnacles	Coromandel Range	1♀	-37.047	175.716	729
Mt Te Aroha	Kaimai Range	2♀/1♂	-37.533	175.742	939
Te Araroa	East Cape	2♀/1♂	-37.639	178.359	40
Mt Karioi	Waikato	1♀	-37.861	174.799	696
Mt Hikurangi	Raukumara Range	1♀/1♂	-37.912	178.055	1435
Mt Pirongia	Waikato	3♀	-37.983	175.109	723
Lake Tikitapu	Rotorua	1♀	-38.189	176.327	423
Pukahunui Valley	Rotorua	1♀	-38.740	176.654	699
Lake Waikaremoana	Te Urewera	3♀	-38.780	177.141	658–703
Ruakituri Valley	Ruakituri	1♀	-38.791	177.456	252
Pureora Forest Park	Taupo Lake	1♀/1♂	-38.795	175.590	760
Takarere Road	Ahimanawa Range	1♀	-39.061	176.541	619
Mt Tongariro, Ketetahi Track	Central Volcanoes	4♀/6♂	-39.099	175.648	1086–1258
Mt Ruapehu, Whakapapa Village	Central Volcanoes	9♀/11♂	-39.236	175.555	934–1603
Mt Kaweka	Kaweka Range	5♀/3♂	-39.288	176.405	1021–1608
Mt Ruapehu, Turoa Village	Central Volcanoes	18♀/12♂	-39.303	175.529	1241–1690
Military Ground, Mangaio Stream	Rangipo Desert	8♀/12♂	-39.307	175.746	1100
Mt Kuripapango	Kaweka Range	2♀/2♂	-39.358	176.344	678–1312
Ngaruroro Valley	Kaweka Range	4♀	-39.385	176.333	514–677
Golden Crown	Ruahine Range	1♀	-39.626	176.295	1260
Corner Hut	Ruahine Range	2♀	-39.631	176.173	1193
Armstrong Saddle	Ruahine Range	3♀	-39.783	176.165	1368
Whanahuia Mountains	Ruahine Range	3♀/4♂	-39.891	176.019	1042–1427
Herepai Peak	Tararua Range	3♀	-40.687	175.516	1083
Mt Dundas	Tararua Range	4♀	-40.726	175.447	1460
Arete Peak	Tararua Range	10♀	-40.745	175.434	1289–1404
Mt Holdsworth	Tararua Range	5♀/2♂	-40.883	175.423	1285
Mt Hector	Tararua Range	2♀	-40.926	175.266	1160–1440

Figure S2.1. Visual representation of morphological features used to characterise phenotypic variation in *Sigaus piliferus*. Body dimensions (top panel): left hind femur length (FL) and maximum width (FW), and mid-line pronotum length (PL) and maximum width (PW). Geometric morphometrics (bottom panel) used 14 landmarks around the margin of the pronotum (circles). Images were organised into thin-plate spline (TPS) files and landmarks were digitised and scale-calibrated using TPSDIG2 2.29 (Rohlf, 2015), which captures the spatial coordinates of landmarks and transforms them into geometric data. Adult female (left) and male (right) to the same scale for illustrative purposes. Measurement and imaging were done by the same person to minimise operator error.

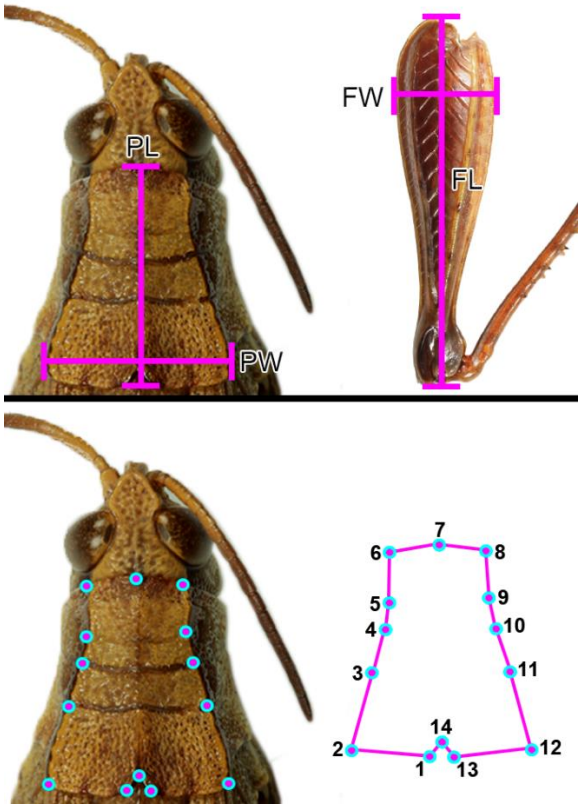

Figure S2.2. Differences in repeatability of body dimensions (top: FL, femur length; FW, femur width; PL, pronotum length; PW, pronotum width) and shapes (bottom: L01–L14, Landmarks 01–14) estimated with experimental replication. For this, we randomly selected five males and five females to then remeasured body dimensions and redigitased landmarks five times, remounting specimens between successive measurements and digitalisations. Repeatability (R; the ratio of intra-observer variance) for body dimensions and pronotal shape (i.e., Procrustes coordinates) was calculated with the R package 'rptR' 0.9.22 (Stoffel et al., 2017). In addition, we calculated percentage measurement error (%ME; the amount of variation within individuals among replicates) over all shapes based on a PERMANOVA design using the R package 'geomorph'. We found high measurement consistency for body size (R > 0.9670, mean = 0.9989, SE = 0.0002) and shape (R > 0.9134, mean = 0.9516, SE = 0.0228), though differences in repeatability of individual traits were noted. Mean measurement error (%ME) for shapes was low (2.54%) and PERMANOVA results indicated the replicate factor was not significant (P = 1.000) while specimen factor was (P < 0.001). These results indicated that morphological data use here are highly reproducible with a technical measurement error biologically negligible.

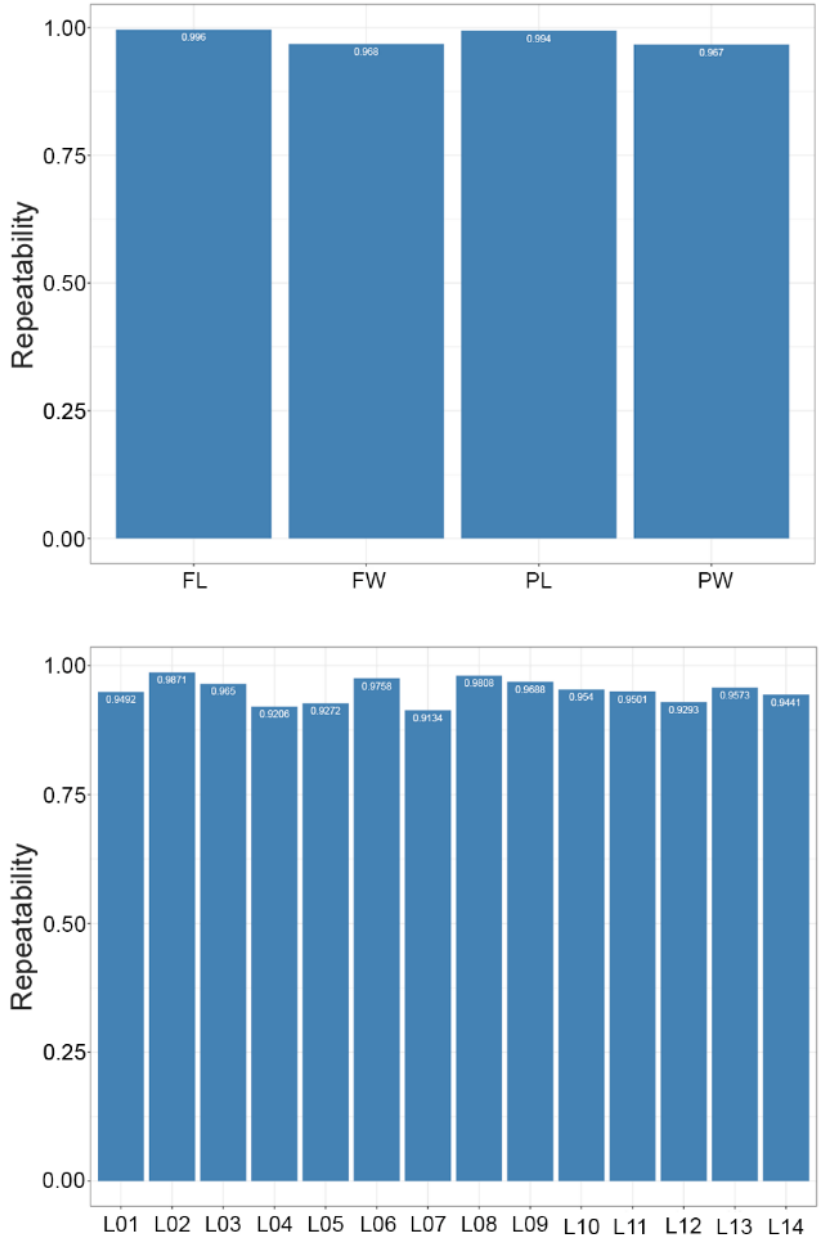

Figure S2.3. Morphological analyses indicated *Sigaus piliferus* exhibit sexual dimorphism in the studied traits as depicted by boxplots of body dimensions and pronotum centroid size based on the landmark configuration (a–e) and a Principal Component Analysis (PCA) of pronotal shape using sex as a grouping factor (f). Barplot showing the variation described by each principal component (PC), with meaningful PCs indicated.

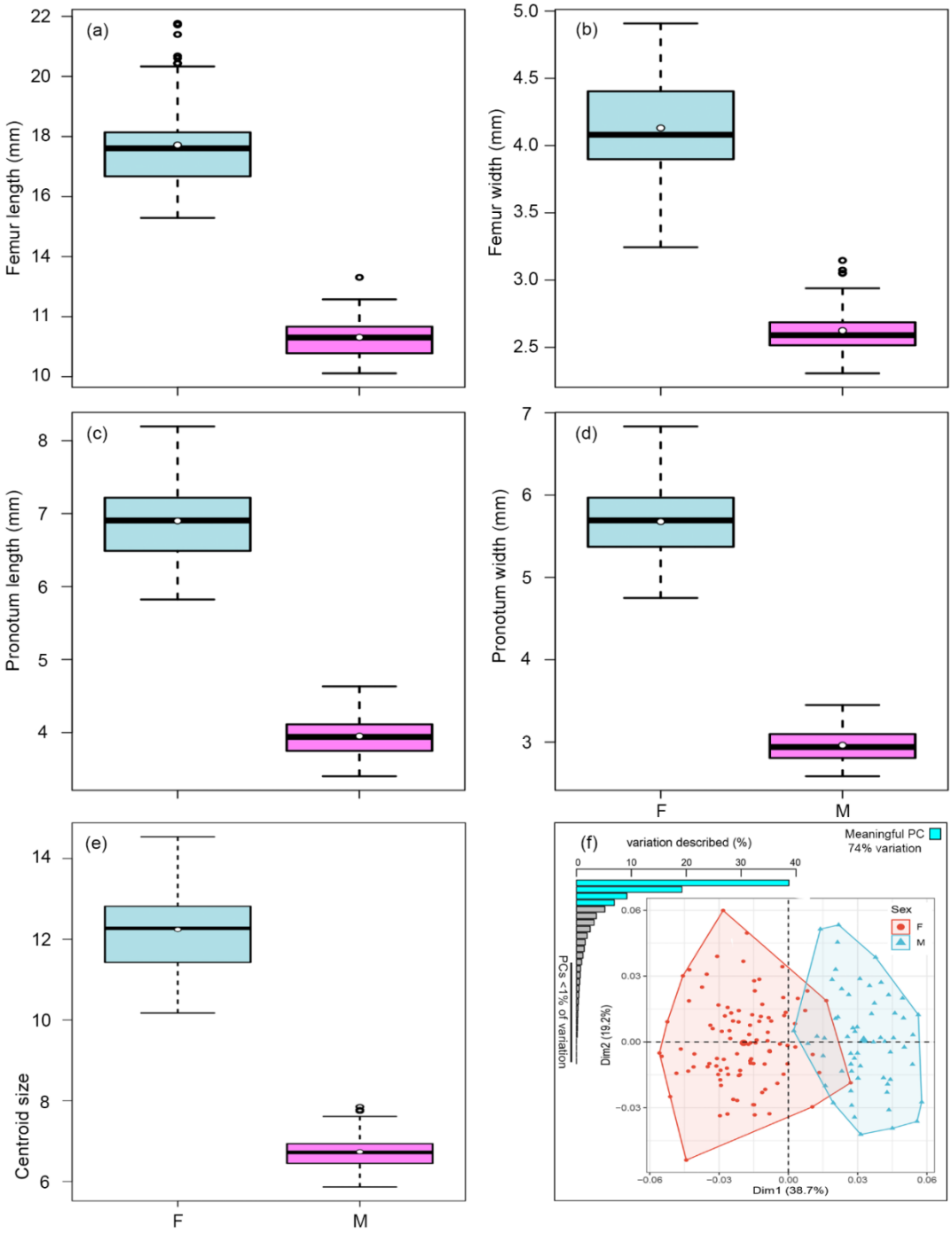

Appendix 3. Supplementary information about ecological niche modelling and niche comparisons methods and results.

Table S3.1. Environmental predictor variables investigated for estimating and projecting the potential niche of *Sigaus piliferus*. Four variables describing geodiversity (soil type) and topographic traits (slope, aspect, and roughness) were derived from a fundamental soil layer and a digital elevation model (Meza-Joya et al., 2013) obtained from the New Zealand Land Resource Information System portal (https://lris.scinfo.org.nz). Variable selection was carried out using the R package 'fuzzySim' 3.0 (Barbosa 2015), which implements a stepwise selection procedure considering correlations among variables, false discovery rate, and parsimony. We also appraised the ecological relevance of selected variables favouring those expected to reflect a more direct influence on occurrences of these grasshopper species (e.g., temperature attributes: Carmelet-Rescan et al., 2021; Koot et al., 2022; Meza-Joya et al., 2013). Variables retained for final modelling depicting their Variance Inflation Factor (VIF) value. Variable type is shown (dyn = dynamic, sta = static, con = continuous, cat = categorical).

Code	Description	Variable	VIF
bio1	Annual mean temperature (°C)	dyn, con	-
bio2	Annual mean diurnal range (°C)	dyn, con	1.5658
bio3	Isothermality (%)	dyn, con	-
bio4	Temperature seasonality (SD, °C)	dyn, con	-
bio5	Max temperature of warmest month (°C)	dyn, con	-
bio6	Min temperature of coldest month (°C)	dyn, con	-
bio7	Temperature annual range (°C)	dyn, con	-
bio8	Mean temperature of wettest quarter (°C)	dyn, con	1.1870
bio9	Mean temperature of driest quarter (°C)	dyn, con	1.3428
bio10	Mean temperature of warmest quarter (°C)	dyn, con	-
bio11	Mean temperature of coldest quarter (°C)	dyn, con	-
bio12	Annual precipitation (mm)	dyn, con	-
bio13	Precipitation of wettest month (mm)	dyn, con	-
bio14	Precipitation of driest month (mm)	dyn, con	1.1411
bio15	Precipitation seasonality (CV, %)	dyn, con	1.3938
bio16	Precipitation of wettest quarter (mm)	dyn, con	-
bio17	Precipitation of driest quarter (mm)	dyn, con	-
bio18	Precipitation of warmest quarter (mm)	dyn, con	-
bio19	Precipitation of coldest quarter (mm)	dyn, con	-
slope	Slope (°)	sta, con	-
asp	Aspect (°)	sta, con	-
rough	Roughness (°)	sta, con	-
soil	Soil type (class)	sta, cat	-

Table S3.2. Optimised models for *Sigaus piliferus* showed a greater performance when compared to default models as indicated by AUC values. Model performance was estimated by randomly splitting our data into training (80%) and testing (20%) datasets. The training dataset was further split into five random folds to perform cross-validation. Evaluation metric on the training (AUC_{TRAIN}) and the test (AUC_{TEST}) datasets as the arithmetic mean across all cross-validation folds are shown.

Algorithm	**Default model**		**Optimised model**	
	AUC_{TRAIN}	AUC_{TEST}	AUC_{TRAIN}	AUC_{TEST}
Generalised Boosting	0.9878	0.9837	0.9978	0.9939
Random Forest	0.9998	0.9847	1.0000	0.9925
Maximum Entropy	0.9902	0.9824	0.9985	0.9942

Table S3.3. Best performing parameters used for refitting the final models for *Sigaus piliferus*. Tuneable hyperparameter were tested as implemented in the R package 'SDMtune' 1.1.4 (Vignali et al., 2021). Default values as in the R package 'Biomod2' 3.4.6 (Thuiller et al., 2020). For details about the meaning of hyperparameter see the respective package documentation. Feature classes for Maximum Entropy are (l) linear, (q) quadratic, (p) product, and (h) hinge.

Algorithm	**Tuneable options**	**Default**	**Settings tested**	**Best parameters**
Generalised	number of trees	2500	750, 1250, 2500, 5000	1250
Boosting	interaction depth	7	1, 3, 7, 10	3
	shrinkage	0.001	0.0005, 0.001, 0.002, 0.004	0.004
	bag fraction	0.50	0.25, 0.50, 0.75, 1	1
Random	# sampled variables	sqrt(#var)	1, 1.5, 2, 2.5, 3, 3.5, 4	2
Forest	number of trees	500	250, 500, 1000, 2000	2000
	size of terminal nodes	5	1, 5, 10, 15, 20	1
Maximum	feature classes	lqpht	l, lq, lh, lqp, lqph, lqpht	lqpht
Entropy	Regularisation multiplier	1	0.1, 0.5, 1, 1.5, 2, 2.5, 3	0.5

Figure S3.1. Occurrence data for *Sigaus piliferus* based on a presence-absence database with 1,188 sites used in ecological niche modelling (geodetic datum WGS84), including 1,053 absences and 135 presences. Map projection: NZGD2000.

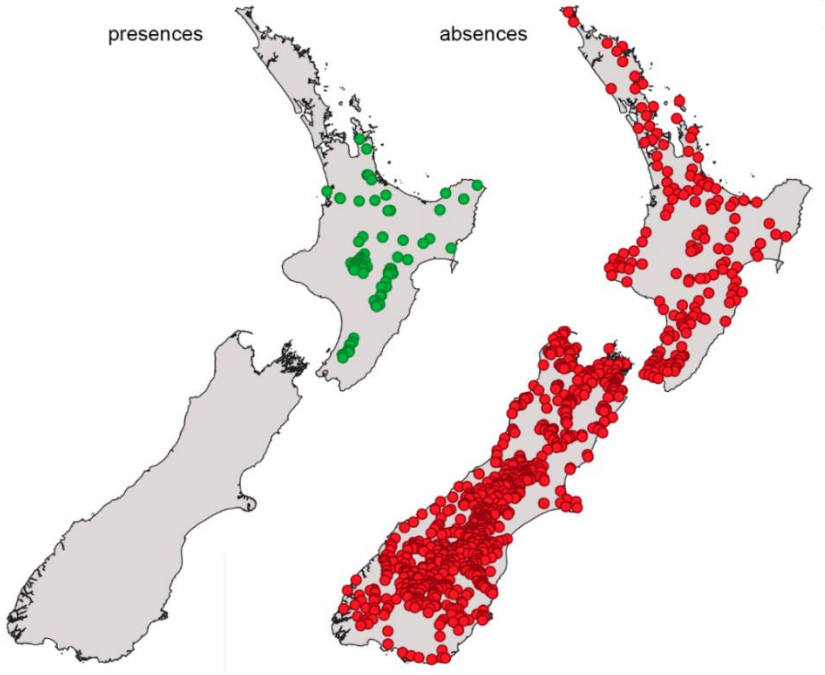

Figure S3.2. Spatial block arrangement of presence-absence data for one of the folds used for modelling the ecological niche of *Sigaus piliferus*. The study region was divided into 39 equal-sized square blocks (~150 × 150 km), which were allocated into five folds for cross-validation, each containing a similar proportion of presence/absence records. Optimal block size was calculated based on 10,000 sample points to estimate the effective autocorrelation range of all predictor variables. Map projection: NZGD2000.

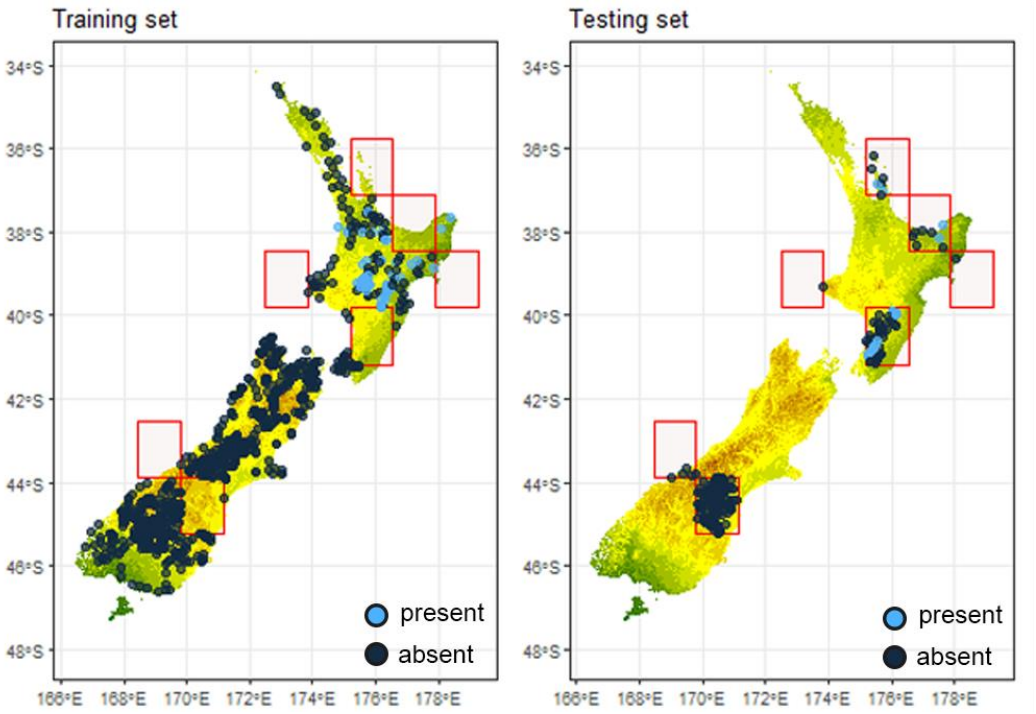

Figure S3.3. Individual models for *Sigaus piliferus* showed good to excellent predictive performance as indicated by their Receiver Operating Characteristic (ROC) and True Skill Statistic (TSS). Generalised Boosting Model (GBM), Random Forest (RF), and Maximum Entropy (MaxEnt).

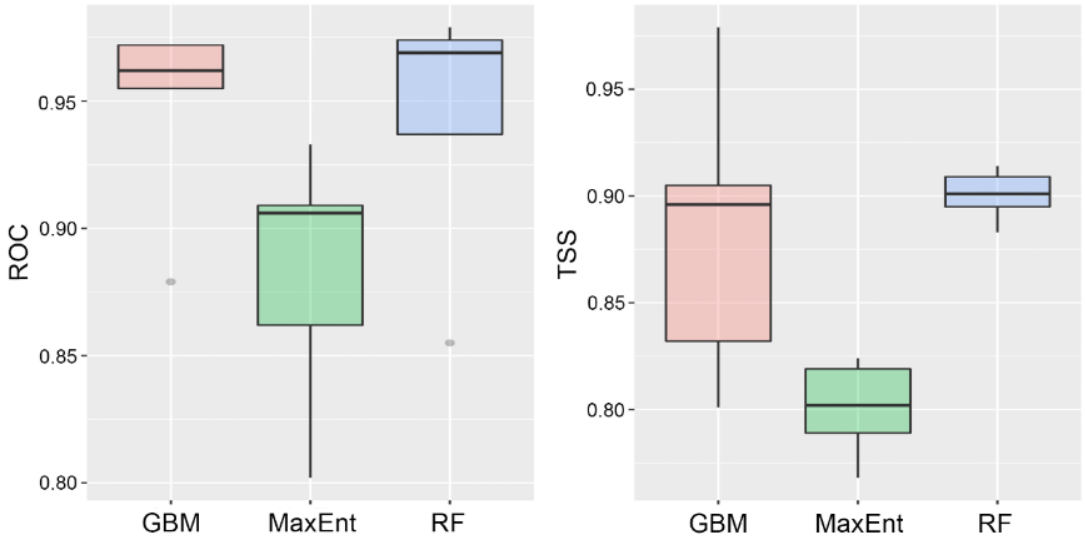

Figure S3.4. Precipitation and temperature related predictors were more influential to estimate the potential niche of *Sigaus piliferus* as indicated by the ensemble model variable importance. Variable importance scores (%) and confidence bars (95%) are reported. Variable importance scores for individual models were calculated by subtracting the mean correlation score of each predictor from 1, with scores closest to 1 indicating important variables. Variable importance for the final ensemble (EMmw) model was calculated by applying the weightings used for the ensemble forecasting to the variable importance scores for individual models, summing values by variable and then dividing by three, that is, the number of modelling methods used (Fletcher et al., 2016). Variable codes as in Table S1.1.

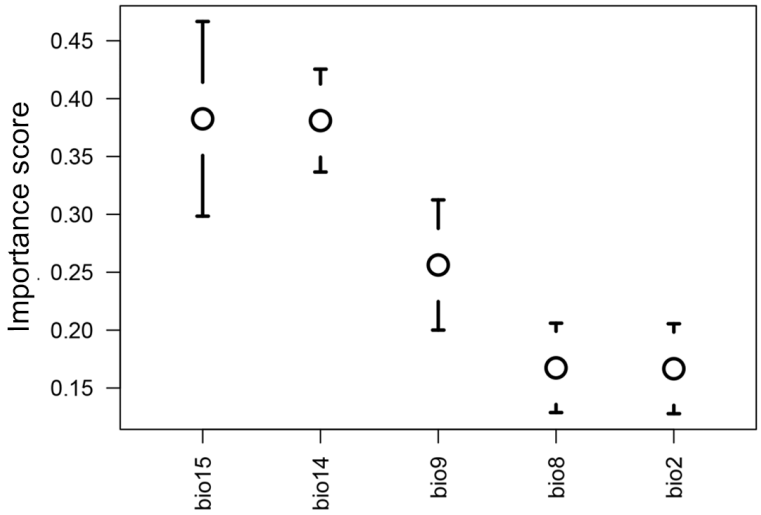

Figure S3.5. Predicted shifts in suitable niche space for *Sigaus piliferus* (mean-weighted ensemble models) in New Zealand under three past epochs (last interglacial, last glacial maximum, and mid-Holocene), current time, and two future scenarios (RCP 4.5 and RCP 8.5). Oruanui eruption (~25.5 ka) at last glacial maximum after Wilson (2001). Map projection: NZGD2000.

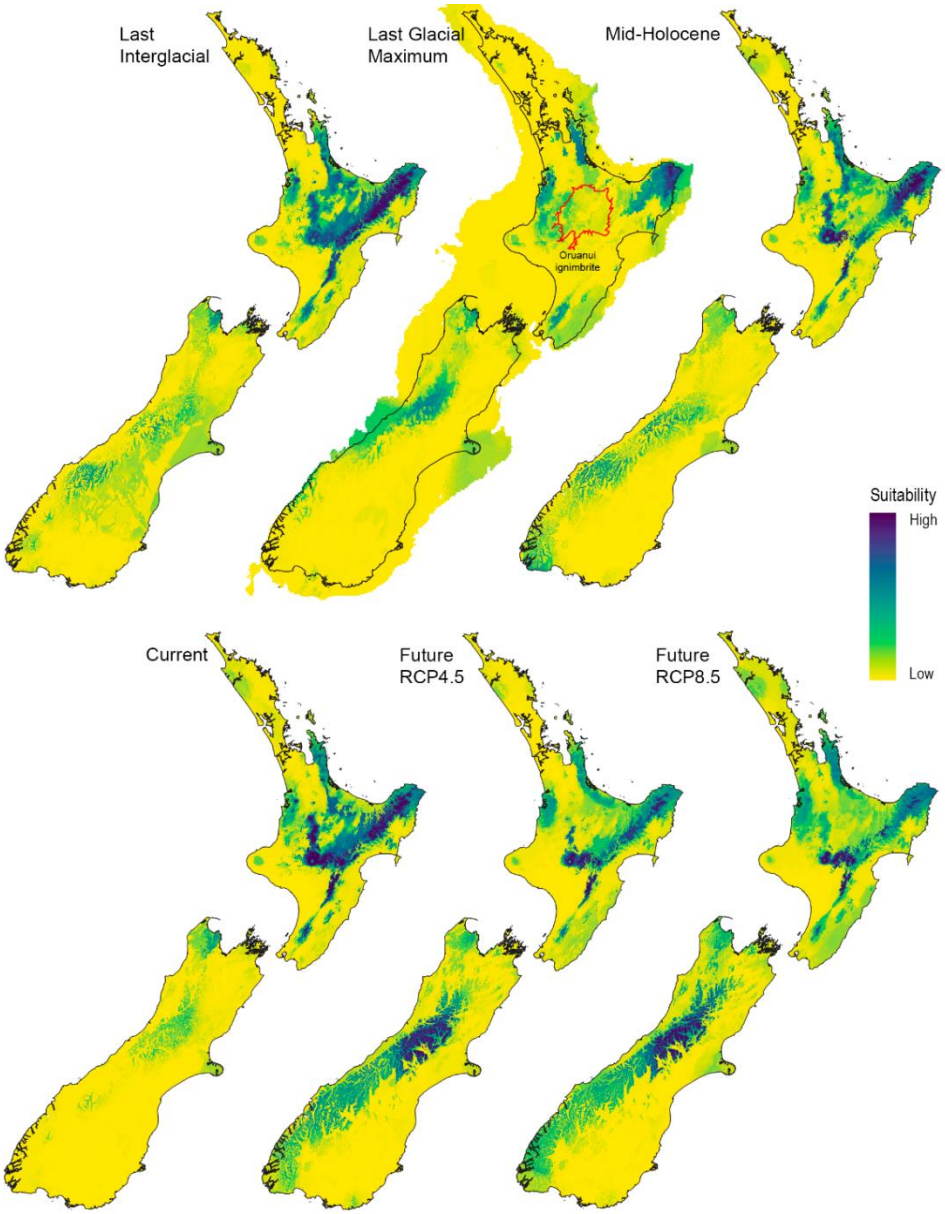

Figure S3.6. Areas of strict extrapolation based on multivariate environmental similarity surface indicate climate novelty, that is, climate conditions that differ from those used for model calibration. Notice that areas of strict extrapolation were fairly minimal and marginally overlapped with binary predictions (cut-off = 488.5) of suitable space in all climate scenarios (>2%), expect in RCP8.5 (28% overlaid). Oruanui eruption (~25.5 ka) at last glacial maximum after Wilson (2001). Map projection: NZGD2000.

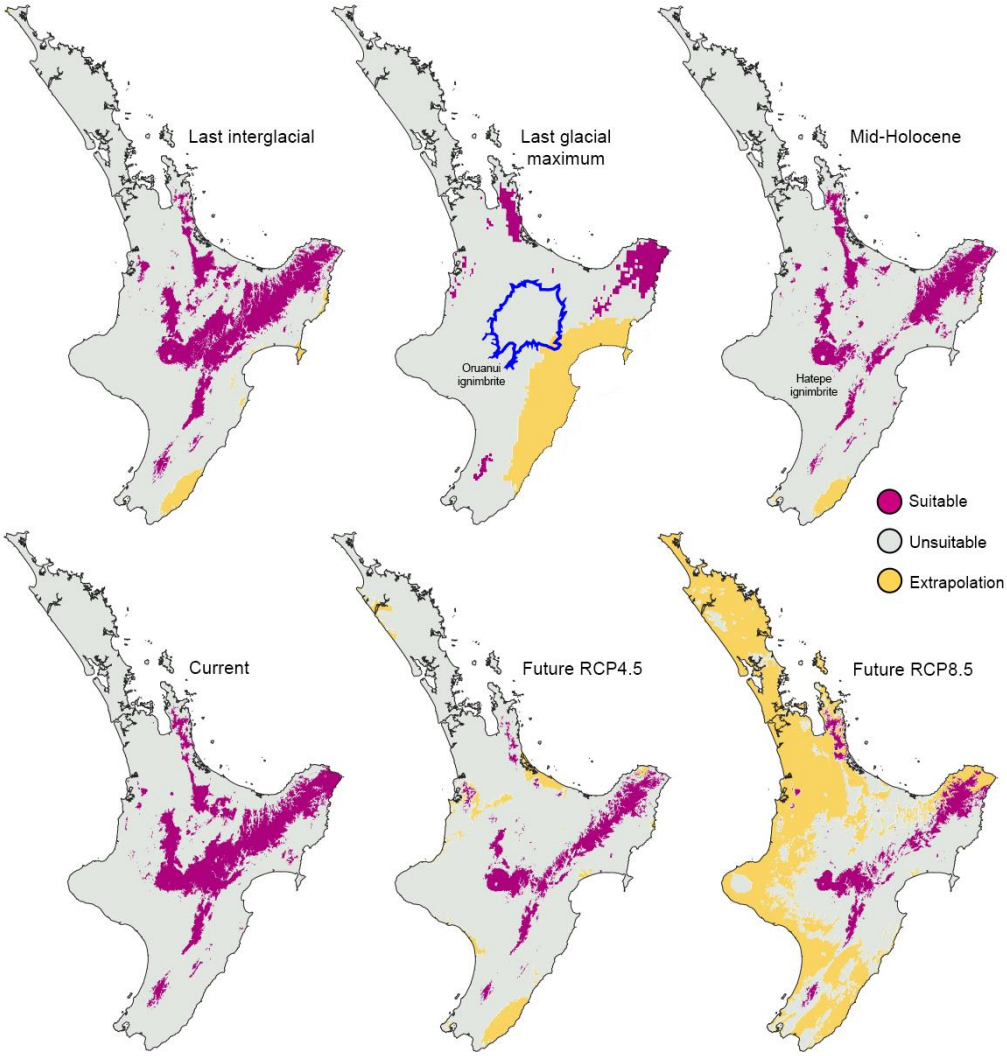

Appendix 4. Supplementary information about genotype-phenotype-environment associations.

Figure S4.1. Most relevant climatic factors contributing to body size differentiation among populations of *Sigaus piliferus* as inferred from the best-fitted multiple matrix regression with randomization model.

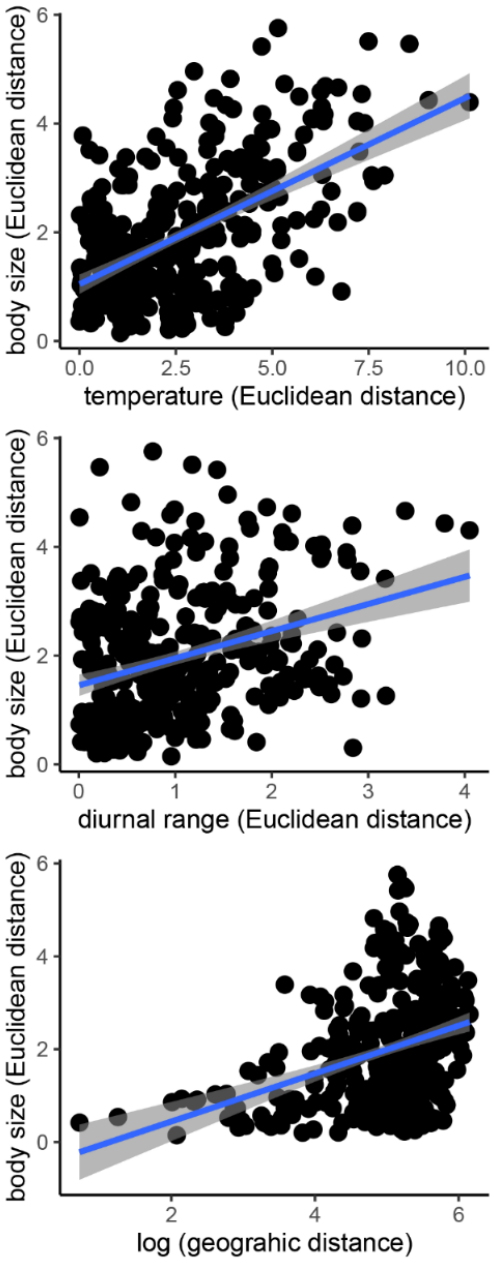

Supplementary references (not include in the main text)

Galbreath, K. E., Hafner, D. J., & Zamudio, K. R. (2009). When cold is better: Climate-driven elevation shifts yield complex patterns of diversification and demography in an alpine specialist (American pika, Ochotona princeps). *Evolution*, *63*(11), 2848–2863. https://doi.org/10.1111/j.1558-5646.2009.00803.x

Lanfear, R., Frandsen, P. B., Wright, A. M., Senfeld, T., & Calcott, B. (2017). Partitionfinder 2: New methods for selecting partitioned models of evolution for molecular and morphological phylogenetic analyses. *Molecular Biology and Evolution*, *34*(3), 772–773. https://doi.org/10.1093/molbe v/msw260

Stoffel, M. A., Nakagawa, S., & Schielzeth, H. (2017). rptR: Repeatability estimation and variance decomposition by generalized linear mixed-effects models. *Methods in Ecology and Evolution*, *8*(11), 1639–1644. https://doi.org/10.1111/2041-210X.12797

Rambaut, A., Drummond, A. J., Xie, D., Baele, G., & Suchard, M. A. (2018). Posterior summarisation in Bayesian phylogenetics using tracer 1.7. *Systematic Biology*, *67*(5), 901–904. https://doi.org/10.1093/sysbi o/syy032

Rogers, A. R., & Harpending, H. (1992). Population growth makes waves in the distribution of pairwise genetic differences. *Molecular Biology and Evolution*, *9*(3), 552–569. https://doi.org/10.1093/oxfor djournals.molbev.a040727

“In the lower classes of the animal kingdom, the greater size of the females seems generally to depend on their developing an enormous number of ova; and this may to a certain extent hold good with insects.”

(Darwin, 1874, p. 278)

Brachaspis nivalis, a scree-dwelling grasshopper within the New Zealand alpine radiation. Mating pair at Allan’s Basin, Craigieburn Forest Park, South Island.

Chapter Five

Climate correlates of body size and sexual dimorphism clines among mountaintop insect populations

MASSEY UNIVERSITY
TE KUNENGA KI PŪREHUROA
UNIVERSITY OF NEW ZEALAND

GRADUATE RESEARCH SCHOOL

STATEMENT OF CONTRIBUTION
DOCTORATE WITH PUBLICATIONS/MANUSCRIPTS

We, the student and the student's main supervisor, certify that all co-authors have consented to their work being included in the thesis and they have accepted the student's contribution as indicated below in the Statement of Originality.

Student name:	Fabio Leonardo Meza Joya
Name and title of main supervisor:	Steven A. Trewick
In which chapter is the manuscript/published work?	Chapter 5

Describe the contribution that the student and members of the supervisory team have made to the manuscript/published work:[1]

Conceptualization and data collection: Fabio Leonardo Meza-Joya, Steven A. Trewick and Mary Morgan-Richards; Data curation and analysis: Fabio Leonardo Meza-Joya; Visualization and writing – original draft: Fabio Leonardo Meza-Joya; Writing – review and editing: Steven A. Trewick and Mary Morgan-Richards; Funding acquisition: Fabio Leonardo Meza-Joya, Steven A. Trewick and Mary Morgan-Richards; Supervision: Steven A. Trewick and Mary Morgan-Richards.

Please select one of the following three options:

○	The manuscript/published work is published or in press Please provide the full reference of the research output:
○	The manuscript is currently under review for publication Please provide the name of the journal:
◉	It is intended that the manuscript will be published, but it has not yet been submitted to a journal

Student's signature:	Fabio Leonardo Meza Joya Digitally signed by Fabio Leonardo Meza Joya Date: 2024.01.02 15:02:00 +13'00'	Main supervisor's signature:	Digitally signed by Steve Trewick Date: 2024.01.09 10:38:07 +13'00'

This form should be placed at the beginning of each relevant thesis chapter.

[1] Refer to the Massey University Publishing and Authorship guidelines (OneMassey for staff, Stream for students) and/ or Contributor Roles Taxonomy (CRediT) guidelines for guidance.

Abstract

Aim: Ecological variation in local conditions is a major factor driving phenotypic evolution, yet the ultimate causes and proximate mechanisms underlying morphological disparities are poorly understood. Environmental clines serve as analogues for predicting species responses to the current climate warming. Here, we tested for biogeographic clines in body size and sexual size dimorphism in three alpine species with overlapping ranges and explored the climate correlates that best predict phenotypic variation.

Location: Te Waipounamu (South Island), Aotearoa (New Zealand).

Taxon: Endemic alpine adapted Catantopinae grasshoppers.

Methods: We surveyed mountaintop populations of three flightless, partially co-distributed and closely related alpine grasshopper species endemic to the Southern Alps of New Zealand. Distinct body size components from 881 adult grasshoppers were analysed: structural size, body mass, and body condition. We used Bayesian generalised linear models to test for biogeographic clines in body size and sexual size dimorphism, and to explore climate–size associations.

Results: Body size in three ecologically similar alpine grasshopper species show distinct geographic trends and climatic associations across the same region, yet relationships were species and trait dependant. We found latitudinal size trends consistent with Bergmann's rule, but non-linear clines or lack thereof were evident, particularly when examining elevational trends. Female grasshoppers exhibit the greatest proportional changes in size that led to contrasting patterns of size dimorphism. Temperature alone do not explain patterns of size variation in the studied grasshopper system.

Main conclusions: Widespread clinal variation in body size suggests the studied alpine grasshoppers can respond via morphological change to varied environmental conditions. Contrary to our expectation of conspecific clines, variation in size was species dependant, and the direction and magnitude of change varied with the examined metric. Distinct climatic factors influence body size trends of three co-distributed cold-adapted species. Examining alternative size components at once will be important to better understand ecogeographic patterns and make robust inferences of the general effects of climate change on body size.

Keywords: alpine species, Aotearoa New Zealand, climate change, convergent evolution, ecogeographical rules, climatic gradients.

Introduction

Biogeographic clines in morphology—whether across latitude or elevation—can illuminate the evolutionary forces driving organismal trait disparity and inform phenotypic adjustments to changing environmental conditions (De Frenne et al., 2013; Endler, 1977; Hodkinson, 2005; Keller et al., 2013). Climate varies across the landscape according to latitude and elevation, and such climate isoclines serve as analogues for studying species responses to climate warming effects (De Frenne et al., 2013; Hodkinson, 2005). Climate usually becomes colder as elevation and latitude increase, but the spatial rate of change is much higher when moving across elevation than latitude as hallmarked by rapid changes in temperature over shorter (~100 m) vertical distances relative to changes of the same approximate magnitude over much longer (~100 km) horizontal distances (De Frenne et al., 2013; Hodkinson, 2005; Jump et al., 2009). The gradual decrease in temperature with latitude accentuates differences between other climate-related covariates, particularly light availability and day length, which does not covary strongly with elevation (De Frenne et al., 2013; Hodkinson, 2005). Notably, the elevational gradient on mountains results in a decrease of partial pressure of atmospheric gases, including oxygen and carbon dioxide, while other factors such precipitation (as rain or snow), wind speed, and radiation input generally increase (Barry, 1992; Hodkinson, 2005; Jump et al., 2009; Keller et al., 2013). Thus, nearby sites on steep slopes may experience very different climate and atmospheric regimes.

Where latitude and elevation gradients intersect in the alpine zone of high-latitude mountains, manifold climate factors interact to create the environmental envelopes within which species persist (Koot et al., 2022). Many insect species are broadly distributed along biogeographic gradients, such that populations at their extremes experience dissimilar local conditions, mostly with respect to temperature, that can lead to phenotypic disparities (e.g. Bulgarella et al., 2015; Chapter 4; Yadav et al., 2020). There are several well-established ecogeographical rules describing convergent patterns of phenotypic variation with geography, and the widespread existence of these patterns by itself may reflect their capacity to adapt to fluctuating environmental conditions (Mayr, 1956; Millien et al., 2006). While commonly interpreted as adaptive, the mechanisms for such broad-scale trends remain largely speculative; despite this, these rules have gained renewed interest since the pace of the anthropogenic climate crisis

became apparent (e.g. Delhey et al., 2020; Gardner et al., 2011; Tian & Benton, 2020). Phenotypic differentiation among regional populations can result from either genetic adaptation, phenotypic plasticity or both (Keller et al. 2013; Minards et al., 2014). Moreover, it often is less clear whether observed patterns of variation reflect the influence of random forces such as genetic drift (Keller et al. 2013; Minards et al., 2014). Seeking parallel patterns of phenotypic evolution among co-distributed species provides a powerful means to infer adaptive processes of trait variation (Minards et al., 2014).

Organism body size is a master trait related to almost all biological processes, from individual performance to ecosystem function (Chown & Gaston, 2010; Ohlberger, 2013; Whitman, 2008). Geographic variation in size is the most pervasive, yet poorly-understood phenomenon in nature (Blackburn et al., 1999; Blanckenhorn & Demont, 2004; Stillwell et al., 2007). Of the many rules purported to describe widespread clinal patterns in size across taxa, Bergmann's rule (Bergmann, 1847) has continuously generated interest among evolutionary ecologists. Originally formulated for homeothermic vertebrates, it describes a trend where larger species (or individuals) occur at higher, colder latitudes and elevations, owing to the relative thermal efficiency of a lower surface-to-volume ratio (Bergmann, 1847; James, 1970; Mayr, 1956). While this mechanism does not apply to ectotherms (Atkinson, 1994, Blackburn et al., 1999), parallels have been observed in Orthoptera and other insects, but in this case the counter-gradient seems to be the rule rather than the exception (Bidau et al., 2016; Shelomi, 2012; Mousseau, 1997; Whitman, 2008). The existence of opposing insect size clines indicates that the mechanisms underlying size variation differ across species and likely populations (Yadav et al., 2020), probably reflecting the influence of environmental factors, such as temperature affecting growth and developmental rates, which ultimately determine insect body size (Atkinson, 1994; Chown & Gaston, 2010; Whitman, 2008).

Sex-related differences in adult body size, termed sexual size dimorphism (SSD), are also thought to vary in a predictable manner with overall size within lineages following Rensch's rule, that is, SSD decreases with size (hypoallometry) when females are the larger sex, but increases with size (hyperallometry) when males are larger (Abouheif & Fairbairn, 1997; Fairbairn, 1997; Rensch, 1960). While the mechanisms creating this pattern remain obscure, SSD trends consistent with Rensch's rule are common in taxa with larger males (Abouheif & Fairbairn, 1997; Fairbairn, 1997), but seldom seen in taxa

where females are larger, such as Orthoptera and other insects (Blanckenhorn et al., 2007; Hochkirch & Gröning, 2008; Teder & Tammaru, 2005). The evolution of larger female insects is traditionally attributed to strong maternal size–fecundity effects (Blanckenhorn et al., 2007; Fairbairn, 1997; Stillwell et al., 2010), and this might explain the converse Rensch's pattern often found in this group (Fairbairn, 1997). Variation in insect SSD also includes differences among populations, as observed across latitudinal gradients (Blanckenhorn et al., 2006; Horne et al., 2019; Rohner et al., 2018; Stillwell et al., 2007). Although the drivers of these clines are not clear, a substantial amount of this variability is likely due to sex differences in growth and/or development (Blanckenhorn et al., 2007; Stillwell et al., 2010; Rohner et al., 2018; Teder & Tammaru, 2005), which are strongly dependent on environmental factors such nutrition and temperature (Atkinson, 1994; Davidowitz et al., 2004; Stillwell et al., 2010).

A remarkable aspect of the alpine environment of New Zealand—Aotearoa—is the high diversity and endemism of brachypterous and flightless insect communities (Buckley et al., 2022; Nakano et al., 2023). Such alpine insects are of particular interest for exploring patterns and climate drivers of morphological disparity, as they might rely on phenotypic responses to cope with ongoing environmental change due to dispersal restrictions to track suitable conditions (see Chevin & Hoffmann, 2017). This is the situation of the flightless alpine grasshopper species product of an endemic radiation associated primarily with the Southern Alps—Kā Tiritiri o Te Moana—of New Zealand (Koot et al. 2020). These grasshoppers exhibit high, spatially structured genetic diversity (at least at mitochondrial level), with little or no sharing of haplotypes among mountain populations, indicative of long-term extrinsic barriers (Carmelet-Rescan et al., 2021; Meza-Joya et al., 2023). The latitudinal gradient of the Southern Alps is expected to result in cooler conditions to the south compared to the north, and this correlates with the elevation of montane alpine habitats that tends to be higher in the north and lower in the south of the island (Wardle, 2008). This is particularly relevant for widespread alpine insects as associations between body size and climate may depend on geography (e.g. Dillon et al., 2006; Chapter 4; Yadav et al., 2020).

Here we explore patterns of geographic variation in adult body size in three widespread flightless, co-distributed, and closely-related alpine grasshopper species (Acrididae) endemic to the Southern Alps of New Zealand: *Brachaspis nivalis* (Hutton), *Paprides*

nitidus (Hutton), and *Sigaus australis* (Hutton). We assessed whether Bergmann clines occur across latitude and elevation at intraspecific level. Environmental gradients provide powerful settings to infer ecological and evolutionary processes driving phenotypic changes (Endler 1977). Unlike latitudinal gradients, which comprise gradual variation in temperature and other climate-related covariates (e.g. light availability and day length), elevational gradients incorporate strong clinal variation in temperature and oxygen availability (De Frenne et al., 2013; Hodkinson, 2005). Despite steep clines, the studied alpine grasshoppers are connected by gene flow along elevation, while populations on separate mountain ranges along latitude are genetically isolated (Meza-Joya et al., 2023; Trewick et al., 2000). Thus, one might expect contrasting patterns, and most notably drivers, of phenotypic differentiation along these gradients. By contrasting size variation in three related species across genetically-connected (elevation) and disrupted gradients (latitude) it might be possible to infer the influence of gene flow creating or constraining patterns of phenotype variation (Lenormand, 2002). Although these species tend to occupy slightly different climate envelopes (Meza-Joya et al., 2023) and show some degree of micro-habitat partitioning (Bigelow, 1967; Nakano et al., 2023; White, 1974), they experience similar climates along their co-distributed ranges. If body size is primarily driven by common direct climatic effects acting at regional scales, we expect parallel climatic clines (see Endler, 1977). The marked female-biased size dimorphism of these grasshoppers (Bigelow, 1967) suggests the largest sex might exhibit the greatest proportional changes in body size across biogeographic and climate gradients—opposite to Rensch's rule—creating clinal variation in size dimorphism (Blanckenhorn et al. 2006; Horne et al., 2019; Stillwell et al., 2007).

Materials and Methods

Study site and grasshopper collections

We surveyed alpine populations of *B. nivalis*, *P. nitidus* and *S. australis* on six mountains on the Southern Alps, New Zealand (Figure 1): Mt McRae, Mt Temple, Hamilton Peak, Mt Hutt, Fox Peak, and Mt Cardrona. These mountains embrace latitudinal and elevational gradients encompassing most of these species' ranges, thus capturing distinct climatic and ecological features of their environmental envelopes. Sampling took place

along transects divided into 100–200m elevation intervals (hereafter, sampling sites) that ranged in length between 411 and 761 m depending on terrain steepness and accessibility. Adult grasshoppers were collected by hand during summer when they are active (late January to early March 2015–2023) from 33 sampling sites as follows: five at Fox Peak, Hamilton Peak, Mt Hutt, and Mt Temple; six at Mt McRae; seven at Mt Cardrona (Figure 1; Table S1). Species name, sex, and maturity were identified using morphological traits following Bigelow (1967).

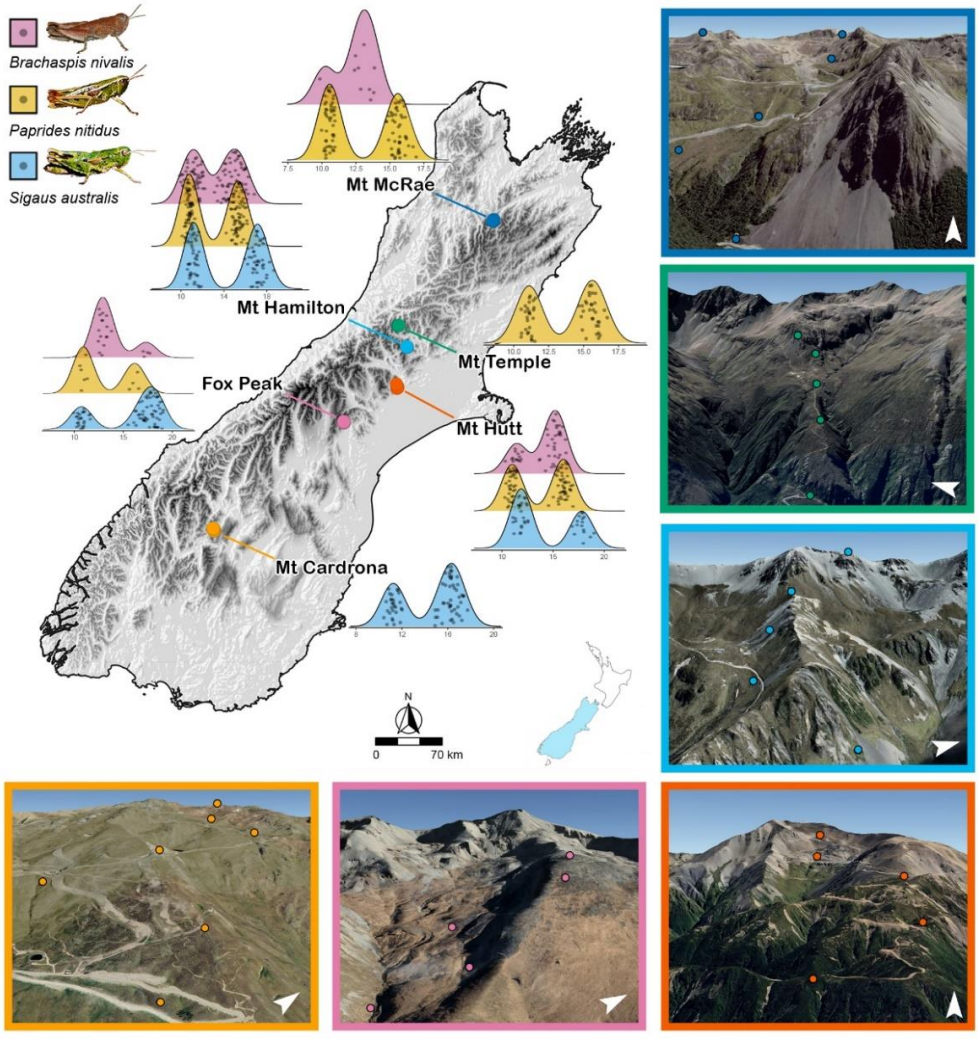

Figure 1. Map of South Island, New Zealand depicting sampling sites on six mountains for *Brachaspis nivalis*, *Paprides nitidus* and *Sigaus australis*. Density plots illustrating body size variation across mountain populations using femur length (mm) as a proxy of overall size (Meza-Joya et al., 2022). Note these species exhibit female-biased size dimorphism (females larger than males). Insets show three-dimensional projections for each sampled mountains with dots showing sampling sites and arrow heads pointing north (https://www.google.com). Map projection: NZGD2000.

Body size and body condition data

Body size, separable into structural (i.e. linear body dimensions) and mass components, was examined to investigate biogeographic size clines across these grasshoppers' latitudinal and elevational ranges. While structural size and mass are closely related in these species (Meza-Joya et al., 2022), each may be affected differently by environmental factors (Bailey et al., 2020; Canale et al., 2016). Insect adult structural size is a largely static trait controlled during development by gene-environment interactions, whereas body mass is a dynamic trait determined by a combination of structural size and body condition, which is itself determined by reproductive phase and resources availability (Cardilini et al., 2016; Chown & Gaston, 2010; Meza-Joya et al., 2022; Whitman, 2008).

We explore three non-independent linear dimensions as surrogates of structural size (Figure S1): left hind femur length (FL), maximum left femur width (FW) and mid-line pronotum length (PL). Unlike body length, these metrics are not arbitrary affected by preservation and are informative for examining phenotypic variation in New Zealand grasshoppers (e.g. Bigelow, 1967; Dowle et al., 2014; Meza-Joya et al., 2022; Chapter 4). Measurements were taken from 881 adult grasshoppers (*B. nivalis* = 113♀, 92♂; *P. nitidus* = 200♀, 194♂; *S. australis* = 163♀, 119♂; Table S1) using an Olympus SZX7 stereomicroscope with Olympus SC100 image capture and Olympus cellSens Dimension v1.6 software (Olympus Corporation, Japan). For all species, femur length was closely correlated with other size components in our datasets, including body mass (Pearson's $R \geq 0.960$, $P < 0.001$; Figure S2). Moreover, this metric is considered the best single linear predictor of overall body size in the studied grasshopper species (Meza-Joya et al., 2022), hence, we selected this metric as a general index of structural size in downstream analyses. Repeatability analyses showed that our morphometric dataset is highly reproducible with a technical measurement error biologically negligible (Figure S3).

Body mass was examined by measuring fresh mass (FM) from field-collected specimens (± 0.001 mg) using a Sartorius Quintix35-1S digital scale (Sartorius Lab Instruments GmbH & Co, Germany). For grasshoppers collected before 2020—which lack fresh mass estimates—we measured ethanol-preserved mass (PM), which was then converted to fresh mass using species-specific mass-to-mass regression equations from Meza-Joya et al. (2022). This approach has proved high accuracy (prediction errors < 0.011 g) for predicting fresh mass in all three grasshopper species studied here (Meza-Joya et al.,

2022). As body mass estimates in the studied grasshopper species carry substantial unexplained variance related to inter-individual differences in body condition (Meza-Joya et al., 2022), we used the 'scaled mass index' ($\hat{M}_i$) proposed by Peig & Green (2009) as a proxy of individual body condition (i.e. body mass corrected for structural size): $\hat{M}_i = M_i [L_0/L_i] \wedge b_{SMA}$, where M_i and L_i are the FM and FL of individual i respectively; b_{SMA} is the scaling exponent estimated by the standardized major axis (SMA) regression of M on L; and L_0 is the mean FL value for the study population. Here we used FL as structural proxy as this metric is expected to best explain the fraction of mass associated with structural size (see Meza-Joya et al., 2022). Figure S4 summarises distribution plots illustrating variation in size components across populations of our focal species.

Environmental parameters

Mountaintop insects face relatively brief periods of favourable climate conditions due to seasonality effects on mountain environments, hence, one may expect that body size would respond to climate seasonality, isothermality, and limiting factors such as temperature and precipitation extremes (e.g. Baroni & Masoero, 2018; Beck et al., 2016; Beerli et al., 2019). Conditions encountered during the growing season are also influential for growth and size of diapausing organisms (Beck et al., 2016; Beerli et al., 2019), and this may be the case for the alpine grasshoppers studied here as their phenology and growth is likely influenced by temperature and precipitation regimens during growing in summer and snow-lie duration during diapause in winter (White & Sedcole, 1991). Here we explored 18 variables measuring distinct aspects of the above-mentioned factors as potential predictors of body size variation in our focal species (Table S1). Climate layers (spanning 1981–2010) were obtained from the climatologies at high resolution for the Earth's and land surface areas (CHELSA) database v2.1 (Karger et al., 2017, 2021) at 30 arc-sec resolution (~1 km^2). While the time period of this dataset (1981–2010) does not perfectly fit our grasshopper collections (2015–2023), these variables are expected to better capture the relative magnitude of current climate trends than alternative datasets based on older climate series (e.g. McCarthy et al., 2021). Closely correlated predictors were removed from further analysis to ensure the variables retained for modelling did not show multicollinearity (see Table S3). Figure S5 summarises the association of the six selected environmental variables with latitude and elevation.

Statistical analyses

Following Bergmann's rule—larger individuals at colder, higher latitudes and elevations—we first tested for body size clines across both gradients using Bayesian generalised linear mixed models (B-GLMMs). This approach was favoured given convergence issues with the likelihood maximisation algorithm, which likely relate to our modest sample sizes and unbalanced sampling among mountains, sites and years (see Bolker et al., 2009). Because the hypotheses being tested concerns body size variation within species, individual size was used as the unit of analysis. For this, we used three distinct size metrics as response variables: (i) femur length (FL), (ii) fresh mass (FM), and (iii) body condition ($\hat{M}i$). Models included latitude (absolute), elevation, sex as fixed effects; and sex as an interaction term with latitude and elevation to infer geographic variation in SSD (latitude × sex + elevation × sex). Radom effects (i.e. grouping factors) accounting for non-independence of specimens from the same mountain population (1|population), sampling site (1|site), and collection year (1|year) were included. Preliminary plots suggested instances of non-linear links between size traits and latitude, so competing models with both linear and quadratic terms for this covariate were fitted. Model selection used the Watanabe-Akaike information criterion (WAIC) and pseudo-BMA weighting with Bayesian bootstrap with the R packages 'performance' 0.10.4 (Lüdecke et al., 2021) and 'loo' 2.0.0 (Vehtari et al., 2020): lower WAIC values, and higher pseudo-BMA weights indicate better model fit (Table S4).

We then examined how body size variation (i.e. FL, FM, and $\hat{M}_i$) relates to spatial climate variation using six independent, not strongly correlated predictors (see Table S3). We examined the importance of each variable using a projection predictive variable selection approach with the R package 'projpred' 2.6.0 (Piironen et al., 2023), as this method provides an excellent trade-off between model complexity and accuracy. For this, we first fitted separate reference models for each species and size proxy including all relevant predictors plus sex, and then sought for the model with the smallest number of predictors that best explain size variation in our datasets. Reference models only included additive main effects without sex interactions, as their inclusion would have increased model complexity beyond the limits of our datasets. To get a useful predictor ranking, we manually delayed the random terms to the last position during the selection process. Reference models used weakly informative regularized horseshoe priors as we expect

some of the predictors might be irrelevant (Piironen et al., 2023), and weakly informative priors for the other parameters. The resulting informative predictors (Figure S6) were used to fit species-specific B-GLMMs, this time including sex as an interaction term with each predictor (see Table S4 for details on model syntaxis). Inspection of preliminary plots suggested linear responses, thus quadratic terms were not considered.

All B-GLMMs were fitted using the R packages 'rstanarm' 2.21.3 (Goodrich et al., 2020) and unless otherwise indicated, models used gaussian distribution with identity link and default weakly informative priors centred on zero and 2.5 standard deviations. Continuous predictors were standardised by centring and dividing by two standard deviations to improve model performance and interpretability (Gelman, 2008). Models used four chains of 50^3 iterations, discarding the first half as burn-in and saving every 10th sample, and adapt deltas of 0.999. Model convergence was checked by examining trace plots of posterior samples and making sure that Rhat ($\hat{R}$) values for each parameter were close to 1.0 (Gelman & Rubin, 1992). Model fit was assessed by examining graphical posterior predictive checks and model assumptions were checked by inspecting regression diagnostic plots obtained with the R package 'performance'. Bayesian R^2 conditional (R^2_c) and marginal (R^2_m) were estimated using the R package 'bayestestR' 0.12.1 (Makowski et al., 2019) to infer the percentage of variance explained by the model and fixed effects, respectively (Nakagawa & Schielzeth, 2013). We reported the posterior medians, a point effect estimate, and the 95% Bayesian high density intervals (HDI), a metric of uncertainty, for all parameters in the models. We also reported the probability of direction (pd), an index of effect existence, and the full region of practical equivalence (ROPE), and index of effect significance (Makowski et al., 2019). Here pd > 99% were inferred as indicative of the existence of an effect and parameter estimates were considered "significant" if both the 95% HDI did not overlap zero and ROPE < 1%. Model results were visualised using the R package 'interactions' 1.1.5 (Long, 2022).

Results

All models ran smoothly with no post-sampling warnings, and diagnostic statistics shown convergence for all parameters (Table S5). Model assumptions were consistently met, and only subtle and harmless deviations from homoscedasticity were detected (see Knief & Forstmeier, 2021). Posterior-projection predictive checks showed that all models were able to fairly generate similar predictions to that from the observed response values.

Conditional R^2 scores ranged from 0.582 to 0.978 (mean = 0.869 ± 0.117 SD), indicating that in most cases a reasonable amount of the variance in our datasets is explained by the models. As expected, sex had a strong effect on FL and FM across all fitted models (Table 1 and 2), but no effect was detected on M̂i (i.e. FM corrected by FL).

The three grasshopper species considered here varied considerably in body size across latitude, yet relationships were species and trait dependant (Figure 2 and S7; Table 1). The fixed effects in our models explained the majority of variance in FL (> 74.2%) and FM (> 64.8%), but only a residual amount (< 13.5%) in M̂i (Table 1). Estimates (median [95% HDI]) from the best-fitted models for *B. nivalis* revealed that body size significantly increases with latitude according to Bergmann's rule (ROPE < 1%), regardless the size trait examined (FL = 3.03 [1.33, 4.68]; FM = 1.42 [0.57, 2.20]; M̂i = 0.08 [0.02, 0.15]). Yet the low explanatory power of the fixed factors in the latter model (R^2_m = 0.135) indicates biological irrelevance. Significant linear interactions with sex were also found for FL (−0.92 [−1.60, −0.29]), while both interactions (linear/quadratic) were significant in FM (−0.80 [−1.14, −0.47]/−0.34 [−0.67, −0.03]). These interaction revealed that females exhibit slightly steeper latitudinal clines than males, hence, SSD increases accordingly with latitude in both traits (Figure 2a–b). In contrast, we found no main effects of latitude on *P. nitidus*, yet significant but very weak quadratic latitude × sex interactions were detected for FL (−4.54 [−6.01, −3.02]) and FM (−0.41 [−0.67, −0.16]). This interactions indicate that males and females follow opposite (quadratic) trajectories in these traits, resulting in size divergence and increased SSD towards southern latitudes, particularly for FL (Figure 2c–d). Likewise, we found no evidence of main effects of latitude on *S. australis*, but again there were significant interactions (linear/quadratic) with sex for FL (5.85 [3.70, 8.13]/9.76 [7.38, 12.09]) and FM (1.47 [1.09, 1.88]/0.85 [0.42, 1.25]), showing that these traits increase quadratically with latitude only in females, thus SSD increase at mid-latitudes in both cases (Figure 2e–f). We found no evidence for relationships between body size and elevation across species and size proxies, either as a main effect or in interaction with sex (Table 1; Figure S7).

Table 1. Relationships between latitude and elevation and body size for three alpine grasshopper species (*Brachaspis nivalis*, *Paprides nitidus* and *Sigaus australis*) endemic to South Island, New Zealand. Median ± AD (median absolute deviation), CI = credible interval, Pd = probability of direction, ROPE = full region of practical equivalence. Significant parameters are in bold. Estimates for other parameters are in Table S6.

Parameter	Femur length				Fresh mass				Body condition			
	Median ± AD	**CI (95%)**	**Pd**	**ROPE**	**Median ± AD**	**CI (95%)**	**Pd**	**ROPE**	**Median ± AD**	**CI (95%)**	**Pd**	**ROPE**
(a) *Brachaspis nivalis*												
latitude	**3.03 ± 0.70**	**1.33, 4.68**	**99.63**	**0.29**	**1.42 ± 0.29**	**0.57, 2.20**	**99.37**	**0.06**	**0.08 ± 0.02**	**0.02, 0.15**	**99.04**	**0.58**
latitude^2	N/A	N/A	N/A	N/A	0.66 ± 0.45	-0.57, 1.86	90.49	1.91	N/A	N/A	N/A	N/A
elevation	0.49 ± 0.31	-0.14, 1.17	94.26	15.46	0.05 ± 0.03	-0.02, 0.11	93.76	16.04	-0.01 ± 0.01	-0.03, 0.01	92.11	19.88
sex	**-3.69 ± 0.10**	**-3.87, -3.50**	**100**	**0.00**	**-0.35 ± 0.01**	**-0.37, -0.32**	**100**	**0.00**	0.01 ± 0.01	-0.01, 0.02	78.90	53.01
latitude × sex	**-0.92 ± 0.33**	**-1.60, -0.29**	**99.65**	**0.96**	**-0.80 ± 0.17**	**-1.14, -0.47**	**100**	**0.00**	0.03 ± 0.02	-0.02, 0.08	89.98	9.12
latitude^2 × sex	N/A	N/A	N/A	N/A	**-0.34 ± 0.16**	**-0.67, -0.03**	**99.21**	**0.95**	N/A	N/A	N/A	N/A
elevation × sex	-0.19 ± 0.19	-0.55, 0.17	84.59	50.12	-0.02 ± 0.02	-0.07, 0.02	84.06	40.15	0.01 ± 0.01	-0.01, 0.04	84.81	23.05
R^2 conditional/marginal	0.936/0.742				0.906/0.677				0.765/0.135			
(b) *Paprides nitidus*												
latitude	1.96 ± 1. 86	-3.57, 8.14	83.29	4.67	0.13 ± 0.25	-0.65, 0.84	69.18	6.02	-0.03 ± 0.05	-0.15, 0.07	76.00	6.86
latitude^2	3.63 ± 1.56	-0.36, 7.83	95.82	1.18	0.23 ± 0.22	-0.38, 0.78	83.76	3.99	N/A	N/A	N/A	N/A
elevation	0.04 ± 0.09	-0.13, 0.22	68.38	98.71	0.01 ± 0.02	-0.02, 0.04	64.37	82.48	0.01 ± 0.01	-0.01, 0.02	67.47	40.55
sex	**-4.78 ± 0.04**	**-4.86, -4.70**	**100**	**0.00**	**-0.43 ± 0.01**	**-0.45, -0.42**	**100**	**0.00**	0.00 ± 0.01	-0.01, 0.01	76.49	54.56
latitude × sex	1.12 ± 0.78	-0.39, 2.64	92.80	8.64	-0.22 ± 0.13	-0.47, 0.05	94.89	3.45	0.01 ± 0.01	-0.02, 0.02	50.19	38.01
latitude^2 × sex	**-4.54 ± 0.76**	**-6.01, -3.02**	**100**	**0.00**	**-0.41 ± 0.13**	**-0.67, -0.16**	**99.94**	**0.11**	N/A	N/A	N/A	N/A
elevation × sex	0.07 ± 0.08	-0.10, 0.24	78.59	97.80	0.01 ± 0.01	-0.03, 0.03	51.52	87.56	-0.02 ± 0.01	-0.04, 0.00	95.45	11.10
R^2 conditional/marginal	0.978/0.957				0.928/0.834				0.754/0.028			
(c) *Sigaus australis*												
latitude	-6.25 ± 5.02	-21.40, 7.80	87.74	1.65	-1.69 ± 1.37	-5.18, 2.03	87.60	1.06	-0.07 ± 0.07	-0.24, 0.10	83.84	5.27
latitude^2	-9.21 ± 5.17	-25.43, 4.06	95.12	1.12	-1.20 ± 1.54	-6.07, 2.13	82.02	1.39	N/A	N/A	N/A	N/A
elevation	0.45 ± 0.15	-0.15, 0.75	99.65	16.79	0.05 ± 0.02	0.00, 0.10	98.78	17.35	0.01 ± 0.01	-0.01, 0.04	85.01	26.76
sex	**-5.99 ± 0.07**	**-6.13, -5.85**	**100**	**0.00**	**-0.63 ± 0.01**	**-0.65, -0.60**	**100**	**0.00**	-0.01 ± 0.01	-0.02, 0.01	76.07	51.69
latitude × sex	**5.85 ± 1.12**	**3.70, 8.13**	**100**	**0.00**	**1.47 ± 0.20**	**1.09, 1.88**	**100**	**0.00**	0.01 ± 0.01	-0.02, 0.04	81.02	29.25
latitude^2 × sex	**9.76 ± 1.22**	**7.38, 12.09**	**100**	**0.00**	**0.85 ± 0.22**	**0.42, 1.25**	**100**	**0.00**	N/A	N/A	N/A	N/A
elevation × sex	-0.55 ± 0.14	-0.93, -0.18	98.97	4.09	-0.01 ± 0.02	-0.06, 0.04	69.29	76.79	0.02 ± 0.01	-0.01, 0.05	90.50	20.77
R^2 conditional/marginal	0.971/0.894				0.941/0.648				0.728/0.087			

Table 2. Relationships between climate and body size of three alpine grasshopper species (*Brachaspis nivalis*, *Paprides nitidus* and *Sigaus australis*) endemic to South Island, New Zealand. Median ± AD (median absolute deviation), CI = credible interval, Pd = probability of direction, ROPE = full region of practical equivalence. Significant parameters are in bold. Abbreviations: isothermality (isotherm), temperature seasonality (temp season), mean air temperature of the driest quarter (temp driest qtr), precipitation seasonality (prec season). Estimates for other parameters are in Table S7.

Parameter	Femur length				Fresh mass				Body condition			
	Median ± AD	**CI (95%)**	**Pd**	**ROPE**	**Median ± AD**	**CI (95%)**	**Pd**	**ROPE**	**Median ± AD**	**CI (95%)**	**Pd**	**ROPE**
(a) *Brachaspis nivalis*												
temp driest qtr	**-2.23 ± 0.76**	**-3.77, -0.69**	**99.71**	**0.59**	**-0.24 ± 0.08**	**-0.41, -0.08**	**99.66**	**0.34**	N/A	N/A	N/A	N/A
isotherm	-1.45 ± 1.00	-3.95, 0.60	92.70	4.75	-0.18 ± 0.11	-0.44, 0.05	94.56	3.48	N/A	N/A	N/A	N/A
prec season	N/A	N/A	N/A	N/A	N/A	N/A	N/A	N/A	**-0.10 ± 0.03**	**-0.16, -0.01**	**99.17**	**0.70**
temp season	N/A	N/A	N/A	N/A	N/A	N/A	N/A	N/A	0.02 ± 0.02	-0.03, 0.07	83.56	12.78
sex	**-3.75 ± 0.09**	**-3.92, -3.57**	**100**	**0.00**	**-0.36 ± 0.01**	**-0.38, -0.34**	**100**	**0.00**	0.00 ± 0.01	-0.01, 0.02	71.30	58.40
temp driest qtr × sex	**0.84 ± 0.31**	**0.24, 1.45**	**99.63**	**0.97**	**0.20 ± 0.04**	**0.13, 0.28**	**100**	**0.00**	N/A	N/A	N/A	N/A
isotherm × sex	0.24 ± 0.19	-0.14, 0.61	90.07	39.95	0.03 ± 0.02	-0.01, 0.08	90.98	29.16	N/A	N/A	N/A	N/A
prec season × sex	N/A	N/A	N/A	N/A	N/A	N/A	N/A	N/A	**-0.04 ± 0.01**	**-0.06, -0.01**	**99.55**	**0.97**
temp season × sex	N/A	N/A	N/A	N/A	N/A	N/A	N/A	N/A	-0.03 ± 0.02	-0.07, 0.00	97.01	5.14
R^2 conditional/marginal	0.940/0.627				0.919/0.583				0.811/0.249			
(b) *Paprides nitidus*												
prec season	-0.44 ± 0.16	-0.81, 0.02	97.22	12.53	-0.04 ± 0.02	-0.08. 0.01	95.29	23.76	N/A	N/A	N/A	N/A
temp season	N/A	N/A	N/A	N/A	N/A	N/A	N/A	N/A	**-0.05 ± 0.01**	**-0.08, -0.02**	**99.69**	**0.38**
temp driest qtr	N/A	N/A	N/A	N/A	N/A	N/A	N/A	N/A	0.03 ± 0.02	-0.01, 0.06	93.93	5.86
sex	**-4.82 ± 0.04**	**-4.90, -4.74**	**100**	**0.00**	**-0.44 ± 0.01**	**-0.45, -0.43**	**100**	**0.00**	0.00 ± 0.01	-0.01, 0.01	53.81	58.21
prec season × sex	**0.31 ± 0.08**	**0.16, 0.47**	**100**	**0.98**	**0.06 ± 0.01**	**0.03, 0.08**	**100**	**0.58**	N/A	N/A	N/A	N/A
temp season × sex	N/A	N/A	N/A	N/A	N/A	N/A	N/A	N/A	0.01 ± 0.01	-0.02, 0.03	69.00	25.43
temp driest qtr × sex	N/A	N/A	N/A	N/A	N/A	N/A	N/A	N/A	0.03 ± 0.02	0.00, 0.07	95.77	4.54
R^2 conditional/marginal	0.977/0.961				0.928/0.855				0.582/0.084			
(c) *Sigaus australis*												
isotherm	**1.16 ± 0.18**	**0.78, 1.51**	**100**	**0.04**	**0.21 ± 0.03**	**0.15, 0.28**	**100**	**0.00**	0.05 ± 0.05	-0.05, 0.14	83.64	7.93
temp wettest qtr	N/A	N/A	N/A	N/A	N/A	N/A	N/A	N/A	0.02 ± 0.04	-0.05, 0.10	74.40	14.73
sex	**-6.18 ± 0.08**	**-6.34, -6.02**	**100**	**0.00**	**-0.68 ± 0.01**	**-0.70, -0.65**	**100**	**0.00**	-0.01 ± 0.01	-0.02, 0.01	82.76	48.81
isotherm × sex	**-0.81 ± 0.16**	**-0.12, -0.50**	**100**	**0.09**	**-0.23 ± 0.02**	**-0.27, -0.18**	**100**	**0.00**	-0.03 ± 0.02	-0.07, 0.00	95.43	8.68
temp wettest qtr × sex	N/A	N/A	N/A	N/A	N/A	N/A	N/A	N/A	-0.05 ± 0.02	-0.09, -0.01	98.87	2.77
R^2 conditional/marginal	0.961/0.943				0.927/0.821				0.691/0.033			

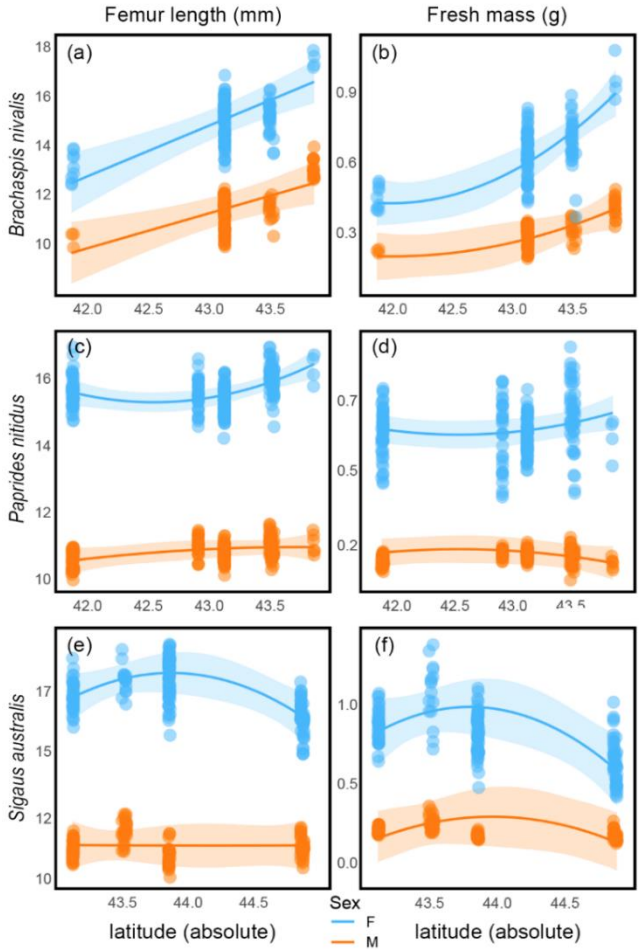

Figure 2. Significant latitudinal trends in three alpine grasshoppers (*Brachaspis nivalis*, *Paprides nitidus* and *Sigaus australis*) endemic to South Island (New Zealand). Note that females exhibit the greatest proportional changes in body size, resulting in latitudinal variation in size dimorphism. Shading represents uncertainty (95% high density intervals).

Predictors capturing seasonal shifts in temperature and precipitation were ranked highest and selected as informative most often (Table S3). The most important predictors varied among species and size proxies (Figure S6), yet the same set of variables was always retained as informative for both FL and FM. The fixed effects in these models explained most of variance in FL (> 62.7%) and FM (> 58.3%), but only a residual amount of variance (< 24.9%) in M̂i (Figure 3 and S8; Table 2). We found significant negative relationships between temperature of the driest quarter and both FL and FM in *B. nivalis*, both as a main effect (FL = −2.23 [−3.77, −0.69], FM = −0.24 [−0.41, −0.08]) or in interaction with sex (FL = 0.84 [0.24, 1.45], 0.20 [0.13, 0.28]), showing that females exhibit steeper slopes in both traits, particularly for FM (Figure 3a–b). A significant link between M̂i and precipitation seasonality was also found (−0.10 [−0.16, −0.01]) but with

a low coefficient (R^2_m = 0.349). While precipitation seasonality was retained as the most informative predictor for *P. nitidus* FL and FM, we only detected significant but weak interactions with sex in both cases (FL = 0.31 [0.16, 0.47], FM = 0.06 [0.03, 0.08]), but these trends likely have little biological significance (Figure 3c–d). We also found a main effect of temperature seasonality on M̂i (−0.05 [−0.08, −0.02]), but the low explanatory power of the fixed factors in the latter model (R^2_m = 0.084) indicates biological irrelevance. We found significant positive links between isothermality and both FL and FM in *S. australis*, both as a main effect (FL = 1.16 [0.78, 1.51], FM = 0.21 [0.15, 0.28]) and in interaction with sex (FL = −0.81 [−0.12, −0.50], −0.23 [−0.27, −0.18]), indicating that females exhibit steeper slopes in both traits, especially for FM (Figure 3e–f).

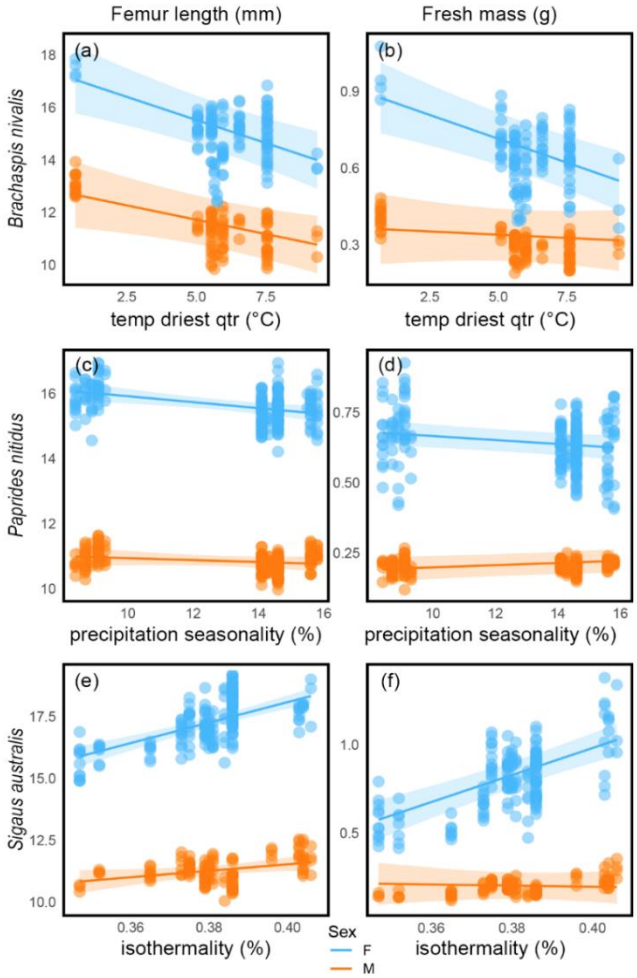

Figure 3. Relationships showing significant effects of environmental factors on female and male body size in three alpine grasshoppers (*Brachaspis nivalis*, *Paprides nitidus* and *Sigaus australis*) endemic to South Island (New Zealand). Shading represents uncertainty (95% high density intervals). Abbreviations: temperature of the driest quarter (temp driest qtr).

Discussion

Understanding how phenotype changes across biogeographic gradients is germane for making general inferences about the potential effects of climate change on biota (Delhey et al., 2020; Gardner et al., 2011; Tian & Benton, 2020). Here we sampled mountaintop populations of three flightless and partially co-distributed alpine grasshopper species endemic to the Southern Alps of New Zealand to investigate geographic clines in adult body size and sexual size dimorphism (SSD). We have assessed the influence of climate on differentiation of distinct size components: structural size (FL), body mass (FM) and body condition ($\hat{M}i$). We found sex differences accounted for most variance in structural size and body mass, as expected from a system with strong female-biased SSD (Bigelow, 1967), but not in body condition (i.e. FM corrected by FL). This indicates that variation in body mass in these grasshoppers is mostly dependent on sexual differences in femur length, and thus overall body size, as more mass without the respective increase in leg would be disadvantageous, particularly for flightless grasshoppers that rely on jumping for locomotion and predator avoidance (Meza-Joya et al., 2022).

As expected, body size did not vary consistently with elevation for any of the three alpine grasshopper species examined (Horne et al., 2018; Minards et al., 2014). The lack of size variation despite sampling twelve transects of between 383 and 761 m elevation is an important observation. In contrast, conspecific clines in size were detected over the latitudinal range for all three species but were species specific, with the direction and magnitude of change dependent on metric (e.g. Bidau et al., 2016; Ciplak et al., 2008). Consistent with Bergmann's rule, body size in *B. nivalis* increased with latitude regardless of sex or size proxy examined. In contrast, non-linear clines or lack thereof were evident in the other studied species (*P. nitidus* and *S. australis*). While the lack of elevation–size clines suggest no temperature effects, our climate models indicate otherwise, suggesting confounding factors disguise any effect of temperature on body size along this gradient (Horne et al., 2018). As individual movement in the flightless, alpine grasshoppers studied here is more likely across elevation than latitude (Koot et al., 2022; Meza-Joya et al., 2023), the lack of elevation–size clines we observed likely reflects the influence of individual movement and genetic mixture across different elevations (Dillon et al., 2006; Horne et al., 2018; Keller et al., 2013). Thus, these grasshoppers provide evidence that gene flow is a constraining evolutionary force within

mountain populations. The observed latitudinal-size clines may reflect mostly genetic differences between populations (Horne et al., 2018, 2019; Keller et al., 2013), given the postglacial isolation history of the mountaintop populations may have resulted not only in genetic divergence (Meza-Joya et al., 2023) but also in phenotypic differentiation via local selective forces (e.g. Chapter 4).

According to the temperature–size rule, ectotherms grow faster and mature at smaller sizes with warming (Angilletta & Dunham, 2003; Atkinson, 1994; Kingsolver & Huey, 2008). In keeping with this expectation, *B. nivalis* body size decreases with the temperature of the driest quarter, suggesting that the temperature this grasshopper encounters during its activity peak (i.e. summertime) is an important proximate predictor of Bergmann's rule. This fits well with the preferred habitat of this species, as on scree areas it may be more sensitive to direct temperature effects. Adult size in ectotherms also covaries with oxygen availability, which also covaries with elevation, yet evidence for such oxygen–size relationships is fragmentary for terrestrial insects (Horne et al., 2015). Likewise, body size variation in *S. australis* was positively related with isothermality (FL and FM), that is, larger sizes are found in more thermally variable environments. This size increase may relate seasonal resource variability in unpredictable alpine environments, as small sizes would increase starvation risk under unfavourable conditions (Arnett and Gotelli, 2003; Cushman et al., 1993; Lindstedt & Boyce, 1985). Notably, *P. nitidus* body size seems to be temperature insensitivity, rather size variation is weakly correlated with precipitation seasonality, which is a proxy of the west–east rain shadow gradient of the study region (Griffiths & McSaveney, 1983). Here, slightly larger sizes are found in areas with a more even annual precipitation distribution, suggesting reduced resource availability in areas with uneven rainfall regimens might be influential for phenotypic differentiation (Teta et al., 2022). However, this pattern requires further verification as our sampling is biased towards drier, eastern mountains. Nevertheless, high-resolution climate layers are needed as microclimate heterogeneity originated by the complex local topography of the Southern Alps (see Barry, 1992) may be influential for phenotypic variation (see Horne et al., 2018).

Sex-specific variation in body size clines determine the degree to which SSD varies across environmental gradients (Blanckenhorn et al. 2006; Horne et al., 2019; Stillwell et al., 2007). Consistent with this, we found female grasshoppers exhibit the greatest

proportional changes in size, opposite to Rensch's rule (Stillwell et al., 2010; Horne et al., 2019; Rohner et al., 2018; Teder & Tammaru, 2005). Fecundity selection is expected to mediate female-biased SSD in insects (Blanckenhorn et al., 2007; Fairbairn, 1997; Stillwell et al., 2010), yet sex differences in developmental time can also produce the same output when female size increases at expenses of a prolonged development (Esperk et al., 2007; Horne et al., 2019; Teder, 2014). Insect females can develop to larger sizes through a higher number of instars than males (Esperk et al., 2007; Laiolo et al., 2013; Teder, 2014), and this is true of females of our focal species, which include one extra nymphal instar than smaller-bodied males (Hudson, 1970; White, 1974). As plasticity in instar number is required for such sexual differences to evolve (Esperk et al., 2007), female grasshoppers may add supernumerary instars during development to become larger than males and better adjust their size to favourable local conditions (see Esperk et al., 2007; Horne et al., 2019; Rohner et al., 2018) and this has been observed in other montane acridid grasshoppers (Laiolo et al., 2013). Therefore, plasticity and/or natural selection during development may lead to adjustments in female body size accordingly to the prevailing local conditions (Baroni & Masoero, 2018).

In all three grasshopper species, greater variability in female size often led to substantial changes in SSD, although the magnitude of change varied between size proxies (e.g. Bidau et al., 2016; Blanckenhorn et al., 2006; Laiolo et al., 2013). Notably, neither sex exhibited elevational size clines, akin to recent findings in a wide range of arthropods, including orthopterans (Horne et al., 2019). While this implies both sexes respond similarly to environmental change along elevation mostly via plastic responses (Horne et al., 2018, 2019), genotypic mixing and/or individual movement across this gradient may conceal any sex-specific response. Females of the species considered here also exhibited greater plasticity in response to climate factors, suggesting the largest sex is more condition dependent, which is common in insects, including grasshoppers (Laiolo et al., 2013; Rohner et al., 2018). Likewise, we found female body mass changed more readily than structural size in response to climate. Thus supports the idea that size proxies capturing match nutritional conditions and local resource availability display steeper clines than those accounting for structural size alone and implies that condition dependence accentuates SSD (Laiolo et al., 2013; Rohner et al., 2018). As a great deal of variation in body size is female-biased, we predict sexually dimorphic plasticity will be crucial for population persistence under climate change (see Hangartner et al., 2022).

Our findings add to the mounting evidence that distinct size components can be affected in different ways by the environment, which complicate inferences about the impacts of climate change on morphology (e.g. Bailey et al., 2020; Canale et al., 2016). While the examined geographic and climatic predictors explained a reasonable amount of variation in structural size and body mass, the large proportion of unexplained variance in body condition likely reflect inter-individual differences in body composition (e.g. water and fat content), food intake and reproductive status (see Meza-Joya et al., 2022). Indeed, the used statistical proxy of body condition ($\hat{M}i$) is expected to capture most (if not all) variation related to such factors, thus inferences from analyses based on this index alone can be difficult to interpret and so the ultimate causes of variation in this trait. Although body mass alone seems a reasonable size indicator in the studied species, changes in mass can relate changes in either structural size, body condition or both (Bailey et al., 2020). The difficulties associated with analysing spatial (or temporal) changes in a composite trait such as body size are not unique to insects (e.g. Bailey et al., 2020; Canale et al., 2016; McLean et al., 2018), and this might explain some of the discrepancies observed when comparing studies using both structural size and mass metrics (e.g. Canale et al., 2016). Examining alternative size components at once would allow at minimum a better interpretation of ecogeographic patterns and drawing more consistent conclusions about the effects of climate change on morphology (Bailey et al., 2020; Canale et al., 2016).

In the grasshopper species here considered, common trends between femur length and fresh mass in response to climate variation likely reflect actual variation in overall body size. Deeping our understanding of the fitness costs of such changes in body size is urgently needed (see Kingsolver & Huey, 2008). This is particularly relevant as decline in organismal body size has been proposed as a general response to anthropogenic global warming (Gardner et al., 2011). In rule with this, warm conditions seem to favour smaller sizes in *B. nivalis*. Thus, we might expect intraspecific size declines under warming for this and other species with strong temperature–size relationships. However, we have also seen that up and down the same mountain no strong clines in body size exist, suggesting that grasshopper populations might not be able to response with the speed necessary to match current climate warming. Climate-driven range shifts can also reduce assemblages' mean body size if Bergmann's rule is acting at interspecific level along the geographic gradients over which species are moving (Wu et al., 2018). New Zealand grasshoppers show interspecific positive size–elevation cline suiting Bergmann's rule

(Bigelow, 1967) and poleward and upward range shifts have also been anticipated for our focal species under warming (Koot et al., 2022; Meza-Joya et al., 2023). As dispersal for these grasshoppers is more likely across elevation, we expect uphill shifts to bring smaller species into higher elevations reducing the overall assemblage size profile (see Wu et al., 2018). Larger body size is often related to greater fitness, thus size reduction at species and assemblage level might affect fitness accordingly (Kingsolver & Huey, 2008), and this has the potential to disrupt trophic interactions, which in turn might alter the size structure of entire communities (Ohlberger, 2013). The New Zealand alpine environment harbours other wing-reduced and flightless animal lineages with limited dispersal ability and increased body sizes relative to their lower elevation counterparts (Goldberg et al., 2008; McCulloch & Waters, 2018), thus size restructuring due to global warming would be geographically and taxonomically widespread.

Acknowledgements

We are grateful to the New Zealand Department of Conservation for granting access and approval to collect from the Conservation Estate (Authorization Number: 49878-RES and 97397-FLO). We thank the ski fields and managers who allowed us to access field sites. We also acknowledge our field partners: Eliana Ramos, Mari Nakano, Cheten Dorji, Evans Effah, and Andrea Clavijo. This research was assisted by a grant from the Miss E. L. Hellaby Indigenous Grasslands Research Trust and a doctoral scholarship from Massey University (awarded to FLMJ). Open access publishing facilitated by Massey University, as part of the Wiley -Massey University agreement via the Council of Australian University Librarians.

References

Abouheif, E., & Fairbairn, D. J. (1997). A comparative analysis of allometry for sexual size dimorphism: Assessing Rensch's rule. *The American Naturalist*, *149*(3), 540–562. https://doi.org/10.1086/286004

Angilletta, M. J., & Dunham, A. E. (2003). The temperature-size rule in ectotherms: Simple evolutionary explanations may not be general. *The American Naturalist*, *162*(3), 332–342. https://doi.org/10.1086/377187

Arnett, A. E., & Gotelli, N. J. (2003). Bergmann's rule in larval ant lions: Testing the starvation resistance hypothesis. *Ecological Entomology*, *28*(6), 645–650. https://doi.org/10.1111/j.1365-2311.2003.00554.x

Atkinson, D. (1994). Temperature and organism size–a biological law for ectotherms? *Advances in Ecological Research*, *25*, 1–58. https://doi.org/10.1016/S0065-2504(08)60212-3

Bailey, L. D., Kruuk, L. E., Allen, R., Clayton, M., Stein, J., & Gardner, J. L. (2020). Using different body size measures can lead to different conclusions about the effects of climate change. *Journal of Biogeography*, *47*, 1687–1697. https://doi.org/10.1111/jbi.13850

Baroni, D., & Masoero, G. (2018). Complex influence of climate on the distribution and body size of an Alpine species. *Insect Conservation and Diversity*, *11*(5), 435–448. https://doi.org/10.1111/icad.12296

Barry, R. G. (1992). Mountain climatology and past and potential future climatic changes in mountain regions: A review. *Mountain Research and Development*, *12*, 71–86. https://doi.org/10.2307/3673749

Beck, J., Liedtke, H. C., Widler, S., Altermatt, F., Loader, S. P., Hagmann, R., ... & Fiedler, K. (2016). Patterns or mechanisms? Bergmann's and Rapoport's rule in moths along an elevational gradient. *Community Ecology*, *17*(2), 137–148. https://doi.org/10.1556/168.2016.17.2.2

Beerli, N., Bärtschi, F., Ballesteros-Mejia, L., Kitching, I. J., & Beck, J. (2019). How has the environment shaped geographical patterns of insect body sizes? A test of hypotheses using sphingid moths. *Journal of Biogeography*, *46*(8), 1687–1698. https://doi.org/10.1111/jbi.13583

Bergmann, C. (1847). Über die verhältnisse der wärmeökonomie der thiere zu ihrer grösse. *Göttinger Studien*, *3*, 595–708.

Bidau, C. J., Taffarel, A., & Castillo, E. R. (2016). Breaking the rule: Multiple patterns of scaling of sexual size dimorphism with body size in orthopteroid insects. *Revista*

de la Sociedad Entomológica Argentina, *75*(1-2), 11–36. https://www.biotaxa.org/RSEA/article/view/22294

Bigelow, R. S. (1967). *The grasshoppers (Acrididae) of New Zealand*. University of Canterbury Publications.

Blackburn, T. M., Gaston, K. J., & Loder, N. (1999). Geographic gradients in body size: A clarification of Bergmann's rule. Diversity and Distributions, *5*(4), 165–174. https://doi.org/10.1046/j.1472-4642.1999.00046.x

Blanckenhorn, W. U., & Demont, M. (2004). Bergmann and converse Bergmann latitudinal clines in arthropods: Two ends of a continuum? *Integrative and Comparative Biology*, *44*, 413–424. https://doi.org/10.1093/icb/44.6.413

Blanckenhorn, W. U., Dixon, A. F., Fairbairn, D. J., Foellmer, M. W., Gibert, P., van der Linde, K., … Wiklund, C. (2007). Proximate causes of Rensch's rule: Does sexual size dimorphism in arthropods result from sex differences in development time? *The American Naturalist*, *169*, 245–257. https://doi.org/10.1086/510597

Blanckenhorn, W. U., Stillwell, R. C., Young, K. A., Fox, C. W., & Ashton, K. G. (2006) When Rensch meets Bergmann: Does sexual size dimorphism change systematically with latitude? *Evolution*, *60*, 2004–2011. https://doi.org/10.1111/j.0014-3820.2006.tb01838.x

Bolker, B. M., Brooks, M. E., Clark, C. J., Geange, S. W., Poulsen, J. R., Stevens, M. H. H., & White, J. S. S. (2009). Generalized linear mixed models: A practical guide for ecology and evolution. *Trends in Ecology & Evolution*, *24*(3), 127–135. https://doi.org/10.1016/j.tree.2008.10.008

Buckley, T. R., Hoare, R. J., & Leschen, R. A. (2022). Key questions on the evolution and biogeography of New Zealand alpine insects. *Journal of the Royal Society of New Zealand*, *54*(1), 30–54. https://doi.org/10.1080/03036758.2022.2130367

Bulgarella, M., Trewick, S. A., Godfrey, A. J. R., Sinclair, B. J., Morgan-Richards, M. (2015). Elevational variation in adult body size and growth rate but not in metabolic rate in the tree weta *Hemideina crassidens*. *Journal of Insect Physiology*, *75*, 30–38. http://dx.doi.org/10.1016/j.jinsphys.2015.02.012

Canale, C. I., Ozgul, A., Allaine, D., & Cohas, A. (2016). Differential plasticity of size and mass to environmental change in a hibernating mammal. *Global Change Biology*, *22*(10), 3286–3303. https://doi.org/10.1111/gcb.13286

Cardilini, A. P., Buchanan, K. L., Sherman, C. D., Cassey, P., & Symonds, M. R. (2016). Tests of ecogeographical relationships in a non-native species: What rules avian morphology? *Oecologia*, *181*, 783–793. https://doi.org/10.1007/s00442-016-3590-9

Carmelet-Rescan, D., Morgan-Richards, M., Koot, E. M., & Trewick, S. A. (2021). Climate and ice in the last glacial maximum explain patterns of isolation by distance inferred for alpine grasshoppers. *Insect Conservation and Diversity*, *14*(5), 568–581. https://doi.org/10.1111/icad.12488

Chevin, L. M., & Hoffmann, A. A. (2017). Evolution of phenotypic plasticity in extreme environments. *Philosophical Transactions of the Royal Society B: Biological Sciences*, *372*(1723), 20160138. https://doi.org/10.1098/rstb.2016.0138

Chown, S. L., & Gaston, K. J. (2010). Body size variation in insects: A macroecological perspective. *Biological Reviews*, *85*(1), 139–4169. https://doi.org/10.1111/j.1469-185X.2009.00097.x

Chown, S. L., & Klok, C. J. (2003). Altitudinal body size clines: Latitudinal effects associated with changing seasonality. *Ecography*, *26*(4), 445–455. https://doi.org/10.1034/j.1600-0587.2003.03479.x

Ciplak, B., Sirin, D., Taylan, M. S., & Kaya, S. (2008). Altitudinal size clines, species richness and population density: Case studies in Orthoptera. *Journal of Orthoptera Research*, *17*(2), 157–163. https://doi.org/10.1665/1082-6467-17.2.157

Cushman, J. H., Lawton, J. H., & Manly, B. F. J. (1993). Latitudinal patterns in European ant assemblages: Variation in species richness and body size. *Oecologia*, *95*, 30–37. https://doi.org/10.1007/BF00649503

Davis, M. B., & Shaw, R. G. (2001). Range shifts and adaptive responses to quaternary climate change. *Science*, *292*(5517), 673–679. https://doi.org/10.1126/science.292.5517.673

Davidowitz, G., D'Amico, L. J., & Nijhout, H. F. (2004). The effects of environmental variation on a mechanism that controls insect body size. *Evolutionary Ecology Research*, *6*, 49–62. http://www.evolutionary-ecology.com/abstracts/v06/1643.html

De Frenne, P., Graae, B. J., Rodríguez-Sánchez, F., Kolb, A., Chabrerie, O., Decocq, G., ... & Verheyen, K. (2013). Latitudinal gradients as natural laboratories to infer species' responses to temperature. *Journal of Ecology*, *101*(3), 784–795. https://doi.org/10.1111/1365-2745.12074

Delhey, K., Dale, J., Valcu, M., & Kempenaers, B. (2020). Why climate change should generally lead to lighter coloured animals. *Current Biology*, *30*(23), R1406–R1407. https://doi.org/10.1016/j.cub.2020.10.070

Dillon, M. E., Frazier, M. R., & Dudley, R. (2006). Into thin air: Physiology and evolution of alpine insects. *Integrative and Comparative Biology*, *46*(1), 49–61. https://doi.org/10.1093/icb/icj007

Dowle, E. J., Morgan-Richards, M., & Trewick, S. A. (2014). Morphological differentiation despite gene flow in an endangered grasshopper. *BMC Evolutionary Biology*, *14*, 216. https://doi.org/10.1186/s12862-014-0216-x

Endler, J. A. (1977). *Geographic variation, speciation, and clines*. Princeton University Press.

Esperk, T., Tammaru, T., Nylin, S., & Teder, T. (2007). Achieving high sexual size dimorphism in insects: Females add instars. *Ecological Entomology*, *32*(3), 243–256. https://doi.org/10.1111/j.1365-2311.2007.00872.x

Fairbairn, D. J. (1997). Allometry for sexual size dimorphism: Pattern and process in the coevolution of body size in males and females. *Annual Review of Ecology and Systematics*, *28*, 659–687. https://doi.org/10.1146/annurev.ecolsys.28.1.659

Fairbairn, D. J., Blanckenhorn, W. U., & Székely, T. (2007). Sex, size and gender roles: Evolutionary studies of sexual size dimorphism. Oxford University Press.

Gardner, J. L., Peters, A., Kearney, M. R., Joseph, L., & Heinsohn, R. (2011). Declining body size: A third universal response to warming? *Trends in Ecology & Evolution*, *26*(6), 285–291. https://doi.org/10.1016/j.tree.2011.03.005

Gelman, A. (2008). Scaling regression inputs by dividing by two standard deviations. *Statistics in Medicine*, *27*(15), 2865–2873. https://doi.org/10.1002/sim.3107

Gelman, A., & Rubin, D. B. (1992). Inference from iterative simulation using multiple sequences. *Statistical Science*, *7*(4), 457–472. https://www.jstor.org/stable/2246093

Goldberg, J., Trewick, S. A., & Paterson, A. M. (2008). Evolution of New Zealand's terrestrial fauna: A review of molecular evidence. *Philosophical Transactions of the Royal Society of London B: Biological Sciences*, *363*, 3319–3334. https://doi.org/10.1098/rstb.2008.0114

Goodrich, B., Gabry, J., Ali, I., & Brilleman, S. (2023). rstanarm: Bayesian applied regression modeling via Stan. https://cran.r-project.org/package=rstanarm

Griffiths, G. A., & McSaveney, M. J. (1983). Distribution of mean annual precipitation across some steepland regions of New Zealand. *New Zealand Journal of Science*, *26*(2), 197–209.

Hangartner, S., Sgrò, C. M., Connallon, T., & Booksmythe, I. (2022). Sexual dimorphism in phenotypic plasticity and persistence under environmental change: An extension of theory and meta-analysis of current data. *Ecology Letters*, *25*(6), 1550–1565. https://doi.org/10.1111/ele.14005

Hochkirch, A., & Gröning, J. (2008) Sexual size dimorphism in Orthoptera (sens. Str.): A review. *Journal of Orthoptera Research*, *17*, 189–196. https://doi.org/10.1665/1082-6467-17.2.189

Hodkinson, I. D. (2005). Terrestrial insects along elevation gradients: Species and community responses to altitude. *Biological Reviews of the Cambridge Philosophical Society*, *80*, 489–513. https://doi.org/10.1017/S1464793105006767

Horne, C. R., Hirst, A. G., & Atkinson, D. (2015). Temperature-size responses match latitudinal-size clines in arthropods, revealing critical differences between aquatic and terrestrial species. *Ecology Letters*, *18*(4), 327–335. https://doi.org/10.1111/ele.12413

Horne, C. R., Hirst, A. G., & Atkinson, D. (2018) Insect temperature–body size trends common to laboratory, latitudinal and seasonal gradients are not found across altitudes. *Functional Ecology*, *32*, 948–957. https://doi.org/10.1111/1365-2435.13031

Horne, C. R., Hirst, A. G., Atkinson, D. (2019). A synthesis of major environmental-body size clines of the sexes within arthropod species. *Oecologia*, *190*, 343–353. https://doi.org/10.1007/s00442-019-04428-7

Hudson, L. (1970). Identification of the immature stages of New Zealand alpine acridid grasshoppers (Orthoptera). *Transactions of the Royal Society of New Zealand (Biological Science)*, *12*(17), 185–208.

James, F. C. (1970). Geographic size variation in birds and its relationship to climate. *Ecology*, *51*(3), 365–390. https://doi.org/10.2307/1935374

Jump, A. S., Mátyás, C., & Peñuelas, J. (2009). The altitude-for-latitude disparity in the range retractions of woody species. *Trends in Ecology & Evolution*, *24*(12), 694–701. https://doi.org/10.1016/j.tree.2009.06.007

Karger, D. N., Conrad, O., Böhner, J., Kawohl, T., Kreft, H., Soria-Auza, R. W., ... & Kessler, M. (2017). Climatologies at high resolution for the earth's land surface areas. *Scientific data*, *4*(1), 1–20. https://doi.org/10.1038/sdata.2017.122

Karger, D. N., Conrad, O., Böhner, J., Kawohl, T., Kreft, H., Soria-Auza, R. W., ... & Kessler, M. (2017). *Climatologies at high resolution for the earth's land surface areas*. EnviDat. https://doi.org/10.16904/envidat.228.v2.1

Keller, I., Alexander, J. M., Holderegger, R., & Edwards, P. J. (2013). Widespread phenotypic and genetic divergence along altitudinal gradients in animals. *Journal of Evolutionary Biology*, *26*, 2527–2543. https://doi.org/10.1111/jeb.12255

Kingsolver, J., & Huey, R. (2008). Size, temperature, and fitness: Three rules. *Evolutionary Ecology Research*, *10*(2), 251–268.

Knief, U., & Forstmeier, W. (2021). Violating the normality assumption may be the lesser of two evils. *Behavior Research Methods*, *53*, 2576–2590. https://doi.org/10.3758/s13428-021-01587-5

Koot, E. M., Morgan-Richards, M., & Trewick, S. A. (2020). An alpine grasshopper radiation older than the mountains, on Kā Tiritiri o te Moana (Southern Alps) of Aotearoa (New Zealand). *Molecular Phylogenetics and Evolution*, *147*, 106783. https://doi.org/10.1016/j.ympev.2020.106783

Koot, E. M., Morgan-Richards, M., & Trewick, S. A. (2022). Climate change and alpine adapted insects: Modelling environmental envelopes of a grasshopper radiation. *Royal Society Open Science*, *9*, 211596. https://doi.org/10.1098/rsos.211596

Laiolo, P., Illera, J. C., & Obeso, J. R. (2013). Local climate determines intra-and interspecific variation in sexual size dimorphism in mountain grasshopper

communities. *Journal of Evolutionary Biology*, *26*(10), 2171–2183. https://doi.org/10.1111/jeb.12213

Lenormand, T. (2002). Gene flow and the limits to natural selection. *Trends in Ecology & Evolution*, *17*(4), 183–189. https://doi.org/10.1016/S0169-5347(02)02497-7

Lindstedt, S. L., & Boyce, M. S. (1985). Seasonality, fasting endurance, and body size in mammals. *The American Naturalist*, *125*(6), 873–878. https://doi.org/10.1086/284385

Long, J. A. (2019). interactions: Comprehensive, user-friendly toolkit for probing interactions. https://cran.r-project.org/package=interactions

Lovich, J. E., & Gibbons, J. W. (1992). A review of techniques for quantifying sexual size dimorphism. *Growth, Development & Aging*, *56*, 269–269.

Lüdecke, D., Ben-Shachar, M. S., Patil, I., Waggoner, P., & Makowski, D. (2021). performance: An R package for assessment, comparison and testing of statistical models. *Journal of Open Source Software*, *6*(60), 3139. https://doi.org/10.21105/joss.03139

Makowski, D., Ben-Shachar, M. S., & Lüdecke, D. (2019). bayestestR: Describing effects and their uncertainty, existence and significance within the Bayesian framework. *Journal of Open Source Software*, *4*(40), 1541. https://doi.org/10.21105/joss.01541

Mayr, E. (1956). Geographical character gradients and climatic adaptation. *Evolution*, *10*, 105–108. https://doi.org/10.1111/j.1558-5646.1956.tb028 36.x

McCarthy, J. K., Leathwick, J. R., Roudier, P., Barringer, J. R. F., Etherington, T. R., Morgan, F. J., Odgers, N. P., Price, R. H., Wiser, S. K., & Richardson, S. J. (2021). New Zealand Environmental Data Stack (NZEnvDS): A standardised collection of spatial layers for environmental modelling and site characterisation. *New Zealand Journal of Ecology*, *45*(2), 1–8. https://www.jstor.org/stable/48621886

McCulloch, G. A., & Waters, J. M. (2018). Does wing reduction influence the relationship between altitude and insect body size? A case study using New Zealand's diverse stonefly fauna. *Ecology and Evolution*, *8*(2), 953–960. https://doi.org/10.1002/ece3.3713

McLean, N., Van Der Jeugd, H. P., & van de Pol, M. (2018). High intra-specific variation in avian body condition responses to climate limits generalisation across species. *PLoS One*, *13*(2), e0192401. https://doi.org/10.1371/journal.pone.0192401

Meza-Joya. F. L., Morgan-Richards, M., Koot, E. M., & Trewick, S. A. (2023). Global warming leads to habitat loss and genetic erosion of alpine biodiversity. *Journal of Biogeography*, *50*, 961–975. https://doi.org/10.1111/jbi.14590

Meza-Joya, F. L., Morgan-Richards, M., & Trewick, S. A. (2022). Relationships among body size components of three flightless New Zealand grasshopper species (Orthoptera, Acrididae) and their ecological applications. *Journal of Orthoptera Research*, *31*(1), 91–103. https://doi.org/10.3897/jor.31.79819

Millien, V., Kathleen Lyons, S., Olson, L., Smith, F. A., Wilson, A. B., & Yom-Tov, Y. (2006). Ecotypic variation in the context of global climate change: Revisiting the rules. *Ecology Letters*, *9*(7), 853–869. https://doi.org/10.1111/j.1461-0248.2006.00928.x

Minards, N. A., Trewick, S. A., Godfrey, A. J. R., & Morgan-Richards, M. (2014). Convergent local adaptation in size and growth rate but not metabolic rate in a pair of parapatric Orthoptera species. *Biological Journal of the Linnean Society*, *113*(1), 123–135. https://doi.org/10.1111/bij.12304

Mousseau, T. A. (1997). Ectotherms Follow the Converse to Bergmann's Rule. *Evolution*, *51*(2), 630–632. https://doi.org/10.1111/j.1558-5646.1997.tb02453.x

Nakagawa, S., & Schielzeth, H. (2013). A general and simple method for obtaining R2 from generalized linear mixed-effects models. *Methods in Ecology and Evolution*, *4*(2), 133–142. https://doi.org/10.1111/j.2041-210x.2012.00261.x

Nakano, M., Morgan-Richards, M., Clavijo-McCormick, A., & Trewick, S. A. (2023). Abundance and distribution of antennal sensilla on males and females of three sympatric species of alpine grasshopper (Orthoptera: Acrididae: Catantopinae) in Aotearoa New Zealand. *Zoomorphology*, *142*, 51–62. https://doi.org/10.1007/s00435-022-00579-z

Ohlberger, J. (2013). Climate warming and ectotherm body size–from individual physiology to community ecology. *Functional Ecology*, *27*(4), 991–1001. https://doi.org/10.1111/1365-2435.12098

Peig, J., & Green, A. J. (2009). New perspectives for estimating body condition from mass/length data: The scaled mass index as an alternative method. *Oikos*, *118*(12), 1883–1891. https://doi.org/10.1111/j.1600-0706.2009.17643.x

Piironen, J., Paasiniemi, M., Catalina, A., Weber, F., & Vehtari, A. (2023). projpred: Projection Predictive Feature Selection. https://cran.r-project.org/package=projpred

R Core Team. (2022). R: A language and environment for statistical computing. https://www.r-project.org

Rensch, B. (1960). Evolution above the species level. Columbia University Press.

Rohner, P. T., Teder, T., Esperk, T., Lüpold, S., & Blanckenhorn, W. U. (2018). The evolution of male-biased sexual size dimorphism is associated with increased body size plasticity in males. *Functional Ecology*, *32*(2), 581–591. https://doi.org/10.1111/1365-2435.13004

Shelomi, M. (2012). Where are we now? Bergmann's rule sensu lato in insects. *The American Naturalist*, *180*(4), 511–519. https://doi.org/10.1086/667595

Stillwell, R. C., Blanckenhorn, W. U., Teder, T., Davidowitz, G., & Fox, C. W. (2010). Sex differences in phenotypic plasticity affect variation in sexual size dimorphism in insects: From physiology to evolution. *Annual Review of Entomology*, *55*, 227–245. https://doi.org/10.1146/annurev-ento-112408-085500

Stillwell, R. C., Morse, G. E., Fox, C. W. (2007). Geographic variation in body size and sexual size dimorphism of a seed-feeding beetle. *American Naturalist*, *170*, 358–369. https://doi.org/10.1086/520118

Teder, T. (2014). Sexual size dimorphism requires a corresponding sex difference in development time: A meta-analysis in insects. *Functional Ecology*, 28(2), 479–486. https://doi.org/10.1111/1365-2435.12172

Teder, T., & Tammaru, T. (2005). Sexual size dimorphism within species increases with body size in insects. *Oikos*, *108*(2), 321–334. https://doi.org/10.1111/j.0030-1299.2005.13609.x

Teta, P., de la Sancha, N. U., D'Elía, G., & Patterson, B. D. (2022). Andean rain shadow effect drives phenotypic variation in a widely distributed Austral rodent. *Journal of Biogeography*, *49*(10), 1767–1778. https://doi.org/10.1111/jbi.14468

Tian, L., & Benton, M. J. (2020). Predicting biotic responses to future climate warming with classic ecogeographic rules. *Current Biology*, *30*(13), R744-R749. https://doi.org/10.1016/j.cub.2020.06.003

Trewick, S. A., Wallis, G. P., & Morgan-Richards, M. (2000). Phylogeographical pattern correlates with Pliocene mountain building in the alpine scree weta (Orthoptera, Anostostomatidae). *Molecular Ecology*, *9*(6), 657–666. https://doi.org/10.1046/j.1365-294x.2000.00905.x

Vehtari, A., Gabry, J., Magnusson, M., Yao, Y., Bürkner, P., Paananen, T., & Gelman, A. (2023). loo: Efficient leave-one-out cross-validation and WAIC for Bayesian models. https://cran.r-project.org/package=loo

Wardle, P. (2008). New Zealand Forest to alpine transitions in global context. *Arctic, Antarctic, and Alpine Research*, *40*, 240–249. https://doi.org/10.1657/1523-0430(06-066)[WARDLE]2.0.CO;2

White, E. G. (1974). A quantitative biology of three New Zealand alpine grasshopper species. *New Zealand Journal of Agricultural Research*, *17*(2), 207–227. https://doi.org/10.1080/00288233.1974.10421001

White, E. G., & Sedcole, J. R. (1991). A 20-year record of alpine grasshopper abundance, with interpretations for climate change. *New Zealand Journal of Ecology*, *15*,139–152. https://www.jstor.org/stable/24053567

Whitman, D. W. (2008). The significance of body size in the Orthoptera: A review. *Journal of Orthoptera research*, *17*(2), 117–134. https://doi.org/10.1665/1082-6467-17.2.117

Wu, C. H., Holloway, J. D., Hill, J. K., Thomas, C. D., Chen, I. C., & Ho, C. K. (2019). Reduced body sizes in climate-impacted Borneo moth assemblages are primarily explained by range shifts. *Nature Communications*, *10*, 4612. https://doi.org/10.1038/s41467-019-12655-y

Yadav, S., Stow, A., & Dudaniec, R. Y. (2020). Elevational partitioning in species distribution, abundance and body size of Australian alpine grasshoppers (*Kosciuscola*). *Austral Ecology*, *45*(5), 609–620. https://doi.org/10.1111/aec.12876

Supporting Information

Table S1. Sampling information for three alpine grasshoppers (*Brachaspis nivalis*, *Paprides nitidus* and *Sigaus australis*) endemic to South Island, New Zealand. Site: Rainbow Ski Club (RS), Temple Basin Ski Area (TB), Broken River Ski Area (BR), Mt Hutt Ski Area (MH), Fox Peak Ski Club (FP), and Cardrona Alpine Resort (CR). Not recoded (NR).

					Number of specimens		
Latitude	**Longitude**	**Mountain**	**Site**	**Elevation**	***B. nivalis***	***P. nitidus***	***S. australis***
-41.88410	172.85990	Mt McRae	RS1	1286 m	NR	4♂	NR
-41.88152	172.85721	Mt McRae	RS2	1396 m	NR	15♀, 6♂	NR
-41.87920	172.85940	Mt McRae	RS3	1462 m	NR	18♀,	NR
-41.87230	172.86210	Mt McRae	RS4	1620 m	NR	8♀, 10♂	NR
-41.86690	172.86400	Mt McRae	RS5	1727 m	3♀, 1♂	6♀, 5♂	NR
-41.88202	172.84633	Mt McRae	RS6	1856 m	6♀, 2♂	3♂	NR
-42.91076	171.56564	Mt Temple	TB1	1070 m	NR	2♀	NR
-42.91061	171.56946	Mt Temple	TB2	1245 m	NR	4♀, 5♂	NR
-42.90982	171.57435	Mt Temple	TB3	1335 m	NR	12♀,	NR
-42.90912	171.57930	Mt Temple	TB4	1450 m	NR	13♀, 9♂	NR
-42.90807	171.58074	Mt Temple	TB5	1547 m	NR	1♀, 3♂	NR
-43.12545	171.68959	Hamilton Peak	BR1	1386 m	19♀, 5♂	14♀,	NR
-43.12575	171.68624	Hamilton Peak	BR2	1482 m	13♀,	27♀,	13♀, 13♂
-43.12442	171.68449	Hamilton Peak	BR3	1578 m	15♀,	7♀, 13♂	11♀, 7♂
-43.12276	171.68298	Hamilton Peak	BR4	1671 m	8♀, 11♂	9♀, 10♂	12♀, 11♂
-43.11962	171.68139	Hamilton Peak	BR5	1797 m	13♀,	11♀,	8♀, 10♂
-43.53211	171.54027	Mt Hutt	MH1	1095 m	NR	10♀, 4♂	4♂
-43.52537	171.55258	Mt Hutt	MH2	1207 m	3♀, 3♂	13♀, 6♂	8♀, 7♂
-43.51309	171.54942	Mt Hutt	MH3	1440 m	2♂	9♀, 15♂	5♀, 10♂
-43.49518	171.53568	Mt Hutt	MH4	1610 m	15♀, 4♂	17♀,	3♀, 4♂
-43.48946	171.53427	Mt Hutt	MH5	1856 m	14♀, 5♂	NR	NR
-43.86180	170.80790	Fox Peak	FP1	1319 m	NR	1♀, 3♂	8♀, 3♂
-43.85839	170.80744	Fox Peak	FP2	1402 m	2♀, 3♂	NR	11♀, 3♂
-43.85690	170.80370	Fox Peak	FP3	1506 m	1♂	2♀, 2♂	10♀, 3♂
-43.85260	170.80790	Fox Peak	FP4	1600 m	4♂	1♀, 1♂	20♀, 8♂
-43.85200	170.80500	Fox Peak	FP5	1702 m	2♀, 7♂	NR	8♀, 8♂
-44.87469	168.96662	Mt Cardrona	CR1	1215 m	NR	NR	11♀, 3♂
-44.88080	168.95830	Mt Cardrona	CR2	1340 m	NR	NR	7♀, 4♂
-44.88070	168.95530	Mt Cardrona	CR3	1440 m	NR	NR	2♀, 3♂
-44.87720	168.95340	Mt Cardrona	CR4	1540 m	NR	NR	5♀, 5♂
-44.86090	168.95510	Mt Cardrona	CR5	1640 m	NR	NR	5♀, 3♂
-44.86010	168.95000	Mt Cardrona	CR6	1740 m	NR	NR	7♀, 3♂
-44.85684	168.94611	Mt Cardrona	CR7	1865 m	NR	NR	9♀, 7♂

Table S2. Variables initially examined to quantify the influence of local environment on body size variation in three alpine grasshoppers (*Brachaspis nivalis*, *Paprides nitidus* and *Sigaus australis*) endemic to South Island, New Zealand. All variables were retrieved from the climatologies at high resolution for the Earth's and land surface areas (CHELSA) portal (https://chelsa-climate.org).

Variable name	**Units**
mean annual air temperature	°C
mean diurnal air temperature range	°C
isothermality	%
temperature seasonality	°C/100
annual air temperature range	°C
mean air temperature of the wettest quarter	°C
mean air temperature of the driest quarter	°C
precipitation amount of wettest month (Aug[1])	kg m^{-2} yr^{-1}
precipitation amount of driest month (Feb)	kg m^{-2} yr^{-1}
precipitation seasonality	%
precipitation amount of wettest quarter	kg m^{-2} yr^{-1}
precipitation amount of driest quarter	kg m^{-2} yr^{-1}
mean annual climate moisture	kg m^{-2} yr^{-1}
growing season length	days
growing degree days heat sum above 5°C	°C
mean temperature of the growing season	°C
precipitation of the growing season	kg m^{-2} yr^{-1}
snow cover days	days

Table S3. Predictors used to quantify the influence of local environment on body size variation in three alpine grasshoppers (*Brachaspis nivalis*, *Paprides nitidus* and *Sigaus australis*) endemic to South Island, New Zealand. Selection of relevant variables used a variance inflation factor (VIF) analysis in the R package 'usdm' 1.1-18 (Naimi et al., 2014), and strongly correlated variables (Pearson's correlation $r > 0.7$) were removed from further analysis. All precipitation-related variables in our dataset were highly correlated between them and with other predictors ($r > 0.813$), thus only precipitation seasonality was retained during the elimination process. The linear correlation coefficients between predictors ranges between 0.133 (growing season length ~ temperature seasonality) and 0.630 (growing season length ~ mean air temperature of the driest quarter). Variables retained as informative for each size proxy per species after projection predictive variable selection (see Figure S6).

Variable name	***Brachaspis nivalis***	***Paprides nitidus***	***Sigaus australis***
isothermality	FL/FM	-	FL/FM/M̂i
temperature seasonality	M̂i	M̂i	-
mean air temperature of the driest quarter	FL/FM	M̂i	-
mean air temperature of the wettest quarter	-	-	M̂i
precipitation seasonality	M̂i	FL/FM	-
growing season length	-	-	-

Table S4. Geographic variation in body size components (FL, femur length; FM, fresh mass; M̂I, body condition) of three alpine grasshopper species (*Brachaspis nivalis, Paprides nitidus* and *Sigaus australis*) endemic to South Island (New Zealand) was in most cases best explained by models incorporating quadratic terms for latitude and elevation. Lower WAIC values and higher pseudo-BMA weights indicate better model fit. Bayesian conditional R^2 values show the amount of variance explained by each model.

Species	**Model**	**WAIC**	**Weights**	$\boldsymbol{R^2_{\text{conditional}}}$
Brachaspis nivalis	**FL (linear)**	**355.1**	**0.746**	**0.936**
	FL (quadratic)	358.5	0.254	0.938
	FM (quadratic)	**-496.9**	**0.700**	**0.906**
	FM (linear)	-493.4	0.300	0.898
	M̂i (linear)	**-710.1**	**0.716**	**0.765**
	M̂i (quadratic)	-707.9	0.284	0.770
Paprides nitidus	**FL (quadratic)**	**350.4**	**0.993**	**0.978**
	FL (linear)	384.4	0.007	0.973
	FM (quadratic)	**-1,026.4**	**0.807**	**0.928**
	FM (linear)	-1,019.7	0.193	0.915
	M̂i (linear)	**-1,375.9**	**0.663**	**0.758**
	M̂i (quadratic)	-1,371.5	0.337	0.747
Sigaus australis	**FL (quadratic)**	**480.3**	**0.999**	**0.971**
	FL (linear)	539.2	0.001	0.962
	FM (quadratic)	**-487.1**	**0.962**	**0.941**
	FM (linear)	-473.5	0.038	0.926
	M̂i (linear)	**-795.7**	**0.680**	**0.733**
	M̂i (quadratic)	-793.0	0.320	0.728

Table S5. Posterior summary statistics for all definitive Bayesian linear mixed models examining biogeographic and environmental clines in body size components (FL, femur length; FM, fresh mass; M̂I, body condition) of three alpine grasshoppers (*Brachaspis nivalis*, *Paprides nitidus* and *Sigaus australis*) endemic to South Island, New Zealand. Diagnostic statistics indicated good model performance and convergence for all parameters included in the models as depicted by mean values ± standard deviation (SD) for the Rhat convergence diagnostic (R̂), effective posterior sample size (ESS), and Monte-Carlo Standard Error (MCSE). All models had the same random structure: (1| population) + (1|site) + (1|year). See Table S3 for variable abbreviations.

Model syntaxis (excluding random structure)	**R̂ ± SD**	**ESS ± SD**	**MCSE ± SD**
(a) *Brachaspis nivalis*			
FL ~ latitude × sex + elevation × sex	9,909 ± 185.9	1.000 ± 0.001	0.005 ± 0.008
FM ~ latitude^2 × sex + elevation × sex	9,821 ± 297.0	1.000 ± 0.001	0.002 ± 0.008
M̂i ~ latitude × sex + elevation × sex	9,937 ± 355.7	1.000 ± 0.002	0.002 ± 0.008
FL ~ temp driest qtr × sex + isotherm × sex	9,838 ± 352.3	1.000 ± 0.001	0.004 ± 0.009
FM ~ temp driest qtr × sex + isotherm × sex	9,894 ± 245.7	1.000 ± 0.001	0.002 ± 0.009
M̂i ~ prec season × sex + temp season	9,807 ± 331.1	1.000 ± 0.001	0.001 ± 0.008
(b) *Paprides nitidus*			
FL ~ latitude^2 × sex + elevation × sex	9,670 ± 401.1	1.000 ± 0.001	0.004 ± 0.010
FM ~ latitude^2 × sex + elevation × sex	9,899 ± 300.0	1.000 ± 0.001	0.002 ± 0.009
M̂i ~ latitude × sex + elevation × sex	9,858 ± 267.7	1.000 ± 0.001	0.002 ± 0.008
FL ~ prec season × sex	9,674 ± 354.5	1.000 ± 0.001	0.002 ± 0.009
FM ~ prec season × sex	9,891 ± 257.2	1.000 ± 0.001	0.001 ± 0.009
M̂i ~ temp season × sex + temp driest qtr × sex	9,837 ± 298.5	1.000 ± 0.001	0.001 ± 0.009
(c) *Sigaus australis*			
FL ~ latitude^2 × sex + elevation × sex	9,802 ± 263.2	1.000 ± 0.001	0.009 ± 0.017
FM ~ latitude^2 × sex + elevation × sex	9,833 ± 267.9	1.000 ± 0.001	0.003 ± 0.009
M̂i ~ latitude × sex + elevation × sex	9,813 ± 342.5	1.000 ± 0.001	0.002 ± 0.009
FL ~ isotherm × sex	9,737 ± 318.2	1.000 ± 0.001	0.003 ± 0.010
FM ~ isotherm × sex	9,856 ± 333.3	1.000 ± 0.001	0.002 ± 0.010
M̂i ~ isotherm × sex + temp wettest qtr × sex	9,775 ± 385.4	1.000 ± 0.001	0.002 ± 0.009

Table S6. Significant effects of latitude and elevation on body size components of three alpine grasshoppers (*Brachaspis nivalis*, *Paprides nitidus* and *Sigaus australis*) endemic to South Island, New Zealand. Median ± AD = point median estimate ± median absolute deviation, CI = credible interval (95% highest density interval), Pd = probability of direction, ROPE = full region of practical equivalence, σ = within-group variability, τ = between-group variability, ICC = intra-class correlation coefficient. The conditional R^2 indicates the amount of variance explained by the model, while the marginal R^2 considers only the variance of the fixed effects. Fixed terms with significant effects are in bold. N/A = parameters not included in the best fitted-model.

Parameter	Femur length				Fresh mass				Body condition			
	Median ± AD	**CI (95%)**	**Pd**	**ROPE**	**Median ± AD**	**CI (95%)**	**Pd**	**ROPE**	**Median ± AD**	**CI (95%)**	**Pd**	**ROPE**
(a) *Brachaspis nivalis*												
(intercept)	15.22 ± 0.38	14.32, 16.12	100	0.00	0.63 ± 0.05	0.50, 0.76	100	0.00	0.50 ± 0.02	0.44, 0.55	100	0.00
latitude	**3.03 ± 0.70**	**1.33, 4.68**	**99.63**	**0.29**	**1.42 ± 0.29**	**0.57, 2.20**	**99.37**	**0.06**	**0.08 ± 0.02**	**0.02, 0.15**	**99.04**	**0.58**
latitude^2	N/A	N/A	N/A	N/A	0.66 ± 0.45	-0.57, 1.86	90.49	1.91	N/A	N/A	N/A	N/A
elevation	0.49 ± 0.31	-0.14, 1.17	94.26	15.46	0.05 ± 0.03	-0.02, 0.11	93.76	16.04	-0.01 ± 0.01	-0.03, 0.01	92.11	19.88
sex	**-3.69 ± 0.10**	**-3.87, -3.50**	**100**	**0.00**	**-0.35 ± 0.01**	**-0.37, -0.32**	**100**	**0.00**	0.01 ± 0.01	-0.01, 0.02	78.90	53.01
latitude × sex	**-0.92 ± 0.33**	**-1.60, -0.29**	**99.65**	**0.96**	**-0.80 ± 0.17**	**-1.14, -0.47**	**100**	**0.00**	0.03 ± 0.02	-0.02, 0.08	89.98	9.12
latitude^2 × sex	N/A	N/A	N/A	N/A	**-0.34 ± 0.16**	**-0.67, -0.03**	**99.21**	**0.95**	N/A	N/A	N/A	N/A
elevation × sex	-0.19 ± 0.19	-0.55, 0.17	84.59	50.12	-0.02 ± 0.02	-0.07, 0.02	84.06	40.15	0.01 ± 0.01	-0.01, 0.04	84.81	23.05
Random effects												
σ	0.555				0.068				0.039			
$\tau_{population}$	0.566				0.007				0.002			
τ_{site}	0.248				0.002				0.001			
τ_{year}	0.129				0.002				0.003			
ICC	0.750				0.710				0.760			
$R^2_{conditional/marginal}$	0.936/0.742				0.906/0.677				0.765/0.135			
(b) *Paprides nitidus*												
(intercept)	15.63 ± 0.12	15.31, 15.96	100	0.00	0.65 ± 0.03	0.58, 0.71	100	0.00	0.36 ± 0.03	0.30, 0.43	100	0.00
latitude	1.96 ± 1. 86	-3.57, 8.14	83.29	4.67	0.13 ± 0.25	-0.65, 0.84	69.18	6.02	-0.03 ± 0.05	-0.15, 0.07	76.00	6.86
latitude^2	3.63 ± 1.56	-0.36, 7.83	95.82	1.18	0.23 ± 0.22	-0.38, 0.78	83.76	3.99	N/A	N/A	N/A	N/A
elevation	0.04 ± 0.09	-0.13, 0.22	68.38	98.71	0.01 ± 0.02	-0.02, 0.04	64.37	82.48	0.01 ± 0.01	-0.01, 0.02	67.47	40.55
sex	**-4.78 ± 0.04**	**-4.86, -4.70**	**100**	**0.00**	**-0.43 ± 0.01**	**-0.45, -0.42**	**100**	**0.00**	0.00 ± 0.01	-0.01, 0.01	76.49	54.56
latitude × sex	1.12 ± 0.78	-0.39, 2.64	92.80	8.64	-0.22 ± 0.13	-0.47, 0.05	94.89	3.45	0.01 ± 0.01	-0.02, 0.02	50.19	38.01
latitude^2 × sex	**-4.54 ± 0.76**	**-6.01, -3.02**	**100**	**0.00**	**-0.41 ± 0.13**	**-0.67, -0.16**	**99.94**	**0.11**	N/A	N/A	N/A	N/A
elevation × sex	0.07 ± 0.08	-0.10, 0.24	78.59	97.80	0.01 ± 0.01	-0.03, 0.03	51.52	87.56	-0.02 ± 0.01	-0.04, 0.00	95.45	11.10

Random effects												
σ	0.366				0.064				0.041			
$\tau_{population}$	0.089				0.002				0.003			
τ_{site}	0.016				0.001				0.001			
τ_{year}	0.019				0.003				0.002			
ICC	0.510				0.570				0.750			
$R^2_{conditional/marginal}$	0.978/0.957				0.928/0.834				0.754/0.028			
(c) *Sigaus australis*												
(intercept)	17.30 ± 0.30	16.43, 18.17	100	0.00	0.83 ± 0.08	0.63, 1.05	99.99	0.01	0.51 ± 0.04	0.39, 0.61	100	0.00
latitude	-6.25 ± 5.02	-21.40, 7.80	87.74	1.65	-1.69 ± 1.37	-5.18, 2.03	87.60	1.06	-0.07 ± 0.07	-0.24, 0.10	83.84	5.27
latitude^2	-9.21 ± 5.17	-25.43, 4.06	95.12	1.12	-1.20 ± 1.54	-6.07, 2.13	82.02	1.39	N/A	N/A	N/A	N/A
elevation	0.45 ± 0.15	-0.15, 0.75	99.65	16.79	0.05 ± 0.02	0.00, 0.10	98.78	17.35	0.01 ± 0.01	-0.01, 0.04	85.01	26.76
sex	**-5.99 ± 0.07**	**-6.13, -5.85**	**100**	**0.00**	**-0.63 ± 0.01**	**-0.65, -0.60**	**100**	**0.00**	-0.01 ± 0.01	-0.02, 0.01	76.07	51.69
latitude × sex	**5.85 ± 1.12**	**3.70, 8.13**	**100**	**0.00**	**1.47 ± 0.20**	**1.09, 1.88**	**100**	**0.00**	0.01 ± 0.01	-0.02, 0.04	81.02	29.25
latitude^2 × sex	**9.76 ± 1.22**	**7.38, 12.09**	**100**	**0.00**	**0.85 ± 0.22**	**0.42, 1.25**	**100**	**0.00**	N/A	N/A	N/A	N/A
elevation × sex	-0.55 ± 0.14	-0.93, -0.18	98.97	4.09	-0.01 ± 0.02	-0.06, 0.04	69.29	76.79	0.02 ± 0.01	-0.01, 0.05	90.50	20.77
Random effects												
σ	0.544				0.098				0.057			
$\tau_{population}$	0.580				0.039				0.005			
τ_{site}	0.068				0.001				0.001			
τ_{year}	0.140				0.007				0.002			
ICC	0.730				0.830				0.700			
$R^2_{conditional/marginal}$	0.971/0.894				0.941/0.648				0.728/0.087			

Table S7. Significant effects of climate factors on body size components of three alpine grasshoppers (*Brachaspis nivalis*, *Paprides nitidus* and *Sigaus australis*) endemic to South Island, New Zealand. Median ± AD = point median estimate ± median absolute deviation, CI = credible interval (95% highest density interval), Pd = probability of direction, ROPE = full region of practical equivalence, σ = within-group variability, τ = between-group variability, ICC = intra-class correlation coefficient. The conditional R^2 indicates the amount of variance explained by the model, while the marginal R^2 considers only the variance of the fixed effects. Fixed terms with significant effects are in bold. N/A = parameters not included in the best fitted-model. Abbreviations as in Table 2.

Parameter	Femur length				Fresh mass				Body condition			
	Median ± AD	**CI (95%)**	**Pd**	**ROPE**	**Median ± AD**	**CI (95%)**	**Pd**	**ROPE**	**Median ± AD**	**CI (95%)**	**Pd**	**ROPE**
(a) *Brachaspis nivalis*												
(intercept)	15.53 ± 0.56	14.07, 16.72	100	0.00	0.70 ± 0.07	0.55, 0.86	100	0.00	0.46 ± 0.03	0.40, 0.53	100	0.00
temp driest qtr	**-2.23 ± 0.76**	**-3.77, -0.69**	**99.71**	**0.59**	**-0.24 ± 0.08**	**-0.41, -0.08**	**99.66**	**0.34**	N/A	N/A	N/A	N/A
isotherm	-1.45 ± 1.00	-3.95, 0.60	92.70	4.75	-0.18 ± 0.11	-0.44, 0.05	94.56	3.48	N/A	N/A	N/A	N/A
prec season	N/A	N/A	N/A	N/A	N/A	N/A	N/A	N/A	**-0.10 ± 0.03**	**-0.16, -0.01**	**99.17**	**0.70**
temp season	N/A	N/A	N/A	N/A	N/A	N/A	N/A	N/A	0.02 ± 0.02	-0.03, 0.07	83.56	12.78
sex	**-3.75 ± 0.09**	**-3.92, -3.57**	**100**	**0.00**	**-0.36 ± 0.01**	**-0.38, -0.34**	**100**	**0.00**	0.00 ± 0.01	-0.01, 0.02	71.30	58.40
temp driest qtr × sex	**0.84 ± 0.31**	**0.24, 1.45**	**99.63**	**0.97**	**0.20 ± 0.04**	**0.13, 0.28**	**100**	**0.00**	N/A	N/A	N/A	N/A
isotherm × sex	0.24 ± 0.19	-0.14, 0.61	90.07	39.95	0.03 ± 0.02	-0.01, 0.08	90.98	29.16	N/A	N/A	N/A	N/A
prec season × sex	N/A	N/A	N/A	N/A	N/A	N/A	N/A	N/A	**-0.04 ± 0.01**	**-0.06, -0.01**	**99.55**	**0.97**
temp season × sex	N/A	N/A	N/A	N/A	N/A	N/A	N/A	N/A	-0.03 ± 0.02	-0.07, 0.00	97.01	5.14
Random effects												
σ	0.556				0.068				0.040			
$\tau_{population}$	1.308				0.014				0.001			
τ_{site}	0.233				0.002				0.001			
τ_{year}	0.075				0.005				0.003			
ICC	0.840				0.820				0.710			
$R^2_{conditional/marginal}$	0.940/0.627				0.919/0.583				0.811/0.249			
(b) *Paprides nitidus*												
(intercept)	15.68 ± 0.10	15.44, 15.95	100	0.00	0.65 ± 0.02	0.59, 0.71	100	0.00	0.37 ± 0.02	0.33, 0.41	100	0.00
prec season	-0.44 ± 0.16	-0.81, 0.02	97.22	12.53	-0.04 ± 0.02	-0.08. 0.01	95.29	23.76	N/A	N/A	N/A	N/A
temp season	N/A	N/A	N/A	N/A	N/A	N/A	N/A	N/A	**-0.05 ± 0.01**	**-0.08, -0.02**	**99.69**	**0.38**
temp driest qtr	N/A	N/A	N/A	N/A	N/A	N/A	N/A	N/A	0.03 ± 0.02	-0.01, 0.06	93.93	5.86
sex	**-4.82 ± 0.04**	**-4.90, -4.74**	**100**	**0.00**	**-0.44 ± 0.01**	**-0.45, -0.43**	**100**	**0.00**	0.00 ± 0.01	-0.01, 0.01	53.81	58.21
prec season × sex	**0.31 ± 0.08**	**0.16, 0.47**	**100**	**0.98**	**0.06 ± 0.01**	**0.03, 0.08**	**100**	**0.58**	N/A	N/A	N/A	N/A
temp season × sex	N/A	N/A	N/A	N/A	N/A	N/A	N/A	N/A	0.01 ± 0.01	-0.02, 0.03	69.00	25.43
temp driest qtr × sex	N/A	N/A	N/A	N/A	N/A	N/A	N/A	N/A	0.03 ± 0.02	0.00, 0.07	95.77	4.54

Random effects												
σ	0.375				0.063				0.041			
$\tau_{population}$	0.053				0.001				0.001			
τ_{site}	0.023				0.001				0.001			
τ_{year}	0.016				0.003				0.002			
ICC	0.410				0.510				0.540			
$R^2_{conditional/marginal}$	0.977/0.961				0.928/0.855				0.582/0.084			
(c) *Sigaus australis*												
(intercept)	17.54 ± 0.14	17.17, 17.89	100	0.00	0.88 ± 0.04	0.77, 0.99	100	0.00	0.49 ± 0.03	0.41, 0.56	100	0.00
isotherm	**1.16 ± 0.18**	**0.78, 1.51**	**100**	**0.04**	**0.21 ± 0.03**	**0.15, 0.28**	**100**	**0.00**	0.05 ± 0.05	-0.05, 0.14	83.64	7.93
temp wettest qtr	N/A	N/A	N/A	N/A	N/A	N/A	N/A	N/A	0.02 ± 0.04	-0.05, 0.10	74.40	14.73
sex	**-6.18 ± 0.08**	**-6.34, -6.02**	**100**	**0.00**	**-0.68 ± 0.01**	**-0.70, -0.65**	**100**	**0.00**	-0.01 ± 0.01	-0.02, 0.01	82.76	48.81
isotherm × sex	**-0.81 ± 0.16**	**-0.12, -0.50**	**100**	**0.09**	**-0.23 ± 0.02**	**-0.27, -0.18**	**100**	**0.00**	-0.03 ± 0.02	-0.07, 0.00	95.43	8.68
temp wettest qtr × sex	N/A	N/A	N/A	N/A	N/A	N/A	N/A	N/A	-0.05 ± 0.02	-0.09, -0.01	98.87	2.77
Random effects												
σ	0.601				0.095				0.056			
$\tau_{population}$	0.047				0.006				0.004			
τ_{site}	0.044				0.001				0.001			
τ_{year}	0.077				0.006				0.002			
ICC	0.420				0.610				0.680			
$R^2_{conditional/marginal}$	0.961/0.943				0.927/0.821				0.691/0.033			

Figure S1. Visual representation of morphological features used to characterise adult structural body size variation in three alpine grasshoppers (*Brachaspis nivalis*, *Paprides nitidus* and *Sigaus australis*) endemic to South Island, New Zealand. Body dimensions: left hind femur length (FL), maximum left femur width (FW) and mid-line pronotum length (PL).

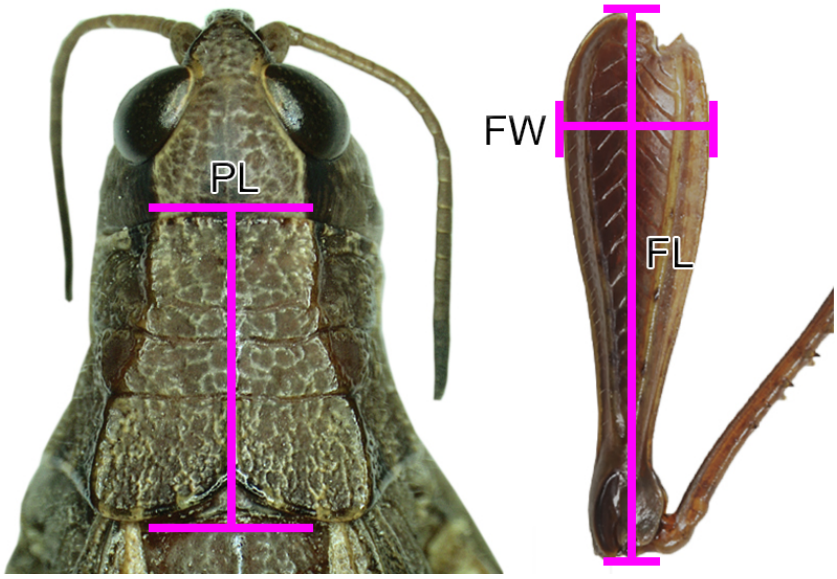

Figure S2. Relationships between body dimensions (mm) and mass estimates (g) and in three New Zealand grasshopper species (*Brachaspis nivalis, Paprides nitidus* and *Sigaus australis*) endemic to South Island, New Zealand. Pairwise correlation coefficients between body size proxies (FL, left hind femur length; FW, maximum left femur width; PL, mid-line pronotum length; FM, fresh mass) are shown. Significant ($p < 0.001$) correlations are denoted by three asterisks (***). Measurements were done by the same person to minimise operator error.

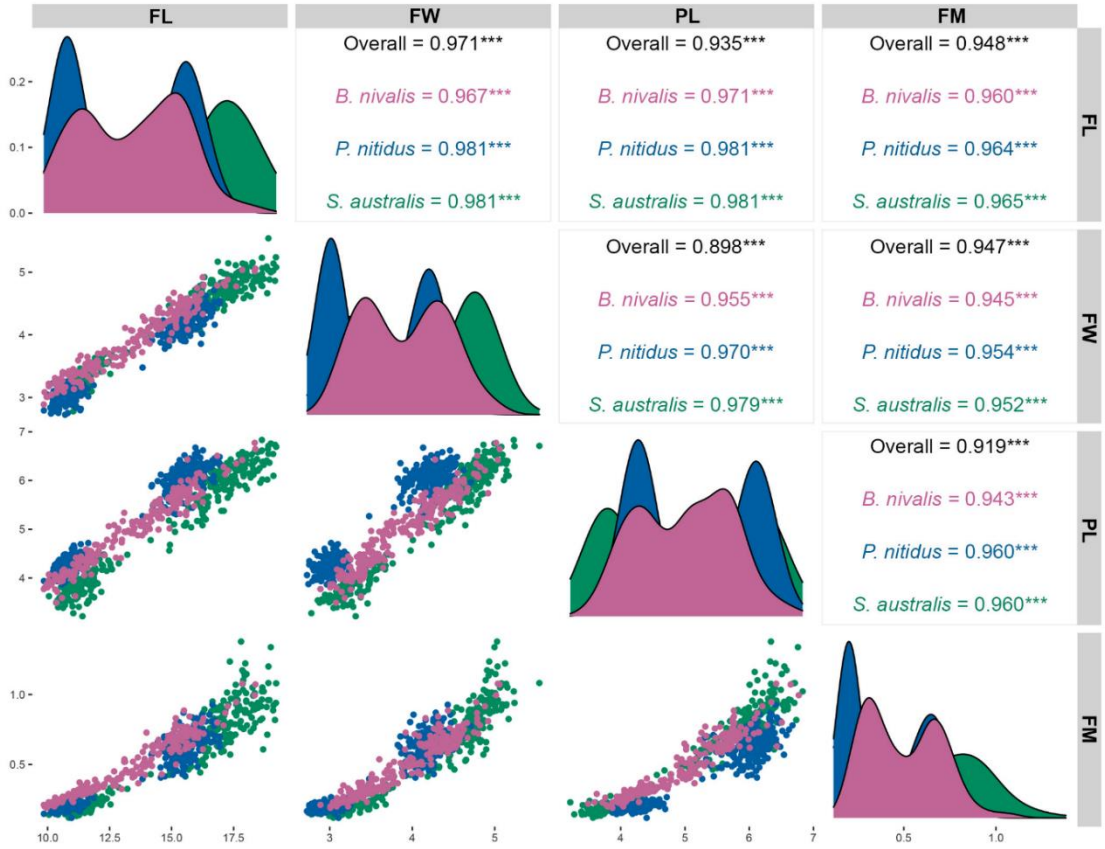

Figure S3. Repeatability (R) analyses of the studied body size dimensions (FL, left hind femur length; FW, maximum left femur width; PL, mid-line pronotum length) in three New Zealand grasshopper species (*Brachaspis nivalis*, *Paprides nitidus* and *Sigaus australis*) endemic to South Island, New Zealand, indicated high reproducibility with a technical measurement error biologically negligible. For estimations we randomly selected five males and five females per species to then remeasured body dimensions five times, remounting specimens between successive measurements. Repeatability was calculated independently for size proxy (top panel), species (middle panel) and sexes (bottom panel) with the R package rptR (Stoffel et al., 2017), using specimen as a grouping term. The ratio of intra-observer variance (i.e., R) was calculated as the among-group variance (VG) over the sum of group-level and within-group (residual) variance (VR): R = VG / (VG + VR). White points indicate mean values.

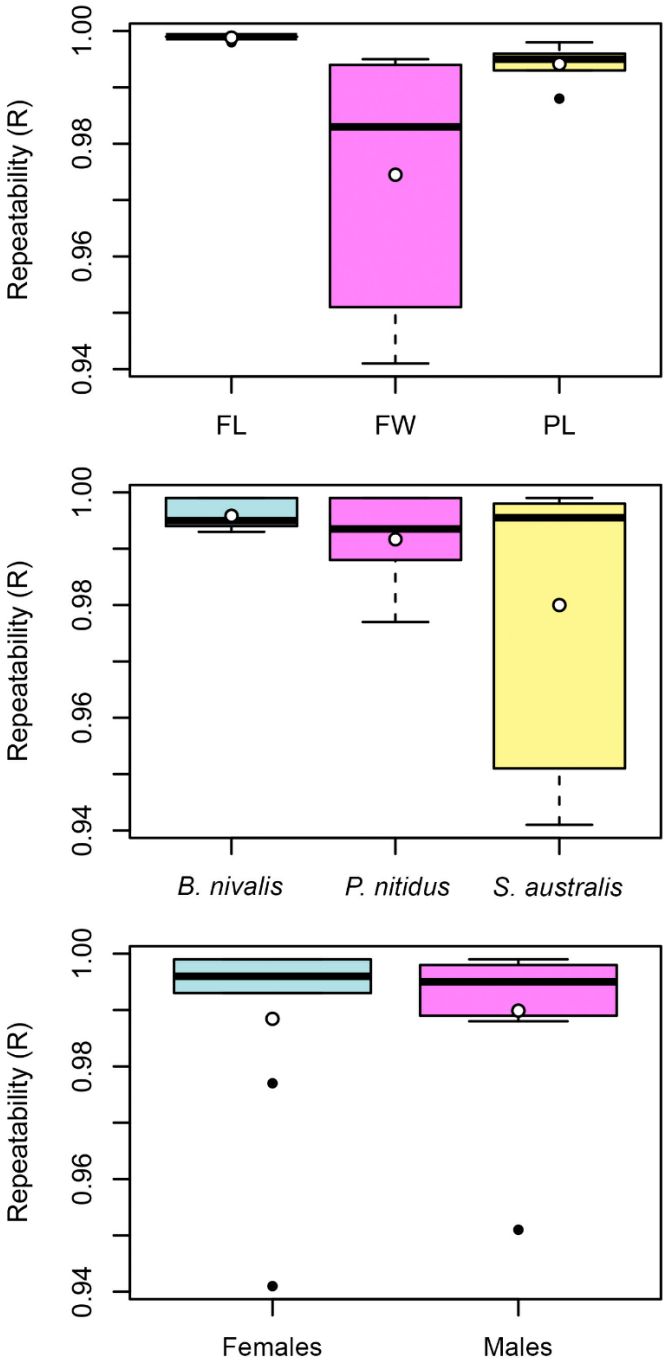

Figure S4. Density plots showing differences in size components in three New Zealand grasshopper species (*Brachaspis nivalis*, *Paprides nitidus and Sigaus australis*) endemic to South Island, New Zealand. Plots are arranged by mountain and latitude (north to south). Note female-biased size dimorphism (i.e. females larger than males) is evident in femur length and fresh mass, but not in body condition (see main text for details).

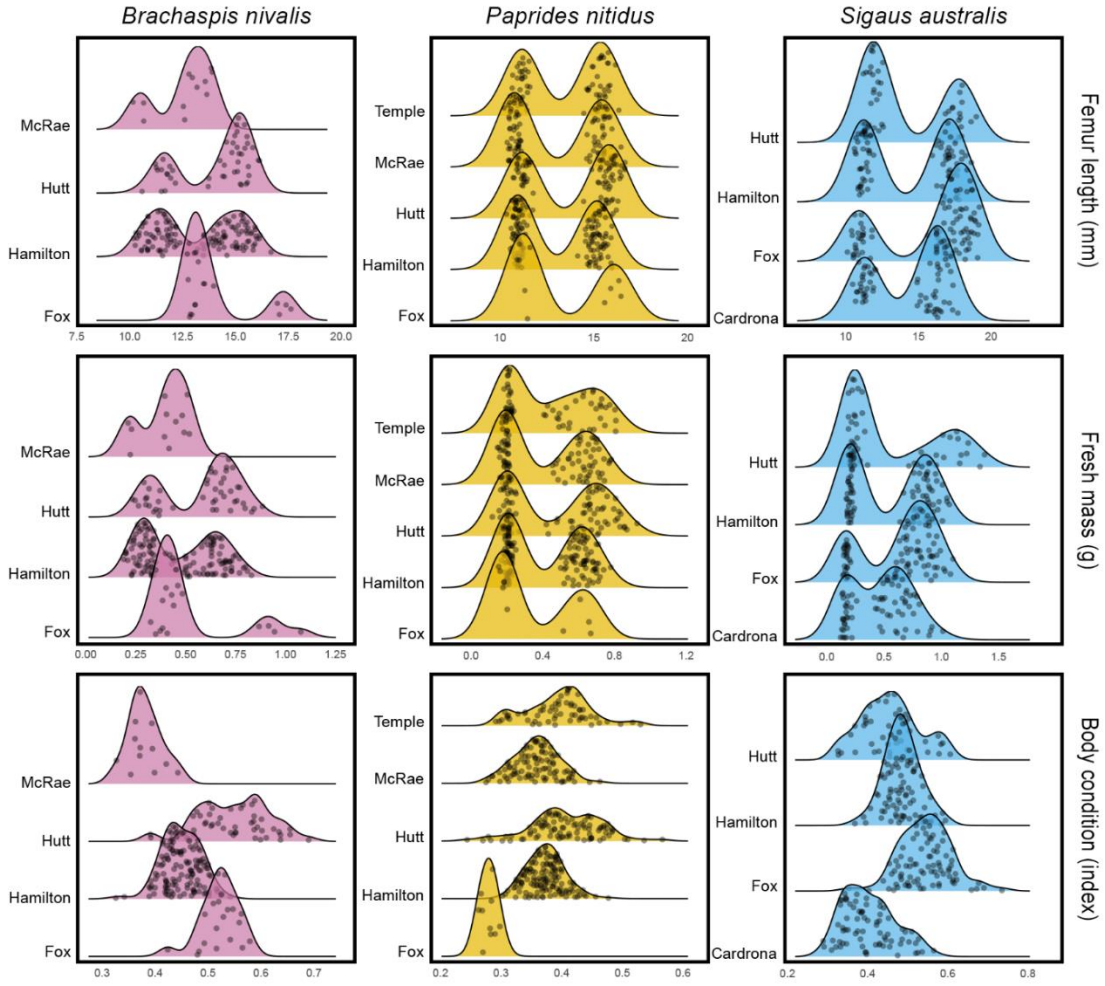

Figure S5. Scatterplot showing linear associations between both absolute latitude (right panels) and elevation (left panels) and the six predictors (see Table S3 for details) used to quantify the influence of climate on body size variation in three alpine grasshoppers (*Brachaspis nivalis*, *Paprides nitidus* and *Sigaus australis*) endemic to South Island, New Zealand.

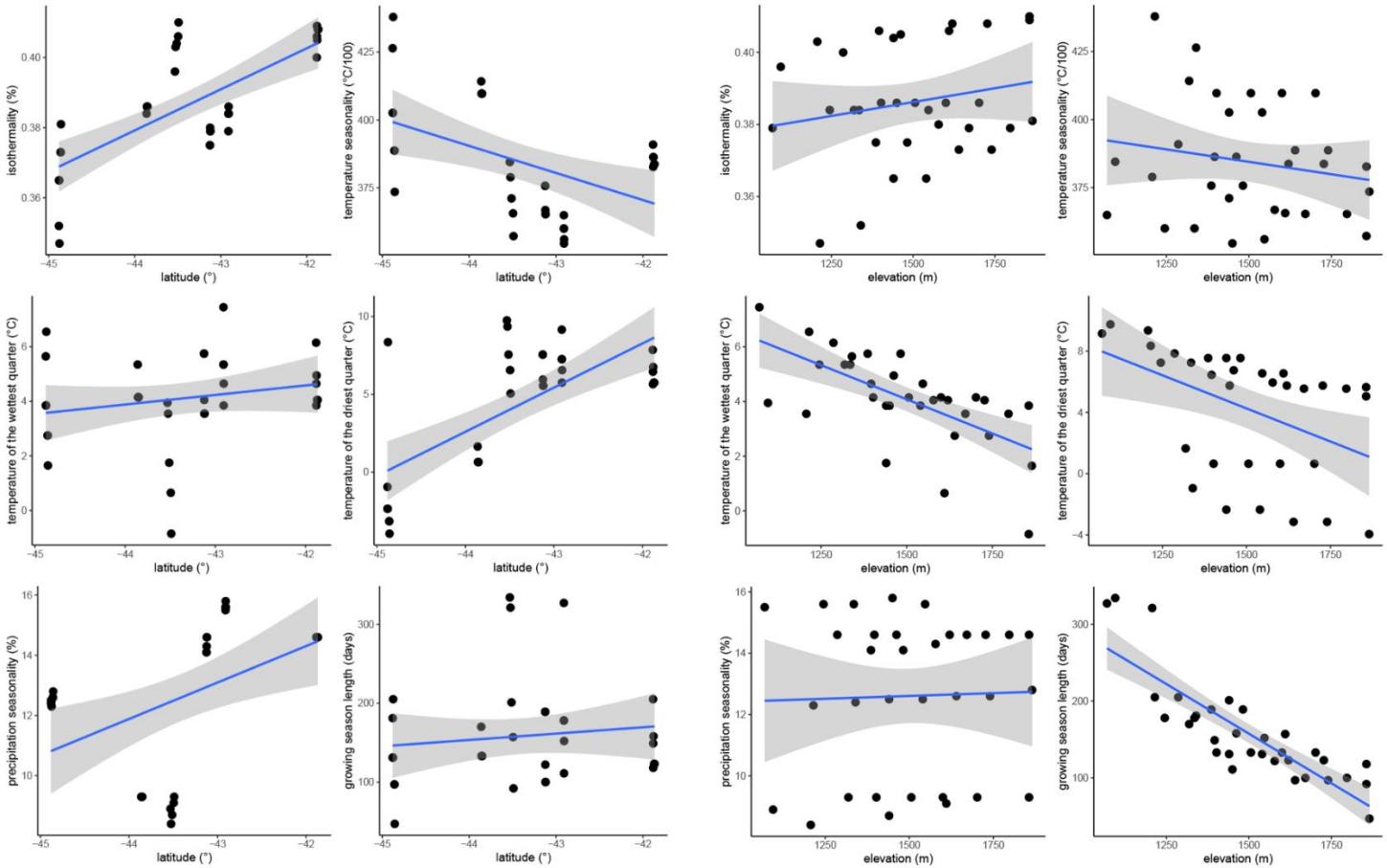

Figure S6. Projection predictive variable selection for climate factors explaining variation in body size components of three alpine grasshoppers (*Brachaspis nivalis*, top panel; *Paprides nitidus*, middle panel; and *Sigaus australis*, bottom panel) endemic to South Island, New Zealand. Ranking of climate predictors based on the difference in the expected log predictive density (ELPD) and root-mean-squared error (RMSE) between the reference model and the fitted submodels. When overlapping, ranking points were slightly jittered for clarity. Solid points indicate predictors selected as relevant, others add only marginal model improvement. Abbreviations: isothermality (isotherm), temperature seasonality (temp season), mean air temperature of the wettest quarter (temp wettest qtr), mean air temperature of the driest quarter (temp driest qtr), precipitation seasonality (prec season), growing season length (grow length).

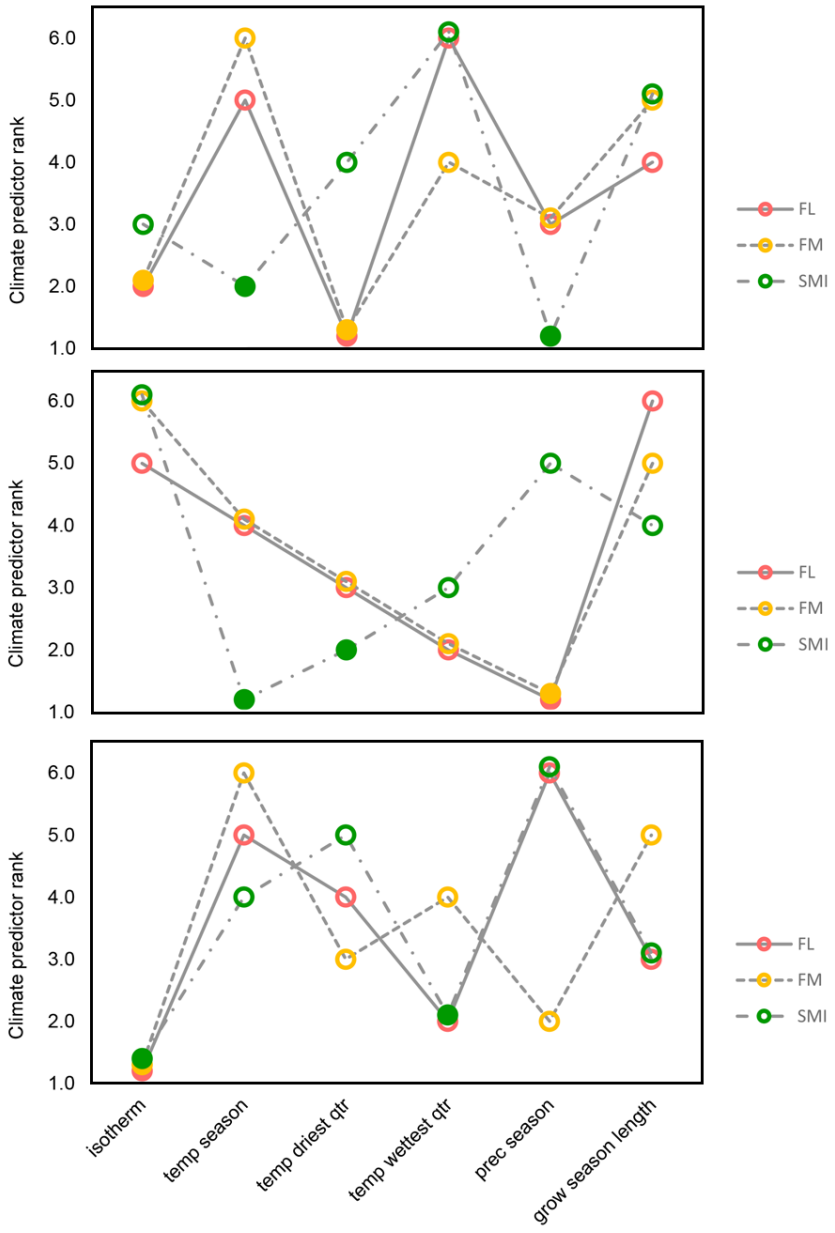

Figure S7. Posterior parameter estimates for the best-fitted models examining the effects of latitude and elevation on body size components (FL, femur length; FM, fresh mass; M̂I, body condition) of three alpine grasshopper species (*Brachaspis nivalis*, *Paprides nitidus* and *Sigaus australis*) endemic to South Island, New Zealand. The inner uncertainty interval 75% (thick horizontal lines) and the outer uncertainty interval 95% (thin horizontal lines) are shown. The midpoint estimates show the posterior medians of the Markov chain Monte Carlo (MCMC) draws using Hamiltonian Monte Carlo (HMC) sampling. Midpoints in blue indicate significant effects (i.e. 95% HDI did not overlap zero and ROPE < 1%).

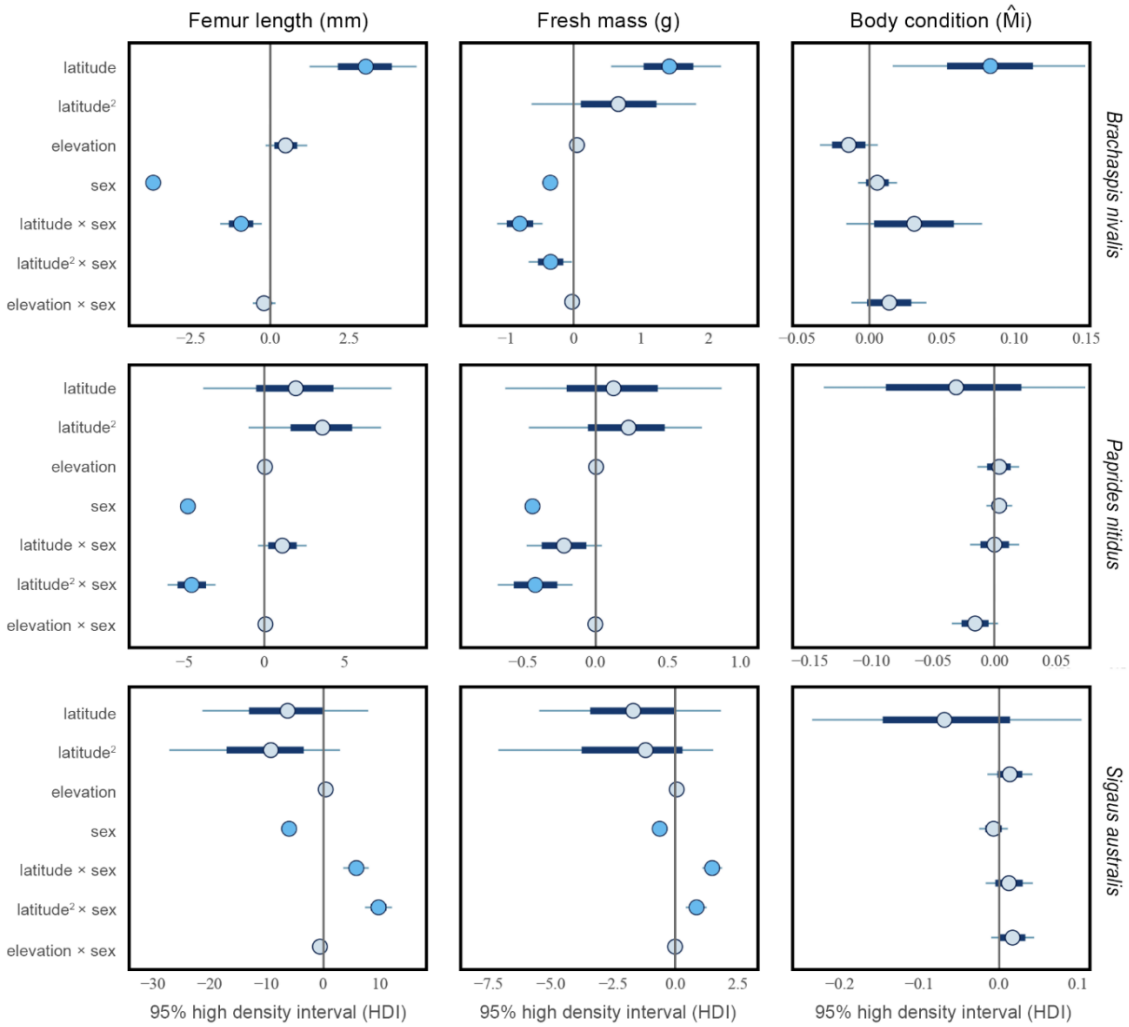

Figure S8. Posterior parameter estimates for the final models examining the effects of climatic factors on body size components (FL, femur length; FM, fresh mass; M̂i, body condition) of three alpine grasshopper species (*Brachaspis nivalis*, *Paprides nitidus* and *Sigaus australis*) endemic to South Island, New Zealand. The inner uncertainty interval 75% (thick horizontal lines) and the outer uncertainty interval 95% (thin horizontal lines) are shown. The midpoint estimates show the posterior medians of the Markov chain Monte Carlo (MCMC) draws using Hamiltonian Monte Carlo (HMC) sampling. Midpoints in blue indicate significant effects (i.e. 95% HDI did not overlap zero and ROPE < 1%). Abbreviations: isothermality (isotherm), temperature seasonality (temp season), mean temperature of the wettest quarter (temp wettest qtr), mean temperature of the driest quarter (temp driest qtr), precipitation seasonality (prec season).

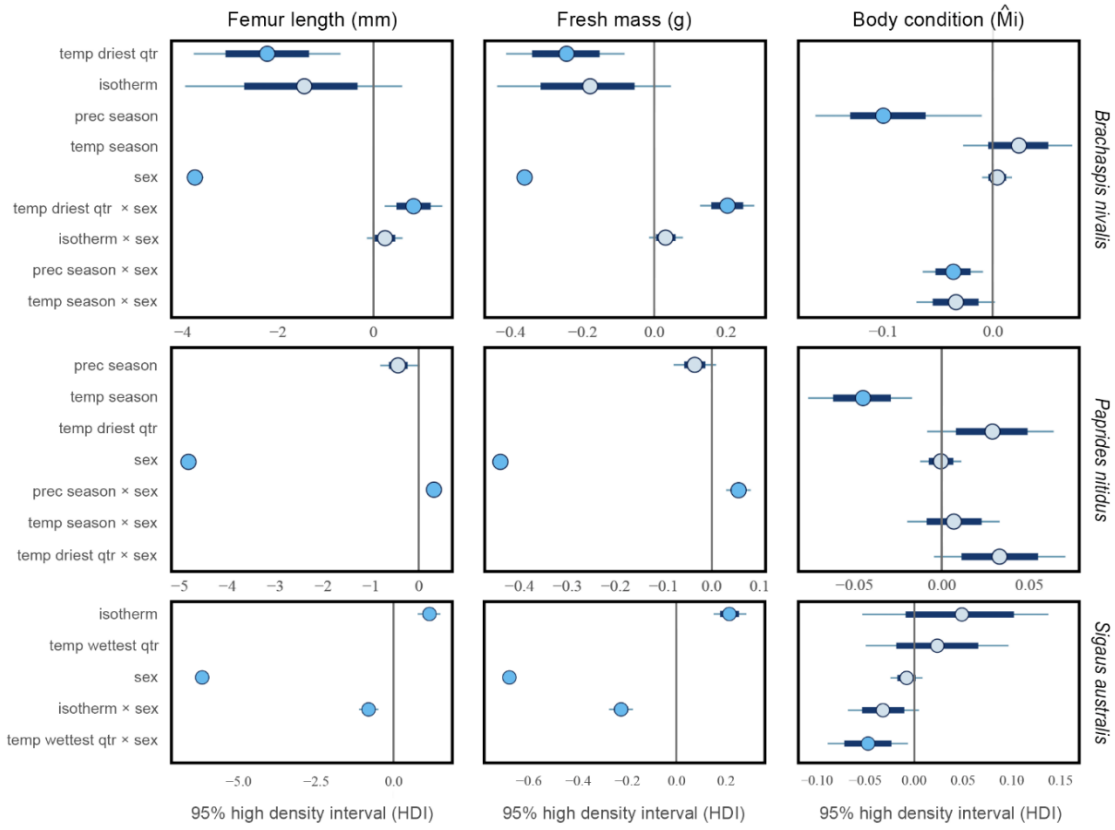

Supplementary references

Naimi, B., Hamm, N. A., Groen, T. A., Skidmore, A. K., & Toxopeus, A. G. (2014). Where is positional uncertainty a problem for species distribution modelling? *Ecography*, *37*(2), 191–203. https://doi.org/10.1111/j.1600-0587.2013.00205.x

Stoffel, M. A., Nakagawa, S. & Schielzeth, H. (2017). rptR: Repeatability estimation and variance decomposition by generalized linear mixed-effects models. *Methods in Ecology and Evolution*, *8*, 1639–1644. https://doi.org/10.1111/2041-210X.12797

“Hence, when the warmth had fully returned, the same arctic species, which had lately lived in a body together on the lowlands of the Old and New Worlds, would be left isolated on distant mountain-summits (having been exterminated on all lesser heights) and in the arctic regions of both hemispheres.”

(Darwin, 1859, p. 367)

Sigaus villosus, a mountaintop-dwelling grasshopper within the New Zealand alpine radiation. Nervous Knob, Hamilton Peak, Craigieburn Forest Park, South Island.

Chapter Six

General discussion: Forecasting the future of alpine habitat specialists

"This model will be a simplification and an idealization, and consequently a falsification. It is to be hoped that the features retained for discussion are those of greatest importance in the present state of knowledge."

(Turing, 1952, p. 5)

Thesis conclusions: the foreseen future of New Zealand alpine insects

Climatic, biological, and geophysical factors controlled population structuring of flightless, cold-adapted grasshopper species during the Pleistocene with a legacy of spatially separate intraspecific lineages. Temperature is a key predictor of species' ranges in the studied grasshopper system but fails to fully-predict patterns of phenotypic variation. Departures from current climatic conditions are projected to vary with geography, and so species exposure and vulnerability to global warming, and this might strongly influence potential responses. While distinct climate envelopes indicate microhabitat segregation at inter and intraspecific levels, all studied species are expected to experience severe habitat reduction and fragmentation as rising temperatures drive suitable habitat to higher elevations, resulting in population contractions, range shifts, local extinctions and genetic erosion. Although current levels of intraspecific diversity, both genetic and phenotypic, suggest adaptative potential, the rate of habitat loss predicted over the next 50 years of warming will lead to smaller and more-fragmented populations with reduced adaptive potential (Willi et al., 2006). They are unlikely to have the genotypic scope to respond to natural selection arising directly from rapid climate change and other anthropogenic threats (Bowler et al., 2020). Species of New Zealand alpine grasshopper co-occur throughout their ranges (Bigelow, 1967; Trewick & Morris, 2008; Trewick et al., 2023) and interact with other biotic and abiotic elements that likely affect their ability to persist under environmental change (see Thompson & Fronhofer, 2019). Critically, differences in niche features between diverging intraspecific lineages

suggest distinct responses to climate change, and this has implications for prioritising conservation actions and management strategies.

The New Zealand alpine environment harbours other wing-reduced and flightless animal lineages with limited dispersal ability and increased body sizes relative to their lower elevation counterparts (Goldberg et al., 2008; McCulloch & Waters, 2018), thus distributional and phenotypic restructuring in response to global warming would be geographically and taxonomically widespread. This would lead to novel biological communities with rewired size profiles and ecological interactions (e.g. Wu et al., 2019) that are also exposed to biological invasions (see Hulme, 2017). Beyond range and phenotypic shifts, other relevant biotic responses (e.g. phenological and behavioural) remain poorly studied. While our current understanding of species responses to climate change comes from studies on gradual warming (Thakur et al., 2022), extreme climatic events and interactions with other anthropogenic threats might expose alpine biota to selective pressures not encountered by their ancestors (see Harvey et al., 2020). Other potentially valuable key research fields include thermal biology of alpine life, genetic basis of alpine adaptations and biological invasion processes and effects on alpine environments (see Buckley et al., 2022). An important finding of the present research on alpine grasshoppers is that closely related species are predicted to respond in different ways to climate change, suggesting such responses are more evolutionarily labile than conserved (Diamond, 2018). The thermal environment is a powerful abiotic driver of evolution, and as we face unparalleled rates of warming, understanding how temperature hinder or foster evolution is critical (McGaughran et al., 2021).

Species range shift forecast and uncertainty

Ecological niche modelling (ENM) is the keystone tool for predicting warming-driven range shifts, particularly models using a purely correlative approach that directly links species occurrences and primarily climatic predictors (Briscoe et al., 2019; Dormann et al., 2012; Wiens et al., 2009). Although data-friendly (relying on either presence-only or presence-absence data), correlative models are limited in their predictions and transferability to novel conditions, and ignore the biological mechanism(s) driving biotic responses to climate change (Briscoe et al., 2019; Dormann et al., 2012), including

physiology, biotic interactions, demography, evolution, dispersal, and spatial climate gradients (Urban et al., 2016). Like any mathematical models, ENMs make assumptions, both biological (e.g. equilibrium and habitat saturation) and statistical (e.g. bias, imperfect detection), and incorporate uncertainties related to the scale choice and accuracy of the input data, including that from climatic general circulation models (Briscoe et al., 2019; Dormann et al., 2012; Wiens et al., 2009). More critically, the circular nature of the modelling process precludes any attempt for hypothesis testing (i.e. the modelled causal relationship), as the same data used for hypothesis formulation cannot be use for testing (Dormann et al., 2012).

Several methods to boost inferences from correlative models have been applied to New Zealand alpine specialist, including ensemble forecasting to ensure multiple projections are integrated (e.g. Carmelet-Rescan et al., 2021; Koot et al., 2022; Meza-Joya et al., 2023; Chapter 4), statistical procedures to reduce overfitting and consider extrapolation risks (e.g. Meza-Joya et al., 2023; Chapter 4), pre-modelling methods to account for past human-driven fire regimes promoting range shifts and post-modelling analyses to detect spatial patterns of vulnerability and exposure to global warming (e.g. Meza-Joya et al., 2023). Accompanying correlative modelling with alternative methods such as phylogeography and historical demography (e.g. Carmelet-Rescan et al., 2021; King et al., 2020; Meza-Joya et al., 2023; Chapter 4), linear and geometric morphometrics (Carmelet-Rescan et al., 2021; Meza-Joya et al., 2023; Chapter 4), range shift statistics (Koot et al., 2022), genotype-phenotype-environment associations (Chapter 4), and climate niche factor analyses (Meza-Joya et al., 2023; Chapter 4) offers a way to explore biological mechanism(s) and species sensitivities and exposures to climate. Yet, reconciling inferences from distinct approaches is challenging, each method has its own assumptions, and ambiguous or conflicting results can hinder confidence (e.g. Marske et al., 2011; Chapter 4). As raising temperatures push alpine environments uphill and novel biotic interactions become apparent, models that explicitly incorporate ecological processes are promising to improve range shift forecasts and increase our understanding of the mechanisms that drive range dynamics (Briscoe et al., 2019; Urban et al., 2016).

A number of approaches exist to explicitly state the processes omitted by correlative models, often called process-based (or mechanistic) models (but see Connolly et al., 2017). By simulating the mechanisms driving range and population dynamics, such

models are expected to inform more realistic projections of species' responses to climate change (Briscoe et al., 2019; Urban et al., 2016). Nevertheless while promising, process-explicit methods also make assumptions (reviewed in Briscoe et al., 2019), some of them (e.g. unbiased sampling) shared with correlative models, are data-hungry and their application often require substantial computing power and technical expertise (Briscoe et al., 2019; Diamond, 2018; Dormann et al., 2012). Hybrid models offer promising alternative to overcome the limitations of both purely correlative and mechanistic models, by combining both approaches and allowing the use of multiple data types (Diamond, 2018; Dormann et al., 2012). This could improve range shift forecasts by simulating processes that might drive responses to climate change, such as dispersal ability and evolution of range-limiting traits (e.g. body size) to track their preferred niche; physiological tolerances and exposure and vulnerability patterns; evolutionary potential and local adaptation to persist in place; and novel biotic interactions. Although hybrid modelling approaches may improve predictions of species responses to global warming, there is no silver bullet in ENM, and the best approach will depend on the specific questions being asked and data availability (Dormann et al., 2012; Briscoe et al., 2019).

Data limitations, challenges, and opportunities

Alpine ecosystems are under increasing anthropogenic pressure (Frazier & Brewington, 2019; Greenwood & Jump, 2014; Pauli & Halloy, 2019), but efforts to predict the future of alpine life are hindered by considerable data challenges. The harsh environmental conditions of the alpine zone pose logistical challenges for sampling: most alpine systems are difficult to access, and sampling (especially for alpine invertebrates) is typically limited to the summer season, making data spatially, temporally, and taxonomically biased. Indeed, a small portion of the alpine environments have been systematically surveyed by researchers, and this is true of the Southern Alps of New Zealand, where large alpine tracts remaining unsurveyed. This has resulted in a general lack of ecological, distributional, phenotypic, and molecular data for most alpine species. Data scarcity, though, is not restricted to the biotic components of these systems. Available climatic data used for ENM are too coarse (1-km scale size) and ignore relevant local topographic factors that create fine-scale variation in climate (Zellweger et al., 2019) that can create microrefugia for some alpine species under global warming (e.g. Meineri & Hylander,

2017). We know, for example, that many New Zealand alpine species show fine-scale micro-habitat partitioning (e.g. Bigelow, 1967; Meudt et al., 2009; White, 1974). Notably, these species have shifted their ranges following Polynesian fires (Halloy & Mark, 2003), but we lack spatial data on historical fire regimens to account for this phenomena. Filling these major data gaps is crucial to understand how alpine diversity is distributed and the mechanisms underlying its spatial variation, and to improve forecasts of responses to climate change and other anthropogenic threats.

Although systematic data collection efforts using standardised sampling protocols are essential to overcome current data limitations, they are usually time consuming and costly. Meanwhile, scientific literature and natural history collections contain large amounts of valuable data for elucidating biodiversity responses to environmental change (Holmes et al., 2016; Le Guillarme & Thuiller, 2022; Millien et al., 2006; Shaffer et al., 1998). Historical location data (e.g. records from museums, journal articles, and field notes) hold value for inferring range shifts (Shaffer et al., 1998; Tingley & Beissinger, 2009) using distinct modelling approaches. Wildlife observations from citizen science programs (e.g. iNaturalist NZ, https://inaturalist.nz) are increasingly available online, enabling rapid access to locality data. While data from such sources are usually opportunistic occurrence data and presence surveys, and can carry geolocation errors, a variety of approaches ease such limitations. For instance by generating target-group absences or pseudo-absences to generate presence-absence data (Mateo et al., 2010) and using geolocation-correction methods (e.g. point-radius or nearest geographical point) to adjust imprecisely georeferenced data (Smith et al., 2022) in a way that best informs range forecasts. In New Zealand, studies accounting for these issues have proved effective for improving the statistical accuracy of range shift forecasts for alpine and non-alpine species (e.g. Carmelet-Rescan et al., 2021; Koot et al., 2022; Sivyer et al., 2018; Mathias et al., 2023; Meza-Joya et al., 2023).

Natural history collections are key sources of long-term data for examining morphological (Millien et al., 2006) and genetic shifts (Holmes et al., 2016) in response to climate change. While obtaining reliable morphological data from museum specimens can be difficult due to fixation (e.g. chemical agents affecting body mass) and preservation issues (e.g. fragmentation or loss of appendages), allometric scaling models have helped to overcome such limitations (Kendall et al., 2019; Meza-Joya et al., 2022).

These models have proved efficient for obtaining mass estimates to test changes in beetle body size in response to global warming (e.g. Tseng et al., 2018) and butterfly biomass over space and time (e.g. Macgregor et al., 2019, Kinsella et al., 2020), and have provided an effective tool to overcome body mass sampling gaps in our alpine grasshoppers (Chapter 5). Moreover, museum specimens have been central to examination of ecogeographical rules describing relationships between body size and climate (reviewed in Millien et al., 2006). As fixation and preservation are also critical for DNA recovery, most genetic studies using historical samples are limited to small fragments from few loci (Card et al., 2021; Holmes et al., 2016). Despite this, studies using historical and modern population of alpine squirrels have shown the value of museum specimens for detecting warming-driven genetic erosion and restructuring (Bi et al., 2013; Rubidge et al., 2012).

A New Zealand case study: Resurveying to infer insect-host plant shifts over time

Phytophagous insects and the plants they feed on have been interacting in complex but synchronic ways for millions of years (Labandeira, 2013). Environmental shifts can modify plant-insect interactions by influencing host plant defence responses to insects (Jamieson et al., 2017). Thus, insect herbivores are under strong selection pressure to find quality host plants in changing environments (Bruce et al., 2015). Despite this co-dependency, the responses of insect herbivores and their host plants to rapid global warming are typically studied in isolation (Kerner et al., 2023). Previous studies on New Zealand alpine systems have shown wide fluctuations in the relative contribution of plants to grasshopper diets (Watson, 1970) and fine-scale ecological partitioning when grasshopper species occur in sympatry (Bigelow, 1967; White, 1974). This suggests that grasshopper occurrences depend on the presence of microhabitats with suitable host plants. While longitudinal alpine vegetation monitoring has a long history in New Zealand (e.g. Evans, 1973; Dickinson et al., 1992; Duncan et al., 2001), historical surveys accounting for both plant and insect taxa are rare, hindering our ability to study compositional changes in alpine insect in response to vegetation dynamics over time.

Watson's (1970) study provides a marvellous opportunity overcome this limitation. To illustrate this point, we resurveyed 14 historical alpine plots in two adjacent catchments (Broken River and Camp Stream) in Craigieburn Forest Park (Figure 1) to explore fine-scale changes in alpine grasshopper richness in response to vegetation dynamics over time. These plots were first sampled during the summer season of 1968/1969 (hereafter

1969; Watson, 1970) and then during the same season in 2023. The same field methods were used in 1969 and 2023 to allow direct comparisons (see Appendix 1). At the landscape scale, the vegetation cover in the study area has not change substantially during the last 54 years (Figure 2), so one might expect that the vegetation features and grasshopper ocurrences reported by Watson (1970) to remain relatively stable. To test this simple prediction, we compared three distinct metrics between sampling year: grasshopper species richness, percentage of vegetation cover, and host-plant species richness (see Table S1). Vegetation metrics were chosen as they are expected to influence grasshopper species occurrences (Watson, 1970).

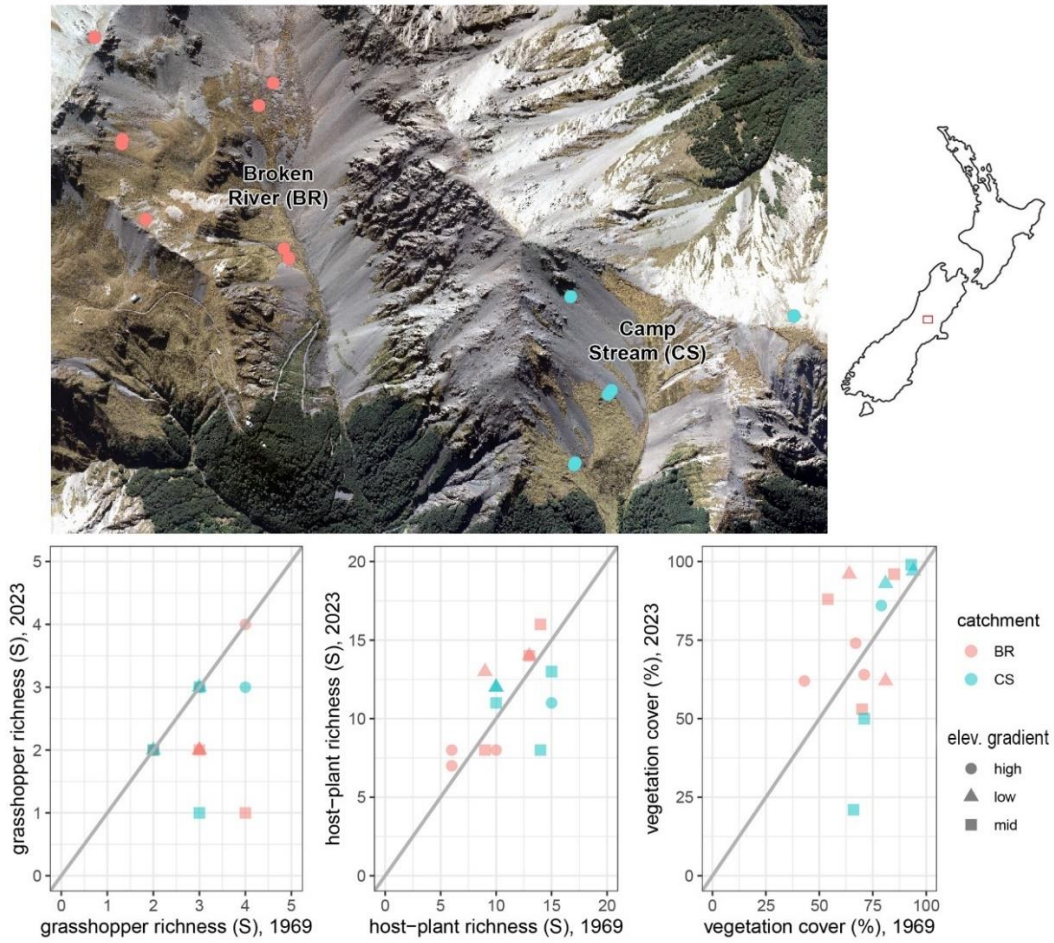

Figure 1. Orthophotography of the study area in Craigieburn Forest Park taken in the flying season (summer period) 2015–2016 (top). The inset map shows the location of study area in central South Island, New Zealand. Plots comparing three distinct metrics between sampling year (bottom). Points above the line indicate higher values in 2023, while those below indicate higher values in 1969. Points on the diagonal line represent similar values between surveys. For practical purposes, the elevational gradient was divided into three zones (low [1341–1400 m], mid [1401–1539 m], high [1540–1829 m]).

Figure 2. Photographs comparing vegetation cover on Camp Stream (1,324 m; up), Allan's Basin (1,616 m; centre), and Nervous Knob (1,820 m, bottom) in 1969 (left photos by R. N. Watson) and 2023.

Contrary to our prediction, there was a decline in grasshopper species richness across plots between sampled periods (Figure 1). Despite this directional change, all four grasshopper species detected in 1969 were detected in 2023: *Brachaspis nivalis* (Hutton), *Paprides nitidus* Hutton, *Sigaus australis* (Hutton), and *Sigaus villosus* Salmon. This

indicates that changes in composition resulted from reordering of species occurrences rather than changes in species richness over time. On the other hand, vegetation cover and host-plant richness showed increased values in most plots (n = 9). This suggests that the explored vegetation traits are poor predictors of changes in grasshopper occurrences. Though by no means robust comparisons, this brief example shows the value of resurveying historical plots to infer biotic responses to vegetation dynamics. While promising, this approach has some methodological limitations that must be considered (e.g. relocation errors, seasonal biases, and observer errors; see Appendix 1), as these issues can skew observed shifts from actual patterns (Kapfer et al., 2017).

Novel technologies to overcome data challenges

Novel data capture technologies such as environmental DNA (eDNA) and remote-sensing imagery are exciting prospects to overcome the logistical limitations of traditional surveys in alpine environments. Indeed, environmental DNA (eDNA) metabarcoding might increase survey capacity in terrestrial alpine environments. Unlike traditional surveys, eDNA offers a rapid and (potentially) cost-efficient approach for assessing biodiversity (Hassan et al., 2022; Pascher et al., 2022). While eDNA metabarcoding has rapidly gained impetus in freshwater alpine monitoring (e.g. Mächler et al., 2021; Lim et al., 2022; Chacko et al., 2023), technical issues related to quantifying biases associated with DNA spread, limited reference databases, and capture and degradation of DNA in terrestrial systems must be considered (Hassan et al., 2022; Pascher et al., 2022). Despite this limitations, eDNA metabarcoding is a tool with potential to support and complement biological monitoring (Pascher et al., 2022; Veilleux et al., 2021).

Remote-sensing imagery can be used to assess vegetation cover shifts across multiple spatial scales in near real-time, with on-ground surveys validating and complementing remote data (Turner, 2014). Remotely-sensed high-resolution (HR) satellite/aerial images from Google Earth Pro™ (Google, Inc.) have informed treeline positioning in New Zealand (Rita et al., 2023), and multispectral satellite images from Google Earth Engine (Gorelick et al., 2017) have shown decadal warming-driven vegetation greening (productivity gain) in the European Alps (e.g. Rumpf et al., 2022). Time series imagery from Google Earth has revealed climate-driven treeline dynamics in Asian alpine mountains over the last two decades (e.g. Zou et al., 2022). Combining historical aerial

photographs with new satellite images (e.g. Luo & Dai, 2013) and on-ground surveys (Cazzolla Gatti et al., 2019) has informed alpine treeline shifts over the half century in Asian mountains, overcoming long-term availability associated with HR satellite imagery. Nevertheless, remote sensing (e.g. laser scanning, hyperspectral and thermal imaging) is advancing microclimate modelling, and this can overcome scale-size issues for modelling range shifts (Zellweger et al., 2019).

Taking full advantage of such cutting-edge technologies requires significant technical skills and computational muscle, which can hamper potential applications. A variety of tools such as Google Earth Engine (Gorelick et al., 2017) and NeSI (https://www.nesi.org.nz) assist large-scale processing tasks and complex geospatial and bioinformatic workflows, respectively. State-of-the-art algorithms may also help to overcome data scarcity challenges. For instance, novel deep-learning-based named entity recognition (NER) systems such as TaxoNERD (Le Guillarme & Thuiller, 2022) help access multi-taxa information (e.g. distribution, traits, diet) from biodiversity literature. Geographic information systems can facilitate data storage, integration, analysis, and sharing (e.g. https://linaria.obsnev.es). Likewise, novel free and open-source software packages such as chelsa-cmip6 (Karger et al., 2023) allow generation of high resolution climate change projections for user defined spatial and temporal extents, that can improve detection of microrefugia under global warming (e.g. Meineri & Hylander, 2017). While advancing ground based data collection efforts is essential, these novel technologies can help to overcome some of the current data gaps, enabling more robust forecasts.

Concluding remarks

Climate change is driving enhanced rates of warming in high-elevation ecosystems across the globe, and alpine animals are responding in a myriad of ways. While distributional and morphological shifts are the most visible ways in which alpine specialists respond to selective pressures imposed by planetary heating, other responses remain poorly studied (e.g. phenological and behavioural). As we face unparalleled rates of warming, our capacity to predict the future of alpine biodiversity is crucial to inform decision-making, but this task is impaired by data limitations and challenges due to uncertainties on how to characterise the adaptive capacity of biotic units across the population-species continuum.

This research illustrates how, by using multiple data types and integrating a wide range of tools, such predictions can be improved, and uncertainty can be reduced. Future efforts to explicitly incorporate the processes underpinning species' responses to climatic factors using hybrid modelling approaches might enhance the biological realism of our predictions and open opportunities to addressing a range of questions, but gathering such data is a big challenging and the pace of environmental change may be overwhelming. Boosting scientific capability to envisage the foreseeable trajectory of alpine environments and their associated biota requires taking full advantage and make good use of all data and tools we have at hand, critically funding, data integration and sharing, and regular resurveys and long-term monitoring needs to be prioritised.

References

Bailey, L. D., Kruuk, L. E., Allen, R., Clayton, M., Stein, J., & Gardner, J. L. (2020). Using different body size measures can lead to different conclusions about the effects of climate change. *Journal of Biogeography*, *47*, 1687–1697. https://doi.org/10.1111/jbi.13850

Bi, K. E., Linderoth, T., Singhal, S., Vanderpool, D., Patton, J. L., Nielsen, R., ... & Good, J. M. (2019). Temporal genomic contrasts reveal rapid evolutionary responses in an alpine mammal during recent climate change. *PLoS Genetics*, *15*(5), e1008119. https://doi.org/10.1371/journal.pgen.1008119

Bigelow, R. S. (1967). *The grasshoppers (Acrididae) of New Zealand*. University of Canterbury Publications.

Bowler, D. E., Bjorkman, A. D., Dornelas, M., Myers-Smith, I. H., Navarro, L. M., Niamir, A., ... & Bates, A. E. (2020). Mapping human pressures on biodiversity across the planet uncovers anthropogenic threat complexes. *People and Nature*, *2*(2), 380–394. https://doi.org/10.1002/pan3.10071

Briscoe, N. J., Elith, J., Salguero-Gómez, R., Lahoz-Monfort, J. J., Camac, J. S., Giljohann, K. M., ... & Guillera-Arroita, G. (2019). Forecasting species range dynamics with process-explicit models: Matching methods to applications. *Ecology Letters*, 22(11), 1940–1956. https://doi.org/10.1111/ele.13348

Bruce, T. J. (2015). Interplay between insects and plants: Dynamic and complex interactions that have coevolved over millions of years but act in milliseconds. *Journal of Experimental Botany*, *66*(2), 455–465. https://doi.org/10.1093/jxb/eru391

Buckley, T. R., Hoare, R. J., & Leschen, R. A. (2022). Key questions on the evolution and biogeography of New Zealand alpine insects. *Journal of the Royal Society of New Zealand*, *54*(1), 30–54. https://doi.org/10.1080/03036758.2022.2130367

Card, D. C., Shapiro, B., Giribet, G., Moritz, C., & Edwards, S. V. (2021). Museum genomics. *Annual Review of Genetics*, *55*, 633–659. https://doi.org/10.1146/annurev-genet-071719-020506

Carmelet-Rescan, D., Morgan-Richards, M., Koot, E. M., & Trewick, S. A. (2021). Climate and ice in the last glacial maximum explain patterns of isolation by distance inferred for alpine grasshoppers. *Insect Conservation and Diversity*, *14*(5), 568–581. https://doi.org/10.1111/icad.12488

Cazzola Gatti, C. R., Callaghan, T., Velichevskaya, A., Dudko, A., Fabbio, L., Battipaglia, G., & Liang, J. (2019). Accelerating upward treeline shift in the Altai Mountains under last-century climate change. *Scientific Reports*, *9*(1), 7678. https://doi.org/10.1038/s41598-019-44188-1

Connolly, S. R., Keith, S. A., Colwell, R. K., & Rahbek, C. (2017). Process, mechanism, and modeling in macroecology. *Trends in Ecology & Evolution*, *32*(11), 835–844. https://doi.org/10.1016/j.tree.2017.08.011

Diamond, S. E. (2018). Contemporary climate-driven range shifts: Putting evolution back on the table. *Functional Ecology*, *32*(7), 1652–1665. https://doi.org/10.1111/1365-2435.13095

Dickinson, K. J. M., Mark, A. F., & Lee, W. G. (1992). Long-term monitoring of non-forest communities for biological conservation. *New Zealand Journal of Botany*, *30*(2), 163–179. https://doi.org/10.1080/0028825X.1992.10412896

Dormann, C. F., Schymanski, S. J., Cabral, J., Chuine, I., Graham, C., Hartig, F., ... & Singer, A. (2012). Correlation and process in species distribution models: Bridging a dichotomy. *Journal of Biogeography*, *39*, 2119–2131. https://doi.org/10.1111/j.1365-2699.2011.02659.x

Duncan, R. P., Webster, R. J., & Jensen, C. A. (2001). Declining plant species richness in the tussock grasslands of Canterbury and Otago, South Island, New Zealand. *New Zealand Journal of Ecology*, *25*(2), 35–47. http://www.jstor.org/stable/24055296

Evans, G. R. (1973). *The Alpine and Upper Montane Grasslands of the Eyre Mountains*. Forest Research Institute.

Frazier, A. G., Brewington, L., Goldstein, M. I., & DellaSala, D. A. (2020). *Current changes in alpine ecosystems of Pacific Islands*. In M. I. Goldstein & D. A. DellaSala (Eds.), *Encyclopedia World's Biomes* (pp. 607–619). Elsevier. https://doi.org/10.1016/B978-0-12-409548-9.11881-0

Goldberg, J., Trewick, S. A., & Paterson, A. M. (2008). Evolution of New Zealand's terrestrial fauna: A review of molecular evidence. *Philosophical Transactions of the Royal Society of London B: Biological Sciences*, *363*, 3319–3334. https://doi.org/10.1098/rstb.2008.0114

Gorelick, N., Hancher, M., Dixon, M., Ilyushchenko, S., Thau, D., & Moore, R. (2017). Google Earth Engine: Planetary-scale geospatial analysis for everyone. *Remote sensing of Environment*, *202*, 18–27. https://doi.org/10.1016/j.rse.2017.06.031

Greenwood, S., & Jump, A. S. (2014). Consequences of treeline shifts for the diversity and function of high altitude ecosystems. *Arctic, Antarctic, and Alpine Research*, *46*(4), 829–840. https://doi.org/10.1657/1938-4246-46.4.829

Halloy, S. R., & Mark, A. F. (2003). Climate-change effects on alpine plant biodiversity: A New Zealand perspective on quantifying the threat. *Arctic, Antarctic, and Alpine Research*, *35*, 248–254. https://doi.org/10.1657/1523-0430(2003)035[0248:CEOAPB]2.0.CO;2

Harvey, J. A., Heinen, R., Gols, R., & Thakur, M. P. (2020). Climate change-mediated temperature extremes and insects: From outbreaks to breakdowns. *Global Change Biology*, *26*(12), 6685–6701. https://doi.org/10.1111/gcb.15377

Holmes, M. W., Hammond, T. T., Wogan, G. O., Walsh, R. E., LaBarbera, K., Wommack, E. A., ... & Nachman, M. W. (2016). Natural history collections as windows on evolutionary processes. Molecular Ecology, 25(4), 864–881. https://doi.org/10.1111/mec.13529

Hulme, P. E. (2017). Climate change and biological invasions: Evidence, expectations, and response options. *Biological Reviews*, *92*(3), 1297–1313. https://doi.org/10.1111/brv.12282

Jamieson, M. A., Burkle, L. A., Manson, J. S., Runyon, J. B., Trowbridge, A. M., & Zientek, J. (2017). Global change effects on plant-insect interactions: The role of phytochemistry. *Current Opinion in Insect Science*, *23*, 70–80. https://doi.org/10.1016/j.cois.2017.07.009

Karger, D. N., Chauvier, Y., & Zimmermann, N. E. (2023). chelsa-cmip6 1.0: A python package to create high resolution bioclimatic variables based on CHELSA ver. 2.1 and CMIP6 data. *Ecography*, *6*, e06535. https://doi.org/10.1111/ecog.06535

Kendall, L. K., Rader, R., Gagic, V., Cariveau, D. P., Albrecht, M., Baldock, K. C., ... & Bartomeus, I. (2019). Pollinator size and its consequences: Robust estimates of body size in pollinating insects. *Ecology and Evolution*, *9*(4), 1702–1714. https://doi.org/10.1002/ece3.4835

Kerner, J. M., Krauss, J., Maihoff, F., Bofinger, L., & Classen, A. (2023). Alpine butterflies want to fly high: Species and communities shift upwards faster than their host plants. *Ecology*, *104*, e3848. https://doi.org/10.1002/ecy.3848

King, K. J., Lewis, D. M., Waters, J. M., & Wallis, G. P. (2020). Persisting in a glaciated landscape: Pleistocene microrefugia evidenced by the tree wētā Hemideina maori in central South Island, New Zealand. *Journal of Biogeography*, *47*, 2518–2531. https://doi.org/10.1111/jbi.13953

Kinsella, R. S., Thomas, C. D., Crawford, T. J., Hill, J. K., Mayhew, P. J., & Macgregor, C. J. (2020). Unlocking the potential of historical abundance datasets to study biomass change in flying insects. *Ecology and Evolution*, *10*(15), 8394–8404. https://doi.org/10.1002/ece3.6546

Koot, E. M., Morgan-Richards, M., & Trewick, S. A. (2022). Climate change and alpine adapted insects: Modelling environmental envelopes of a grasshopper radiation. *Royal Society Open Science*, *9*, 211596. https://doi.org/10.1098/rsos.211596

Labandeira, C. C. (2013). A paleobiologic perspective on plant-insect interactions. *Current Opinion in Plant Biology*, *16*(4), 414–421. https://doi.org/10.1016/j.pbi.2013.06.003

Le Guillarme, N., & Thuiller, W. (2022). TaxoNERD: Deep neural models for the recognition of taxonomic entities in the ecological and evolutionary literature. *Methods in Ecology and Evolution*, *13*(3), 625–641. https://doi.org/10.1111/2041-210X.13778

Luo, G., & Dai, L. (2013). Detection of alpine tree line change with high spatial resolution remotely sensed data. *Journal of Applied Remote Sensing*, *7*(1), 073520. https://doi.org/10.1117/1.JRS.7.073520

MacGregor, C. J., Williams, J., Bell, J., & Thomas, C. (2019). Moth biomass increases and decreases over 50 years in Britain. *Nature Ecology & Evolution*, *3*, 1645–1649. https://doi.org/10.1038/s41559-019-1028-6

Mächler, E., Salyani, A., Walser, J. C., Larsen, A., Schaefli, B., Altermatt, F., & Ceperley, N. (2021). Environmental DNA simultaneously informs hydrological and biodiversity characterization of an Alpine catchment. *Hydrology and Earth System Sciences*, *25*(2), 735–753. https://doi.org/10.5194/hess-25-735-2021

MacLean, H. J., Kingsolver, J. G., & Buckley, L. B. (2016). Historical changes in thermoregulatory traits of alpine butterflies reveal complex ecological and evolutionary responses to recent climate change. *Climate Change Responses*, *3*, 13. https://doi.org/10.1186/s40665-016-0028-x

Marske, K. A., Leschen, R. A., & Buckley, T. R. (2011). Reconciling phylogeography and ecological niche models for New Zealand beetles: Looking beyond glacial refugia. *Molecular Phylogenetics and Evolution*, *59*(1), 89–102. https://doi.org/10.1016/j.ympev.2011.01.005

Mateo, R. G., Croat, T. B., Felicísimo, A. M., & Muñoz, J. (2010). Profile or group discriminative techniques? Generating reliable species distribution models using pseudo-absences and target-group absences from natural history collections. *Diversity and Distributions*, *16*(1), 84–94. https://doi.org/10.1111/j.1472-4642.2009.00617.x

Mathias, S., van Galen, L. G., Jarvie, S., & Larcombe, M. J. (2023). Range reshuffling: Climate change, invasive species, and the case of *Nothofagus* forests in Aotearoa New Zealand. *Diversity and Distributions*, *29*, 1402–1419. https://doi.org/10.1111/ddi.13767

McCulloch, G. A., & Waters, J. M. (2018). Does wing reduction influence the relationship between altitude and insect body size? A case study using New Zealand's diverse stonefly fauna. *Ecology and Evolution, 8*(2), 953–960. https://doi.org/10.1002/ece3.3713

McGaughran, A., Laver, R., & Fraser, C. (2021). Evolutionary responses to warming. *Trends in Ecology & Evolution*, *36*(7), 591–600. https://doi.org/10.1016/j.tree.2021.02.014

Meineri, E., & Hylander, K. (2017). Fine-grain, large-domain climate models based on climate station and comprehensive topographic information improve microrefugia detection. *Ecography*, *40*(8), 1003–1013. https://doi.org/10.1111/ecog.02494

Meudt, H. M., Lockhart, P. J., & Bryant, D. (2009). Species delimitation and phylogeny of a New Zealand plant species radiation. *BMC Evolutionary Biology*, *9*(1), 1–17. https://doi.org/10.1186/1471-2148-9-111

Meza-Joya, F. L., Morgan-Richards, M., & Trewick, S. A. (2022). Relationships among body size components of three flightless New Zealand grasshopper species (Orthoptera, Acrididae) and their ecological applications. *Journal of Orthoptera Research, 31*(1), 91–103. https://doi.org/10.3897/jor.31.79819

Meza-Joya. F. L., Morgan-Richards, M., Koot, E. M., & Trewick, S. A. (2023). Global warming leads to habitat loss and genetic erosion of alpine biodiversity. *Journal of Biogeography, 50*, 961–975. https://doi.org/10.1111/jbi.14590

Millien, V., Kathleen Lyons, S., Olson, L., Smith, F. A., Wilson, A. B., & Yom-Tov, Y. (2006). Ecotypic variation in the context of global climate change: Revisiting the rules. *Ecology Letters*, *9*(7), 853–869. https://doi.org/10.1111/j.1461-0248.2006.00928.x

Pascher, K., Švara, V., & Jungmeier, M. (2022). Environmental DNA-based methods in biodiversity monitoring of protected areas: Application range, limitations, and needs. *Diversity*, *14*(6), 463. https://doi.org/10.3390/d14060463

Pauli, H., & Halloy, S. (2019). *High mountain ecosystems under climate change*. Oxford University Press. https://doi.org/10.1093/acrefore/97801 90228 620.013.764

Reji Chacko, M., Altermatt, F., Fopp, F., Guisan, A., Keggin, T., Lyet, A., ... & Pellissier, L. (2023). Catchment-based sampling of river eDNA integrates terrestrial and aquatic

biodiversity of alpine landscapes. *Oecologia*, 202, 699–713. https://doi.org/10.1007/s00442-023-05428-4

Rita, A., Saracino, A., Cieraad, E., Saulino, L., Zotti, M., Idbella, M., ... & Bonanomi, G. (2023). Topoclimate effect on treeline elevation depends on the regional framework: A contrast between Southern Alps (New Zealand) and Apennines (Italy) forests. *Ecology and Evolution*, *13*(1), e9733. https://doi.org/10.1002/ece3.9733

Rubidge, E. M., Patton, J. L., Lim, M., Burton, A. C., Brashares, J. S., & Moritz, C. (2012). Climate-induced range contraction drives genetic erosion in an alpine mammal. *Nature Climate Change*, *2*, 285–288. https://doi.org/10.1038/nclimate1415

Rumpf, S. B., Gravey, M., Brönnimann, O., Luoto, M., Cianfrani, C., Mariethoz, G., & Guisan, A. (2022). From white to green: Snow cover loss and increased vegetation productivity in the European Alps. *Science*, *376*, 1119–1122. https://doi.org/10.1126/science.abn669

Shaffer, H. B., Fisher, R. N., & Davidson, C. (1998). The role of natural history collections in documenting species declines. *Trends in Ecology & Evolution*, *13*(1), 27–30. https://doi.org/10.1016/S0169-5347(97)01177-4

Sivyer, L., Morgan-Richards, M., Koot, E., & Trewick, S. A. (2018). Anthropogenic cause of range shifts and gene flow between two grasshopper species revealed by environmental modelling, geometric morphometrics and population genetics. *Insect Conservation and Diversity*, *11*, 415–434. https://doi.org/10.1111/icad.12289

Smith, A. B., Murphy, S. J., Henderson, D., & Erickson, K. D. (2023). Including imprecisely georeferenced specimens improves accuracy of species distribution models and estimates of niche breadth. *Global Ecology and Biogeography*, *32*(3), 342–355. https://doi.org/10.1111/geb.13628

Thakur, M. P., Risch, A. C., & van der Putten, W. H. (2022). Biotic responses to climate extremes in terrestrial ecosystems. *iScience*, *25*(7), 104559. https://doi.org/10.1016/j.isci.2022.104559

Thompson, P. L., & Fronhofer, E. A. (2019). The conflict between adaptation and dispersal for maintaining biodiversity in changing environments. *Proceedings of the National Academy of Sciences of the United States of America*, *116*(42), 21061–21067. https://doi.org/10.1073/pnas.19117 96116

Tingley, M. W., & Beissinger, S. R. (2009). Detecting range shifts from historical species occurrences: New perspectives on old data. *Trends in Ecology & Evolution*, *24*(11), 625–633. https://doi.org/10.1016/j.tree.2009.05.009

Trewick, S. A., Koot, E. M., & Morgan-Richards, M. (2023). Māwhitiwhiti Aotearoa: Phylogeny and synonymy of the silent alpine grasshopper radiation of New Zealand (Orthoptera: Acrididae). *Zootaxa*, 5383(2), 225–241. https://doi.org/10.11646/zootaxa.5383.2.7

Trewick, S. A., & Morris, S. (2008). *Diversity and Taxonomic Status of Some New Zealand Grasshoppers*. Science & Technical Publishing Department of Conservation https://www.doc.govt.nz/globalassets/docum ents/science-and-technical/drds2 90.pdf

Tseng, M., Kaur, K. M., Soleimani Pari, S., Sarai, K., Chan, D., Yao, C. H., ... & Fograscher, K. (2018). Decreases in beetle body size linked to climate change and warming temperatures. *Journal of Animal Ecology*, *87*(3), 647–659. https://doi.org/10.1111/1365-2656.12789

Turner, W. (2014). Sensing biodiversity. *Science*, *346*, 301–302. https://doi.org/10.1126/science.1256014

Urban, M. C., Bocedi, G., Hendry, A. P., Mihoub, J. B., Pe'er, G., Singer, A., ... & Travis, J. M. (2016). Improving the forecast for biodiversity under climate change. *Science*, *353*, aad8466. https://doi.org/10.1126/science.aad8466

Veilleux, H. D., Misutka, M. D., & Glover, C. N. (2021). Environmental DNA and environmental RNA: Current and prospective applications for biological monitoring. *Science of the Total Environment*, *782*, 146891. https://doi.org/10.1016/j.scitotenv.2021.146891

Watson, R. N. (1970). *The feeding behaviour of alpine grasshoppers (Acrididae: Orthoptera), in the Craigieburn Range, Canterbury, New Zealand*. [Master's thesis, University of Canterbury]. Research@Lincoln Repository. https://hdl.handle.net/10182/4000

White, E. G. (1974). A quantitative biology of three New Zealand alpine grasshopper species. *New Zealand Journal of Agricultural Research*, *17*(2), 207–227. https://doi.org/10.1080/00288233.1974.10421001

White, E. G., & Sedcole, J. R. (1991). A 20-year record of alpine grasshopper abundance, with interpretations for climate change. *New Zealand Journal of Ecology*, *15*,139–152. https://www.jstor.org/stable/24053567

Wiens, J. A., Stralberg, D., Jongsomjit, D., Howell, C. A., & Snyder, M. A. (2009). Niches, models, and climate change: Assessing the assumptions and uncertainties. *Proceedings of the National Academy of Sciences*, *106*, 19729–19736. https://doi.org/10.1073/pnas.0901639106

Willi, Y., Van Buskirk, J., & Hoffmann, A. A. (2006). Limits to the adaptive potential of small populations. *Annual Review of Ecology, Evolution, and Systematics*, *37*, 433–458. https://doi.org/10.1146/annurev.ecols ys.37.091305.110145

Wu, C. H., Holloway, J. D., Hill, J. K., Thomas, C. D., Chen, I. C., & Ho, C. K. (2019). Reduced body sizes in climate-impacted Borneo moth assemblages are primarily explained by range shifts. *Nature Communications*, *10*, 4612. https://doi.org/10.1038/s41467-019-12655-y

Zellweger, F., De Frenne, P., Lenoir, J., Rocchini, D., & Coomes, D. (2019). Advances in microclimate ecology arising from remote sensing. *Trends in Ecology & Evolution*, *34*(4), 327–341. https://doi.org/10.1016/j.tree.2018.12.012

Zou, F., Tu, C., Liu, D., Yang, C., Wang, W., & Zhang, Z. (2022). Alpine treeline dynamics and the special exposure effect in the Hengduan Mountains. *Frontiers in Plant Science, 13*, 861231. https://doi.org/10.3389/fpls.2022.861231

Supporting Information

Appendix 1. Supplementary methods for the New Zealand case study: Resurveying to infer insect-host plant shifts over time.

Vegetation plot resurveying is a well-established method for monitoring vegetation dynamics over time (Douda et al., 2023; Futschik et al., 2019; Kapfer et al., 2017). While promising, this approach has some limitations that can lead to misleading inferences (Kapfer et al., 2017): relocation error (i.e. changes in plot position), seasonal bias (i.e. seasonal shifts in sampling), and observer error (i.e. shifts in detectability and misidentifications). Relocation errors can vary from negligible for permanently marked plots to significant for quasi-permanent (known location but unmarked) and non-traceable (unknown location) plots (Kapfer et al., 2017), yet errors can be reduced by considering information available from the original study (e.g. maps, plot location descriptions, elevation, aspect, slope, photographs). A sensible approach to avoid seasonal bias is resampling during a phenological period comparable to the historical survey (Kapfer et al., 2017). Although observer error cannot be fully avoided (reviewed in Morrison, 2016), simple data aggregation methods (e.g. merging species at genus level or functional classes: grasses, herbs, and shrubs) can reduce observer effects while informing vegetation trends, yet identification to the lowest possible taxonomic level is desirable prior to aggregation, particularly for threatened and invasive species (Boch et al., 2022).

Here, I resurveyed 14 historical alpine plots originally visited during the summer season of 1968/1969 by R. N. Watson then at the University of Canterbury (Watson, 1970). These plots are located along two elevational transects, each extending from near the timberline to the ridges of the mountains. For each of these plots, Watson (1970) provides data on grasshopper occurrences, vegetation cover and vascular plant species richness, along with plot-specific covariates including elevation, aspect, and slope. Watson (1070) also provided aerial imagery of the study area, which were uploaded to Google Earth Pro™ (Google, Inc.) to locate the plots, while accounting elevation, aspect, and slope features. Location uncertainty was estimated as 30 m based on the size of the location dots in Watson's (1970) map. Plots were 10 × 20 m, pegged up and down the slope, and vegetation cover was quantified using a point analyser frame method from 500 points, taken from 25 random locations (4 m^2) located within a 200 m^2 area (Watson, 1970). The raw data obtained for this method is expressed as a frequency (i.e. relative proportion of each species in the vegetation and the ground cover occupied by them), thus for a given species *i* the percentage of cover (C) can be estimated as: C = (total hits on *i*/500) × 100 (Watson, 1970). Plant species were identified in field with the assistance of an experienced botanist (Dr Claire Newell). Taxonomic nomenclature follows that of the New Zealand Plant Conservation Network (www.nzpcn.org). Host-plant species richness was estimated for each plot based on the top-ranked plant species included into the studied grasshoppers' diet (Table S1). The occurrence of grasshopper species inside each plot was recorded as we walked through, and was coded as absent (0) or present (1), and then the number of grasshopper species per plot was estimated. Species were identified using morphological traits (e.g. pronotum margin, subgenital plate, and epiproct) following Bigelow (1967).

Table S1. Top-ranked plant species included into the studied grasshoppers' diet. Ranking based on data from Table 13 in Watson (1970).

Rank	Species	Authority
1	*Poa colensoi*	Hook.f.
2	*Anisotome aromatica*	Hook.f.
3	*Celmisia viscosa*	Hook.f.
4	*Gaultheria depressa*	Hook.f.
5	*Celmisia lyallii*	Hook.f.
6	*Luzula* spp.	-
7	*Coprosma* spp.	-
8	*Polytrichum juniperinum*	Hedw.
9	*Austroblechnum penna-marina*	(Poir.) Kuhn
10	*Wahlenbergia albomarginata*	Hook.

Supplementary references (not include in the main text)

Boch, S., Küchler, H., Küchler, M., Bedolla, A., Ecker, K. T., Graf, U. H., ... & Bergamini, A. (2022). Observer-driven pseudoturnover in vegetation monitoring is context-dependent but does not affect ecological inference. *Applied Vegetation Science, 25*(3), e12669. https://doi.org/10.1111/avsc.12669

Douda, J., Doudová, J., Holeštová, A., Chudomelová, M., Vild, O., Boublík, K., ... & Hédl, R. (2023). Historical sampling error: A neglected factor in long-term biodiversity change research. *Biological Conservation, 286*, 110317. https://doi.org/10.1016/j.biocon.2023.110317

Futschik, A., Winkler, M., Steinbauer, K., Lamprecht, A., Rumpf, S. B., Barančok, P., ... & Pauli, H. (2020). Disentangling observer error and climate change effects in long-term monitoring of alpine plant species composition and cover. *Journal of Vegetation Science, 31*(1), 14–25. https://doi.org/10.1111/jvs.12822

Kapfer, J., Hédl, R., Jurasinski, G., Kopecký, M., Schei, F. H., & Grytnes, J. A. (2017). Resurveying historical vegetation data–opportunities and challenges. *Applied Vegetation Science*, *20*(2), 164–171. https://doi.org/10.1111/avsc.12269

Morrison, L. W. (2016). Observer error in vegetation surveys: A review. *Journal of Plant Ecology, 9,* 367–379. https://doi.org/10.1093/jpe/rtv077

In loving memory of my grandpa "Rul". My heart aches knowing I have to go through life without your stories, jokes, and kindness.